INSTITUTO SUPERIOR DE ENGENHARIA DO PORTO
MESTRADO EM ENGENHARIA MECÂNICA




Desenvolvimento de um processo de recuperação de louça sanitária através da tecnologia laser

RÚBEN DANIEL FERNANDES DE SOUSA COSTA
setembro de 2021

POLITÉCNICO
DO PORTO

Instituto Superior de Engenharia do Porto

DEVELOPMENT OF A RECOVERY PROCESS FOR SANITARY WARE USING LASER TECHNOLOGY

Rúben Daniel Fernandes de Sousa Costa

2021

ISEP – School of Engineering, Polytechnic of Porto

Mechanical Engineering Department – Materials and Manufacturing Technologies

POLITÉCNICO DO PORTO

isep Instituto Superior de Engenharia do Porto

POLITÉCNICO
DO PORTO

Instituto Superior de Engenharia do Porto

DEVELOPMENT OF A RECOVERY PROCESS FOR SANITARY WARE USING LASER TECHNOLOGY

Rúben Daniel Fernandes de Sousa Costa

1160913

Dissertation presented to ISEP – School of Engineering to fulfil the requirements necessary to obtain a Master's degree in Mechanical Engineering, carried out under the guidance of Doctor Luís Miguel Pereira Durão, Coordinator Professor at ISEP – School of Engineering, Polytechnic of Porto, and Doctor Arnaldo Manuel Guedes Pinto, Adjunct Professor at ISEP – School of Engineering, Polytechnic of Porto.

2021

ISEP – School of Engineering, Polytechnic of Porto

Mechanical Engineering Department

POLITÉCNICO DO PORTO

isep Instituto Superior de Engenharia do Porto

POLITÉCNICO
DO PORTO

“Education is the most powerful weapon which you can use to change the world.”

Nelson Mandela

JURY

President

<Academic Grade and Name>

<Category, Institution>

Supervisor

Luís Miguel Pereira Durão, PhD

Coordinator Professor, ISEP – School of Engineering, Polytechnic of Porto

Second supervisor

Arnaldo Manuel Guedes Pinto, PhD

Adjunct Professor, ISEP – School of Engineering, Polytechnic of Porto

Examiner

Fernando Jorge Lino Alves, PhD

Associate Professor, FEUP – Faculty of Engineering, University of Porto

ACKNOWLEDGEMENTS

Firstly, I would like to thank my parents and brother for being my background and guaranteeing I would have all the means to carry on.

Secondly, a special word to my girlfriend, Marta Barbosa, for always accompanying me closely throughout this journey that has been our master's degree, always giving the best advice and walking side by side with me both academically and in life.

A word of gratitude to ISEP, the institution which welcomed me during these five years, and a warming word of affection to those teachers, too many to enumerate, who turned their everyday work into the pleasure of transmitting knowledge with passion.

A special thanks to my supervisors in this project, Prof. Luis Durão and Prof. Arnaldo Pinto, who always showed their availability to understand the problem since the very beginning of the dissertation, giving their best efforts to help me when I needed. Thank you so much, Prof. Olga Trabulo, for the English revision of the entire dissertation.

Thank you to Mr. Paulo Reis, operational assistant at ISEP, who lent his ceramic tile cutter tool for the project, Prof. Sandra Ramos and Eng. Fátima Andrade, from ISEP, for the help offered with the statistical analysis and the optical microscope use, respectively. Thank you as well to Eng. Rui Rocha, from CEMUP, for the possibility of doing the scanning electronic microscope (SEM) analysis of the samples in study.

My gratitude to ARCH Valadares, the company which hosted my curricular internship, especially to Eng. Rocha Ferreira and Eng. Susete Soares, for teaching me the sanitary ware ceramic industry's pillars, but also to Pedro Barbeiro, my co-worker in this project.

My appreciation to Eng. Samuel Santos, from CicloFapril, as well as Mr. Daniel Matos and Christopher, from Tabor, without whom the practical work for this project would not have been able to be conducted.

Last but not least, my sincerest thanks to my friends from this course in ISEP and those from TAISEP, who taught me that college is much more than a degree, taking me among themselves in the most memorable adventures and making me see the world.

KEYWORDS

Sanitary ware, laser technology, defects, pinholes, cracks

ABSTRACT

The ceramic sanitary ware industry is widespread all over the world. It employs thousands of people and, consequently, has a high financial impact on the global and national economy. The factories associated with this industry are vital in the 21st century as they have a daily production of the most diverse sanitary ware products, which refer to a higher level of comfort for the population. Due to these important items, the words quality and innovation are always present and, consequently, multifunctional teams work incessantly on their continuous improvement.

Over the years, some changes have been made in the sanitary ware manufacturing process in order to achieve maximum efficiency. However, due to factors inherent to the manufacture of these products, at the end of the production line, there are defects that prevent a small percentage of them from being sold, as they do not reach the required quality.

In order to promote a sustainable economy of resources for the company, it avoids products without the required quality level to be submitted to a new complete production cycle, thus promoting their repair in a simpler and more effective way. With the implementation of laser technology for the recuperation of sanitary ware, replacing the refiring process in the kiln, it is estimated that 9 € will be saved per product, on 5% of an annual production rate of 200,000 pieces. Laser technology, along with its numerous and different applications in the industry field nowadays, has all the means to be capable of performing a correct ink fusion on the defects which appear on ceramic sanitary ware materials, reason why it was tested for this project in a wide range of experimental tests that include provoked defects on ceramic tiles.

Some analysis methods were also used, such as a colour difference reading to compare to the standard one (with a statistical approach), or the optical microscope and SEM-EDS analysis, to complement the understanding of the results. Finally, two quality tests were performed, namely the autoclave and the acids, bases and staining agents' tests, with the purpose of proving this method's effectiveness.

Accordingly, it was concluded that the best results, considering defects caused on a white coloured piece, are obtained with an ethyl alcohol-based ink, and the parameters to be used for the laser interaction are manual firing with a power between 50 and 70 W, and an interaction time of 1 to 3 firings of 10 seconds each without the use of any amplifying lens. These values apply for both pinholes and cracks, with a 50 W power and an interaction of 30 seconds being the best.

PALAVRAS-CHAVE

Louça sanitária, tecnologia laser, defeitos, picadas, fissuras

RESUMO

A indústria cerâmica de artigos para uso sanitário está difundida por todo o mundo. Esta emprega milhares de pessoas e, consequentemente, é responsável por um elevado impacto financeiro na economia global e nacional. As fábricas associadas a esta indústria são vitais no século XXI, uma vez que apresentam uma produção diária dos mais diversos produtos de louça sanitária, que remetem para um elevado nível de conforto da população. Devido a estas peças tão importantes, as palavras qualidade e inovação estão sempre presentes, e como tal, equipas multifuncionais trabalham incessantemente na sua melhoria contínua.

Ao longo dos anos foram efetuadas algumas mudanças no processo de fabrico de louça sanitária com vista a alcançar o expoente máximo da sua eficácia. Contudo, decorrente de fatores inerentes ao fabrico destes produtos, no final da linha de produção surgem defeitos que inviabilizam uma pequena percentagem dos mesmos de serem comercializados, por não terem atingido a qualidade requisitada.

Por forma a promover uma economia sustentável dos recursos para a empresa, evita-se que as peças sem o nível de qualidade exigido sejam submetidas a um novo ciclo completo de produção, promovendo assim a sua reparação de uma forma mais simples e eficaz. Com a implementação da técnica do laser para a recuperação de louça sanitária, substituindo o processo de recozedura no forno, estima-se que serão poupados 9 € por produto, em 5% de uma taxa de produção anual de 200 000 peças. A tecnologia laser, juntamente com as suas numerosas e diferentes aplicações no campo da indústria nos dias de hoje, possui todos os meios para ser capaz de realizar uma correta fusão da tinta nos defeitos que surgem nos materiais cerâmicos sanitários, razão pela qual foi testada para este projeto num vasto conjunto de ensaios experimentais que contemplam defeitos provocados em azulejos cerâmicos.

Utilizaram-se, ainda, alguns métodos de análise, tais como a leitura das diferenças de cor em comparação com o padrão (com uma abordagem estatística), ou o microscópio ótico e a análise SEM-EDS, para complementar a compreensão dos resultados. Por fim, realizaram-se dois ensaios de qualidade, nomeadamente o ensaio do autoclave e dos ácidos, bases e agentes manchantes, com o objetivo de provar a eficácia deste método.

Desta forma, chegou-se à conclusão de que os melhores resultados, considerando defeitos provocados numa peça de cor branca, se obtêm para uma tinta à base de álcool etílico e os parâmetros a usar para a interação laser são o disparo manual com uma potência entre 50 e 70 W e um tempo de interação de 1 a 3 disparos de 10 segundos cada sem o uso de qualquer lente amplificadora. Estes valores aplicam-se quer para picadas, quer para fissuras, sendo a potência de 50 W e 30 segundos de interação os melhores.

SCHLÜSSELWÖRTER

Sanitärkeramik, Lasertechnik, Defekte, Lochfraß, Risse

ABSTRAKT

Die Sanitärkeramikindustrie ist weltweit verbreitet. Es beschäftigt Tausende von Menschen und hat folglich einen hohen finanziellen Einfluss auf die globale und nationale Wirtschaft. Die mit dieser Branche verbundenen Fabriken sind im 21. Jahrhundert von entscheidender Bedeutung, da sie täglich die unterschiedlichsten Sanitärprodukte produzieren, die auf einen höheren Komfort für die Bevölkerung hinweisen. Aufgrund dieser wichtigen Stücke sind die Worte Qualität und Innovation immer präsent und folglich arbeiten multifunktionale Teams unablässig an ihrer kontinuierlichen Verbesserung.

Im Laufe der Jahre wurden einige Änderungen im Herstellungsprozess von Sanitärkeramik vorgenommen, um maximale Effizienz zu erreichen. Aufgrund von Faktoren, die mit der Herstellung dieser Produkte verbunden sind, gibt es jedoch am Ende der Produktionslinie Mängel, die einen kleinen Prozentsatz davon abhalten, verkauft zu werden, da sie nicht die erforderliche Qualität erreichen.

Um eine nachhaltige Ressourcenschonung für das Unternehmen zu fördern, vermeidet es, Produkte ohne das geforderte Qualitätsniveau einem neuen kompletten Produktionszyklus zu unterziehen und fördert so deren Reparatur einfacher und effektiver. Mit der Einführung der Lasertechnologie zur Rekuperation von Sanitärkeramik, die den Nachbrennprozess im Ofen ersetzt, werden schätzungsweise 9 € pro Produkt eingespart, bei 5% einer jährlichen Produktionsrate von 200.000 Stück. Die Lasertechnologie, zusammen mit ihren zahlreichen und unterschiedlichen Anwendungen in der Industrie heutzutage, verfügt über alle Mittel, um eine korrekte Farbschmelze an den Defekten durchzuführen, die auf Sanitärkeramikmaterialien auftreten, weshalb sie für dieses Projekt in einem Jahr getestet wurde breites Spektrum an experimentellen Tests, die provozierte Defekte an Keramikfliesen umfassen.

Einige Analysemethoden wurden ebenfalls verwendet, wie das Ablesen der Farbunterschiede im Vergleich zum Standard (mit einem statistischen Ansatz), oder die optische Mikroskop- und SEM-EDS-Analyse, um das Verständnis der Ergebnisse zu ergänzen. Schließlich wurden zwei Qualitätsprüfungen durchgeführt, nämlich der Autoklav- und der Säure-, Laugen- und Färbemitteltest, um die Wirksamkeit dieser Methode nachzuweisen.

Daraus wurde geschlossen, dass die besten Ergebnisse unter Berücksichtigung von Fehlern, die auf einem weißen Farbstück verursacht werden, mit einer Tinte auf Ethylalkoholbasis erzielt werden, und die für die Laserinteraktion zu verwendendem Parameter sind manuelles Brennen mit einer Leistung zwischen 50 und 70 W, und eine Wechselwirkungszeit von 1 bis 3 Zündungen von jeweils 10 Sekunden ohne Verwendung einer verstärkenden Linse. Diese Werte gelten sowohl für Lochfraß als auch für Risse, wobei 50 W Leistung und eine Interaktion von 30 Sekunden am besten sind.

LIST OF SYMBOLS AND ABBREVIATIONS

List of abbreviations

ABS	Acids, Bases and Staining agents
ANOVA	Analysis of Variance
ARCH	Advanced Research Ceramic Heritage
CAE	Portuguese Classification of Economic Activities
CAGR	Compound Annual Growth Rate
CEMUP	University of Porto Materials Centre
CIELAB	International Commission of Illumination L*a*b* system
CMC	Carboxymethyl cellulose
CO_2	Carbon Dioxide
EBITDA	Earnings before Interest, Taxes, Depreciation and Amortization
FECS	European Federation of Ceramic Sanitaryware Manufacturers
FL	Focal Length
INE	National Institute of Statistics
ISEP	Superior Institute of Engineering of Porto
Laser	Light Amplification by Stimulated Emission of Radiation
LBP	Local Binary Pattern
LMET	Metallography Laboratory
LMEV	Scanning Electron Microscopy Laboratory
MF	Manual Firing
MReLU	Modified Rectified Linear Unit Activation Function
Nd:YAG	Neodymium-doped yttrium aluminium garnet
Nd:YVO_4	Neodymium-doped yttrium orthovanadate
NL	No Lens
P	Laser Power
R	Resolution
RF	Rapid Firing
RIMLV	Rotation Invariant Measure of Local Variance

SEM-EDS	Scanning Electron Microscopy - Energy Dispersive Spectroscopy
SEM	Scanning Electron Microscope
T	Incidence Time
USA	United States of America
UV	Ultraviolet
V	Beam speed (Velocity)
vs	Versus
WA	Water Absorption coefficient
WL	With Lens
Yb-fibre	Ytterbium-Doped fibre

List of units

cm	Centimetre
cm^2	Square Centimetre
dpi	Dot Per Inch
g	Gram
h	Hour
J	Joule
kg	Kilogram
kgf	Kilogram-force
kN	Kilonewton
kW	Kilowatt
M€	Million euros
min	Minute
mm	Millimetre
mm^2	Square Millimetre
mm/s	Millimetre per second
mPa	Millipascal
nm	Nanometre
Pa	Pascal

s	Second
W	Watt
µm	Micrometre
°C	Degree Celsius
€	Euro
”	Inch
%	Percent

List of symbols

a	Type of experiment
a^*	Red-green component of a colour axis
b	Specimen’s number
b^*	Yellow-blue component of a colour axis
c	Sample’s position
C^*	Saturation of the colour
f	Number of factors
l	Number of levels
L^*	Lightness axis
m_0	Mass of the specimen after immersion in water, in grams
m_1	Mass of the dry specimen, in grams
t	Reduction of the number of tests
x	Abscissa axis
y	Ordinate axis
ΔE^*	Colour deviation

GLOSSARY OF TERMS

Barbotine	Clay suspension used for mould fillings.
Kaolin	Hydrated aluminium silicates compound with special characteristics which allow its use in the ceramics manufacturing.
Chamotte	Calcinated clay or kaolin used as an inert raw material to improve part properties (reduction of deformation and thermal shrinkage) in ceramic materials.
Faience	Form of white ceramic which has less kaolin-rich ceramic mass than porcelain and is associated with more plastic clays. Porous mass of white or ivory colouration that has quartz in its constitution and needs subsequent vitrification.
Fine Fire Clay (*Grés*)	Material made from fine-grained clay that can withstand high temperatures and vitrifies between 1150 and 1300 ℃.
Frit	Pre-cast glazed material, produced by rapid solidification of molten material followed by grinding or milling to obtain the required grain size.
Gresanit	Material created by ARCH from fine fire clay (*grés*) but with enhanced characteristics: resistance to crazing, half of the *grés* density, higher mechanical resistance and lower water absorption.
Mulite	Rare mineral derived from silicate formed during the heat treatment of clay.
Thixotropy	Property of a colloidal fluid which translates into a decrease in its viscosity as a function of time when subjected to shear stresses at constant speed.
Vitrification	Process of converting a certain material into a glass or glassy substance by means of heat and/or fusion.

FIGURES INDEX

FIGURE 1 – RED CERAMICS [4] 10
FIGURE 2 – WHITE CERAMICS [5] 10
FIGURE 3 – ASHBY'S CHART: YOUNG'S MODULUS VS DENSITY [7] 11
FIGURE 4 – FRACTURE TOUGHNESS IN DIFFERENT FAMILIES OF MATERIALS [2] 11
FIGURE 5 – SANITARY WARE PRODUCTION (ADAPTED FROM [11]) 12
FIGURE 6 – NAUTILUS WASHBASIN (ADAPTED FROM [10]) 13
FIGURE 7 – MOULD SHAPE VS FINAL WORKPIECE SHAPE (ADAPTED FROM [21]) 16
FIGURE 8 – DEMOULDING THE WORKPIECE FROM THREE PORTIONS OF THE MOULD [23] 17
FIGURE 9 – PROCESS FLOW CHART OF CERAMIC SANITARY WARE INDUSTRY (ADAPTED FROM [24]) 17
FIGURE 10 – APPLICATION OF THE GLAZE TO THE WORKPIECE USING A ROBOTIC ARM [23] 18
FIGURE 11 – LOGOTYPE APPLICATION BY *DECALCOMANIA* 19
FIGURE 12 – FINAL LOGOTYPE 19
FIGURE 13 – SANITARY WARE FIRING [28] 20
FIGURE 14 – GLAZE IN THE MIXING TANK 21
FIGURE 15 – OPAQUE CREAM-COLOURED WASHBASIN [35] 22
FIGURE 16 – RESIDUAL WATERS FORMED DURING THE APPLICATION OF THE GLAZE (ADAPTED FROM [28]) 24
FIGURE 17 – PINHOLES IN SANITARY WARE 26
FIGURE 18 – CRACKS IN SANITARY WARE 27
FIGURE 19 – SHIVERING/PEELING IN SANITARY WARE [49] 27
FIGURE 20 – STAINS IN SANITARY WARE [47] 28
FIGURE 21 – APPLICATION OF LIQUID GLAZE 29
FIGURE 22 – REPAIRED DEFECT - PINHOLES 30
FIGURE 23 – REPAIRED DEFECT - CRACK 30
FIGURE 24 – INCIDENCE OF THE CONCENTRATED UV BEAM 31
FIGURE 25 – ELECTROMAGNETIC SPECTRUM (ADAPTED FROM [52]) 31
FIGURE 26 – LASER MARKING (ADAPTED FROM [54]) 32
FIGURE 27 – LASER ENGRAVING [55] 33
FIGURE 28 – LASER CUTTING [56] 33
FIGURE 29 – LASER LOGOTYPE MARKING [57] 34
FIGURE 30 – MODE OF LIGHT PROPAGATION IN AN OPTICAL FIBRE LASER [60] 35
FIGURE 31 – LASER CLADDING PROCESS [63] 35
FIGURE 32 – LASER DIFFRACTION ON THE SUBSTRATE PARTICLES [65] 37
FIGURE 33 – SUBSTRATE PROCESSING ACCORDING TO THE ENERGY DENSITY AND LASER POWER [65] 38
FIGURE 34 – SEM IMAGES SHOWING SURFACE CRACK GROWTH BEHAVIOUR UNDER LASER SCANNING ROTATIONS BETWEEN LAYERS (ADAPTED FROM [71]) 39
FIGURE 35 – TWO VARIABLES TEST (ADAPTED FROM [77]) 40
FIGURE 36 – THREE VARIABLES TEST (ADAPTED FROM [77]) 40
FIGURE 37 – COMPLETE FACTORIAL DESIGN [77] 41
FIGURE 38 – FRACTIONAL FACTORIAL DESIGN [77] 41

FIGURE 39 – HANGING BASIN LOAD TEST [82] 43
FIGURE 40 – CRAZING IN CERAMIC FAIENCE [84] 43
FIGURE 41 – ARCH VALADARES ENTRANCE [87] 47
FIGURE 42 – SPECIMEN 48
FIGURE 43 – SPECIMEN'S SECTIONAL VIEW 48
FIGURE 44 – SQUARED MATRIX TO PROVOKE DEFECTS 49
FIGURE 45 – PERCUSSION PEN PROVOKING DEFECTS 49
FIGURE 46 – SPECIMEN WITH PROVOKED DEFECTS 49
FIGURE 47 – COMPRESSED AIR GUN 50
FIGURE 48 – CERAMIC TILE SPRAYED WITH GREY MARKING INK 50
FIGURE 49 – WHITE MARKING POWDER 51
FIGURE 50 – SPECIMEN WITH WHITE MARKING INK FILLING THE DEFECTS 52
FIGURE 51 – TROTEC SP1500 LASER SYSTEM [88] 52
FIGURE 52 – JOBCONTROL SOFTWARE [88] 54
FIGURE 53 – COLOURIMETER 54
FIGURE 54 – CIELAB COLOUR SPACE DIAGRAM [90] 55
FIGURE 55 – COLOURIMETER FUNCTIONING 55
FIGURE 56 – OPTICAL MICROSCOPE 56
FIGURE 57 – SCANNING ELECTRONIC MICROSCOPE (SEM) [93] 57
FIGURE 58 – CERAMIC TILE CUTTER 57
FIGURE 59 – TYPES OF LENSES (ADAPTED FROM [88]) 59
FIGURE 60 – FOCAL LENGTH (ADAPTED FROM [88]) 59
FIGURE 61 – REPRESENTATIVE SCHEME OF THE NUMBER OF REALIZED EXPERIMENTS 60
FIGURE 62 – LASER *GABARIT* 61
FIGURE 63 – MANUAL FIRING 62
FIGURE 64 – RAPID FIRING 62
FIGURE 65 – TYPES OF LASER IRRADIATION 63
FIGURE 66 – SPECIMEN (3,4) DEFECTS DISPOSITION 64
FIGURE 67 – SPECIMEN (1,1) 66
FIGURE 68 – SPECIMEN (1,2) 67
FIGURE 69 – SPECIMEN (1,3) 67
FIGURE 70 – SPECIMEN (1,4) 68
FIGURE 71 – SPECIMEN (2,1) 70
FIGURE 72 – SPECIMEN (2,2) 71
FIGURE 73 – SPECIMEN (2,3) 71
FIGURE 74 – SPECIMEN (2,4) 72
FIGURE 75 – WHITE INK FORMED WITH ETHYL ALCOHOL 75
FIGURE 76 – WHITE INK FORMED WITH DILUTED PL960 76
FIGURE 77 – WHITE INK FORMED WITH CONCENTRATED PL960 76
FIGURE 78 – SPECIMEN (3,1) 77
FIGURE 79 – SPECIMEN (3,2) 77
FIGURE 80 – SPECIMEN (3,3) 78
FIGURE 81 – SPECIMEN (3,4) 78

FIGURE 82 – SPECIMEN (4,1) 82
FIGURE 83 – SPECIMEN (4,2) 83
FIGURE 84 – SPECIMEN (5,1) 84
FIGURE 85 – SPECIMEN (5,2) 85
FIGURE 86 – SPECIMEN (5,3) 85
FIGURE 87 – SPECIMEN (5,4) 86
FIGURE 88 – SPECIMEN (6,1) 90
FIGURE 89 – SPECIMEN (6,2) 90
FIGURE 90 – INFLUENCE OF THE LASER POWER IN THE DELTA BY TYPE OF DEFECT 96
FIGURE 91 – SAMPLE (3,1,1) MICROSCOPIC SECTIONAL VIEW 98
FIGURE 92 – SAMPLE (3,1,1) MICROSCOPIC TOP VIEW 98
FIGURE 93 – SAMPLE (3,2,1) MICROSCOPIC VIEW 98
FIGURE 94 – SAMPLE (3,2,2) MICROSCOPIC VIEW 98
FIGURE 95 – SAMPLE (3,2,3) MICROSCOPIC VIEW 99
FIGURE 96 – SAMPLE (3,2,5) MICROSCOPIC VIEW 99
FIGURE 97 – SAMPLE (6,2,6) MICROSCOPIC VIEW 99
FIGURE 98 – SAMPLE (6,2,9) MICROSCOPIC VIEW 99
FIGURE 99 – CERAMIC TILE CUTTER FINISHED SAMPLES 100
FIGURE 100 – SAMPLE (3,2,1) BACKSCATTERED ELECTRON IMAGE 102
FIGURE 101 – SAMPLE (3,2,1) TOPOGRAPHY IMAGE 102
FIGURE 102 – SAMPLE (3,2,1) EDS IMAGE FROM Z1 102
FIGURE 103 – SAMPLE (3,2,3) SEM-EDS WITH A 70X AMPLIFICATION 103
FIGURE 104 – SAMPLE (3,2,3) SEM-EDS WITH A 5000X AMPLIFICATION 103
FIGURE 105 – SAMPLE (6,2,6) SEM-EDS WITH A 70X AMPLIFICATION 103
FIGURE 106 – SAMPLE (6,2,6) SEM-EDS WITH A 250X AMPLIFICATION 103
FIGURE 107 – SAMPLE (6,2,6) SEM-EDS WITH 1000X AMPLIFICATION 104
FIGURE 108 – SAMPLE (6,2,6) SEM-EDS WITH A 375X AMPLIFICATION 104
FIGURE 109 – SAMPLE (3,2,7) SEM-EDS WITH A 50X AMPLIFICATION 104
FIGURE 110 – STANDARD SAMPLE SEM-EDS WITH A 75X AMPLIFICATION 104
FIGURE 111 – SAMPLE (3,2,7) WITH A 10,000X AMPLIFICATION 105
FIGURE 112 – STANDARD SAMPLE WITH A 10,000X AMPLIFICATION 105
FIGURE 113 – AUTOCLAVE 106
FIGURE 114 – SPECIMENS IN THE AUTOCLAVE 106
FIGURE 115 – STANDARD TILE AFTER AUTOCLAVE TEST 107
FIGURE 116 – SPECIMEN (4,1) AUTOCLAVE TEST RESULTS 107
FIGURE 117 – SPECIMEN (5,2) AUTOCLAVE TEST RESULTS 108
FIGURE 118 – ACIDS, BASES AND STAINING AGENTS (ABS) 108
FIGURE 119 – ABS TEST REACTION ON THE DEFECTS 109
FIGURE 120 – ABS TEST RESULTS 109

TABLES INDEX

TABLE 1 – DENSITY AND WATER ABSORPTION RATE OF RED AND WHITE CERAMICS 10
TABLE 2 – FINANCING, IN %, OF THE CERAMIC SANITARY WARE INDUSTRY FROM 2015 TO 2019 [18] 15
TABLE 3 – CAPITAL, IN M€, OF THE CERAMIC SANITARY WARE INDUSTRY IN 2018 AND 2019 [18] 15
TABLE 4 – TYPES OF LASER INTERACTION WITH THE SUBSTRATE 32
TABLE 5 – COMPARISON BETWEEN $CO2$, ND:YAG AND YB-FIBRE LASERS' PROPERTIES 36
TABLE 6 – TROTEC SP1500 RELEVANT ATTRIBUTES 53
TABLE 7 – EXPERIMENTS' ORDER ACCORDING TO THE GLAZE FORMULATION 63
TABLE 8 – SPECIMEN (3,4) DEFECTS POSITION SCHEME 65
TABLE 9 – GREY INK'S SPECIMENS MARKING DISPOSITION 70
TABLE 10 – SPECIMEN (2,1) PARAMETERS 72
TABLE 11 – SPECIMEN (2,2) PARAMETERS 73
TABLE 12 – SPECIMEN (2,3) PARAMETERS 74
TABLE 13 – SPECIMEN (2,4) PARAMETERS 74
TABLE 14 – SPECIMEN (3,1) RESULTS 79
TABLE 15 – SPECIMEN (3,2) RESULTS 79
TABLE 16 – SPECIMEN (3,3) RESULTS 80
TABLE 17 – SPECIMEN (3,4) RESULTS 81
TABLE 18 – SPECIMENS (4,1) AND (4,2) PARAMETERS 83
TABLE 19 – SPECIMEN (5,1) RESULTS 86
TABLE 20 – SPECIMEN (5,2) RESULTS 87
TABLE 21 – SPECIMEN (5,3) RESULTS 88
TABLE 22 – SPECIMEN (5,4) RESULTS 89
TABLE 23 – SPECIMEN (6,1) RESULTS 91
TABLE 24 – SPECIMEN (6,2) RESULTS 92
TABLE 25 – COLOURIMETER VALUES FOR (3,2) SPECIMEN'S PINHOLES 93
TABLE 26 – COLOURIMETER VALUES FOR (5,2) SPECIMEN'S CRACKS 94
TABLE 27 – HYPOTHESIS TEST IN A TWO-WAY ANOVA 95
TABLE 28 – MEAN AND VARIANCE FOR THE DELTA VALUE BY DEFECT 96
TABLE 29 – TWO-WAY ANOVA TEST FOR LASER POWER VS INCIDENCE TIME 97
TABLE 30 – TWO-WAY ANOVA TEST FOR LASER POWER VS BEAM SPEED 97
TABLE 31 – BEST RESULTS OBTAINED WITH EACH PARAMETER 113
TABLE 32 – DISSERTATION'S BALANCE CONSIDERING ITS OBJECTIVES AND RESULTS 114

INDEX

1 INTRODUCTION 3
1.1 Framework 3
1.2 Objectives 4
1.3 Methodology 4
1.4 Structure of the report 4
1.5 Welcoming company 5
2 BACKGROUND 9
2.1 Historical framework 9
2.1.1 Ceramic materials 9
2.1.2 Sanitary ware 12
2.1.3 Impact of the ceramic sanitary ware industry on the economy 13
2.1.3.1 European economy 14
2.1.3.2 Portuguese economy 14
2.2 Manufacturing process 15
2.2.1 Mould production 16
2.2.2 Workpiece production 17
2.2.3 Glazes 20
2.2.3.1 Opacity 21
2.2.3.2 Types of glazes 22
2.2.3.2.1 Low temperature glazes 22
2.2.3.2.2 High temperature glazes 23
2.2.4 Environmental impacts 23
2.3 Defect detection and classification 24
2.3.1 Detection methods 25
2.3.2 Types of defects 26
2.3.2.1 Pinholes 26
2.3.2.2 Cracks 26
2.3.2.3 Shivering/Peeling 27
2.3.2.4 Stains 28

2.4 Sanitary ware recovery processes 28
2.4.1 Hot recovery 28
2.4.2 Cold recovery 30
2.4.3 Laser technology 31
2.4.3.1 Logotype marking 33
2.4.3.2 Surface treatment 34
2.4.3.3 Laser interaction with ceramic materials 37
2.4.3.4 Repair methods using laser technology 39
2.5 Statistical methods for experimental analysis 40
2.5.1 Complete and fractional factorial design 40
2.5.2 ANOVA (Analysis of variance) 41
2.6 Quality control 42
2.6.1 Hanging basin load test 42
2.6.2 Autoclave test 43
2.6.3 Water absorption test 44
3 THESIS DEVELOPMENT 47
3.1 Welcoming company characterization 47
3.2 Materials and methods 48
3.2.1 Materials used 48
3.2.1.1 Specimens 48
3.2.1.2 Inks/Glazes 49
3.2.2 Equipment used 52
3.2.2.1 CO_2 laser system 52
3.2.2.2 Colourimeter 54
3.2.2.3 Microscopes 56
3.2.2.4 Ceramic tile cutter 57
3.2.3 Laser system parameters 58
3.3 Results 59
3.3.1 Experiments conducted with laser 60
3.3.1.1 Regular glaze and frit (1) 66
3.3.1.2 Grey marking ink (2) 69
3.3.1.3 White marking ink 75

3.3.1.3.1 Ethyl alcohol (3) 76
3.3.1.3.2 Diluted PL960 (4) 82
3.3.1.3.3 Concentrated PL960 (5) 84
3.3.1.3.4 Additional experiments (6) 90
3.3.2 Colourimeter analysis 93
3.3.3 Optical microscope analysis 98
3.3.4 Electronic microscope (SEM) analysis 100
3.3.5 Quality tests 105
3.3.5.1 Autoclave test 106
3.3.5.2 Resistance to acids, bases and staining agents (ABS) 108
4 CONCLUSIONS AND PROPOSALS OF FUTURE WORKS 113
4.1 Conclusions 113
4.2 Proposals of future works 115
5 REFERENCES AND OTHER SOURCES OF INFORMATION 119
6 APPENDIX 129
6.1 Appendix 1 – ARCH 2020 Organogram 129
6.2 Appendix 2 – Trotec SP1500 Laser Technical Datasheet 130
6.3 Appendix 3 – Optical Microscope Analysis complete footage 134
6.4 Appendix 4 – SEM-EDS Analysis complete footage 152
6.5 Appendix 5 – Colourimeter Analysis complete set of values 161
6.6 Appendix 6 – Experimental work resume table 164

INTRODUCTION

1.1 Framework

1.2 Objectives

1.3 Methodology

1.4 Structure of the report

1.5 Welcoming company

1 INTRODUCTION

This dissertation is inserted in the ceramic materials field, more specifically in the sanitary ware manufacturing industry, and aims to solve one of its problems: correction of defects which arise during the production of sanitary ware, in a more economical and effective way. This dissertation belongs to the Materials and Manufacturing Technologies branch of the Mechanical Engineering Master's Degree at ISEP – School of Engineering, Polytechnic of Porto. The motivation for its realization consisted mainly in the reduction of waste and energetic consumption in the production of ceramic sanitary ware during its manufacturing process.

1.1 Framework

After firing, sanitary ware products may present superficial defects such as pinholes or small cracks, which make their commercialization unfeasible, appearing in 15 to 20% of the manufactured products. Usually, recovery techniques are employed which involve either refiring the workpiece after glazing or applying a photo-curable acrylic resin under a concentrated ultraviolet (UV) light.

In the first scenario, focus of this study, the workpiece, after being recoated with the application of a glaze the same colour in the location of the defect, is submitted to a new firing in order to fuse the raw glaze which, in the meantime, was applied. Nevertheless, the cost of refiring is expensive and the risk that the workpiece breaks or another defect is evidenced is significant. Until the late 1980's, no refiring was carried out, and the ware produced from the first firing was divided into four categories:

- NOR – Ware which was not defective;
- ECO – Ware with few and not visible defects;
- Third – Ware with clearly visible defects;
- Broken – Ware unusable due to the amount and size of defects.

NOR, without defects, was transported directly to the warehouse. ECO, with few defects, was sold for 80% of the previous price. Third, with more severe defects, was only sold at 50% of the original cost. The broken ones, which were beyond repairing, were destined to landfills. The wares produced with defects only began to be recovered from the 90s, when the theme of sustainability was introduced in Portugal. Even then, until 2002, only about 80% of the products were recovered, and today this percentage has risen to 100%. In spite of this, the recovery method by refiring has several disadvantages which are intended to overcome. This dissertation aims to study the possibility of using other technique for the recovery of sanitary ware, namely the laser technology.

1.2 Objectives

The objectives of this dissertation consist in the development of a new technology in order to recover fired sanitary ware, a process characterized in two main aspects:

- To create a set of glazes (both white and coloured) which fuse at a temperature of 1200 ℃ and whose color difference does not exceed 0.8 in the colourimeter reading, so as not to be distinguishable from the pattern (workpiece) in the user's perspective;
- To create a technique using a laser system that can reach the necessary temperature to achieve a tone identical to the one of the glass and that allows the fusion of the glaze only in the place where it is required to cover the defect.

The ultimate objective is to automate this technique, so that it can be implemented in day-to-day factory operations.

1.3 Methodology

The adopted methodology consists of the following steps:

- Elaboration of the Background;
- Performance of tests in white 150x150 mm tiles with provoked defects through the hot recovery method;
- Definition of the necessary stages to cover the defect with glaze and the use of a CO_2 laser system intended for its fusion;
- Development of a set of glazes which fuse with the laser interaction;
- Performance of tests in white 150x150 mm tiles with provoked defects through the laser technology method;
- Conduction of numerical analyses of the defects' recovery with the colourimeter;
- Realization of a detailed qualitative analysis with an optical microscope;
- Realization of a detailed qualitative analysis with the SEM microscope;
- Conduction of quality control tests to guarantee the solution's effectiveness;
- Study of the automation of the most favourable recovery solution.

1.4 Structure of the report

This dissertation is divided into six main chapters:

- **Introduction**, where the theme is presented and a framework of how it will be developed is made, describing the objectives adopted to achieve them, as well as its structure. A brief approach is also made to the welcoming company;

- **Background**, in which the collection of information relevant to the study in question is done. This chapter provides a theoretical base for the discussing theme, addressing and describing the essential topics for its understanding. Throughout it, the State of the Art is also performed, consisting of a presentation and summary of the main existing articles on the subject;

- **Thesis development**, which, as its name indicates, is the focus of the development of the practical part of the project. It is here that the contents presented in the previous chapter are applied, through an in-depth and detailed description of the work carried out, ending with a discussion of the results obtained by comparison to similar ones already existing in the same field;

- **Conclusions and proposals of future works**, where, finally, the major contributions brought by this work are highlighted. It also describes the tasks to be carried out after the conclusion of the dissertation, in order to finish the project initiated throughout the work that led to this report;

- **References and other sources of information**, which contains every information source used to write this dissertation;

- **Appendix,** the last chapter, with important technical documentation that can be consulted in order to deepen some concepts present in the body of the work.

1.5 Welcoming company

The company responsible for hosting this dissertation is denominated “ARCH – Advanced Research Ceramic Heritage”.

With its headquarters in Valadares, Vila Nova de Gaia, ARCH has national customers who, in 2019, represented 68% of sales and foreign customers who accounted for the remaining 32%. Regarding the suppliers, the national ones comprised 90% of purchases and service supplies, compared to 10% regarding foreign providers. Its annual production is around 200,000 products, which were converted into an annual turnover of 6.5 M€ in 2020.

In 2019, the company already shipped to over thirty countries, with Spain and Italy being the ones with the greatest projection in Europe. Apart from the European continent, the Middle East and Africa are the globe’s most prominent regions.

ARCH has eight different departments which ensure the quality of its production, namely General Management, Finance, Sales, Projects, Technical, Production, Engineering & R&D and Quality. Thus, it has a total of 126 employees corresponding to 222,000 working hours. The regular schedule is from 8am to 5pm, except for the teams that work shifts. Of these 126, only 19 collaborators have a college degree, 2 of them being Mechanical Engineering graduates.

BACKGROUND

2.1 Historical framework

2.2 Manufacturing process

2.3 Defect detection and classification

2.4 Sanitary ware recovery processes

2.5 Statistical methods for experimental analysis

2.6 Quality control

2 BACKGROUND

2.1 Historical framework

The art of pottery is one of the oldest in the world, not only due to the high abundance of clay, but also to its ease of extraction and processing. For this reason, the human being adopted this method, from very early on, to improve his lifestyle by finding various uses for ceramic materials.

The first applications using this technique, in prehistoric times, were simple baskets made from clay, used mainly to store seeds. It was later that the plasticity of clays was discovered, when it was concluded that by adding water to it, it could be moulded, dried in the sun and then its rigidity increased when subjected to high temperatures. This is how ceramic materials emerged [1].

2.1.1 Ceramic materials

A ceramic or ceramic material can be defined as any non-metallic, inorganic material whose structure is totally or partially crystallized after undergoing heat treatment at high temperatures. These may consist of various raw materials, clay being the main one, and have a wide range of structural arrangements [1]. The most common ceramic materials include aluminium oxide (alumina, Al_2O_3) and silicone dioxide (silica, SiO_2), or alternatively, in technical ceramics, silicon carbide (SiC) and silicon nitride (Si_3N_4) [2].

Ceramic materials, in their essence, can be classified into two categories:

- **Traditional** – Encompasses the materials produced from clay-based raw material available in nature. Some examples are tiles, porcelain, paving or sanitary ware;
- **Modern** – Also referred to as advanced or technical, this group includes ceramics with improved technical and mechanical properties, since they are made from materials which do not exist in nature. These are produced synthetically using special chemical and thermal techniques with high purity in order to achieve the desired properties [3].

Within the traditional ceramics, there is also a distinction as to their composition: red clay (roof tiles, bricks - Figure 1) and white clay (faience, porcelain). This last group includes both household ware (plates, flowerpots - Figure 2) and sanitary ware (toilets, sinks). The main factor which distinguishes red ceramics from white ceramics is the respective raw material, specific for each type of ceramic.

Figure 1 – Red ceramics [4]

Figure 2 – White ceramics [5]

Red ceramics are typically manufactured at lower temperatures than white ceramics, a factor resulting in their higher porosity, lower density and lower strength [6]. On the other hand, white ceramics, highly resistant and compact, are composed of materials formed under high pressure in nature and which are subsequently processed at a cycle of temperatures in the factory with a total duration of 15 hours, being the maximum reached at 1200 ℃ over 40 minutes. Therefore, this type of ceramics are glazed products which provide high resistance due to their low porosity, reduced water absorption and their firing process at high temperatures. They also have high flexural and abrasion resistance, superficial hardness, chemical resistance against acid attacks and fire resistance [6].

In Table 1 are represented the estimated values for the density and water absorption rate of the red ceramics by comparison to the white ones. Although the density of the two is not significantly variable, the water absorption rate stands out as the differentiating factor. Red ceramics typically possess a rate between eight and fifteen percent. As for white ceramics, these are divided into faience, with a rate which can reach up to ten percent, and porcelain (namely sanitary ware), whose water absorption rate is so reduced that it tends towards zero, a characteristic that has become a great advantage for the manufacturing of sanitary ware through white ceramic.

Table 1 – Density and water absorption rate of red and white ceramics

Material	Density	Water absorption
Red ceramics	2.65	8 – 15%
Faience	2.62	0 – 10%
Sanitary ware	2.62	≈ 0%

In general, ceramic materials are relatively rigid, very hard and possess a high mechanical strength. However, they are extremely brittle (low ductility) and highly susceptible to fracture, which is why ceramics with greater resistance to fracture have been developed. They are also more resistant to high temperatures and aggressive environments than metals and polymers. Taking into account their optical

characteristics, ceramics can be transparent, translucent or opaque, and some oxide-based ceramics exhibit magnetic behaviour [2].

In Figure 3, it is possible to observe that technical or modern ceramics can exhibit a high density and also have a high stiffness. In the case of non-technical or traditional ceramics, where sanitary ware is found, these present a relatively low density, lower than most metallic materials, and a stiffness lower than that of technical ceramics.

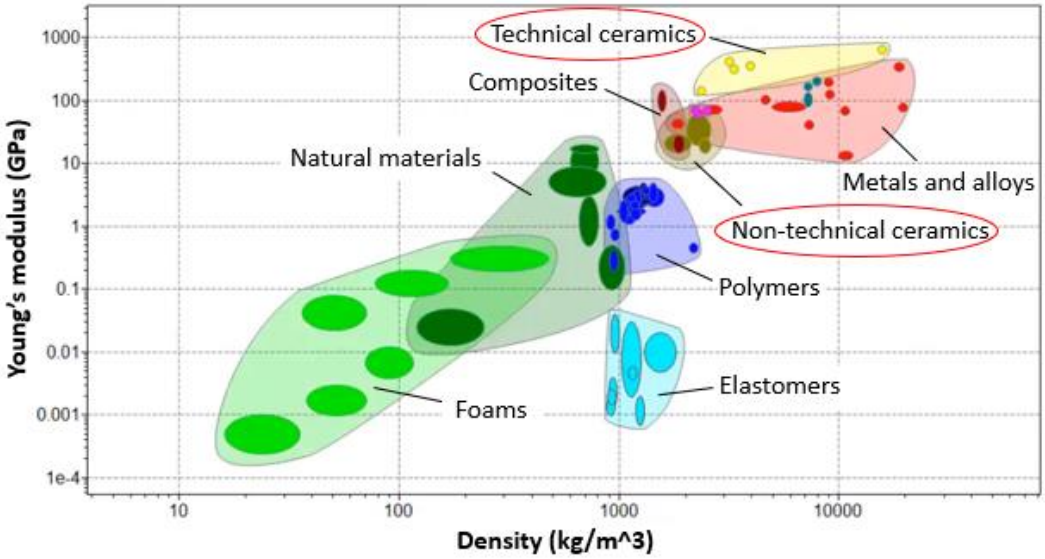

Figure 3 – Ashby's chart: Young's Modulus vs Density [7]

Figure 4 compares different families of materials regarding the Fracture Toughness property. Thus, it is possible to have a more concrete perception that, when handling this type of materials, sometimes a small mistake can cause defects such as cracks or even fractures which make it unfeasible to sell the workpiece. It is necessary to have certain special precautions in their handling, since these materials are fragile and may fracture during their manufacture, storage and transport [6].

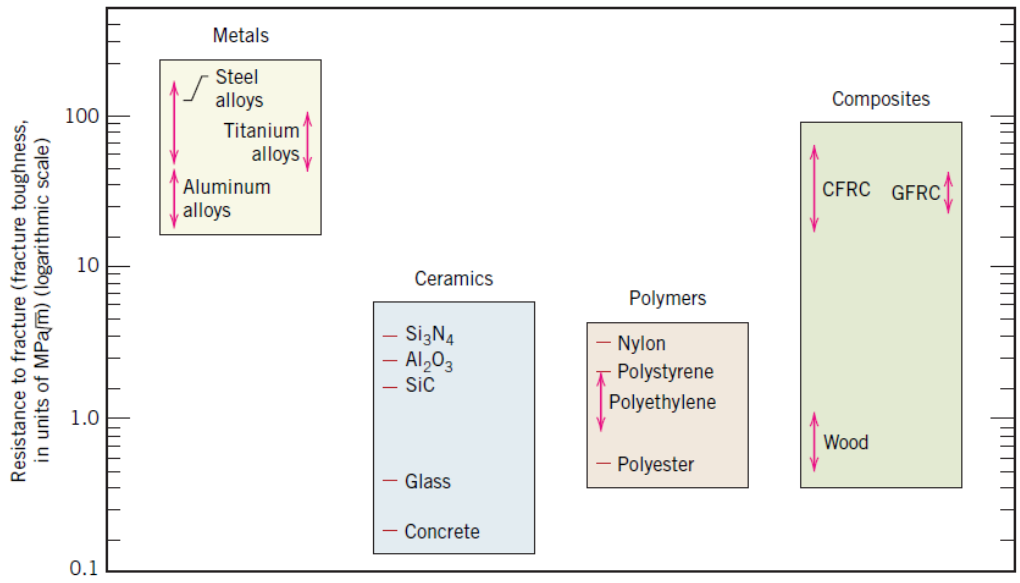

Figure 4 – Fracture Toughness in different families of materials [2]

The existence of several ceramic phases makes it possible to perform combinations of metallic and non-metallic atoms, generating applications for this type of materials in numerous sectors. The structure of the ceramic material is what will define its properties, so it is essential to evaluate this same structure considering the desired final application [1].

Ceramic materials are known for the manufacture of dense structural components, where the existence of porosity is generally associated with defects in the final product. In spite of this, advances in ceramic particle processing technologies associated with scientific and industrial requirements for porous materials with chemical, thermal and structural stability have led to a growing interest in porous ceramic materials [8].

2.1.2 Sanitary ware

Sanitary ceramics, also known as sanitary ware, are part of the traditional white ceramics segment, just like household ware. Composed essentially of aluminium silicates, they usually consist of a ceramic base, over which is a top layer of glaze. The main purpose of this glaze layer is to prevent dirt from adhering to the surface of the product, but also to improve its appearance [9].

The term “sanitary ware” has, as a meaning, the use of clay to produce toilets and bathroom accessories. Some examples include toilets, urinals, washbasins (Figure 5), bidets, bathtubs, shower trays, among others. Bathroom accessories are also manufactured by the same process, including coat hangers, roller racks, soap dishes, shelves, towel racks and sink racks [10]. Nowadays, the designation “sanitary ware” means porcelain obtained through the application of a glaze on its surface, using feldspar, quartz, kaolin and clay as raw materials, and finally submitted to a firing process [9].

Figure 5 – Sanitary ware production (adapted from [11])

Recently, the need has arisen to seek not only hygiene, a vital factor, but also a sense of luxury, comfort and quality in sanitary spaces and bathrooms where sanitary ware is installed. Quality at the aesthetic level can be felt in various ways, such as the sharpness of the image reflected in the surface of a sanitary ware item, its clarity, brightness, colour or visual depth. The latter is directly related to the thickness of the glaze layer applied to the ceramic. For this reason, an enormous variety of sanitary ware is attainable, combining and altering each of these factors, with a focus on manufacturing the best possible model [9]. Figure 6 shows an example of one of Valadares' models [10], the Nautilus washbasin.

Figure 6 – Nautilus washbasin (adapted from [10])

2.1.3 Impact of the ceramic sanitary ware industry on the economy

The global ceramic materials for sanitary purposes market is expected to witness a compound annual growth rate (CAGR) of 6.04% over the period of 2019 to 2026, based on data from 2017 and 2018. This increase in the market value can be attributed to both the rising income levels of the population, resulting in their greater purchasing power, and a greater abundance of available raw materials. This market has some advantages and disadvantages, which influence its growth or decline, respectively [12].

Advantages:

- Increasing levels of construction activities associated to residential and commercial infrastructures;
- Growing adoption of sanitary ceramics due to their chemical resistance, lightweight structure and pressure resistance;
- Growing concern for personal hygiene and cleanliness.

Disadvantages:

- Environmental concerns with disposal and recycling of sanitary ware;
- Price fluctuations of sanitary ware products;
- Lack of housing purchases due to global price fluctuations.

2.1.3.1 European economy

The European ceramics industry is a world leader in the production of high-quality ceramic products, including tiles, bricks or sanitary ware. Most manufacturers are small and medium-sized enterprises, which were hit hard by an economic crisis at international level in 2008, lasting until 2014 [13]. However, with the support of the European Commission, the ceramic industry has shown signs of recovery, becoming competitive once more.

This sector employs more than 338,000 people and has a production value of about 27.8 billion euros. In terms of exports and imports, the United States of America (USA) is the country to which the largest number of exports of ceramic articles from the European Union are made, followed by Switzerland, Russia and Japan. On the other hand, 70% of all imports of these articles come from China, followed by the USA and Thailand [14].

In 1954, the European Federation of Ceramic Sanitaryware Manufacturers (FECS) was created in Switzerland to contribute to the study and resolution of social, statistical and technical-scientific problems that the manufacturers of sanitary ceramics go through in Europe [15].

2.1.3.2 Portuguese economy

According to the National Institute of Statistics (INE), listed in the official document of the Portuguese Classification of Economic Activities (CAE revision 3) and adopted nationally from January 1st, 2008 but still valid today, the Manufacture of Ceramic Articles for Sanitary Uses corresponds to section C – Manufacturing Industries, subclass 23,420 [16].

In 2018, according to the most recent data from INE, this industry had thirteen active companies, with a total turnover of 258,027,043 €, gross added value of 91,922,085 € and gross fixed capital formation of 19,814,875 € [17].

As for the year of 2019, financially accounted for by the Bank of Portugal, fourteen companies were responsible for 39.67% of imports in purchases (70 M€) and 69.15% of exports in sales (181 M€) [18].

Table 2 and Table 3 provide relevant financial information about the ceramic sanitary ware industry between 2015 and 2019, so that its evolution over the last five years on record can be observed.

Table 2 shows that the financial autonomy of companies in the ceramic sanitary ware industry has increased over the years, which demonstrates their growth. On the opposite side, the funding obtained, as well as its cost, has decreased.

Table 2 – Financing, in %, of the ceramic sanitary ware industry from 2015 to 2019 [18]

Year	Financial autonomy	Funding obtained (% assets)	Cost of the obtained funds	Asset profitability
2015	41.3	35.5	3.4	4.3
2016	52.9	25.3	2.2	12.7
2017	59.8	19.9	2.2	19.3
2018	61.5	20.3	1.8	11.3
2019	61.6	19.8	1.9	10.6

With regard to capital, in M€, in sanitary ware industry companies, by the end of 2019, equity, assets and liabilities increased compared to the previous year, as did sales and services rendered, which once again highlights their growth. Nevertheless, the EBITDA and the net income decreased slightly.

Table 3 – Capital, in M€, of the ceramic sanitary ware industry in 2018 and 2019 [18]

Year	Assets	Equity	Liabilities	Sales and services rendered	EBITDA	Net income
2018	376.2	231.4	144.8	258.9	42.5	26.0
2019	391.8	241.5	150.3	261.1	41.6	22.8

2.2 Manufacturing process

The raw materials used in the production of traditional white ceramics consist mainly of clay, feldspar and quartz. Hydro-aluminosilicate materials such as clay and kaolin contribute to increasing their plasticity throughout the manufacturing process as well as their subsequent mechanical strength through mullite formation during sintering, where quartz performs the role of keeping the structure of the workpiece intact and preventing high deformation. This is also where the feldspar is melted, and the amount of liquid phase depends on both this and the type of clay. Thus, the liquid phase mixes with the alumina silicate powder through a viscous flow, resulting in their bonding and consequent formation of a dense mass due to interdiffusion of the phases. The remaining liquid phase subsequently solidifies without crystallization occurring, which generates the glassy appearance of the final product [19].

2.2.1 Mould production

The ceramic sanitary ware industry, similarly to casting, uses moulds as part of its manufacturing process. During the production of the workpieces, their initial shape undergoes significant deformation due to accumulated stresses in the plastic domain and volumetric shrinkage, as observable in Figure 7. Hence, caution must be taken in the design and creation of moulds, since after its production, if its shape is not compatible with the desired one considering the specified tolerances, it can no longer be modified, and a new mould must be produced with the consequential delays and increased costs. It is very common to use a trial-error technique with four to six iterations, which may require several months [20].

In the ceramic sanitary ware industry, plaster moulds (low pressure) are used. There are also acrylic resin moulds (high pressure); however, these are not very flexible to the change of moulds and are more suitable for very high productions. This makes them unfeasible for companies which do not possess a large-scale production, as is the case of ARCH, which is constantly changing between moulds.

During the production process, the mechanical behaviour of the material is not linear, and the deformations recorded may reach 20% of the workpiece original dimensions. Considering that tolerances are only accepted if they do not vary more than 0.5% of their dimensions, the predictability of moulds for sanitary ware represents an extremely challenging engineering problem [20]. Added to these factors is the fact that sanitary ware, especially toilets, have very complex geometries, requiring several sub-moulds for a single model. It was exactly for this reason that techniques of mould predictability through numerical methods began to be developed [21].

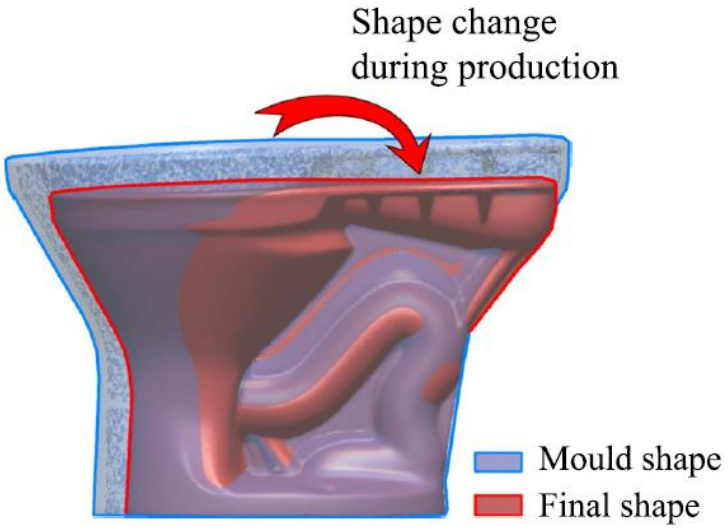

Figure 7 – Mould shape vs final workpiece shape (adapted from [21])

For the production of the mould itself, it is necessary to have one or several mothers [22]. These represent all the surrounding structure of the mould, and it is through the mothers that the mould will be produced, in a similar way to the production of sanitary ware. There are products (for example a toilet) that require the joining of several

separate parts of the mould (Figure 8), the sub-moulds, which will later be joined together through clamps. Each of these required a mother for its manufacture, and in this figure, it is possible to notice three distinct sub-moulds: upper, left and right.

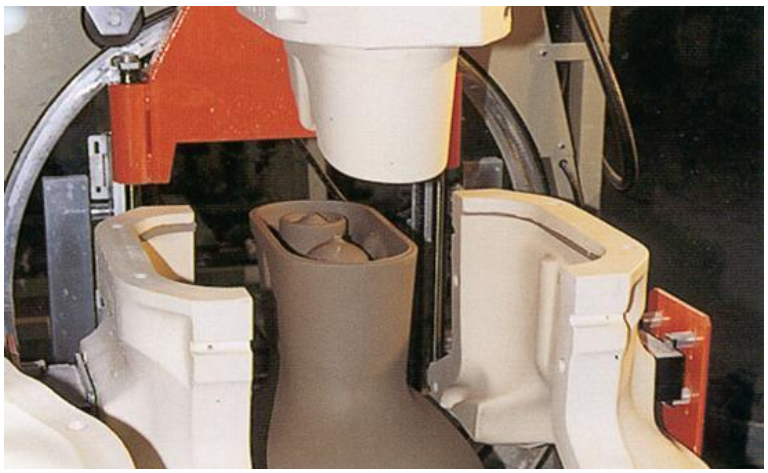

Figure 8 – Demoulding the workpiece from three portions of the mould [23]

2.2.2 Workpiece production

Figure 9 displays a flow chart which contemplates the various stages for the production of sanitary ware, covering each of its phases.

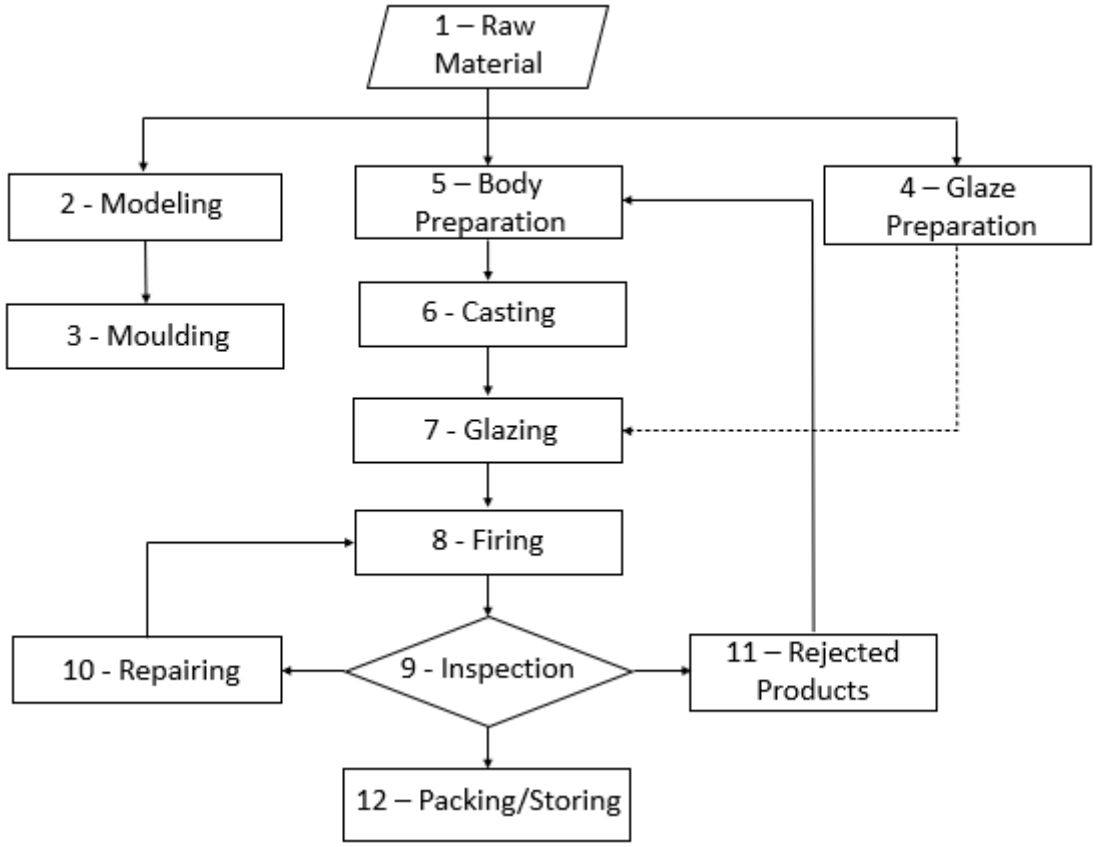

Figure 9 – Process flow chart of ceramic sanitary ware industry (adapted from [24])

Initially, the raw materials (**1**) required for the manufacture of ceramic sanitary ware, such as clay, feldspar and quartz, are gathered. Subsequently, three operations are performed simultaneously, but at different stations. The first is the manufacturing of the mould mother (**2**), where the mould characteristics are already predicted, followed by the manufacturing of the production mould (**3**). For this stage it is necessary to prepare the barbotine, responsible for filling the mould, ending with the drying of the production mould in plaster. In another sector, the glaze (**4**) is prepared for application on the workpieces before firing.

In the main branch, a mixture of the different raw materials is made in what is known as the body preparation (**5**). Then, the traditional casting process begins (**6**), namely the introduction of the paste inside the mould, where it will solidify, and finally the formed components are removed to the outside. These will be subjected to a finishing operation and are then denominated wet pieces or green pieces. At this point, the workpiece already has its final configuration.

After drying, the glaze is applied to both the internal cavities and the external surfaces of the workpiece (**7**), a phase designated glazing, as shown in Figure 10. It is after this process that the company's logotype is marked. Finally, comes the last main step of the ceramic sanitary ware manufacturing process, the firing (**8**). When the workpieces leave the kiln, they are sent through the final quality control, where an inspection (**9**) is conducted with several tests in order to evaluate their conformity. Should there be any problems with the products, these have to be repaired (**10**) and undergo a refiring process. In the event which no repair is possible (**11**), the workpieces are broken and called baked sherd, returning to the initial stage to be recycled. At the end of the process, when the products are ready to be sold, they are stored and then transported (**12**) to the official stores.

Note: The recycling procedure (**11**) is only adopted at ARCH, since at the remaining companies in the same industry, most of the rejected ware is sent to landfills.

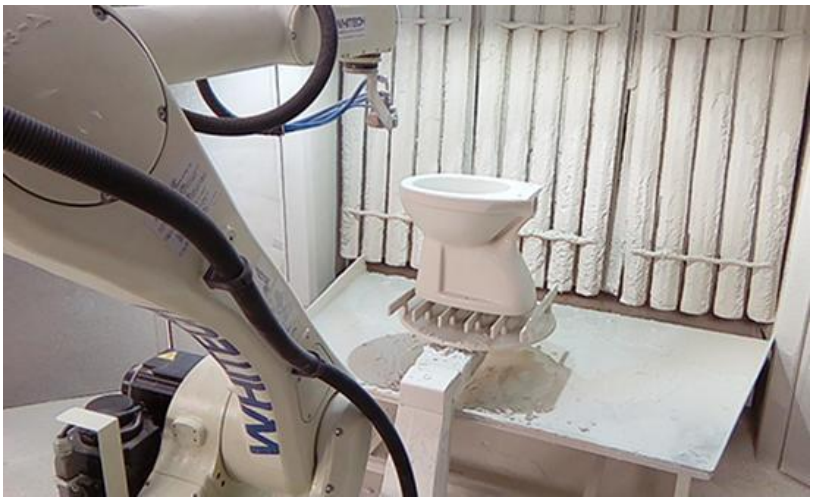

Figure 10 – Application of the glaze to the workpiece using a robotic arm [23]

The use of robotic arms to apply the glaze on the workpieces has already been studied, and *Qian et al.* [25] developed an intelligent robotic system for this use. They argue that although a robotic arm offers less flexibility and adaptability, its working speed and positioning accuracy stand out as great advantages over a manual application.

The application of the logotype, if done manually, is carried out by a technique called *decalcomania*. Initially, the logotype is printed on a paper sheet and afterwards, a yellow jelly is placed on its top which, when immersed in water, sticks the logotype to it. Later, a glue is applied to the appropriate location of the workpiece, and the decal is placed on top of the glue, followed by passing it with a rubber which gives it adherence and removes the air bubbles (Figure 11). Throughout the firing process, the jelly burns, leaving the logotype marked on the workpiece, as can be seen in Figure 12.

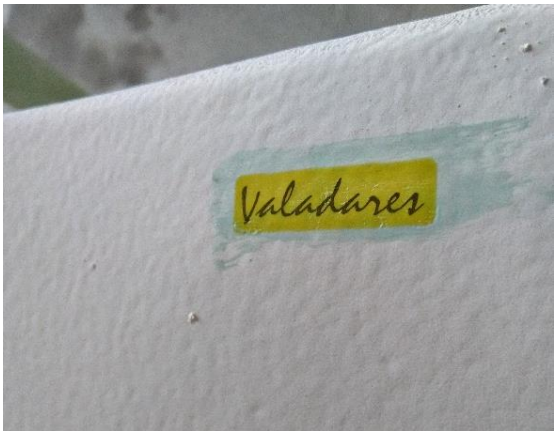

Figure 11 – Logotype application by *decalcomania*

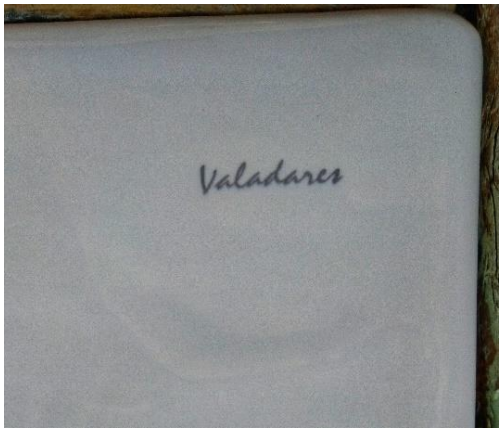

Figure 12 – Final logotype

Every step in the ceramic sanitary ware manufacturing process mentioned by the scheme in Figure 9 can be condensed into three main stages:

- Forming
- Drying
- Firing

During the **forming** phase, the ceramic body, composed of the different raw materials employed to form the sanitary ware, is poured into the mould, but only after its characteristics are conform, particularly the specific weight, viscosity, thixotropy, pH and temperature [26]. The porosity of the mould allows the water to filter, leading to the deposition of a layer of barbotine on its surface. At the moment this layer reaches the desired thickness (about twelve millimetres), the exceeding barbotine is removed in the pouring process. Pressurized air is injected, turning the barbotine sufficiently rigid so as to provide the minimum mechanical strength necessary to be able to extract the formed product from the mould (demoulding) without it collapsing under its own weight. This product is called a green part. After demoulding, the workpieces are finished, namely by removing burrs, cutting/drilling and retouching or fine surface finishing [27].

In the first **drying** phase, the workpieces are exposed to ambient humidity and temperature, which leads to water migration through moisture gradients. The decrease in water content, from 1.5% to 0.5% [26], translates into a swift improvement in mechanical properties. In spite of this, if the drying is too fast, internal stresses arise that may potentially result in the development and propagation of cracks [20]. After this first phase, carried out inside the pottery, the workpiece is subjected to drying with heat from the hot air lost through the kiln at temperatures up to 90 ℃ in its own dryer, the so-called second drying phase.

After the workpieces are completely dry and the glaze applied, it comes to the final phase, the **firing**, where they are transported to the kiln and subjected to a predefined temperature cycle, which reaches a maximum temperature of 1200 ℃, as shown in Figure 13. Here, geometric and dimensional variations occur, due to volumetric shrinkage. When the sintering temperature is reached, the molten phase fills the voids, which causes a complete reorganization of the microscopic ceramic structure [21]. Vitrification of the sanitary products also occurs at this stage.

Figure 13 – Sanitary ware firing [28]

2.2.3 Glazes

Glazes add value to ceramics, improve their appearance, especially in colour and brightness, enhancing the permeability of the products, a crucial attribute, since it allows them to contain liquids (sanitary ware) and solids (household ware). They can also improve other properties of the ceramic body, such as acquiring high abrasion resistance, surface hardness, low porosity and good chemical resistance [29].

A ceramic glaze consists of a thin vitreous layer applied through spray, which provides the workpieces a thickness of 0.8 to 1.6 mm [26]. This consists of compounds formed by powdered raw material mixed with water, which is fused to the surface of a ceramic body through firing. Accordingly, the two will interact, resulting in the interdiffusion of elements between the two. As it is an open system, its chemical composition varies throughout the firing, mainly due to the interaction with the ceramic and volatile behaviour of some of its components [30].

Several studies have been conducted to evaluate the morphological and structural characteristics of glazes as a function of their properties. *Topates et al.* [31] studied the chemical durability of glazes, specifically their corrosion resistance, containing zirconium and *Li et al.* [29] also studied the production of better opaque glazes for tiles with safirine instead of zirconium silicate as an opacifier, i.e., to give them colour. *Cai et al.* [32] investigated the feasibility of developing fast-firing opaque glazes without using zirconium. *Pekkan et al.* [33] developed *temmoku* glazes (created from ferruginous or feldspathic clay with iron oxides) and their respective application in different tiles under the industrial conditions of rapid firing at 1180 °C. *Tezza et al.* [34] analysed the effect of the firing temperature on the photocatalytic activity of anatase ceramic glazes, this is, with titanium dioxide.

From Figure 14 one can observe the glaze being prepared in the mixing tank at ARCH, in Valadares.

Figure 14 – Glaze in the mixing tank

2.2.3.1 Opacity

The appearance and colour of the glaze can be modified through the formation of crystalline compounds resulting from the interaction, dissolution and diffusion of elements between the ceramic and the glaze. Similarly with glass, the colours of the glazes are obtained through the addition of transition metals, subjected to heat in oxidizing or reducing conditions. The colour given to glazes is determined by their nature (iron, copper, manganese, cobalt) and caused by the absorption of light at specific wavelengths of the metal ions [30].

The transparency of the glaze can be reduced by adding to it particles capable of scattering light. Generally large bubbles and undissolved particles, such as quartz, produce a just partially opaque glaze. On the other hand, small particles and newly formed crystalline compounds at the interface between the glaze and the ceramic, such

as calcium and magnesium silicates or aluminosilicates (feldspars), scatter light more efficiently, thus increasing the opacity of the glaze [30].

In Figure 15 it is possible to visualize an example of a sanitary article, namely a cream-coloured washbasin, whose opacity is notoriously high.

Figure 15 – Opaque cream-coloured washbasin [35]

2.2.3.2 Types of glazes

There are very different types of glazes depending on the application in question. For this reason, it is necessary to carry out a detailed investigation when studying the possibility of developing a glaze with its own characteristics. In the research carried out by *Topates et al.* [31], for example, the corrosion resistance of glazes with zirconium in their constitution was studied, and for this it was necessary to perform a careful analysis of four different glazes through image analysis methods taking into account their constituent elements.

Glazes are classified into low temperature glazes, such as those used in sanitary ware, and high temperature glazes.

2.2.3.2.1 Low temperature glazes

Low temperature glazes split into alkaline and tin glazes. Some of the characteristics of these glazes are presented in the following bullet points.

- **Alkaline glazes**

Alkaline glazes are the most commonly used and can be obtained using alkali oxides (Na_2O, K_2O) such as feldspars, adding small amounts of CaO as a stabiliser and fused at low temperatures (900 – 1050 °C). These alkali oxides come from natural alkaline salts, such as hydroxides, carbonates and sulphates.

At the time of production, since several alkali compounds are water soluble, such as sodium carbonate, these migrate into the ceramic or crystallise on the glaze surface during firing. This produces a residue in the glaze, which leaves undissolved components in it. In order to obtain a homogeneous glaze, the alkali compounds must be fused with silica, i.e., fritted, before preparing the glaze. The frit contains a glassy compound that when heated above its softening temperature, produces a viscous liquid which reacts with the ceramic, fusing it and the glaze, and therefore reducing the firing time [30]. The

frit consists of alkaline or alkaline-earth metal oxides, silica, boron oxides and transition metal oxides [36].

- **Tin glazes**

According to *Matin et al.* [37], tin glazes began to be developed in the 8th century on opaque glazed ceramics, both white and yellow, in central and western Asia. To prove this fact, in the paper samples were studied using the SEM-EDS technique, energy dispersive X-ray spectroscopy.

Tin glazes are opaque and fuse at low temperature. Their opacity is increased if small crystals ($\sim 1\ \mu m$) with high refractive index and clean crystalline surfaces, preferably crystallised during fusion, are present in the glaze. Formerly, tin and antimony oxides were used for their production, but since the 19th century these have been replaced by titanium oxide [30].

This type of glaze is an opacifier, used with zirconium silicate, standing out as a viable option due to its reduced cost.

2.2.3.2.2 High temperature glazes

A high temperature glaze, as its name indicates, has a maturation temperature close to 1400 ℃, in contrast to the glazes most commonly chosen for the ceramic sanitary ware industry, which fuse at 1200 ℃. The usual fluxing agents in their constitution are alkaline-earth oxides (CaO and BaO). Glazes with low amounts of CaO at high temperatures can be developed by adding small amounts of Na_2O e K_2O to sand. In order to produce a high temperature glaze, these compounds are added in the form of feldspars, rather than alkaline salt or vegetable ash.

The most important factor in developing such a glaze is for the ceramic body where it will be applied to be able to withstand the high temperature. There are several clays which cannot be fired above 1120 – 1150 ℃, as the vitrification is so extensive that the body deforms rapidly. Therefore, the base material must be carefully studied before applying the glaze [30].

2.2.4 Environmental impacts

The ceramic sanitary ware production industry, due to the scale of its work, is responsible for having a significant impact on the environment. This impact can be assessed in three key areas:

- Air emissions;
- Residual waters;
- Solid waste.

Each of these contributes negatively to an increment in Earth's pollution, which is why techniques have been developed to mitigate this growth, such as substitution to less polluting gases or more "environmentally friendly" raw materials.

Emissions of gases and particles to the atmosphere generally occur during the raw material processing phase and during the firing of the workpieces. In the latter, emissions are generated through the fuels used to generate energy and heat which allow the operation of the kiln for firing. The major pollutants generated in this industry are Sulphur Dioxide (SO_2), Nitrogen Oxides (NO_x), greenhouse gases (essentially CO_2) and Chlorides (HCl) [38].

Residual waters are essentially the end product formed by the water used for cleaning in the mould preparation and moulding stages, but also by other processes such as the application of the glaze (Figure 16) or the workpieces finishing. The residual waters are characterised by being turbid and of varying colours due to the suspension of glaze particles and minerals in its composition [38]. One of the solutions to this problem is to channel them to water treatment plants.

Figure 16 – Residual waters formed during the application of the glaze (adapted from [28])

The solid waste consists of remnants of raw materials, for example clay, from both the production of the mould and the production of the workpieces, fragments resulting from griding or broken refractory material. All this solid waste can be used and reintegrated into ARCH's sanitary ware production process.

2.3 Defect detection and classification

Throughout all the stages that make up the manufacturing process of ceramic sanitary ware and tiles, defects can appear which reduce the value of the workpiece or make it unfit for sale. These defects occur essentially during firing, where the workpieces are subjected to a very high temperature variation, a factor which will alter their physical, chemical and structural properties, but also during the application of the glaze on its surface. For this reason, these two stages are very prone to the development of defects.

The glaze is used as a surface coating for pieces due to its aesthetic appearance and high chemical resistance, which makes it able to withstand contacts with water, acids or other aggressive environments. Despite this, the glaze reacts physically and chemically with the workpiece during firing, which can lead to defects. Even during the manufacturing process, residual stresses are sometimes generated in the workpiece, caused by heterogeneities in its microstructure or by the presence of microscopic defects. These defects can be primary, such as poor glaze placement (lack of adhesion) or secondary if they result from increased humidity or inadequate storage condition [39].

2.3.1 Detection methods

Since the last century there has been an evolution in the methods developed for the detection of surface defects in flat ceramic tiles. The first step is to adopt a visual control technique before storing the products, in order to identify the more obvious defects, that is, visible to the naked eye. *Kumru* [40] presents a decision making technique to facilitate the defect detection process called fuzzy logic. In spite of this, an automatic defect classification and detection system has proven to be faster, more effective and objective than the traditional way of naked eye detection by a human operator [41]. The operator is able to search for defects by tapping with a small hammer on the product, to analyse the emitted sound. Workpieces with good quality emit a characteristic sound, which does not happen with products that possess defects, due to discrepancies in the sound waves. In spite of this, it is a method that brings disadvantages, such as the reliance on the operator's attention level or the surrounding noise [42].

Some of the detection methods involve numerical analysis algorithms with automatic image processing systems, such as *Hanzaei* and *Afshar* [41] who propose the use of the Rotation Invariant Measure of Local Variance (RIMLV). Statistical methods like the histogram curve and Local Binary Pattern (LBP) or structural methods such as *Canny* and *Gauss* [41] frequency domain filters are also employed. *Kesharaju et al.* [43] argued using ultrasound, *Monteiro e Bastos-Filho* [42] analyzed defects through Deep Learning and *Bao et al.* [44] relied on Machine Vision technologies. Furthermore, *Teng et al.* [45] studied a detection method through the improved VGG network, which resorts to the mixed use of image analysis with mathematical functions, notably the Modified Rectified Linear Unit Activation Function (MReLU), and which results in an accuracy 6.46% higher than the function on which the study was based.

These techniques have the great advantage of allowing the identification of defects of very small dimensions, not identifiable by any other type of method and which would put at risk the lifespan of the product, possibly causing a severe failure in its operation after a few years of use. On the other hand, some disadvantages are the complexity of the algorithms that have to be developed, which require extremely skilled manpower to work on, as well as the cost and maintenance of the equipment and softwares needed to identify the defects.

2.3.2 Types of defects

There are several types of defects detected in sanitary ware, including pinholes, cracks, shivering/peeling and stains, each of which will be analysed in detail throughout this subchapter.

Delamination may also occur in tiles due to the presence of air trapped during pressing and the elastic return of the tile [46].

2.3.2.1 Pinholes

The pinholes (Figure 17) are originated in the migration of air from the workpiece, either because it was trapped by the glaze or released too late and the glaze did not close in time. They can also be caused by excessive degassing of soluble salts such as sulphates (SO_4^{2-}) or carbonates (CO_3^{2-}).

The solution to this problem involves adjusting the firing cycle, assessed accordingly to the main cause. One can also adjust the glaze fusibility through its raw materials, or alternatively by reducing the materials in the main body which contain salts or carbon, such as clay [47].

Bazargan e *Dehghanzadeh* [48] carried out studies to evaluate which factors contributed most to the appearance and development of pinholes in sanitary ware. The conclusion they got into was that these defects are caused by the viscosity of the glaze (thixotropy) and its cooling speed, the surface tension of the raw material and the speed at which the workpiece reaches the maximum temperature, as well as its own curvature.

Figure 17 – Pinholes in sanitary ware

2.3.2.2 Cracks

Cracks are generally caused by a lack of concordance between the coefficient of thermal expansion of the base ceramic material and the one of the glaze, known as crazing. In this case, the solution is to approximate the coefficients of both. This can be achieved either by decreasing the coefficient of thermal expansion of the glaze (by incrementing the amount of quartz or reducing the amount of feldspar in its constitution) or by increasing the coefficient of the material, the most favourable option. This can be

accomplished through the addition of quartz (1% increase) to the detriment of another material (usually kaolin) in its constituents or by the use of a *chamotte*, an inert raw material employed in order to enhance the properties of the workpiece, with greater thermal expansion.

There are situations where even after applying these practices, cracks still appear, for example in the autoclave test. This happens due to a high expansion caused by humidity. When this phenomenon occurs, it is common for cracks to appear after a few months or years of product usage, which might be caused by an excess of feldspar in the material, too low firing temperature or the use of a poor quality *chamotte* [47].

In Figure 18 it is possible to observe a crack caused by an effort when demoulding the workpiece in the pottery, another possible cause for its appearance.

Figure 18 – Cracks in sanitary ware

2.3.2.3 Shivering/Peeling

Shivering, or peeling, is generated exactly by the opposite phenomenon to the one of cracks. The disintegration of certain regions (Figure 19) of the sanitary ware glaze occurs in situations where the thermal expansion coefficient of the glaze is too low in comparison to the one of the workpiece to which it is applied.

The solution to this problem consists in increasing the thermal expansion of the glaze by reducing quartz and increasing feldspar in its manufacturing [47].

Figure 19 – Shivering/peeling in sanitary ware [49]

2.3.2.4 Stains

Various types of stains tend to appear on sanitary ware as to their colouring, such as blue, black (as seen in Figure 20), green or brown.

Blue stains are caused due to the blue pigment used as optical whitener in the glaze. The black ones, however, come from raw glazing materials with impurities, for instance, due to iron contamination. The green stains are formed when the *chamotte* has poor quality, i.e., is contaminated with pyrites or copper. In this case, it is also necessary to inspect the manufacturing process. Finally, brown stains are related to the presence of manganese, usually in the water, although they can also be caused by contamination of the raw material of the workpiece.

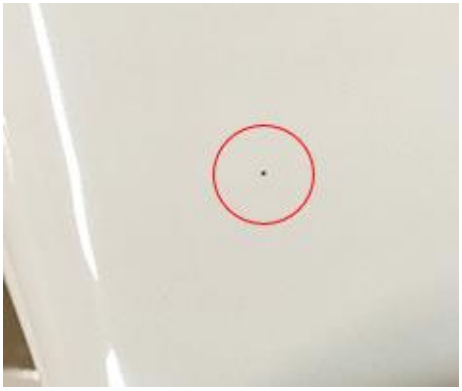

Figure 20 – Stains in sanitary ware [47]

2.4 Sanitary ware recovery processes

The costs which the ceramic sanitary ware industry incurs in all its aspects, as well as the waste generated during its production, have been an increasingly target of awareness around the world and consequently a theme that has motivated the search for solutions to reduce these problems [50].

Currently, the processes used in the industry to repair ceramic sanitary ware include both hot and cold recovery, a criteria which depends mainly on the location of the defects in the product. In this subchapter, a possible sanitary ware recovery process is described, laser technology, along with its applications in the ceramic materials sector nowadays.

2.4.1 Hot recovery

Hot repair is used for defects present in functional and visible areas of the products. In this method, a glaze is initially applied to the location of the defect found in the respective workpiece. After this measure, the entire part is refired, by transporting it back to the kiln where it is submitted to a new thermal treatment, so that the glaze fuses and the final product no longer possesses any problem. For this to happen, the following steps are adopted [51]:

- **Surface preparation**

Regardless of the defect nature, as long as it can be treated, the first step is to perform a proper treatment using abrasion. This is done using a tungsten bur (emery) or a percussion pen to pierce the defect, should it be a pinhole. However, it can be the case that the defect is of considerable size on flat surfaces. In this situation, a drill with a conically shaped enamel stone is also used to smooth out the defect. This ensures smoother curvatures in the defect and a better final finish.

- **Application of liquid glaze**

This stage essentially consists of applying, with the assistance of a brush, the very liquid glaze (Figure 21), so that it spreads homogeneously over the area to be treated. After this is done, it is necessary to dry it with an air compressor, so that the whole defect area is equally covered with glaze before the repair paste is impregnated. After the application of the paste, a layer of glaze can be reapplied to the surface of the repaired defect to improve the final finish and prevent any difference in the product from being visible to the naked eye.

Figure 21 – Application of liquid glaze

In Figure 22 and Figure 23 it is possible to visualize two types of defects where the glaze has already been applied, both in pinholes and a crack. The liquid glaze fills all the free space left by the defect, so that it can fuse with the surface of the workpiece during the new firing process.

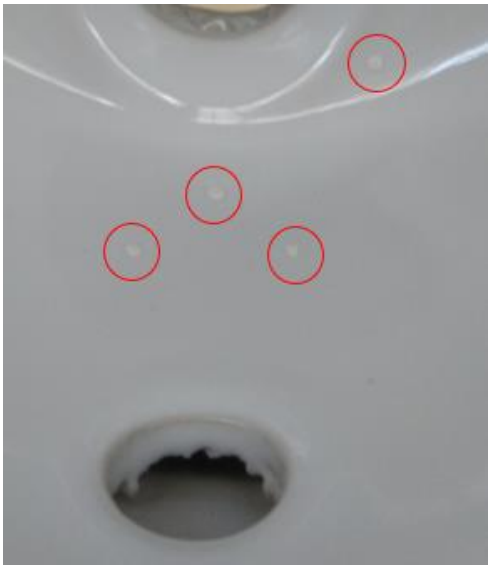

Figure 22 – Repaired defect - Pinholes

Figure 23 – Repaired defect - Crack

- **Refiring**

After these steps, the product is once again placed on a trolley which takes it to the oven to be refired. This process has the same characteristics as the initial firing.

This procedure is effective, managing to repair almost half of the defective workpieces; however, it has two major disadvantages. On the one hand, it makes the process too expensive, since refiring the workpieces involves additional costs, in addition to the time required for them to undergo through a new total kiln cycle, equivalent to twice the initial firing time. On the other hand, there is a high probability of the workpieces developing new defects, with exactly the same origin as the previous ones, which can be even more serious, sometimes culminating in a rupture of the product. This has the aggravating effect of increasing the environmental impact, material and human resources and the fact that the space occupied by the workpieces for repair decreases the total number of products manufactured [51].

2.4.2 Cold recovery

The cold recovery process, in contrast, consists in the application of a photo-curable acrylic resin with concentrated UV beam (Figure 24), which has a spectrum of about 350 nm.

This method holds a major advantage over hot recovery: it is not necessary to subject the products to a new 15-hour cycle at temperatures reaching a maximum of 1200 °C, so it is undoubtedly a less evasive approach. The problem with this technique is the fact that the resin can only be applied either in non-visible or non-functional areas, i.e., areas which do not interfere with the normal functioning of the product. Considering the situation where the resin is applied to a functional area, such as the bottom of a toilet

submerged in water, it will be subjected to a constant erosion action both by the water with which it is in contact and by the debris that regularly flow through it. In this scenario, there is a high probability of the resin being removed by abrasion, which would cause the failure of the equipment [51].

Note: Figure 24 shows a representative picture of the concentrated UV beam focusing on a visible area of the product, so there can be a clear view of the process. In a real cold recovery, the incidence cannot be in that location.

Figure 24 – Incidence of the concentrated UV beam

2.4.3 Laser technology

James Clerk Maxwell, a British physicist and mathematician, devoted his life to the study of electromagnetism and demonstrated that light is a component of the electromagnetic spectrum, observable in Figure 25.

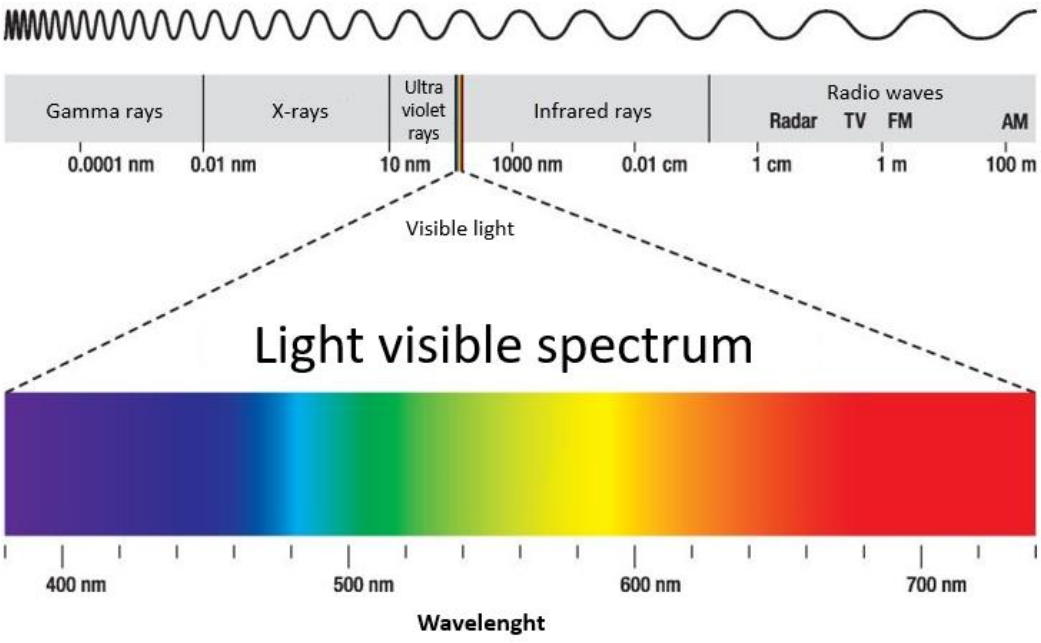

Figure 25 – Electromagnetic spectrum (adapted from [52])

Every wave has the same speed in vacuum, the speed of light (c = 3 x 10^8 m/s) and can be distinguished by their wavelength. There are regions defined by frequency intervals with their own characteristics, the most relevant being ultraviolet and infrared radiation, respectively below and above the visible spectrum of light. This, as the name indicates, represents the set of wavelengths that the human being is able to visualize with the naked eye, being located approximately between 400 and 700 nm [52].

The laser was born from this concept. Acronym for Light Amplification by Stimulated Emission of Radiation, it appeared in 1960 and consists of a device which creates and amplifies a beam of monochromatic light (at a specific wavelength corresponding to a particular colour) of high intensity [53].

The laser interaction with any type of substrate can be divided into three separate operations:

- Marking;
- Engraving;
- Cutting.

These are distinguished essentially due to the power required for each one, as well as the intended purpose, and are represented in detail in Table 4.

Table 4 – Types of laser interaction with the substrate

Type of interaction	Description	Graphic representation
Marking	An ink is placed on the substrate that will fuse through the laser interaction according to a certain pattern. This way, it gets permanently marked on the substrate, whose thickness does not change. In the end, the excess ink is removed, revealing only the desired pattern (Figure 26). Marking can also be done directly on the substrate.	 Figure 26 – Laser marking (adapted from [54])

Engraving	The laser interaction with the substrate removes a layer of the substrate with a small, predefined thickness. The pattern is engraved into the substrate itself (Figure 27), so a slightly high power is required.	 Figure 27 – Laser engraving [55]
Cutting	The laser is programmed with a sufficiently high power so that the interaction with the substrate causes it to penetrate its entire thickness, cutting it to the required pattern (Figure 28). By doing so, a new part is created from the initial substrate.	 Figure 28 – Laser cutting [56]

2.4.3.1 Logotype marking

During its production, sanitary ware also undergoes a process of marking the company logo, which can be carried out by a laser, as a radiant energy source. Marking can be performed by means of an ink placed on the surface of the substrate or directly on the substrate itself.

In the first situation, at least one marking material and a substrate to be marked are placed in reactive contact with each other, i.e., sufficient contact for there to be vitrification between both parts. The marking material may be in the form of powder, paste or film and is generally applied in a thickness between 0.0127 and 2.54 mm. The substance resulting from vitrification can vary in colour, depending on the colour and type of substrate, but also on the marking material. In the case of Figure 29, the marking material used is the orange coating of the thermos bottle [36].

Figure 29 – Laser logotype marking [57]

In the second option, the ceramic material must have at least one additive that is sensitive to radiation, as seen in Figure 29. A laser beam is used as an energy source, which is applied to the surface of the material to be marked, according to the pattern to be produced, so that a colour change is induced in the irradiated areas. For this to happen, the wavelength of the laser beam used can be either in the visible, ultraviolet or near visible infrared range, and the additive sensitive to the radiation is an organic pigment. Additives which absorb the ultraviolet range react at wavelengths between approximately 250 and 380 nm. Despite this, it is preferable to use additives that absorb the visible range of radiation or infrared radiation, with wavelengths between 780 and 2000 nm, approximately. These will react to the incidence of the concentrated laser beam and create the desired pattern [58].

The USA patent for laser marking of ceramic materials, glazes, glass ceramics and glasses [58] argues that the most suitable lasers for this application are pulsed or Nd:YAG lasers with continuous wave multiplied frequency. The laser parameters can be adjusted, in aspects such as the type of pulse or its duration, thus allowing a good adaptation to the requirements of the material to be marked.

2.4.3.2 Surface treatment

Laser technology has provided a large number of benefits with regard to surface treatment on ceramics, mainly due to both the possibility of localised fusion and very high heating and cooling rates.

Currently, the laser is standing out as an alternative tool in the materials processing, more specifically in their surface treatment. Some phenomena resulting from the interaction between the laser and a ceramic material are heating, melting of the surface and its vaporization. According to *Mahmod et al.* [59], one of the most widely used lasers for surface treatment is the Yb-fibre laser. This is explained due to its benefits, namely higher energy conversion efficiency (>30%), higher than Nd:YAG or CO_2, and high localised heating, which contributes to an improved treatment precision.

In Figure 30 the basic structure of an optical fibre laser is noticeable, as well as its light propagation mode, with the beam represented in red. This laser has a double covering, consisting of the cladding and the coating.

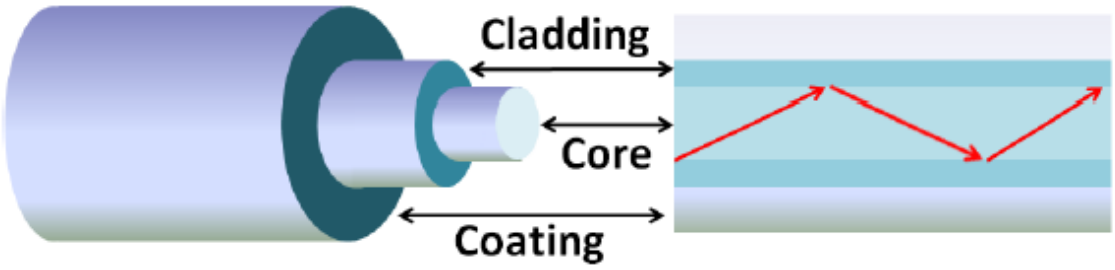

Figure 30 – Mode of light propagation in an optical fibre laser [60]

Basile et al. [61] studied the achievement of a dense glazed layer on ceramics, with a controlled microstructure, by means of a powder glazed coating. This process was possible due to the use of a concentrated laser beam for surface treatment, namely the Nd:YVO_4 laser. Initially, the glazing powder is subjected to the concentrated beam, so it will melt and form a dense and amorphous layer, followed by a subsequently crystallisation occurrence. This way, a glazed coating (10-100 μm) is obtained based on a laser treatment of glaze powder deposited on a ceramic substrate.

An alternative method is the laser cladding, a welding technology which consists of a laser beam focused on the workpiece with a spot of previously stipulated diameter, as depicted on Figure 31. The powder feedstock material is transported to the melt pool by an inert gas through a powder nozzle, and thus, both the powder nozzle and the laser focus will advance along the workpiece surface to coat the entire intended area [62].

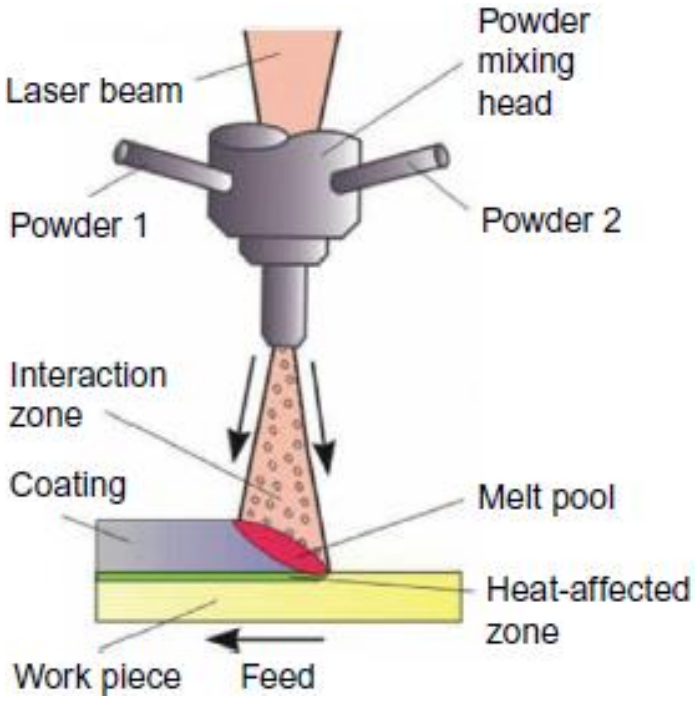

Figure 31 – Laser cladding process [63]

The same type of technology is used in solid oxide fuel cells for glass-ceramic sealants. Although laser welding involves a higher temperature than the usual sintering process in the kiln, it allows a drastic reduction in the time required for operation, namely of only a few minutes. In an in-depth study carried out by *Rodríguez-López et al.* [64], it was concluded that among Nd:YAG, Diode and CO_2 lasers, the latter showed the best results regarding the glaze fusion.

The absorbance factor is dependent on wavelength, being related to the optical response of the material to be processed. In the case of oxides and polymers, the absorbance increases with wavelength, whereas for metals and carbides, the opposite effect is obtained. For this reason, a CO_2 laser has a better absorption than the Nd:YAG and Yb-fibre ones, which are very similar in wavelength, considering the approximate values in Table 5. In spite of this, CO_2 lasers are not able to achieve smaller focussing diameters, in contrast to the Yb-fibre, which can reach higher power densities (output power) and has a better beam quality even than that of the Nd:YAG laser [65]–[68].

Table 5 also presents other relevant properties among the three aforementioned lasers, such as the laser medium and the beam transmission type [69].

Table 5 – Comparison between CO_2, Nd:YAG and Yb-fibre lasers' properties

Laser	CO_2	Nd:YAG	Yb-fibre
Wavelength	10,640 nm	1064 nm	1070 nm
Output power	Up to 15 kW	Up to 4 kW	Up to 20 kW
Laser medium	Gas mixture	Crystal-line rod	Doped fibre
Beam transmission	Mirror, lens	Fibre, lens	Fibre, lens

Nevertheless, the Yb-fiber laser causes visual damage, so it needs protection upon being used. The CO_2 laser, on the other hand, is completely harmless to the operator's safety, has a higher efficiency (around 20%) and is cheaper by comparison to the remaining ones, factors which make it the ideal one to develop the intended work [70].

The use of laser technology proves to be an excellent solution for the recovery of sanitary ware, as it does not lack effectiveness in situations where current methods have drawbacks. Refiring is replaced by a much faster localised heating, saving valuable resources such as time and money. In addition, the laser can be used on small ceramic defects in any area of the workpiece, without harming its normal functioning [71].

2.4.3.3 Laser interaction with ceramic materials

At the moment the laser beam is irradiated, it will interact with the ceramic substrate, causing its fusion. This is a complex process and the control of its parameters is critical to achieve a satisfactory final result, being the irradiated thermal energy per volume of material the most important.

Due to anomalies present in the ceramic substrate, such as low compaction of the particles, which generates inter-granular gaps, it becomes difficult to predict the laser diffusion pattern, given the multiple dispersions and reflections of the laser between the ceramic particles (Figure 32). Therefore, the temperature distribution in the substrate is heterogeneous, leading to uncontrollable heating and cooling phases [65].

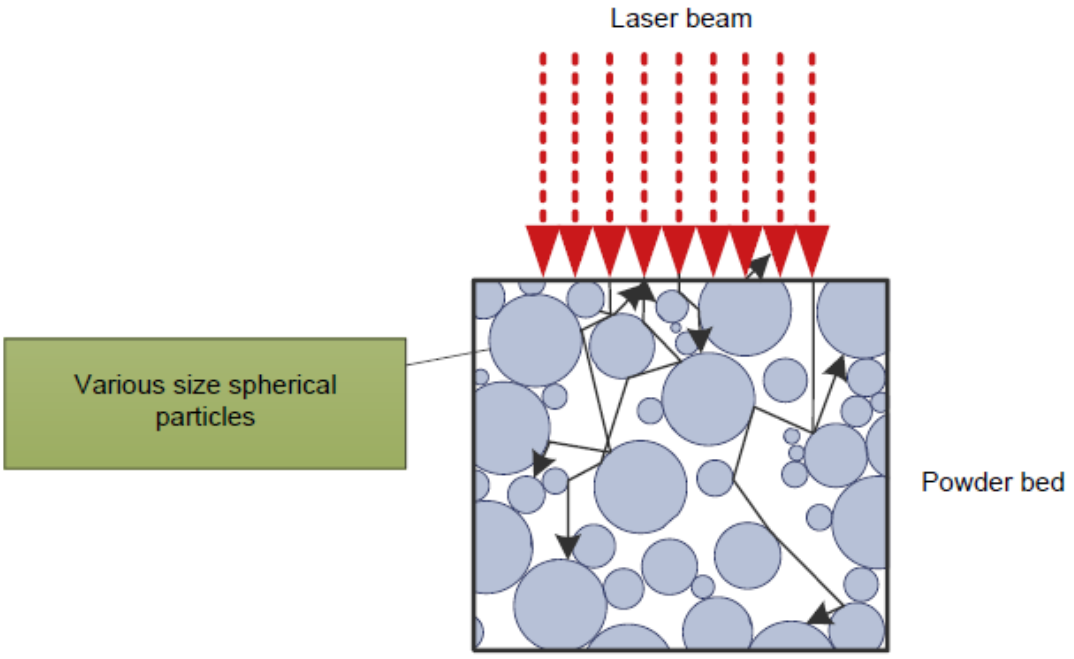

Figure 32 – Laser diffraction on the substrate particles [65]

The most common laser systems used for sintering of ceramics are continuous-wave CO_2 and Yb-fibre lasers. Compared to other commonly used materials in engineering, such as polymers and metals, ceramics have higher melting points and distinct absorption mechanisms, which makes them require a higher energy rate to ensure proper processing through laser interaction.

Consequently, it is necessary to relate various parameters in addition to power, such as the incidence time or the area irradiated by the laser. Only the correct ratio between the energy density [Energy (J) / Area (mm^2)] and the laser power (W) will result in the proper fusion of the substrate, as shown by the graph present in Figure 33, also aiming for a shorter fusion time [65].

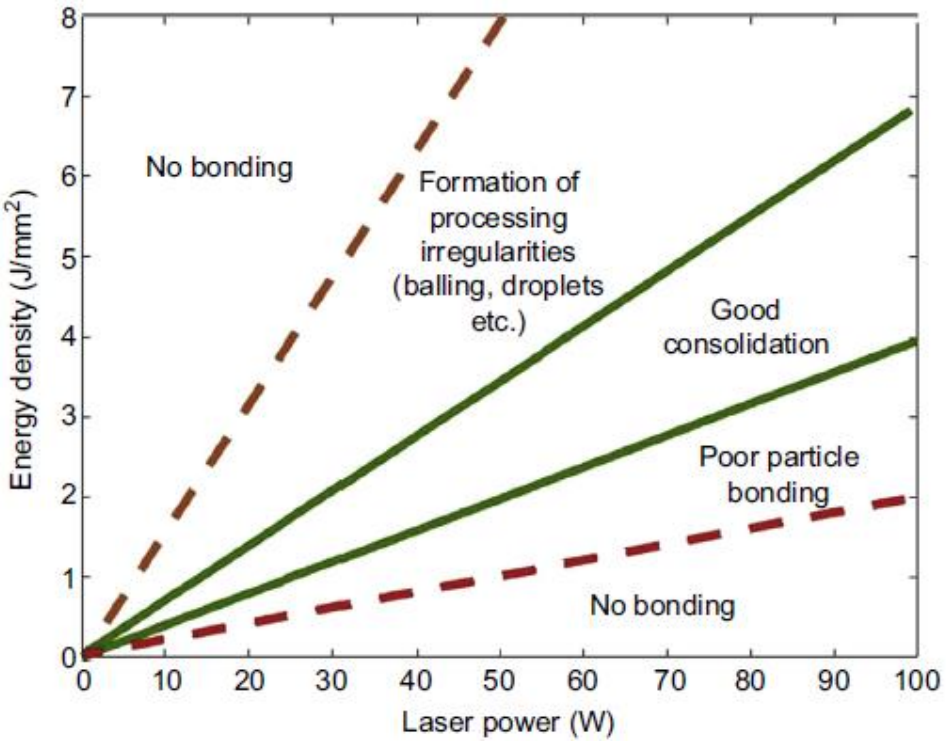

Figure 33 – Substrate processing according to the energy density and laser power [65]

A key aspect to consider is the rapid heating of the substate due to laser incidence. Thermal shock resistance in ceramics is an important factor for applications involving sudden temperature changes, since, due to their brittleness, ceramic materials are susceptible to serious malfunctions when subjected to thermal stress caused by temperature difference [72].

Unlike metals and polymers, which are more resistant to thermal shocks, some attempts to apply the laser to ceramic substrates, such as alumina and zirconia, have resulted in the appearance of cracks. This is justified by the high coefficient of thermal expansion and modulus of elasticity, which caused thermal stresses above the mechanical strength of the material [73]. Rapid heating can produce unwanted cracks in or near the irradiated zone due to the brittleness and low thermal conductivity of ceramics, which cause high thermal gradients and residual stresses to form in the substrate. The parameters of melting temperature and coefficients of thermal expansion of both the glaze and the substate must be controlled so that the resulting stresses in the substrate are lower than its elastic limit stress. The patent *Localized surface glazing of ceramic articles* (1995) [74] addresses the stresses generated from laser incidence and proposes a solution to this problem: by preheating the surface, the temperature difference will not be so high, hence it is possible to avoid cracks and damage to the substrate [75].

2.4.3.4 Repair methods using laser technology

There are also repair methods using laser contemplated in the literature. The patent *Method of thermally glazing an article* [75] addresses a repair method by laser welding, which uses a CO_2 laser with a wavelength of 10,600 nm. These lasers are adopted due to their stability and ability to reach high powers corresponding to temperatures of 1800 and 1900 °C, whose incidence on an area of a few square millimetres can be translated into a fusion of the substrate in only a few seconds.

In a study conducted by *Osvay et al.* [76], a CO_2 laser was used to repair small defects, namely pinholes, with sizes ranging from 0.1 to 0.5 mm. By using the pulsed mode (in contrast to the continuous mode), that is, incidence on a single point at a time, a more effective treatment and greater stability of the laser were obtained.

The patent *Methods for vitrescent marking* [36] refers the use of a laser system for marking which has a wavelength of 1064 nm. After the respective tests, it was concluded that with the original beam width emanating from the laser, the power used ranged from 60 to 100 W, but using the collimator or beam expander, thus expanding the beam in a range of 1.6 to 5x, the power required dropped to 60 to 80 W. This method, on the contrary to the ones presented until then, aimed at marking slightly below the surface (between 0.397 and 3.175 mm deep), so that the final result would be more resistant to low temperatures and abrasion. Nevertheless, other lasers were also used, such as the continuous wave CO_2 laser operating with a wavelength of 10,640 nm and a wide range of energy levels, also with satisfactory results.

Meanwhile, *Wang et al.* [71] developed a technique to produce pure molybdenum by selective fusion, with the aim of reducing cracks in the substrate, having employed a Nd:YAG fibre laser with a maximum power of 400 W. Figure 34 displays an observation in the scanning electron microscope (SEM) where the three scanning shapes used in the tests are depicted: a) 0°, b) 90° e c) 67°. Finally, they came to the conclusion that although there were less cracks in the 90° scanning, in comparison to the 0°, when the same was done at 67°, these decreased not only in quantity but also in dimension.

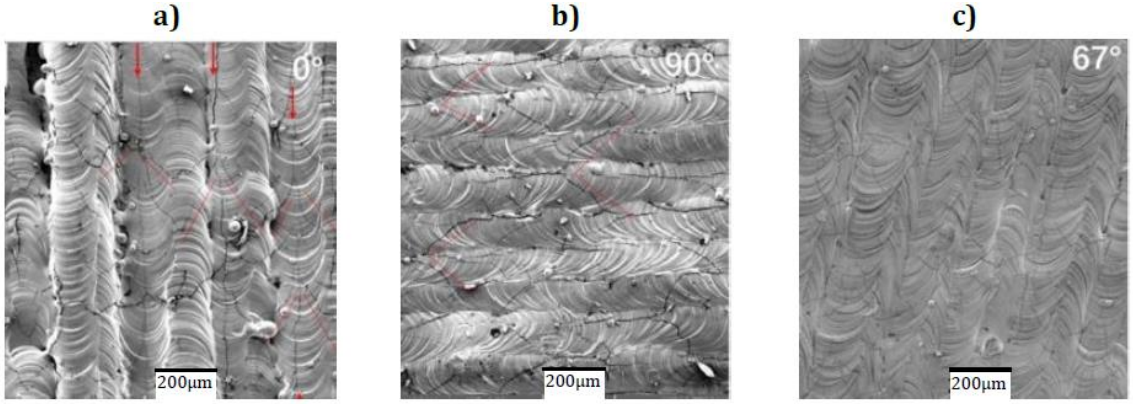

Figure 34 – SEM images showing surface crack growth behaviour under laser scanning rotations between layers (adapted from [71])

2.5 Statistical methods for experimental analysis

At the time of conducting experimental tests as a way to develop the assumptions set out in the literature review with a practical component, several statistical methods can be adopted. The main purpose of these is to ensure the optimisation of the tests, so that they are performed in an organised form, relating the variables under study and identifying which of these will have a greater impact on the results to achieve the defined objectives.

For this reason, the methods to be used are the Complete/fractional factorial design and the ANOVA.

2.5.1 Complete and fractional factorial design

A factorial consists of a set of planned tests which allow the effects that several variables have in relation to a certain goal to be observed. This method has the advantage of being able to vary different values of all variables simultaneously, rather than one at a time, which allows interactions between them to be studied [77].

Complete factorial design

In Figure 35 it is possible to visualize a test with two variables, where the variable A has two values and B has three values, which corresponds to a total of six combinations (2x3=6). In Figure 36 three variables are involved, A, B and C, where each one assumes two different values, constituting eight combinations (2^3 = 8).

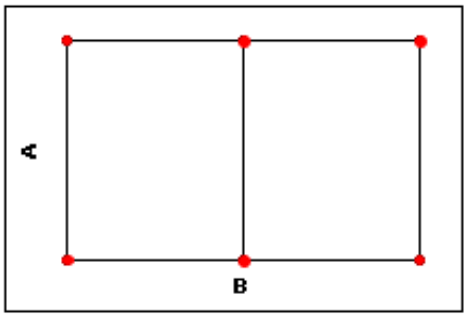

Figure 35 – Two variables test (adapted from [77])

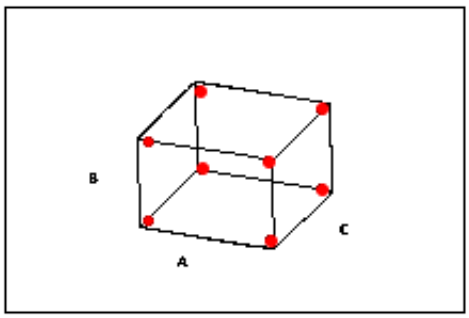

Figure 36 – Three variables test (adapted from [77])

The examples above are both representative of a complete factorial design, that is, relating all the variables and doing tests with the maximum of possible combinations according to the values intended for each variable. In the first case, the number of values (levels) is different for each variable (factor), so the number of combinations is calculated by multiplying the different levels (2x3=6). In the second case, as all factors have the same number of levels, the combinations are calculated through l^f, where f represents the number of factors and l the number of levels. Thus, having three factors and two levels for each, this represents a total of 2^3 = 8 combinations [78].

Fractional factorial design

Besides the complete factorial, there is also the fractional factorial design. As its name indicates, this represents only a fraction of the complete factorial, and it is more frequently used when there is a limitation of available resources or the number of combinations is too high, not being necessary to perform all the tests to reach a viable solution. In this method, the combinations are calculated through l^{f-t}, where f is the number of factors, l the number of levels and t the reduction of the number of tests, or else only a part of the foreseen tests are executed, in a non-linear way. If there is a reduction of the performed tests by half, t=1 [79]. Thus, in the case of having three factors and two levels for each, the complete factorial design would be $2^3 = 8$ (Figure 37) and the respective fractional factorial has $2^{3-1} = 2^2 = 4$ combinations (Figure 38).

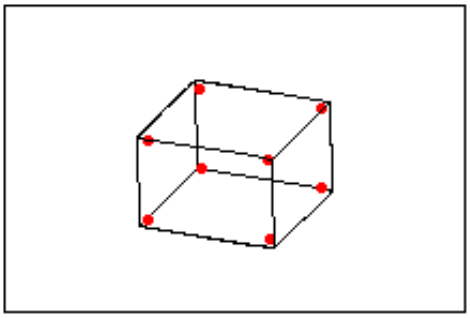

Figure 37 – Complete factorial design [77]

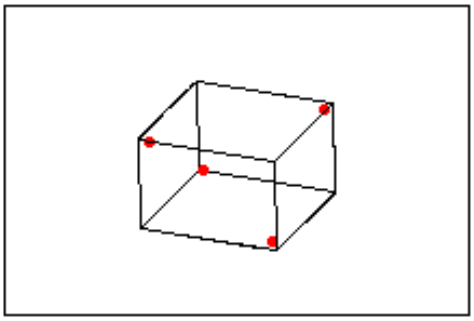

Figure 38 – Fractional factorial design [77]

2.5.2 ANOVA (Analysis of variance)

The variance is a dispersion measure used in the field of statistics to quantify the existing variation in the data of a set of values. As such, it is a parameter which determines the distance of the data of a set of values from the mean [80].

The ANOVA method, or Analysis of Variance, allows the evaluation of the effect that various levels of a factor have on the final result of a certain experimental activity. This way, in a set of experiments with several factors and respective levels, it is possible to study which variable(s) stand out more, contributing to a greater variance in the experiments, and which variables have a reduced variance, and therefore are not so relevant for the final result.

For the conducting of experiments, the ANOVA method is extremely relevant since it allows the analysis of the differences in the variation of parameters and thus to determine which of these are the most important for the final result. Hence, the number of tests is reduced, varying only the relevant parameters. This method has only three assumptions: all samples are drawn from populations with normal distribution, being drawn independently from each other and all populations have a common variance [81].

Furthermore, other statistical methods may also be employed in order to sustain the quantitative results with a mathematical and numerical explanation.

2.6 Quality control

Quality control systems aim to maintain uniformity in the manufactured products, and this is an extremely important process to be carried out before their commercialisation. These products must not present any signs of internal or external defects, otherwise serious problems may arise in their operation, which could even cause harm to the user. According to the standards established in the manufacture of sanitary ware, they must have a life cycle of at least twenty years.

In terms of the physical properties of the product, according to the USA patent on the manufacturing method for sanitary ware [9], it must fulfil at least one of three different conditions:

- A pore area ratio of 3% or less in relation to the total area of a surface obtained by cutting the upper layer of glaze in the direction of its thickness;
- An average pore size of 50 μm or less present in a surface obtained by cutting the upper layer of glaze in the direction of its thickness;
- A difference of 50 μm or less between the maximum and minimum values of the thickness of the upper layer of glaze.

For these reasons and so that there are no monetary or material losses, the entire manufacturing process must be carefully controlled, always guaranteeing the maximum quality of the final products.

Some of the tests carried out on the products to ensure their quality are the hanging basin load test, the autoclave test and the water absorption test.

2.6.1 Hanging basin load test

The hanging basin load test, according to the Portuguese standard *NP EN 997:2012 + A1 2017* [82], is used in suspended sanitary ware, i.e., fixed to a wall, and aims to determine the robustness of the basin, whether it is a toilet, washbasin or bidet.

This test consists in the application of a (4.00 ± 0.05) kN load on the sanitary ware to be tested, for one hour, through a beam with a 100x100 mm cross section, placed in the centre of the upper opening of the basin rim, as shown in Figure 39. In practical cases, this application is carried out for 24 hours, in order to guarantee the robustness of the product.

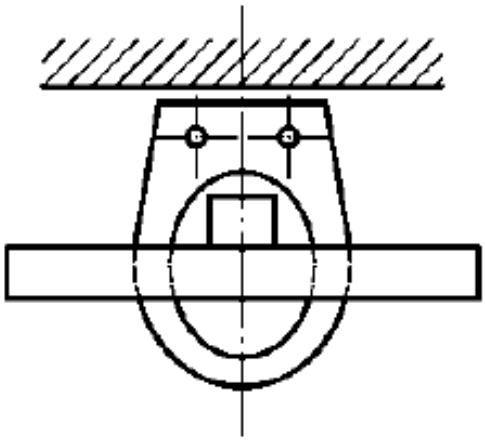

Figure 39 – Hanging basin load test [82]

2.6.2 Autoclave test

The autoclave test is one of the ageing tests performed on tiles and fine fire clay or *gresanit* products. This material is used in the manufacture of larger parts, such as a shower tray, since in this situation the usual sanitary ware suffers deformation.

According to standard *BS EN ISO 10545 – 11:1996* [83], this test provides a guarantee that the product will resist the conditions to which it is subjected throughout its life cycle while fulfilling its function. The sanitary ware should have an area equivalent to about $25{,}000 \pm 150\ \mathrm{mm}^2$, with at least one of its faces glazed.

The product remains fifteen hours inside an autoclave at a temperature of 200 ℃ and subjected to a pressure between 3.0 and 4.0 kgf/cm^2. The focus of this test is to assess the existence of crazing (Figure 40) in the *gresanit*, i.e., whether there is a difference in thermal expansion between the ceramic base and the glaze. Crazing is not allowed in the sanitary products, as it may compromise the user's safety and the quality of the product, leading to fractures in the sanitary ware glaze.

Figure 40 – Crazing in ceramic faience [84]

2.6.3 Water absorption test

In order to carry out this test, three glazed samples must be taken from the same side of a sanitary ware product. The unglazed surface area of the samples shall be approximately 30 cm^2 and the thickness including the glaze about 12 mm. After this step, the samples are allowed to dry at 110 °C for (180 $\pm$ 5) min, then cooled down and weighted to an accuracy of 0.05 g (m_0).

Afterwards, the samples are placed in a bath with demineralized water, which is heated to boiling point and held there for (120 $\pm$ 5) min. Subsequently, the heating process is interrupted and the samples are kept immersed for another (20 $\pm$ 1) h. After their removal from the water and all its cavities dried, the samples are re-weighted, being this mass designated as m_1.

This way, the water absorption coefficient, WA, is calculated using equation 1.

$$\mathrm{WA} = \frac{\mathrm{m}_1 - \mathrm{m}_0}{\mathrm{m}_0} \text{ x } 100 \qquad \text{(Equation 1)}$$

where m_1 represents the mass of the specimen after immersion in water, in g, and m_0 the mass of the dry specimen, in g [82].

In the case of fine fire clay or *gresanit*, the water absorption coefficient must be inferior to 5%, however for a product to be considered as non-defective, its water absorption coefficient must actually be less than or equivalent to 0.5%. *Gresanit*, developed by ARCH, is widely used due to its benefits: it possesses half the weight comparing to identical products of fine fire clay, more than double of its mechanical resistance, it is resistant to crazing throughout its life, unlike the first, and finally it enables products with thicknesses of around 6 mm to be obtained [85].

A chemical resistance test can also be conducted, such as evaluating the basin's resistance to acids, bases and staining agents (ABS), and although these tests are usually performed in a laboratory accredited for that purpose, they can also be done in ARCH's facilities to ensure that the glazed products resist to the chemicals they are in contact with.

In the following chapter, all the concepts discussed in the background will be put into practice, with special focus on the equipment and materials used, the most important being the CO_2 laser system and the sanitary ware specimens. In this manner, all the tests performed in order to achieve the proposed objectives are described, as well as the respective results obtained.

THESIS DEVELOPMENT

3.1 Welcoming company characterization

3.2 Materials and methods

3.3. Results

3 THESIS DEVELOPMENT

3.1 Welcoming company characterization

The name ARCH (Advanced Research Ceramic Heritage) carries with it the historical legacy of the Valadares brand. Throughout a century of existence, this company has stood out in its sector through 100% Portuguese production and a strong environmental component, revolutionising the sanitary ware market with the development of new materials, but also through the applicability of ceramics in various sectors/products.

This company excels with important projects from north to south of Portugal, including Azores and Madeira, and also taking with it the Lusitanian name a bit all over the world, in cities such as Madrid, London, Dubai, Beirut, Abu Dhabi and Luanda [10].

In each letter of its name is hidden the key to its history:

- **Advanced** – Innovation as a design

  Production of highly prestigious articles in the ceramic sanitary ware segment, as well as innovative and exclusive materials;

- **Research** – Research as a working tool

  The technical staff of ARCH is in a constant quest to obtain and conceive new materials and applications;

- **Ceramic** – A universe of creative possibilities

  The ceramic industry is the basis of this company's work and has proven to be essential to historic steps towards innovation;

- **Heritage** – The history and soul of applied knowledge

  Exactly 100 years of existence let the name speak for itself, with recognition and a mark of quality both nationally and internationally [86].

Figure 41 shows the entrance to the ARCH headquarters, in Valadares, Vila Nova de Gaia and ARCH's 2020 Organogram may be consulted in Appendix 1.

Figure 41 – ARCH Valadares entrance [87]

3.2 Materials and methods

Throughout this subchapter are discussed all the materials which were used to perform the necessary tests, as well as the equipment involved in the same process, particularly the laser system and its characterization, but also the colourimeter and the microscopes used to analyse the final samples. Therefore, the laser parameters chosen for a better understanding of the experimental procedure are also described.

3.2.1 Materials used

In order to carry out the experiments for the development of this work, two types of materials were used. Firstly, the specimens, the base material with provoked defects, in which the laser was irradiated, and then the inks/glazes, used to fill the defects. Derived from the interaction with the laser beam, this material fuses, changing its texture and assuming the same appearance and characteristics as the rest of the ceramic product.

3.2.1.1 Specimens

The specimens adopted to conduct these tests are square shaped tiles, as seen in Figure 42, with the dimensions of 150x150x10 mm and manufactured with the exact same formulation of the ceramic sanitary ware. They are composed of a ceramic base followed by a glaze which is applied on its surface, visible through a layer of small thickness (Figure 43), namely 1 mm.

Figure 42 – Specimen

Figure 43 – Specimen's sectional view

After the production of these specimens, a percussion pen was employed for the purpose of generating defects on their surface, alongside with a squared grid (Figure 44 and Figure 45), so that these could be geometrically distanced for an easier laser programming. In some cases, it was also used a tungsten bur (emery) to soften the defect, eliminating its edges.

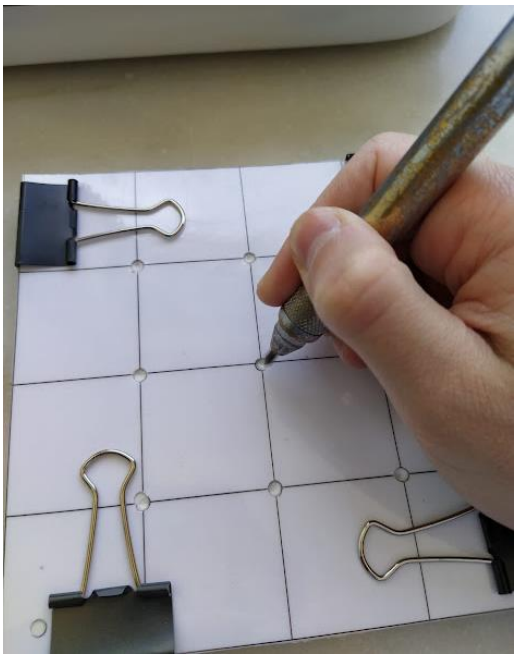

Figure 44 – Squared matrix to provoke defects

Figure 45 – Percussion pen provoking defects

These defects, seen in Figure 46, were simple and small in the first phase, i.e., **pinholes** (top) and then, in the second phase, they became longer, namely **cracks** (bottom).

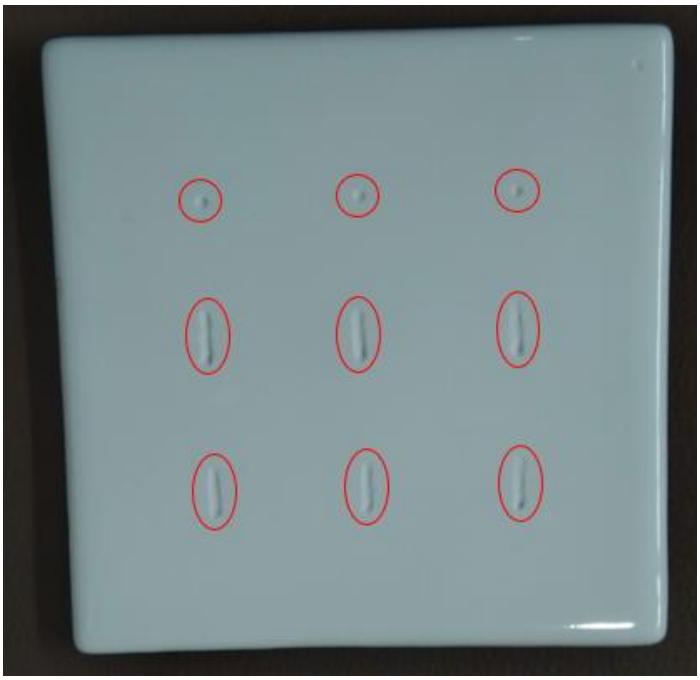

Figure 46 – Specimen with provoked defects

3.2.1.2 Inks/Glazes

Various types of inks or glazes were adopted throughout the experiments, since these were also a factor to be perfectioned, alongside the laser system parameters. Accordingly, four different formulations (low temperature, alkaline glazes) were used which are already employed in the ceramic industry:

- **Regular glaze**

This is the regular glaze which is commonly used in the sanitary ware manufacturing process, precisely in glazing, after the workpieces are formed and before firing in the kiln. It is also used on the current hot recovery process to fill the defects and then submit them to refiring.

- **Frit**

The frit is composed of the regular glaze which is fired at a temperature of 1000 ℃ to release all the carbonates present in its chemical structure. After that, it is poured directly into a container with cold water (room temperature) in order to ensure a strong thermal shock, which causes it to solidify and assume the shape of small granules. The frit's melting point is at 1000 ℃, in contrast to that of the regular glaze, namely 1200 ℃.

- **Grey marking ink**

This type of ink is employed in the laser logotype marking process of white ceramic sanitary ware products in certain companies. In order to be used, firstly the grey powder needs to be mixed with water and a compound denominated Carboxymethyl cellulose (CMC), which acts as a glue to fix the ink. This is added in a certain percentage to the mixture, then is taken to the kiln and fuses, generating the ink.

The grey marking ink is applied to the surface of the specimen, in the form of a spray, using a compressed air gun, as seen in Figure 47. On the other hand, Figure 48 shows the test body, a ceramic sanitary ware tile, after the ink is sprayed on its surface. After the laser interaction, the remaining ink is removed with a piece of paper, revealing only the required pattern, marked on the specimen's surface (**markings**).

Figure 47 – Compressed air gun

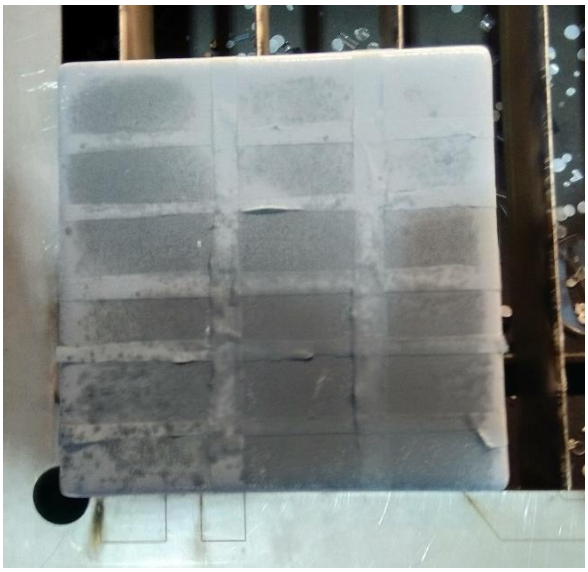

Figure 48 – Ceramic tile sprayed with grey marking ink

- **White marking ink**

The white and shiny marking ink has a similar preparation method to the grey marking ink. It is also generally used in the laser logotype marking process, with the difference that it is used in coloured ceramic sanitary ware products, to form a contrast.

This ink has to be in the liquid state in order to be applied, so the first step is to mix the white powder either with water, ethyl alcohol or a medium. The medium is a particle suspension, a viscous liquid which acts as a fixative, and may be a CMC diluted in water.

Note: The ink used throughout the experiments suffers some changes in its composition, due to the trials to reach the best possible solution, so as it may fuse and fill the defects properly.

In Figure 49 is represented the white marking powder, before mixing with an aqueous medium to form the ink.

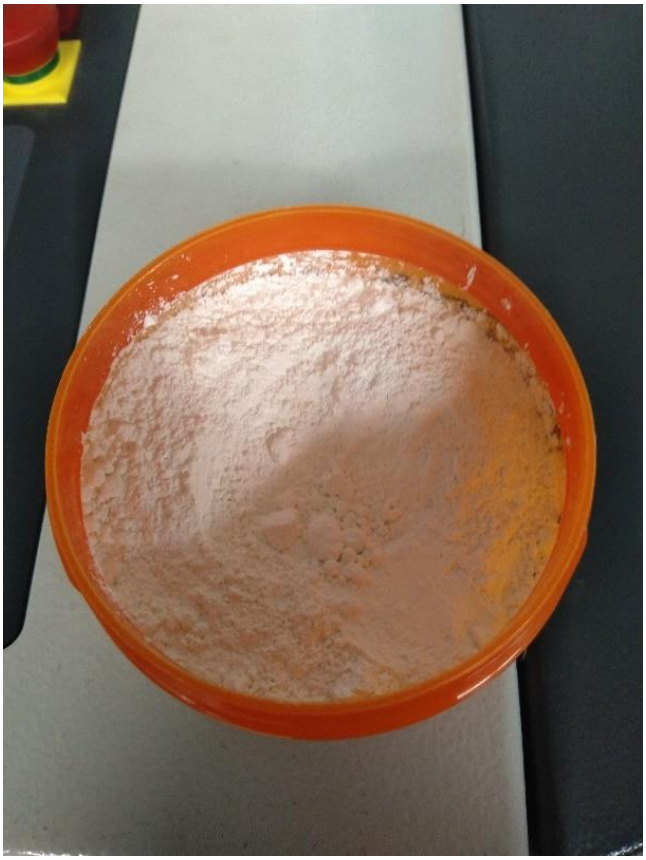

Figure 49 – White marking powder

Figure 50 shows a specimen with two types of provoked defects. The first six are cracks and then the last three are pinholes, each of which is filled with the white marking ink and ready to be submitted to the laser incidence, in order to fuse the ink with the remaining ceramic sanitary ware tile.

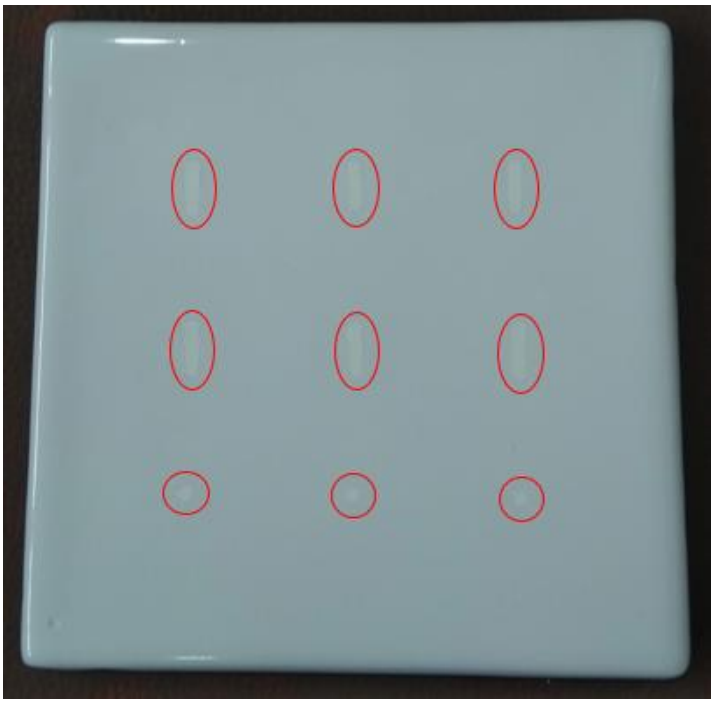

Figure 50 – Specimen with white marking ink filling the defects

3.2.2 Equipment used

The equipment selected to develop this work can be split in two categories. The primary category is the one used to perform the experiments, the CO_2 laser system, whereas the second one includes the instruments responsible for analysing the samples after the experimental phase is completed, comprising not only the colourimeter but also the optical and electronic microscopes.

3.2.2.1 CO_2 laser system

The CO_2 laser system chosen for this project is the Trotec SP1500, as observed by Figure 51. It has a working area of 1500x1250 mm and the maximum workpiece height supported is 53 mm. Although this model's power goes up to 400 W, the system used for the experiments has a power source which only allows it to have a 200 W maximum power. In addition, its laser beam possesses a wavelength of 10,600 nm, being included in the infrared radiation, and has a maximum speed of 1.65 m/s.

Figure 51 – Trotec SP1500 laser system [88]

The laser machine used for this project belongs to TABOR [89] and is present in its facilities. It stands for top quality with minimum maintenance and its flatbed offers a robust, stable work surface for laser marking, engraving and cutting. Some of the most important characteristics of the Trotec SP1500 laser system are described in Table 6 [88]. A full description and technical datasheet are present in Appendix 2.

Table 6 – Trotec SP1500 relevant attributes

Characteristic	Description
Extraction on working head	An extraction hose is assembled directly on the working head of the laser and removes dust and smoke from the material surface during processing. Furthermore, the safety enclosure of the laser machine guarantees the security of its users while working and, at the same time, provides a more efficient dust extraction.
InPack Technology	The *InPack* Technology provides excellent protection for all original components, keeping these maintenance-free and generating higher productivity and lower running costs. Especially the lenses, mirrors, electronics, motors and shafts are assembled in such a way as to prevent any contact with dust. Isolated from the processing zone, the mechanical and electronic components are safe from the debris accumulation.
CeramiCore Technology	The resonance body where the laser radiation is generated is made of 100% ceramic. All the optical elements are bonded onto the ceramic and the gas is energized through the ceramic body. So, with the inexistence of internal metal surfaces, which could damage the balance of the gas mixture, it is possible to work with a pure gas composition over the entire lifetime of the laser source. This way, ceramic lasers can be operated at much higher pressure, resulting in better and faster pulsability, vital for high-speed interaction.

The SP1500 model is also equipped with professional CAD/CAM software, namely the *JobControl*. This software provides a full control of all the laser functions, with the possibility to work alongside graphic design programs such as CorelDraw, Photoshop or AutoCAD. The ability to take advantage of the computer's monitor to work, instead of programming through the laser system mini display, eases the job to be done, increasing the user's productivity. In addition, the processing via colour mapping shows an organized list of up to sixteen simultaneous processes, each of which allows to change the necessary parameters, such as type of laser interaction, laser power, beam speed, number of passes, Z-axis compensation, etc., as represented in Figure 52.

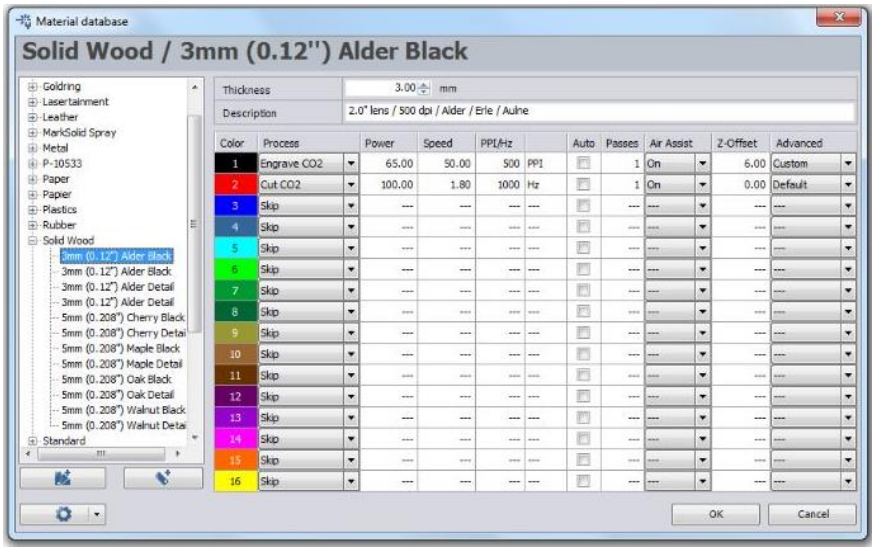

Figure 52 – JobControl software [88]

3.2.2.2 Colourimeter

A colourimeter is an electronic device whose function is to evaluate, according to a certain specific scale, the colour level of a surface, by comparison with standard colours. It can either be used just to quantify the colours of a surface or to compare two different surfaces and calculate the deviation in terms of colours between them.

Figure 53 presents the colourimeter used to analyse the results of the experimental tests, which belongs to ARCH [10] and is present in its facilities. Although it was also possible to use another type of device in order to obtain a proper colour analysis of the specimens, namely the spectrometer, there was a particular reason why this specific equipment was not chosen. The main distinction between the two stands in the range of the wavelengths they are able to measure. Whereas the spectrometer measures a wider range of wavelengths, being most often used to evaluate two different colours, the colourimeter has a specific range of wavelengths, for it is most effective when comparing two samples of the same colour.

Figure 53 – Colourimeter

In order to understand the concept of the colourimeter functioning, one must learn about the CIELAB colour space diagram. Also referred to as L*a*b* colour space, defined by the International Commission on Illumination (CIE), this represents a quantitative relationship of colours on three axes: L* value indicates lightness, and a* and b* area chromaticity coordinates. The vertical axis corresponds to the L* value, which varies from 0 (black) to 100 (white). The a* value is the red-green component of a colour and the b* axis expresses the yellow-blue component. The centre of the plane is neutral or achromatic, and the distance from the central axis is called the chroma (C*), i.e., the saturation of the colour. The angle on the chromaticity axes represents the hue [90].

Figure 54 shows a schematic representation of the CIELAB colour space diagram.

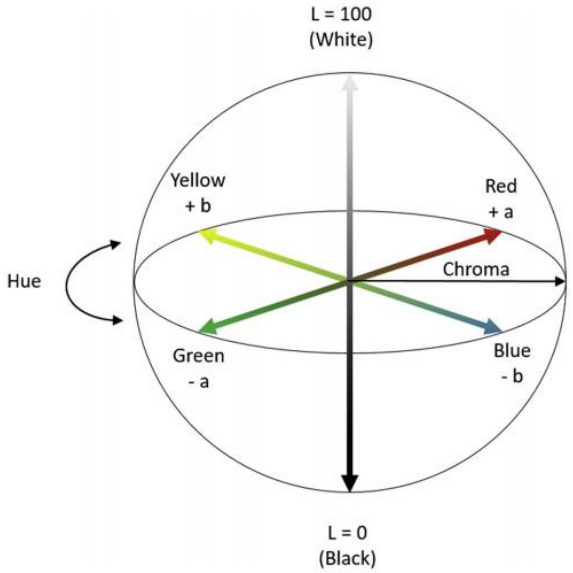

Figure 54 – CIELAB colour space diagram [90]

After the understanding of how the colourimeter works, Figure 55 shows this instrument analysing a black and opaque ceramic sanitary ware surface as an example and the corresponding L*, a* and b* values.

Figure 55 – Colourimeter functioning

These instruments are also able to measure the exact difference in a colour scale between two different parts. The colour deviation (ΔE^*) is calculated by relating the deviation of the three axis' values, as explicit in equation 2, being this deviation shown directly in the colourimeter, alongside the remaining values.

$$\Delta E^* = \sqrt{(\Delta L^*)^2 + (\Delta a^*)^2 + (\Delta b^*)^2} \quad \text{(Equation 2)}$$

3.2.2.3 Microscopes

- **Optical**

The optical microscope, also known as light microscope, usually makes use of the visible light and a system of lenses to generate magnified images of small objects. This device is employed in order to analyse the glaze samples which fill the defects in the ceramic sanitary ware tiles. Figure 56 shows the optical microscope employed, present in ISEP's Metallography Laboratory (LMET) [91], with an 11x maximum amplifying set of lenses. Its model is the *SZ PT Olympus*, alongside with an *Olympus DP70* camera, in order to transpose the pictures seen in the microscope to the computer screen.

Figure 56 – Optical microscope

- **Electronic (SEM)**

The scanning electron microscope (SEM) used, or just electronic microscope, belongs to CEMUP [92] and is present in its facilities, more precisely in the Scanning Electron Microscopy Laboratory (LMEV). It produces images of a sample through the scanning of the workpiece surface with a focused beam of electrons. These electrons then interact with atoms in the sample, producing various signals which contain information about the surface topography and its composition.

This microscope is used mainly to achieve a clear view of the irradiated zone by the laser to an atom level and as a complement to the optical microscope analysis, as seen in Figure 57.

Figure 57 – Scanning electronic microscope (SEM) [93]

3.2.2.4 Ceramic tile cutter

In addition to the already described equipments, there was the need of using a ceramic tile cutter tool as well, due to the SEM-EDS analysis. The electronic microscope which was employed for the experiments' analysis had a very reduced scanning area available to analyse the samples, so the 150x150 mm specimens did not fit in. Consequently, the solution was to use a ceramic tile cutter to divide the tiles in small cubicles, containing just the sufficient space for a sample, i.e., a defect, in it.

Visible in Figure 58, side by side with an already cut sample (on the right), is depicted the ceramic tile cutter tool, which possesses a diamond tip to scratch the tile's glazed surface, thus creating a notch along its entire length. After this procedure, the red handled lever on the left promotes a pressure point in the notch's extremity, at the same time that two metallic pins stabilize the back of the tile, splitting it in two sides.

Figure 58 – Ceramic tile cutter

3.2.3 Laser system parameters

The most important parameters to vary in the laser system are:

- **Laser power (W)**;

This is a key factor in any type of laser interaction. The power varies according to the purpose for which the product is to be used, as its amount is directly proportional to the penetration into the substrate, but also to the type of material where the interaction is performed. A high amount of power can give rise to stress concentration and reduce the lifetime of the product, by fatigue [88]. Its units are the Watt (W).

- **Incidence time (s)**;

In the case of manual firing (pulsed wave), the beam only targets a single point on the part. Thus, the incidence time must be carefully controlled, since although a small amount of time does not cause significant changes in the substrate, if this time is excessive, the negative results of the laser fusion are irreversible. Its units are the seconds (s).

- **Beam speed (m/s)**;

In the case of rapid firing (continuous wave), the beam moves a certain distance (most common in marking) to carry the interaction. The higher the beam speed, the faster the process becomes. However, the laser must have a minimum speed in order to execute the fusion on the substrate. Its units are the metres per second (m/s).

- **Focal length (‘’)**;

The focal length is the distance separating the laser lens from the substrate where it will impact. If the laser is in a vertical position, the focal length is its height in relation to the workpiece. The laser has a certain diameter of focus, which is directly related to the area of interaction on the part where it is going to strike. A lens is also used, fitted to the laser system, in order to reduce the diameter of focus and thus focus on a more precise point on the substrate. The larger the lens, the smaller the area of incidence and the greater the penetration into the substrate. Its units are the inches (‘’).

- **Resolution (dpi)**.

In the case of a marking, the resolution translates into the quality of the final result, according to the number of pixels. The higher the resolution imposed by the laser, the less pixelated the marking will be and, therefore, the higher the visual quality. Its units are the dots per inch (dpi).

In Figure 59 it is possible to see several different types of lenses, with the example of 1.5’’, 2.5’’ e 4.0’’ lenses. In Figure 60, for the specific case of the 2.0’’ lens, there is a schematic representation of the focal length as a function of the laser incidence. The yellow point is incident on the substrate, and the half below that point is the penetration into the specimen.

Figure 59 – Types of lenses (adapted from [88])

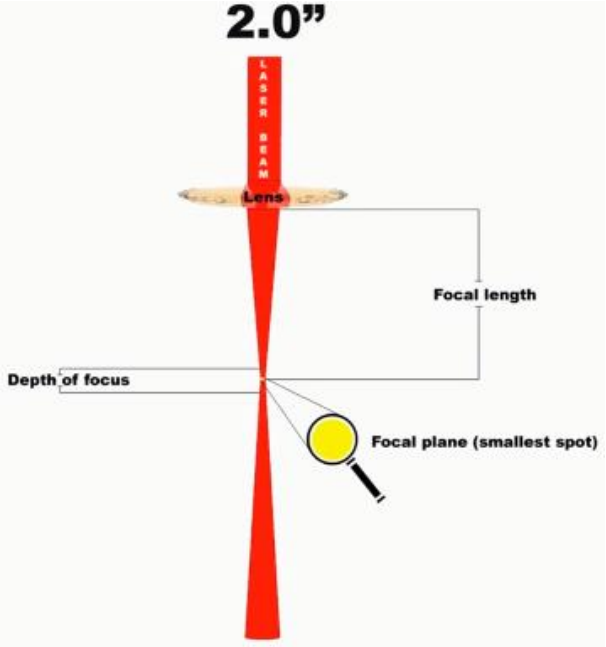

Figure 60 – Focal length (adapted from [88])

3.3 Results

The experiments carried out regarding this dissertation can be categorized in numerous different branches and the scheme present in Figure 61 summarizes them, as the samples converge into an optimal solution with the dissertation's progression.

Speaking in terms of the complete perspective of this project, there is an overall of 21 ceramic tiles used. On their surface, 153 defects were provoked, being 81 pinholes and 72 cracks which, added to the 24 markings, result in 177 samples. Of these, only 154 samples were conducted with laser because, in the end, some of the planned defects were not tested. After the experiments came the analysis step, beginning with a visual inspection to all the 154 samples, through the naked eye. As the ink left some of the defects after the laser interaction, and due to the repetitive nature of this analysis, the colourimeter was only applied to 70 samples. Then, of those, 27 were observed over the optical microscope and 22 were submitted to quality tests. In this last group, there were 3 specimens subjected to the autoclave, being one the standard and the other two with 9 defects each (19 samples in total) and 1 specimen for the ABS test, to analyse the remaining 3 samples. Finally, and at the same time the quality experiments were happening, 5 proceeded to the electronic microscope, finishing the experimental analysis. Appendix 6 contains a synthetic table setting in perspective every experiment done in this practical work, including all the different analysis carried out.

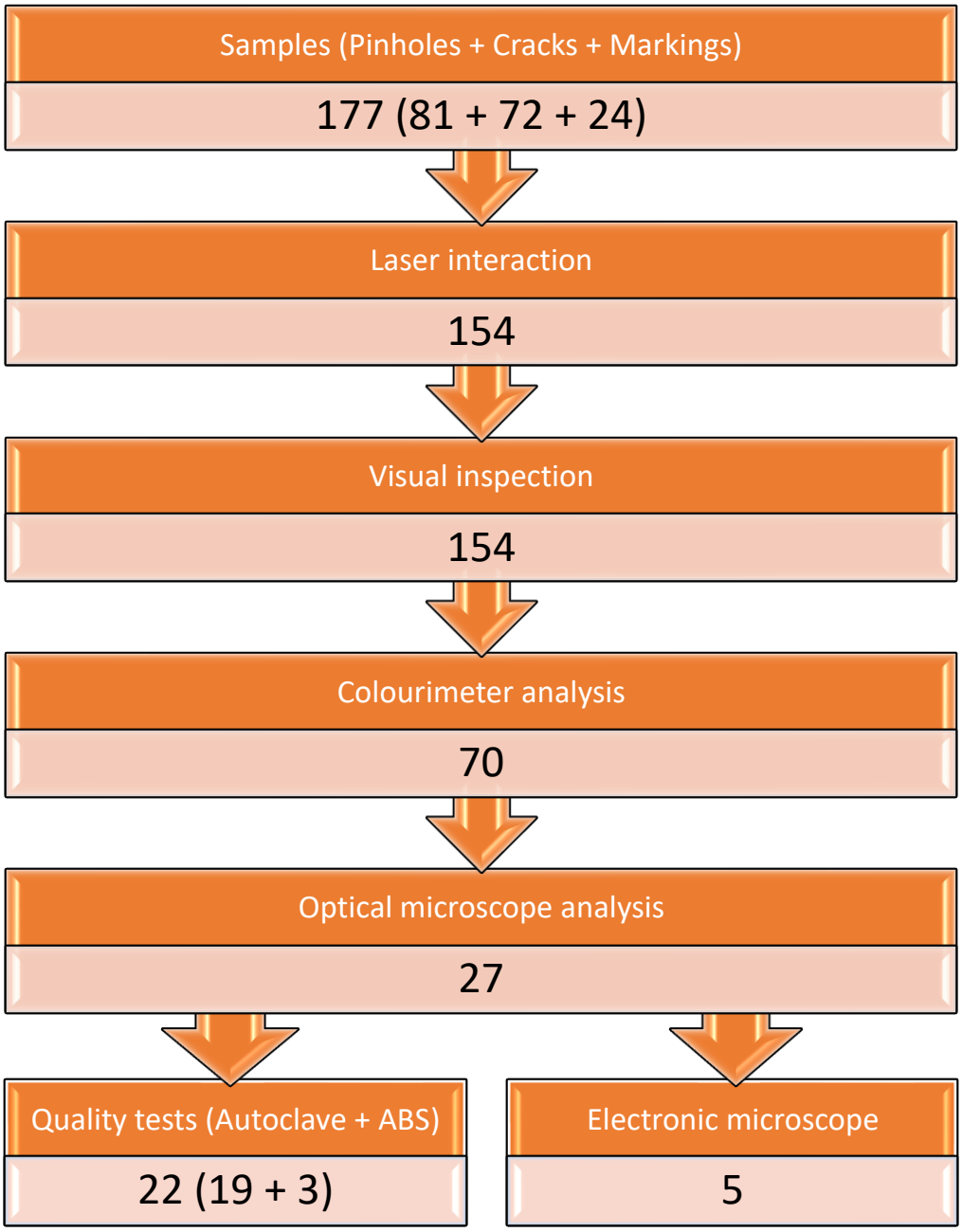

Figure 61 – Representative scheme of the number of realized experiments

3.3.1 Experiments conducted with laser

The laser system utilized for the experimental side of the dissertation, as mentioned before, was the Trotec SP1500 model. This machine, which belongs to the TABOR company, possesses an "L" shaped *gabarit*, a metallic sheet, employed to keep the specimen in the correct position, visible in Figure 62. Through a controlled (x, y) coordinate system in the computer's software, JobControl, the laser point began to focus on the (0, 0) coordinate, manually defined, and with the support from a previously established computational drawing of the defects disposition in the specimen, the laser performed its irradiation in an automatic way.

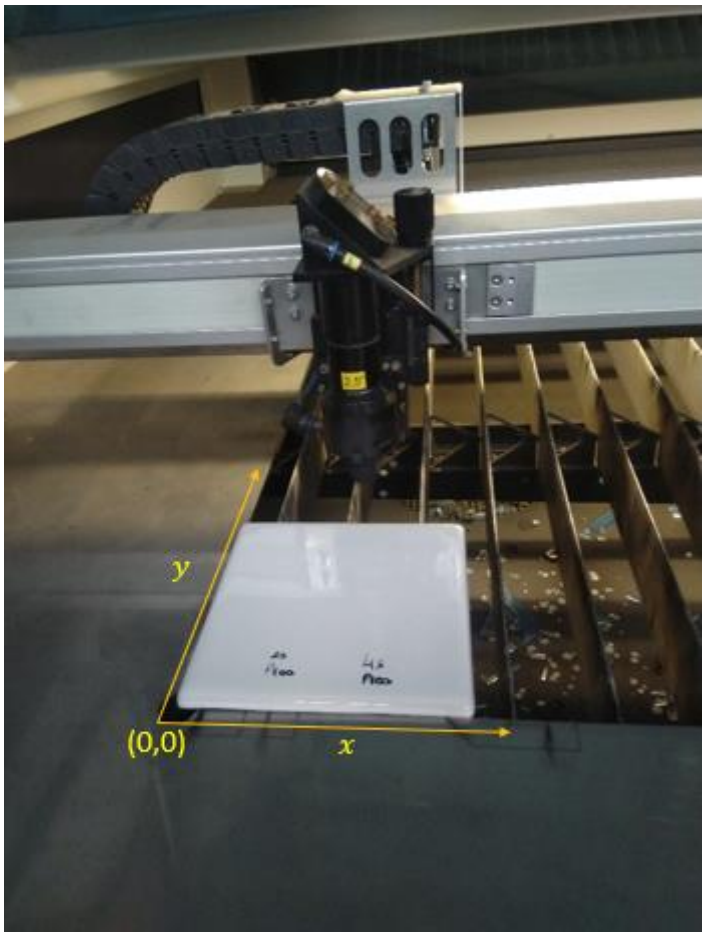

Figure 62 – Laser *gabarit*

When referring to the laser irradiation, the system in question can be operated according to two different approaches:

- **Manual firing (pulsed wave)** – This method is represented by a single firing from the laser system. The beam focuses for a specific duration only on a specific point, for instance a pinhole, placed directly underneath it. Due to safety reasons, each manual firing only lasts for up to ten consecutive seconds; so, if the objective is to extend the incidence time, the manual firings have to be carried on for as long as it's necessary. The corresponding parameters for this methodology are the Laser Power and the Incidence Time.

- **Rapid firing (continuous wave)** – This approach, on the other hand, requires the computer software programming, JobControl, for the laser to work. This is mostly used in larger samples, such as cracks or logotype markings; however, in some cases, it can also be employed in pinholes, focusing on two or more at a time, for just one is too small for this type of interaction. The beam starts at one edge of the crack and repeatedly moves along the *x* axis, slowly moving on the *y* axis, always at the same pre-defined speed, firing the whole sample in stages, instead of directly in one take. The parameters which vary in this method are the Laser Power and the Beam Speed.

As described before, a Manual Firing is one of the laser system's functions, acting solely on a predefined position and performing the beam incidence in a single point, as represented in Figure 63.

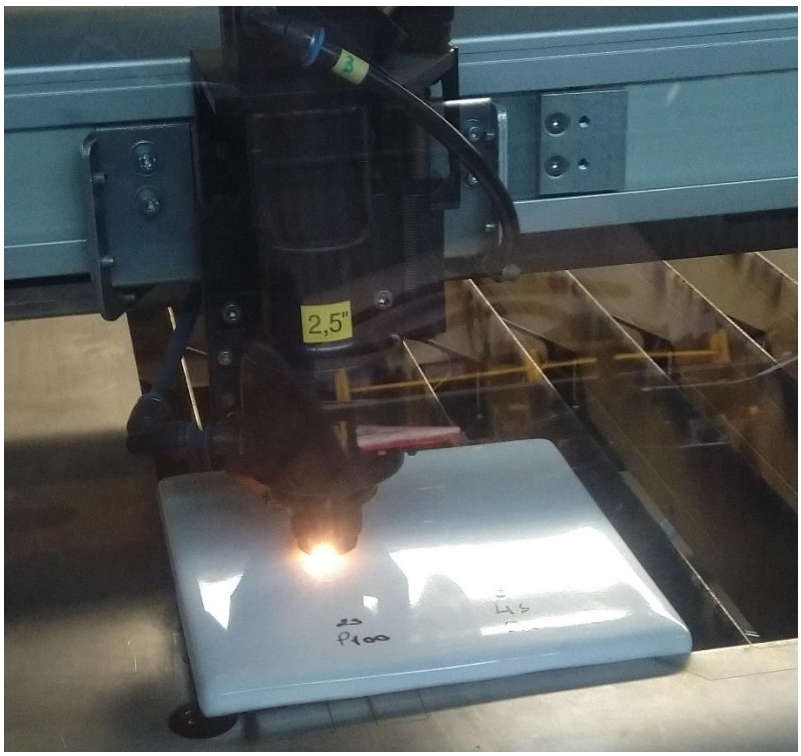

Figure 63 – Manual Firing

On the other hand, Rapid Firing stands as a speed-based function of the laser system's operational set, covering a pre-defined course depending on the samples' geometry. This feature is shown in Figure 64.

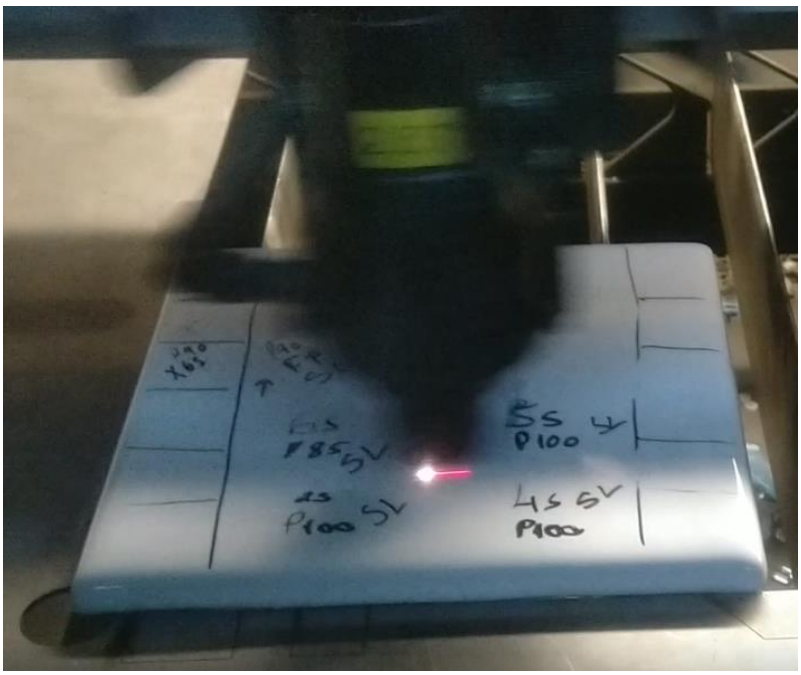

Figure 64 – Rapid Firing

In Figure 65 one may observe an illustration regarding the two types of laser irradiation mentioned above. The red vertical line represents the laser beam. On the left, the manual firing case: it stays above the defect (blue circle) without moving and fusing just the hitting point (red circle). As for the situation on the right, the rapid firing, there are red arrows depicting the path described by the laser beam, covering the defect (blue rectangle) from the top to its bottom.

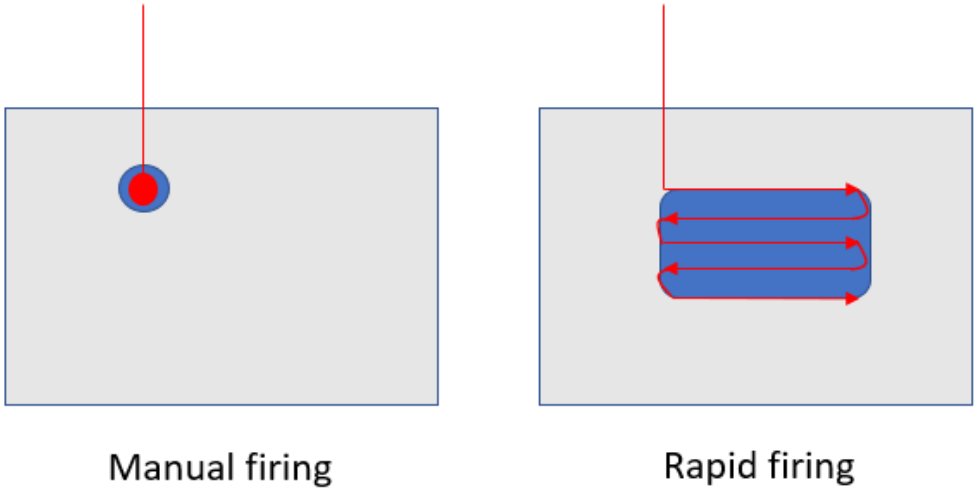

Figure 65 – Types of laser irradiation

The experiments are divided into six different groups, which are established in Table 7.

Table 7 – Experiments' order according to the glaze formulation

Number	Type of ink/glaze employed
1	Regular glaze + Frit
2	Grey marking ink with ethyl alcohol
3	White marking ink with ethyl alcohol
4	White marking ink with diluted PL960
5	White marking ink with concentrated PL960
6	Additional experiments

Each of the listed experiments will be displayed and carefully explained in the following sub-chapters. It is relevant to outline that when the experiments began, there were two different kinds of variables: the laser system parameters and the glaze formulation.

- For this reason, in the first step came the regular glaze and the frit (**1**), both used in a daily basis in the ARCH facilities for the sanitary ware hot recovery.

- Afterwards, the main objective was to unveil the laser's parameters, so a grey ink was used (**2**), which has a wide application in ceramic sanitary ware laser markings.

- As the colour intended was white, the following step was to use a white ink, for the same reason as the one before. Then, and because this ink had good results, came

the preparation of the mixture, when the experiments passed through several different aqueous media, such as ethyl alcohol (**3**), diluted PL960 (**4**), concentrated PL960 (**5**) and finally the additional experiments (**6**), which encompasses one specimen with diluted PL960 and another with ethyl alcohol, as these represented the best results up until that stage.

Considering this determined order and given that each experiment had between two and four specimens in which the laser irradiation was tested, there is a second item relating to the number of the specimen in the same experiment. Lastly, and so as to identify the sample (defect or marking) inside each ceramic tile, a third item was created. In short, a codification comprising three sets of values **(a, b, c)** was arranged in order to refer easily to any given sample, among the 177 in total, where the three factors taken into consideration were the type of the experiment **(a)**, the specimen's number **(b)** and the sample's position **(c)**.

For instance, Figure 66 is referring to the fourth specimen of the third experiment (3,4).

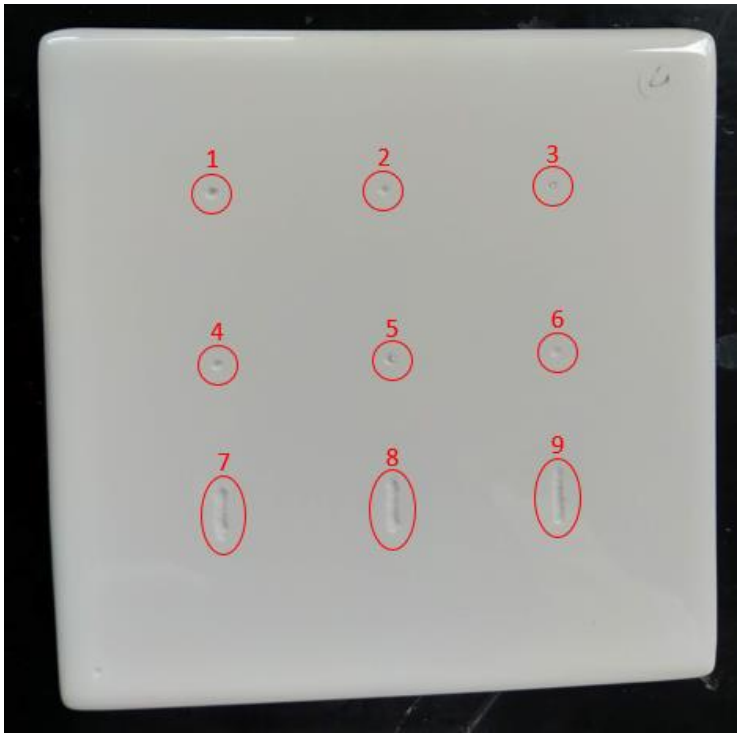

Figure 66 – Specimen (3,4) defects disposition

Considering the ceramic tile mentioned before, it has a total of nine defects, disposed in a 3x3 scheme. As this specimen is identifiable by the (3,4) code, in order to mention each of its defects, it's only necessary to add the respective position that defect occupies in the tile (the **c** coordinate), exactly like depicted in Table 8. This particular specimen starts with the pinhole which goes by the (3,4,1) coordinates and finishes at the (3,4,9) crack, at the other end.

Table 8 – Specimen (3,4) defects position scheme

(3,4,1)	(3,4,2)	(3,4,3)
(3,4,4)	(3,4,5)	(3,4,6)
(3,4,7)	(3,4,8)	(3,4,9)

The experiments with the laser result in a **qualitative classification**. Through the naked eye or even through microscopic analysis only an approximate evaluation can be achieved for the repaired defects' quality. On the other hand, when the colourimeter device is applied to the samples, a **quantitative grading** is permitted, since it can be expressed in numbers, a more precise method, if a defect is well repaired or not, after the exposure to the laser system.

In respect to the parameters used on every experiment, based on the already given description for each one, their practical terms are split in the following:

- **Laser power**

The power source for the laser machine used in this project is 200 W and the power read in its screen is expressed in percentage of the system's maximum power; therefore, for instance, if the appearing value is P25, the actual laser power corresponds to 50 W, and so on.

- **Incidence time (MF)**

The incidence time is only appliable with the manual firing (MF) option. If the incidence time is T20, for example, this means the laser was fired twice in the same spot, each of which had a ten second strike. On the other hand, the incidence time may be 3xT10, meaning that the incidence was in a crack and there were three strikes of ten seconds each, covering the whole crack in three points.

- **Beam speed (RF)**

The beam speed, in turn, is appliable in the rapid firing (RF) situation. The same way as the laser power, this system's maximum beam speed is 1.65 m/s. If the beam speed is V10, the actual beam speed of the laser is 10% of 1.65 m/s, so 0.165 m/s.

- **Focal length (Lens use)**

The default focal length for the laser system is 2.5 inches (2.5''). There was an exception in which the focal length was altered, so as to watch the effect this factor had. Alongside this, there was also the lens factor. During the experiments, some samples had no lens (NL) involved, and in the others a 2.5'' or a 5'' lens (WL) was used.

- **Resolution (marking)**

The resolution is a parameter only applicable on the laser marking system. In this project, the marking was only tested with the grey ink and the values employed were 333 and 1000 dpi.

3.3.1.1 Regular glaze and frit (1)

To begin with the experimental section, the first step was to test the laser in small, provoked defects, namely pinholes. This set of trials included four ceramic tiles: the first two included the defects filled with regular glaze (fusing at 1200 ℃) and the remaining two were filled with frit (fusing at 900 ℃). Both of these formulations are present in ARCH daily to perform the sanitary ware hot recovery in the kiln, reason why they were considered for the laser technique trials.

Figure 67 presents the first tile experimented. It had a small problem, as it broke near defect number six due to poor handling, but it was possible, nevertheless, to fill in and test the twelve pinholes originally intended.

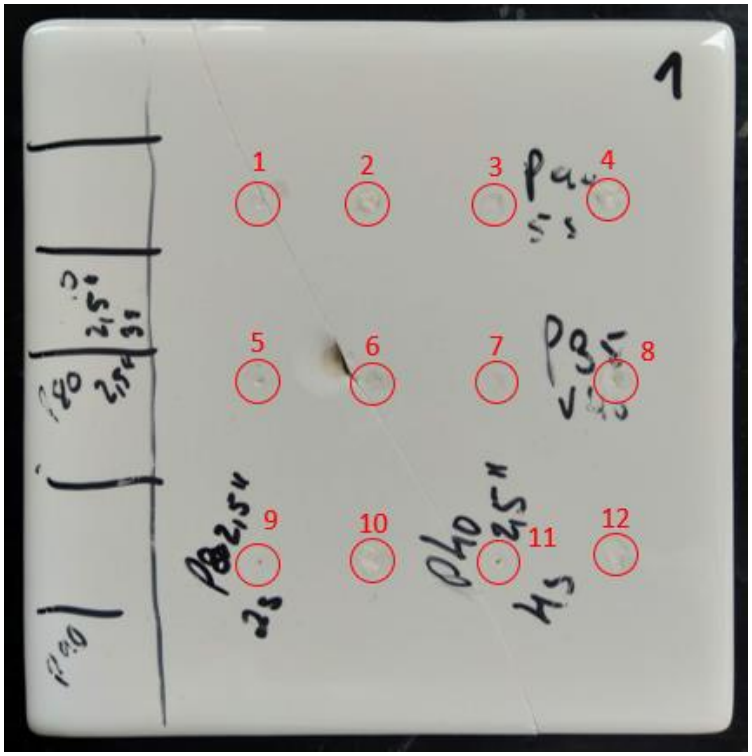

Figure 67 – Specimen (1,1)

Firstly, as visible in Figure 67, left side, the laser was irradiated on a specimen defect free zone, in order to be perceptible to which laser powers the tile would not suffer any alteration. This method ensured that when the glaze was being fused, in the defect zone, the surrounding area would not be affected. Therefore, the objective was to evaluate the maximum power the base material supported without suffering modifications. Firstly, low laser powers were tested, such as P5 and P10. However, as they had no impact on the specimen, in a step-by-step basis, higher laser powers were chosen, resulting in a P35 being the highest value to which there was no thermally affected area.

Afterwards, the laser incidence was performed in the provoked defects, varying the laser power and incidence time parameters, considering that in the first specimen of each formulation – (1,1) and (1,3) – no lens was employed; however, in the second tile – (1,2) and (1,4) – a 2.5'' lens was used.

Figure 68 represents the second specimen, tested with regular glaze and a 2.5'' lens, reason why the defects are pierced, comparing to the first tile. In the lower left corner, there are three additional samples (7, 8 and 9) whose objective was to test different focal distances, although the result was not as clear as intended.

Figure 68 – Specimen (1,2)

The two remaining tiles, both with frit-filled defects, repeated the first half of the experiment's procedure. The first one had twelve pinholes, alongside some other testing directly in the specimen, as represented in Figure 69.

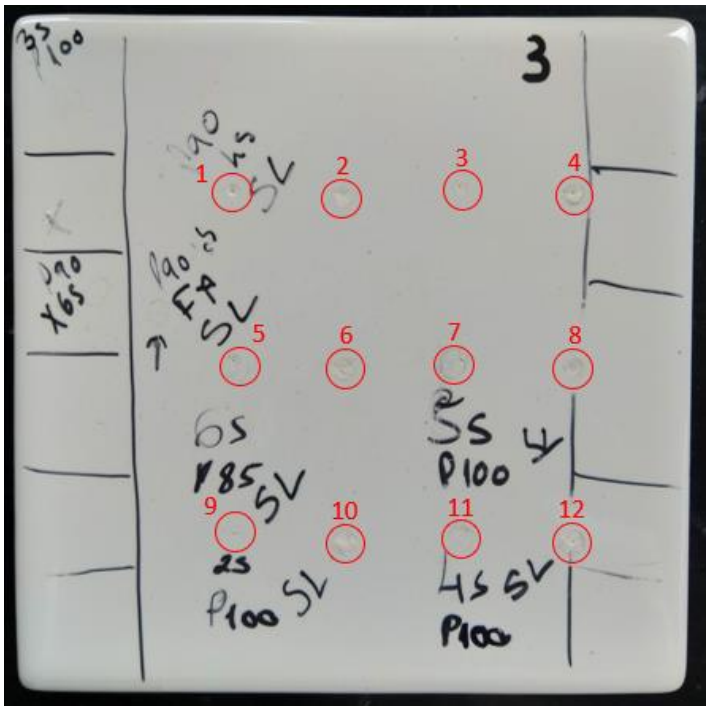

Figure 69 – Specimen (1,3)

The last specimen for these trials, Figure 70, which had a 2.5'' lens use, in addition to its six defects filled with frit had also an extra sample, number 7, that was an engraving directly in the tile's surface, an introduction for the following experiments.

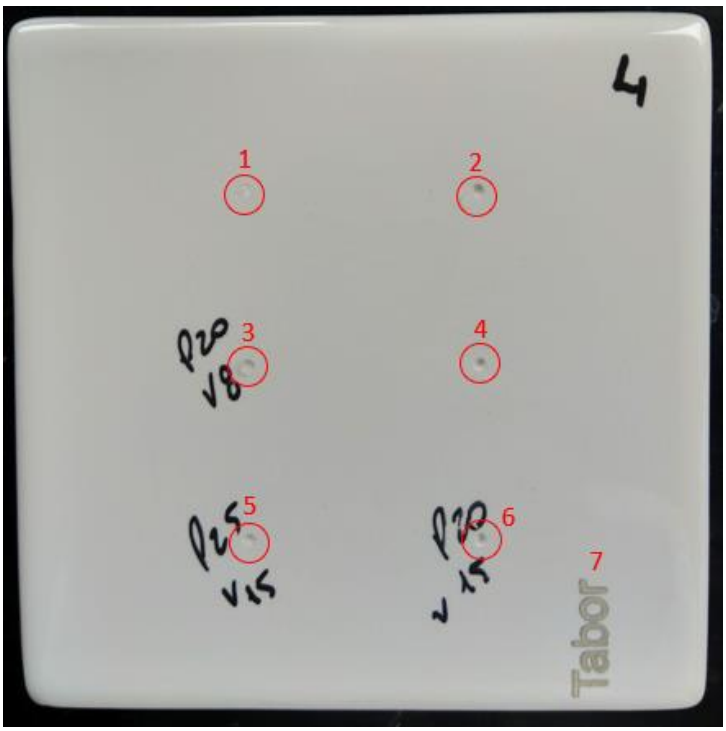

Figure 70 – Specimen (1,4)

When it comes to the results, these were the first experiments conducted, so naturally no perfect score was achieved, as there were many different variables to test. Nonetheless, the best results were:

- **Regular glaze (1,1,8)**

  P35; V45 (RF); WL (2.5'')

  Comment: Although the result was good, it was not achieved in the first try, being the accumulation of several incidences over the same defect with different laser powers. In this case, the beam speed (V) was employed to the entire pinhole row (5, 6, 7 and 8), moving across the line and firing each time it passed over one of the defects.

- **Frit (1,2,1)**

  P45; T10 (MF); NL

  Comment: The frit boiled and partially fused; however, visually there was a notorious difference compared to the remaining tile, besides a thermally affected zone.

- **Frit (1,2,5)**

  P80; T5 (MF); NL

  Comment: It was possible to verify that the frit boiled, though it did not fuse with the rest of the glaze, as it left the defect afterwards, leaving the defect exposed. There was also a thermally affected zone.

Problems encountered:

- There was no comparative term, so it was a very time-consuming, trial-and-error process to vary the different laser parameters in order to be able to boil and fuse the glaze in the defect area;

- Sometimes there were tests in which the laser was not positioned exactly over the defects, since the positioning was done manually, resulting in the laser only hitting and boiling one portion of the defect (white halo barely visible around Figure 68 first six defects, more noticeable in the optical microscope analysis in Appendix 3). Even in the cases where the positioning was automatic through the coordinate system, the point (0,0) was positioned manually, resulting in the same problem;

- In situations where the laser was completely focused on the glaze and it was possible to boil it, there was no correct adherence to the remaining tile, which shows that it did not fuse.

According to what can be seen in the specimens' photos, there are no great visual differences; however, no defect was completely well repaired. The 2.5'' lens brought only bad results, as it perforated the glaze too much; but it was thought that other factors could also be changed to accommodate the lens' use, for example, by altering the focal length, a method which was tested. This way, the reduction on the tile's interaction zone was compensated by the focal distance raise, increasing it again. Despite this attempt, the results did not differ, as the scale in the laser system for the focal length change is not precise enough for this method to work. Therefore, without the lens use (NL) the results were better than with lens (WL).

3.3.1.2 Grey marking ink (2)

In the same way as explained before, the grey marking ink's purpose was to, contrary to the other experiments, create markings of the name "TABOR", the laser owning company, in the ceramic tiles' surface. This way, because the ink's formulation was already proven to be functional with laser interaction, the only unknown factor was within the laser system's parameters. The main objective for this second row of experiments was to investigate which group of laser parameters best resulted in the logotype marking and subsequently apply them to ink-filled defects.

It was also during this procedure that the statistical methods of the Complete and Fractional Factorial Designs were implemented. The ceramic tiles were divided into eighteen blank spaces (Table 9), each of them intended to store one marking. The original idea was to take three sets of parameters and to vary them in an equal amount throughout the specimen, which are the Laser Power (P1, P2 and P3), the Beam Speed (V1, V2 and V3) and the lens adopted (2.5'' and 5''). Through the relation of these three factors, the first two with three levels and the last with two levels, a total of 3x3x2=18 combinations was achieved.

Table 9 – Grey ink's specimens marking disposition

1	2	3
4	5	6
7	8	9
10	11	12
13	14	15
16	17	18

In spite of this, the practical work often suffers some changes in relation to the predicted in a theoretical view; therefore, this Complete Factorial Design quickly turned out to be just a Fractional Factorial Design. The explanation for this matter is that, halfway through the experiments, it was realized that there was no need to conduct the eighteen tests, as the results were too similar to one another (not good), instead of converging to an optimal solution, which reduced the number of experiments.

Alongside the reduction of the experiments, and by observing the first few trials, a different approach was adopted. In place of varying the required parameters in the same proportion to each other, new values for the parameters were tested mainly due to finding a better solution faster, by deciding on every experiment based on the result and parameters used on the previous one. Besides, another parameter was added, namely the laser resolution, which firstly assumed the standard value, 333 dpi, being then modified to the maximum available, 1000 dpi, aiming for a better marking quality.

Figure 71 refers to the first set of the marking experiments, the (2,1) ceramic tile, contemplating fifteen different markings with the grey ink.

Figure 71 – Specimen (2,1)

Similarly, Figure 72 shows the second tile, consisting of only six marking samples.

Figure 72 – Specimen (2,2)

On the other hand, the third specimen (Figure 73), which was intended for extra samples, should these need to be performed, accomodated only two markings and a test in the lower right corner done directly in the ceramic tile.

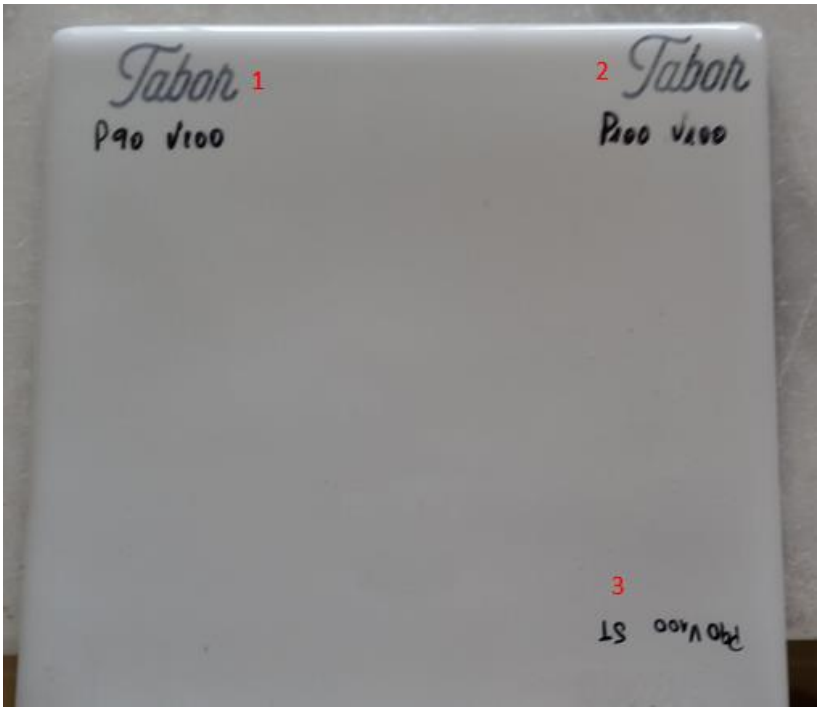

Figure 73 – Specimen (2,3)

Finally, there was also a ceramic tile destined to experiment defects filled with grey ink, just to get the idea of whether the ink would fuse to the remaining specimen or not. The defects in question are pinholes and the six of them are represented in Figure 74.

Figure 74 – Specimen (2,4)

The focal length adopted did not change: 2.5'', and a lens had to be used for the markings. The conditions for these experiments are described in the following tables (Table 10, Table 11, Table 12 and Table 13), being the results explained below each one:

Specimen (2,1)

Table 10 – Specimen (2,1) parameters

1	Lens	2.5''	Laser power	P30
	Resolution	333	Beam speed	V30
2	Lens	2.5''	Laser power	P30
	Resolution	333	Beam speed	V20
3	Lens	2.5''	Laser power	P30
	Resolution	333	Beam speed	V10
4	Lens	2.5''	Laser power	P100
	Resolution	333	Beam speed	V90
5	Lens	2.5''	Laser power	P100
	Resolution	333	Beam speed	V80
6	Lens	2.5''	Laser power	P100
	Resolution	333	Beam speed	V60
7	Lens	2.5''	Laser power	P100
	Resolution	333	Beam speed	V30
8	Lens	2.5''	Laser power	P20
	Resolution	333	Beam speed	V30

9	Lens	2.5''	Laser power	P20
	Resolution	1000	Beam speed	V30
10	Lens	2.5''	Laser power	P100
	Resolution	1000	Beam speed	V30
11	Lens	2.5''	Laser power	P50
	Resolution	1000	Beam speed	V30
12	Lens	2.5''	Laser power	P30
	Resolution	1000	Beam speed	V30
13	Lens	5''	Laser power	P30
	Resolution	1000	Beam speed	V30
14	Lens	5''	Laser power	P20
	Resolution	1000	Beam speed	V30
15	Lens	5''	Laser power	P10
	Resolution	1000	Beam speed	V30

Considering the first whole ceramic tile and its marking experiments, the (2,1,13) and the (2,1,14) undoubtedly originated the best results. On the contrary, the (2,1,15) marking is almost unnoticeable, for the laser power was too reduced in order to be able to fuse the grey ink correctly. The use of the 5'' lens, compared to the 2.5'' one, also brought a better quality to the marking results.

Specimen (2,2)

Table 11 – Specimen (2,2) parameters

1	Lens	5''	Laser power	P25
	Resolution	1000	Beam speed	V40
2	Lens	5''	Laser power	P25
	Resolution	1000	Beam speed	V50
3	Lens	5''	Laser power	P25
	Resolution	1000	Beam speed	V60
4	Lens	5''	Laser power	P30
	Resolution	1000	Beam speed	V50
5	Lens	5''	Laser power	P25
	Resolution	1000	Beam speed	V50
6	Lens	5''	Laser power	P20
	Resolution	1000	Beam speed	V50

The (2,2,1) and (2,2,2) markings showed good results, although the ink was slightly rough. As for the (2,2,3), the beam speed was too high, which transcribed in a less explicit marking. The last three samples were done simultaneously, as the laser beam swept the three at the same time, but with a bad result, concluding that it is preferable to perform each one separately, so that its quality is not negatively affected.

Specimen (2,3)

Table 12 – Specimen (2,3) parameters

1	Lens	2.5''	Laser power	P90
	Resolution	333	Beam speed	V100
2	Lens	2.5''	Laser power	P100
	Resolution	333	Beam speed	V100
3	Lens	2.5''	Laser power	P90
	Resolution	333	Beam speed	V100

It's relevant to underline that the experiments present in this ceramic tile were intercalated with the first one, the (2,1), as the samples (2,3,1) and (2,3,2) were tests for methods used in the first tile. The last sample was another try to observe the difference directly in the specimen's surface.

Specimen (2,4)

The last ceramic tile had six pinholes filled with grey ink, whose experiments were centered around the best parameters used before, notably P25, V50, FL2.5'' , R1000 and WL2.5''. Due to the dark tone of the ink's colour, it was visually hard for the result to be qualified; however, the ink was noted to have fused to the remaining specimen.

The parameters used for this last ceramic tile are present in Table 13. The samples were all tested with the 2.5'' lens.

Table 13 – Specimen (2,4) parameters

1	Laser power	P20	Beam speed	V30
2	Laser power	P25	Beam speed	V40
3	Laser power	P25	Beam speed	V50
4	Laser power	P30	Beam speed	V30
5	Laser power	P30	Beam speed	V40
6	Laser power	P20	Beam speed	V40

The results are converging to around P20/P25/P30 (corresponding to laser powers of 40 to 60 W) and V30/V40/V50 (beam speeds in the 0.495 to 0.825 m/s range), which happens due to the approximation to the correct parameters. Through the naked eye it is possible to see that the ink, although in a dark colour, fused as it should have. The beforementioned laser powers are neither too low for the ink to remain unscathed nor too high to form a thermally affected zone. The same happens with the beam speeds: if these were higher, there would be no time for the ink to fuse and, on the other hand, if they were lower, it would cause the ink to burn or leave the defect. For the explained reasons, these parameters represent values of the most utter importance for the following tests.

3.3.1.3 White marking ink

After the laser parameters for the rapid firing method (RF) were set, it was time to return to the defects' recuperation. In a similar way as the grey marking ink, the white ink employed is used on a daily basis in the ceramic sanitary ware industry to perform the logotype markings in the coloured products. In comparison to the other, this ink has an advantage of being of the same colour as the specimen in which it is put, revealing even in naked eye whether the recovery process through laser technology had a satisfying result or not.

That being said, three different aqueous mediums were experimented to mix with the white powder and create a proper ink to fill the defects:

- **Ethyl alcohol**

Figure 75 shows an ethyl alcohol bottle, side by side with the white powder and a metallic spatula for the mixture.

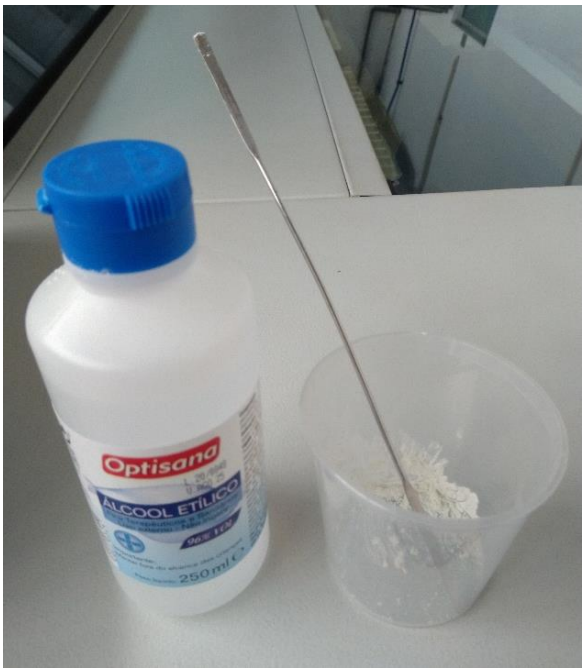

Figure 75 – White ink formed with ethyl alcohol

- **Diluted PL960**

The PL960, seen in Figure 76, is a compound prepared in laboratory which, when diluted, assumes a really liquid and transparent form, remaining with a white colour after mixing with the powder in the box.

Figure 76 – White ink formed with diluted PL960

- **Concentrated PL960**

On the other hand, concentrated PL960 is not so liquid and so it assumes a pink colour after interacting with the white powder, mixture visible in Figure 77.

Figure 77 – White ink formed with concentrated PL960

3.3.1.3.1 Ethyl alcohol (3)

The first experiments with the white powder and ethyl alcohol mixture comprised four ceramic tiles, both containing small defects, i.e., pinholes, and larger ones, the cracks, whose dimensions were a 3 mm diameter for the first group and 3 mm per 13 mm for the latter, approximately.

Figure 78 represents the first specimen for this set of tests. Due to a micro fissure within it, the tile broke at the very first test. However, the experiments continued exactly as planned for the remaining defects. In addition, only the first six samples were tested, because the intention was to finish the pinholes' tests before beginning with the cracks.

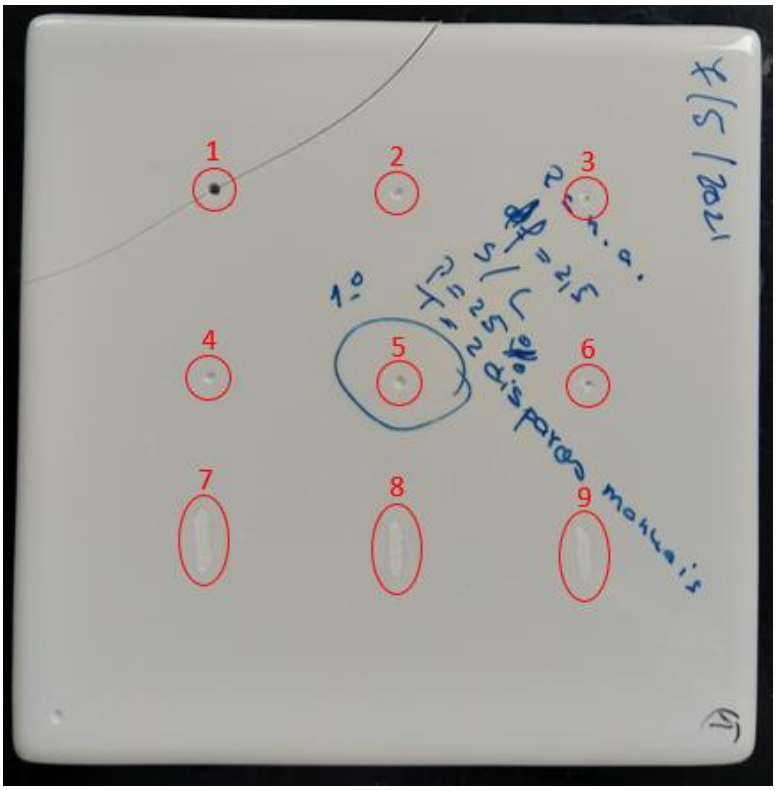

Figure 78 – Specimen (3,1)

As for the second specimen (Figure 79), as opposed to the previous, all nine defects were experimented, although the last three (cracks) were still at a beginning phase, reason why the parameters' choice for these was not the best one, as the point was to observe the laser's reaction to the manual firing (MF) method in larger samples.

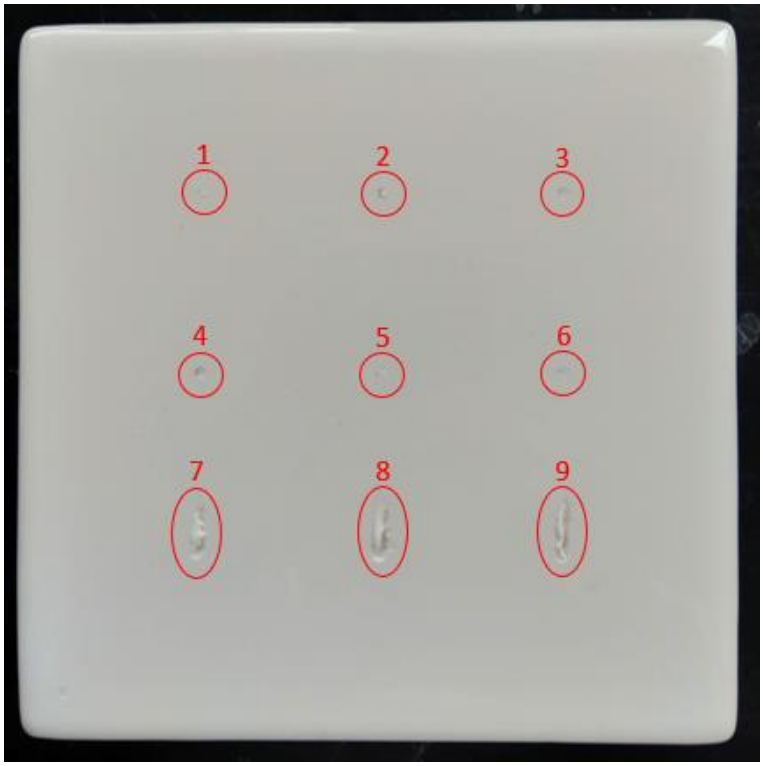

Figure 79 – Specimen (3,2)

Like the specimen (3,1), in the (3,3) tile only the pinholes were tested, leaving the cracks filled with the white ink, but not experimented, fact demonstrated in Figure 80.

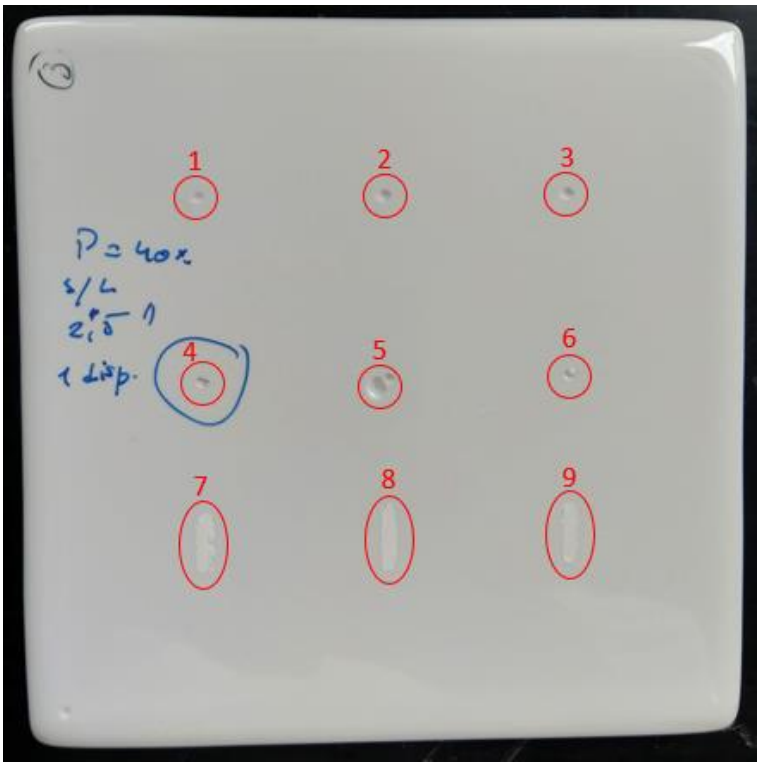

Figure 80 – Specimen (3,3)

Lastly, the fourth ceramic tile of these tests, in Figure 81, was the closing one for this specific set, having its final three defects provoked, but not filled with any kind of ink.

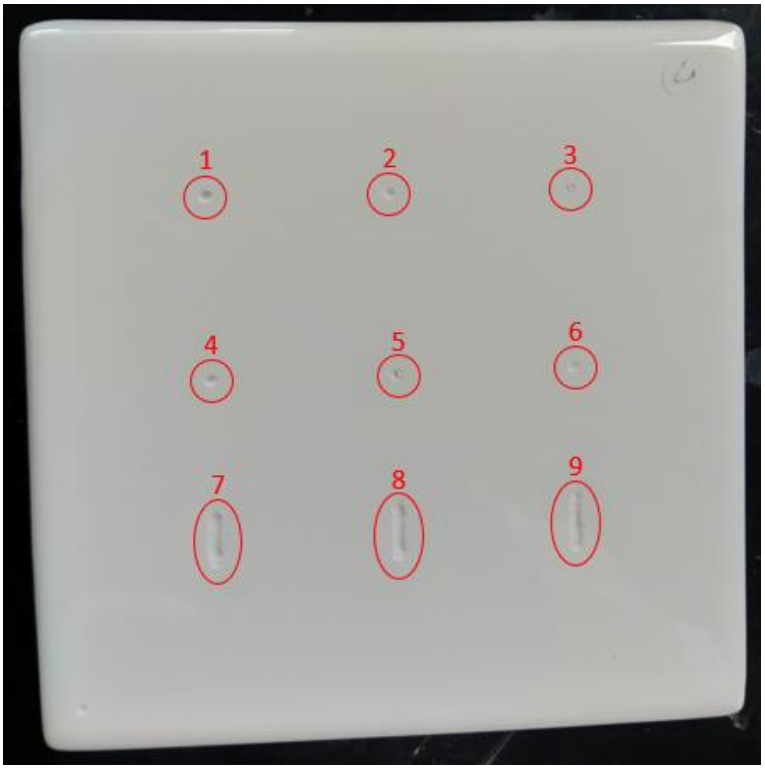

Figure 81 – Specimen (3,4)

The main point of these experiments was to continue and conclude part of the pinholes' tests. Although they were not finished up until this time, the results obtained revealed that the parameters employed were practically correct. It was also decided to experiment on cracks; however, only the (3,2) specimen had them tested. In spite of this, the tests done on the fissures were just to get a hint of how it would look, since the real crack experiments started with the diluted PL960, the fourth set of experiments.

In the upcoming tables (Table 14, Table 15, Table 16 and Table 17), the results for the previous specimens are shown.

Specimen (3,1)

Table 14 – Specimen (3,1) results

1	Laser Power	P60	Incidence time	T5	Lens	WL (2.5'')
	Comment	The tile broke due to a micro fissure within it.				
2	Laser Power	P30	Incidence time	T3	Lens	WL (2.5'')
	Comment	The laser pierced the ink in the defect.				
3	Laser Power	P30	Incidence time	T5	Lens	WL (2.5'')
	Comment	The laser pierced the ink in the defect.				
4	Laser Power	P25	Incidence time	T5	Lens	NL
	Comment	The laser pierced the ink in the defect.				
5	Laser Power	P25	Incidence time	T20	Lens	NL
	Comment	The laser fused the ink, but this one lowered a little.				
6	Laser Power	P25	Incidence time	T5	Lens	WL (2.5'')
	Comment	The laser pierced the ink in the defect.				

The (3,1,5) sample was the best, since the ink fused correctly, although it lowered a little. In order to overcome this problem, in the (3,2) specimen the defects were filled with an ink excess (Figure 79), instead of up until the tile's surface, so that when it lowered, the result would translate in the ink fused at the specimen's surface.

Specimen (3,2)

Table 15 – Specimen (3,2) results

1	Laser Power	P25	Incidence time	T30	Lens	NL
	Comment	The ink fused and spread correctly.				
2	Laser Power	P35	Incidence time	T30	Lens	NL
	Comment	The ink fused, but a bubble was formed.				

3	Laser Power	P35	Incidence time	T30	Lens	NL
	Comment	The ink fused, but lowered a little.				
4	Laser Power	P30	Incidence time	T20	Lens	NL
	Comment	The ink fused, but lowered.				
5	Laser Power	P30	Incidence time	T30	Lens	NL
	Comment	The ink fused and spread correctly.				
6	Laser Power	P35	Incidence time	T30	Lens	NL
	Comment	The ink fused, but lowered a little.				
7	Laser Power	P25	Incidence time	3xT30	Lens	NL
	Comment	The ink fused, but a bubble was formed.				
8	Laser Power	P25	Incidence time	3xT30	Lens	NL
	Comment	The ink fused, but a bubble was formed.				
9	Laser Power	P25	Incidence time	3xT30	Lens	NL
	Comment	The ink fused, but a bubble was formed.				

Specimen (3,3)

Table 16 – Specimen (3,3) results

1	Laser Power	P25	Incidence time	T60	Lens	NL
	Comment	The ink left the defect.				
2	Laser Power	P20	Incidence time	T70	Lens	NL
	Comment	The ink left the defect.				
3	Laser Power	P25	Incidence time	T40	Lens	NL
	Comment	The ink left the defect.				
4	Laser Power	P40	Incidence time	T10	Lens	NL
	Comment	The ink fused, but lowered a little.				
5	Laser Power	P40	Incidence time	T20	Lens	NL
	Comment	The ink left the defect.				
6	Laser Power	P40	Incidence time	T10	Lens	NL
	Comment	The ink fused, but a bubble was formed.				

The main purpose of the (3,3) experiments was to test whether high incidence times would be helpful in fusing the ink better. It's important to outline that whenever the time was above T10, it means that several laser firings were performed and that this number was directly related to the conclusion taken from the previous firing. Put simply, every time a firing was done, the ceramic tile was removed from the laser system and the respective sample analysed, and so, when the incidence time had high values, it meant that the ink had not received enough heat to fuse and had to be tested again.

Moreover, a problem emerged: the red spot in the tile and the fusing point were not completely concentric, due to the lack of lens. Consequently, the fourth specimen was experimented using a 2.5'' lens (increasing the focus) but, at the same time, reducing the focal length, so that the incidence area remained unaltered to compensate.

Specimen (3,4)

In this specimen, the focal length used was of 2.3'', instead of the 2.5'' value used in every other ceramic tile.

Table 17 – Specimen (3,4) results

1	Laser Power	P25	Incidence time	T3	Lens	CL (2.5'')
	Comment	The ink left the defect.				
2	Laser Power	P15	Incidence time	T10	Lens	CL (2.5'')
	Comment	The ink left the defect.				
3	Laser Power	P5	Incidence time	T10	Lens	CL (2.5'')
	Comment	The laser pierced the ink in the defect.				
4	Laser Power	P5	Incidence time	T10	Lens	CL (2.5'')
	Comment	The laser pierced the ink in the defect.				
5	Laser Power	P5	Incidence time	T20	Lens	CL (2.5'')
	Comment	The laser pierced the ink in the defect.				
6	Laser Power	P10	Incidence time	T15	Lens	CL (2.5'')
	Comment	The ink left the defect.				

Despite the assumption initially thought, the lens used did not have a good result; on the contrary. As the laser beam was converging to a single point, most of the outcomes revealed the ink pierced, which is the opposite to the objective intended to accomplish. By the tests conducted until this point, the conclusion was that the lens used negatively affects the laser sanitary ware recovery process, being then discarded hereafter.

Another factor that could not have been entirely correct is the ink formulation, which is why the next experiments introduced a new medium to mix with the white ink: diluted PL960.

3.3.1.3.2 Diluted PL960 (4)

The diluted PL960 set of experiments only consisted of two specimens, each one containing nine provoked defects: six cracks and three pinholes.

The target in these tests was the opposite to the previous ones. While the experiments conducted with the ethyl alcohol medium mixed with the white ink focused on the pinholes' experiments and just had a few cracks to begin testing, the current set reversed the defects' disposition and gave priority to the fissures' samples. Since the pinholes already had most of the experiments dedicated to them, resulting in good conclusions achieved, the focus up until the end of the project was centred in the cracks.

It is visible in Figure 82 that the first six samples have not fused enough and with the naked eye seem not to have been tested at all, in spite of every defect having suffered a laser interaction.

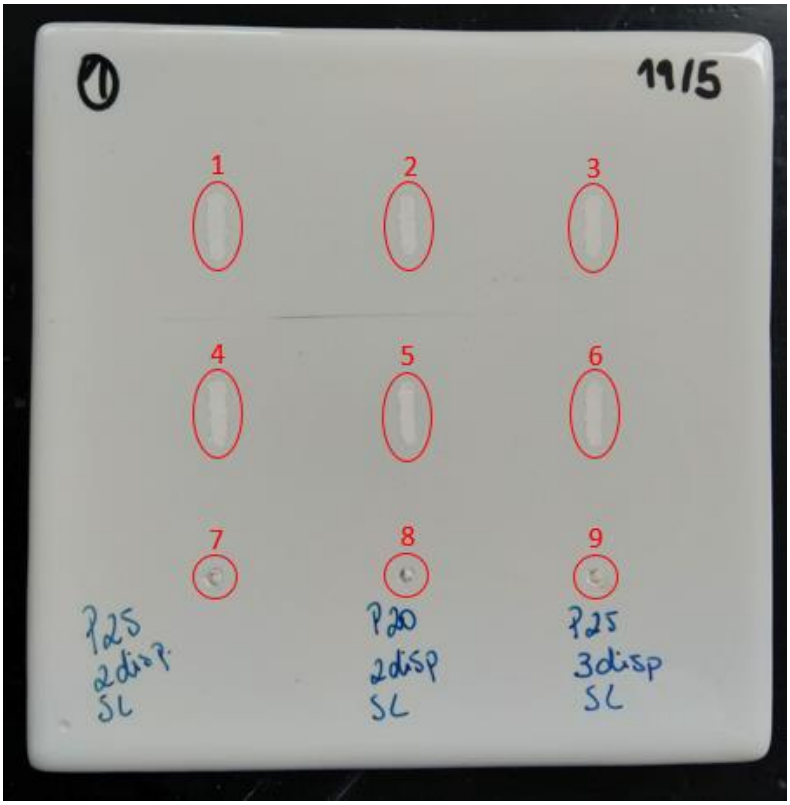

Figure 82 – Specimen (4,1)

By regarding Figure 83, one may see the second ceramic tile, whose fourth sample did not end well, as the heat applied to it was too strong, leaving a dark mark.

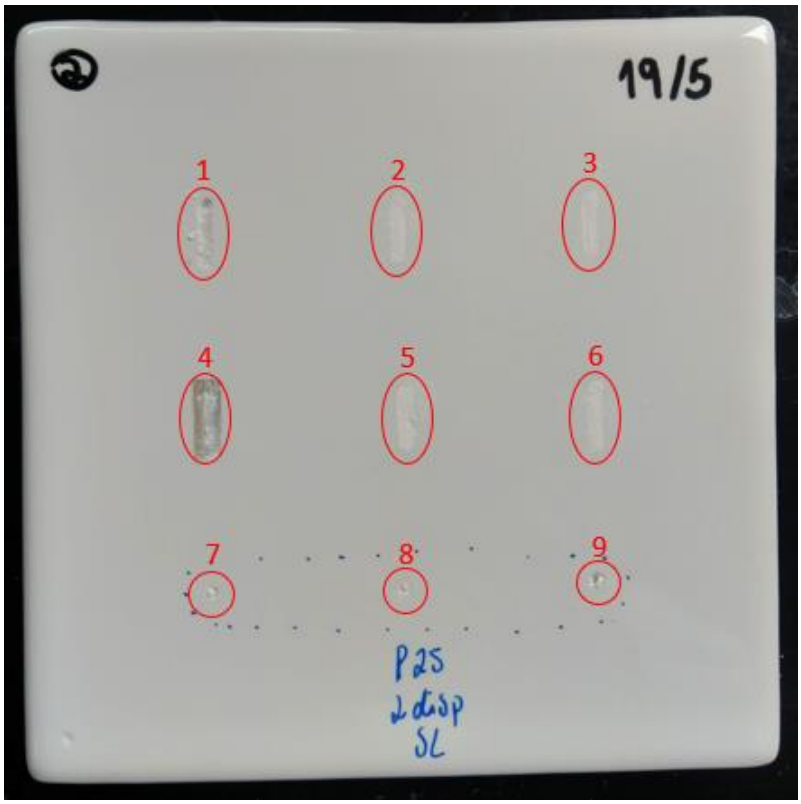

Figure 83 – Specimen (4,2)

The pictures of the current set of experiments undoubtedly show that, as expected, the first testing in cracks did not have the best results. However, the pinholes present at the bottom of the tiles, the last three samples of each one, fused very well, with the only drawback of sometimes forming a small bubble and not spreading perfectly.

This way, the best results in this set arised for the following parameters (Table 18):

Table 18 – Specimens (4,1) and (4,2) parameters

Pinholes						
(4,1,7)	Laser power	P25	Incidence time	T30	Lens	NL
(4,1,8)	Laser power	P20	Incidence time	T20	Lens	NL
(4,1,9)	Laser power	P25	Incidence time	T20	Lens	NL
(4,2,7)	Laser power	P25	Incidence time	T20	Lens	NL
(4,2,8)	Laser power	P25	Incidence time	T20	Lens	NL
(4,2,9)	Laser power	P25	Incidence time	T20	Lens	NL
Cracks						
(4,2,1)	Laser power	P20	Beam speed	V30	Lens	NL

The main objective of this set of experiments was to test the cracks; however, it could not have been worse. Every crack tested in the first specimen almost did not boil, let alone fuse with the tile. This is explained by the low values chosen for the parameters, as it was thought that if the laser power or incidence time was too high, for example, the samples would burn, as ultimately happened to the (4,2,4) sample. The (4,2,1) crack had a good reaction, fusing correctly, but after the laser incidence the ink left the defect, meaning that the recovery did not last long, probably due to the high beam speed, for the ink heated too fast. On the other hand, the pinholes for both of the specimens had good results, fusing well, despite having formed small bubbles in general.

After these results, the tests with other formulations persisted, moving forward to the same compound, PL960, but slightly different, i.e., concentrated instead of diluted. Alongside this, the parameters' values optimisation proceeded as well.

3.3.1.3.3 Concentrated PL960 (5)

The concentrated PL960, as stated before, conferred the ink a pink colour. This affected the experiments negatively, because the laser incidence in the pink ink originated its burning, leaving dark marks inside the ink, which assumed a colour completely different from the desired one, and black lines around the provoked defects, i.e., a black halo which ruined the experiments. Nevertheless, conclusions could be withdrawn from these results, which helped carrying out the testing until the end.

In Figure 84 is shown the first specimen with the concentrated PL960, to whose constitution was added zinc borate.

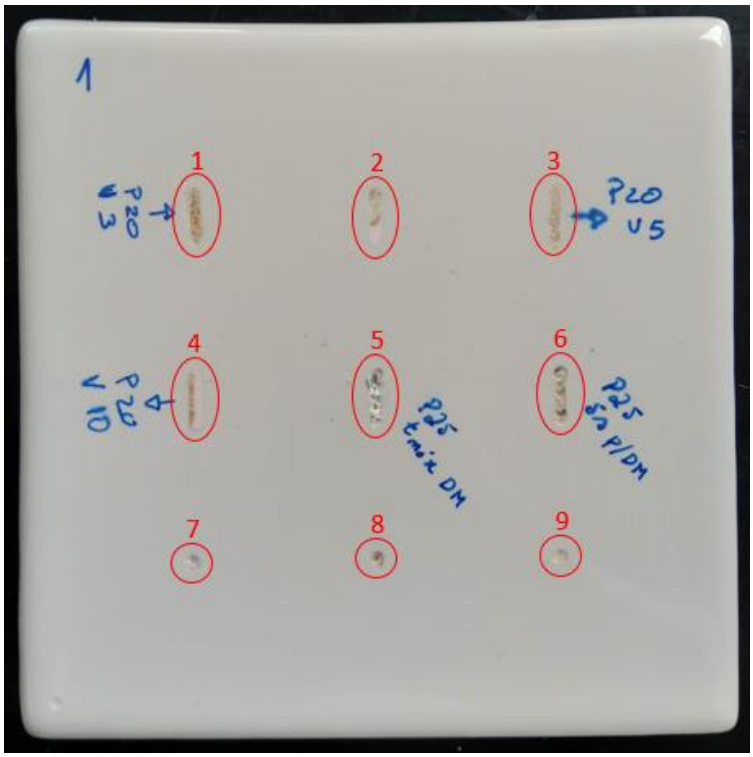

Figure 84 – Specimen (5,1)

Afterwards comes the second specimen, present in Figure 85.

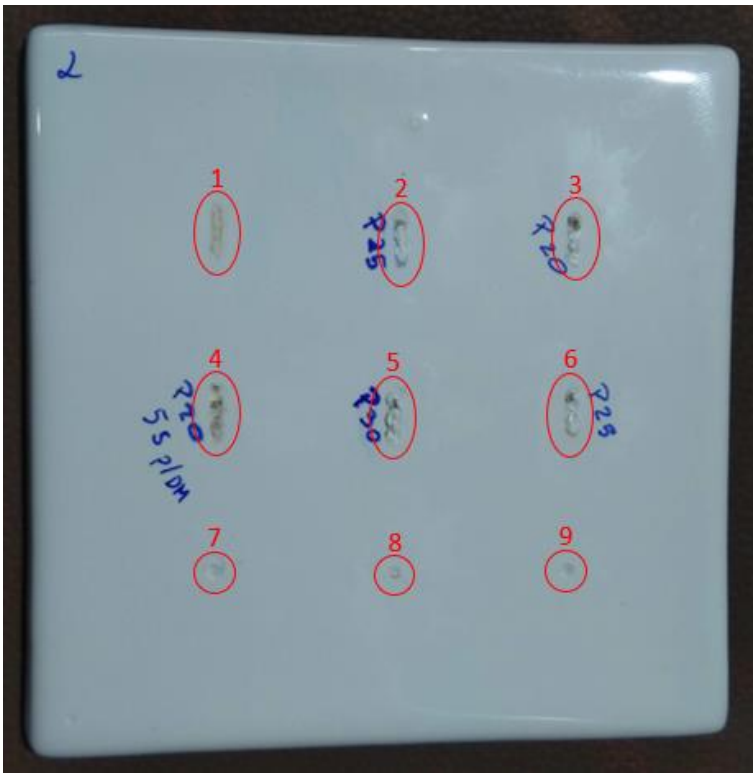

Figure 85 – Specimen (5,2)

In Figure 86 stands the third specimen, concentrated PL960 with zinc borate, like the first one.

Figure 86 – Specimen (5,3)

Finally, Figure 87 represents the fourth and last specimen with the concentrated PL960.

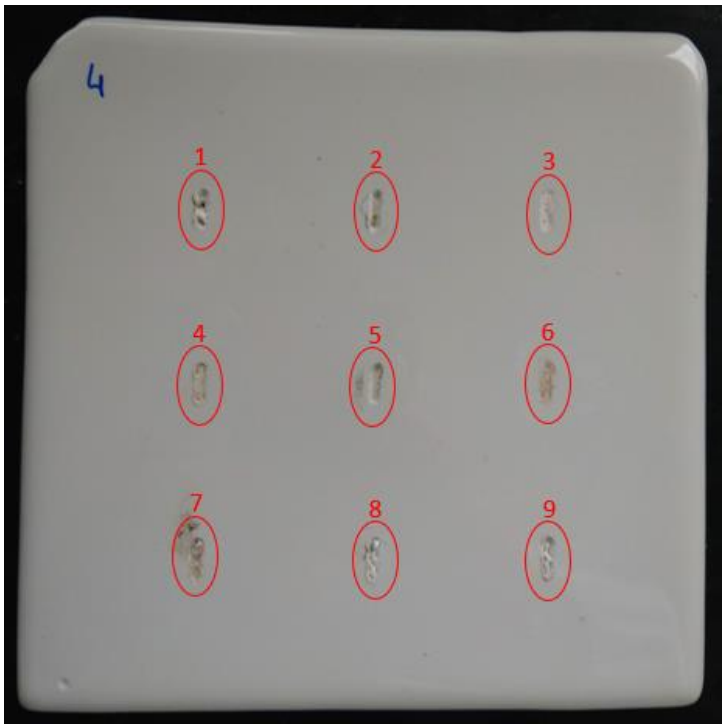

Figure 87 – Specimen (5,4)

As an attempt to overcome the ink bubble forming problem after the laser irradiation, two different formulations were tested:

- Concentrated PL960 with zinc borate;

  This was tested in specimens (5,1) and (5,3).

- Concentrated PL960 without zinc borate;

  This was tested in specimens (5,2) and (5,4).

The zinc borate's purpose was to reduce the superficial tension of the ink, so that it would not form a bubble but instead make it spread correctly.

The results for the shown pictures of the ceramic tiles in this subchapter are described in detail in the following tables (Table 19, Table 20, Table 21 and Table 22).

Specimen (5,1)

Table 19 – Specimen (5,1) results

1	Defect	Crack	Laser power	P20	Beam speed	V3
	Comment	The ink burned.				
2	Defect	Crack	Laser power	P20	Beam speed	V3
	Comment	The ink shredded a little.				
3	Defect	Crack	Laser power	P20	Beam speed	V5
	Comment	The ink burned.				

4	Defect	Crack	Laser power	P20	Beam speed	V10
	Comment	The ink burned.				
5	Defect	Crack	Laser power	P25	Incidence time	3xT10
	Comment	The ink remained white, but formed bubbles.				
6	Defect	Crack	Laser power	P25	Incidence time	3xT5
	Comment	The ink burned.				
7	Defect	Pinhole	Laser power	P25	Incidence time	T10
	Comment	The ink left the defect.				
8	Defect	Pinhole	Laser power	P15	Incidence time	T10
	Comment	The ink burned.				
9	Defect	Pinhole	Laser power	P10	Incidence time	T10
	Comment	The ink didn’t fuse.				

Specimen (5,2)

Table 20 – Specimen (5,2) results

1	Defect	Crack	Laser power	P20	Beam speed	V3
	Comment	The ink didn’t fuse.				
2	Defect	Crack	Laser power	P25	Incidence time	3xT10
	Comment	The ink remained white, but formed bubbles.				
3	Defect	Crack	Laser power	P20	Incidence time	3xT10
	Comment	The first firing burned, but the others didn’t, spreading well.				
4	Defect	Crack	Laser power	P20	Incidence time	3xT5
	Comment	The ink burned in every firing.				
5	Defect	Crack	Laser power	P30	Incidence time	3xT10
	Comment	The ink remained white, but formed a dark line.				
6	Defect	Crack	Laser power	P25	Incidence time	3xT10
	Comment	The first firing burned, but the others didn’t, spreading well.				
7	Defect	Pinhole	Laser power	P25	Incidence time	T10
	Comment	The ink left the defect.				

8	Defect	Pinhole	Laser power	P25	Incidence time	T10
	Comment	The ink left the defect.				
9	Defect	Pinhole	Laser power	P25	Incidence time	T10
	Comment	The ink left the defect.				

In the (5,1) and (5,2) specimens' results, almost every sample suffered the same problems, which were the thermal shock due to the laser interaction in the cold tile's surface, causing an ink burn in the first firing. The remaining ones caused the ink to fuse well, since the defect was already heated.

On the other hand, in the (5,3) specimen only five experiments were carried out, because the results were not converging to a good solution.

Specimen (5,3)

Table 21 – Specimen (5,3) results

1	Defect	Crack	Laser power	P25	Incidence time	3xT20
	Comment	The ink left the defect.				
2	Defect	Crack	Laser power	P25	Beam speed	V5
	Comment	The ink burned.				
3	Defect	Crack	Laser power	P10	Incidence time	3xT10
	Comment	The ink burned.				
4	Defect	Crack	Laser power	P15	Incidence time	3xT10
	Comment	The ink left the defect.				
5	Defect	Crack	Laser power	P40	Incidence time	3xT10
	Comment	The ink burned and formed bubbles.				

There was an attempt, in the fourth ceramic tile of this set of experiments, to prevent the black halo to appear around the defects. By performing a first firing, with a low laser power, i.e., P5, and a moderate beam speed, V10, it was expectable to raise the specimen's temperature in order not to register a thermal shock when doing the laser incidence; however, this method didn't work and the tile kept being affected.

Specimen (5,4)

Table 22 – Specimen (5,4) results

1	Defect	Crack	Laser power	P25	Incidence time	3xT10
	Comment	The ink formed bubbles.				
2	Defect	Crack	Laser power	P25	Incidence time	3xT10
	Comment	The ink left the defect.				
3	Defect	Crack	Laser power	P20	Beam speed	V10
	Comment	The ink didn't fuse.				
4	Defect	Crack	Laser power	P30	Beam speed	V5
	Comment	The ink didn't fuse.				
5	Defect	Crack	Laser power	P40	Beam speed	V5
	Comment	The ink left the defect.				
6	Defect	Crack	Laser power	P50	Beam speed	V20
	Comment	The ink didn't fuse.				
7	Defect	Crack	Laser power	P25	Beam speed	V5
	Comment	The ink burned.				
8	Defect	Crack	Laser power	P25	Incidence time	3xT10
	Comment	The ink formed bubbles.				
9	Defect	Crack	Laser power	P20	Incidence time	3xT10
	Comment	The ink formed bubbles.				

The specimens (5,3) and (5,4), besides burning the ink from the laser interaction, both formed dark lines around the defects, a black halo surrounding the samples, appearing due to the thermal shock. This phenomena happens as a consequence of the formulation employed in this set of experiments, the concentrated PL960, which clearly did not fulfil the requirements needed to correctly fuse the ink and repair the defects.

Beyond the concentrated PL960 being a notoriously bad choice for the composition of the white ink with the objective of fusing it with the laser interaction, the zinc borate addition to the ink did not reveal any important difference, as the ink formed bubbles almost in the same amount in every specimen, whether with zinc borate or not.

The best recorded results with this formulation, although still far from the intended, were the P25 and 3xT10 parameters, which were the main focus for the following and last experiments, the sixth set. Alongside this, the formulations employed during the experimental tests which had the best outcomes were chosen, intended to promote the best results in the final specimens, namely the diluted PL960 and the ethyl alcohol.

3.3.1.3.4 Additional experiments (6)

The additional experiments, as explained before, consist of two ceramic tiles with nine provoked defects each.

The first tile's defects are filled with diluted PL960 mixed white powder (Figure 88).

Figure 88 – Specimen (6,1)

The second specimen's defects have white powder mixed with ethyl alcohol (Figure 89).

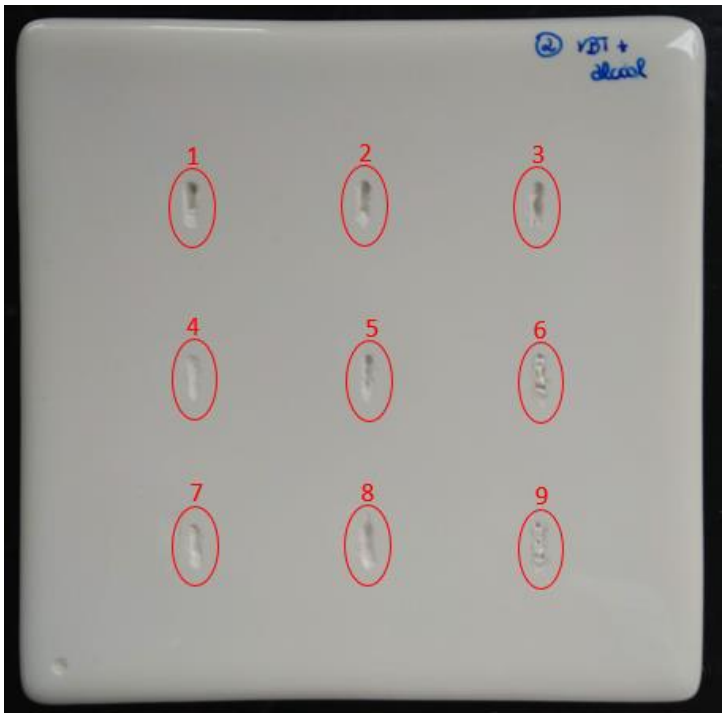

Figure 89 – Specimen (6,2)

The results for these experiments are shown in Table 23 and Table 24.

Specimen (6,1)

Table 23 – Specimen (6,1) results

1	Laser power	P25	Beam speed	V10
	Comment	The ink didn't fuse due to the high beam speed.		
4	Laser power	P25	Beam speed	V5
	Comment	The ink left the defect.		
7	Laser power	P30	Beam speed	V5
	Comment	The ink left the defect.		
2	Laser power	P30	Beam speed	V3
	Comment	The ink left the defect.		
5	Laser power	P30	Beam speed	V1
	Comment	The ink left the defect.		
8	Laser power	P25	Beam speed	V2
	Comment	The ink left the defect.		
3	Laser power	P27	Beam speed	V3
	Comment	The ink left the defect.		
6	Laser power	P27	Beam speed	V3
	Comment	The ink left the defect.		
9	Laser power	P27	Beam speed	V2
	Comment	The ink left the defect.		

This particular specimen did not have good results. Although the ink fused in some samples, in the end it would always leave the defect exposed, as it did not remain attached to the tile.

The reason why the experiments were carried out in a specific and apparently not orderly way, is that the laser treatment had to be in a horizontal disposition, so the specimen suffered a 90° counter clockwise rotation, starting the laser incidence in its lower line and progressively going up the ceramic tile. This method was applied to both this set's specimens.

Specimen (6,2)

Table 24 – Specimen (6,2) results

1	Laser power	P28	Beam speed	V3
	Comment	The ink shredded.		
4	Laser power	P28	Beam speed	V3
	Comment	The ink shredded.		
7	Laser power	P28	Beam speed	V3
	Comment	The ink shredded.		
2	Laser power	P27	Beam speed	V2
	Comment	The ink left the defect.		
5	Laser power	P30	Beam speed	V3
	Comment	The ink left the defect.		
8	Laser power	P35	Beam speed	V3
	Comment	The ink left the defect.		
3	Laser power	P25	Incidence time	3xT10
	Comment	The ink left the defect.		
6	Laser power	P20	Incidence time	3xT10
	Comment	The ink formed a bubble, but spread well.		
9	Laser power	P15	Incidence time	3xT10
	Comment	The ink spread very well, despite small bubbles.		

One of the problems felt during the additional experiments was the laser positioning in comparison to the workpiece. As every defect was a crack and most of the testing was done with the rapid firing function, the programming had to be done through the computer and the JobControl software. This meant drawing the cracks in the software, alongside their disposition in the ceramic tile, which was not always easy because of the small dimensions and the laser system's sensibility.

Nevertheless, in spite of the obstacles, none of the samples showed a dark halo or heat affected zones, a sign of progression in relation to the previous tests. The best results arose with the ethyl alcohol medium, namely samples (6,2,6) and (6,2,9), characterized by laser powers of P20 and P15, respectively, side by side with three manual firings of ten seconds each through the crack. When the laser interacted with the white ink, the alcohol evaporated, making the wet ink fuse inside the defect, at the same time it featured a less rough surface and spread correctly.

3.3.2 Colourimeter analysis

When it comes to the colourimeter analysis, this device was used several times in the resulting samples of the laser experiments. However, many defects had their ink leave the hole after the laser interaction or not fusing at all, reason why the total number of defects analyzed in the colourimeter was only 54, from the initial 153. In addition, three extra samples were also considered, to widen the understanding of these tests, i.e., a crack with the ink that had not been tested with the laser interaction (initial form) and one defect of each (pinhole and crack) whose ink disintegrated, being the analysis done directly in the non-glazed zone of the ceramic material. On top of these 57 samples were added 13 standard analyses, one for each of the specimens which contained the described defects, because a more veracious result was obtained when the comparison was done in relation to the tile that had the defect. This totalizes 70 analyses with the colourimeter.

Although the standard analyses are all taken from the glazed part of the specimens, which supposedly should have the same colour, the colourimeter is a very sensible device, influenced by little variations from the surrounding environment, and so the values for the different specimen's parameters change among one another. The discrepancy of the values may be explained due to the colourimeter's uncertainty, or by factors such as the light and shadows incurring the ceramic tile, its surface roughness or even this machine's positioning on the specimen. As this is a digital device, its uncertainty is estimated by the gap between two consecutive digital values, therefore, 0.1. There was, however, an effort to reduce this influence, by positioning all the samples under the same light/shadow ratio as possible and also to measure the standard values always in the same zone of each specimen, so as to have equal conditions to every analysis done with the colourimeter.

All this does not mean that the colourimeter is not a reliable or effective method, but instead, that it is natural that some values oscillate a bit and as seen in the following tables (Table 25 and Table 26), the obtained values correspond to the qualitative evaluation made.

Table 25 – Colourimeter values for (3,2) specimen's pinholes

Sample	L*	a*	b*	ΔE*
(3,2)	91.8	0.4	1.3	-
(3,2,1)	91.2	0.3	1.1	0.5
(3,2,2)	91.4	0.2	1.5	0.5
(3,2,3)	91.3	0.3	1.5	0.6
(3,2,4)	91.4	0.2	1.7	0.7
(3,2,5)	91.7	0.3	1.2	0.4
(3,2,6)	91.3	0.2	1.6	0.7

The table for the (3,2) specimen which contains its CIELAB colour space diagram parameters shows that these were some of the best results in respect of the laser recovery process of sanitary ware defects, since their colourimeter reading difference (ΔE^*) to the standard is below or equal to the 0.8 value. This was already seen in the visual inspection, and with the microscopic and detailed analysis it can be proved in a more scientific way. Out of 54 defects analysed, only 20 had the delta value below 0.8.

Nonetheless, the opposite is also true as, for example, the (5,2) specimen had some of the worst results in its cracks due to the ink used, which burned, and these reflected in the colourimeter's reading. In this case, the ink had black and dark pink spots after the laser interaction, which lead to a catastrophic raise in the colourimeter reading difference (ΔE^*) to the respective standard specimen.

Table 26 – Colourimeter values for (5,2) specimen's cracks

Sample	L*	a*	b*	ΔE^*
(5,2)	91.6	-0.1	0.8	-
(5,2,1)	91.6	0.1	0.6	1.6
(5,2,2)	87.3	-0.4	1.0	5.3
(5,2,3)	83.8	0.3	2.7	7.1
(5,2,4)	88.2	1.1	4.2	5.2
(5,2,5)	91.1	-0.3	0.6	1.9
(5,2,6)	87.7	0.4	0.6	3.6

The remaining values for the CIELAB colour space diagram parameters are exposed in Appendix 5.

After this brief summary of the colourimeter analysis, a statistical approach was chosen, performed with the SPSS software [95], in a way of supporting the experimental tests carried out with the laser system, namely the ANOVA (Analysis of Variance) method.

The ANOVA method is a statistical technique which allows to evaluate the means of different populations. It compares the means of two or more factors in respect to a certain characteristic, in order to verify if there is a significant difference between its means and if the factors have any influence on the characteristic in study.

The two-way ANOVA test, used for the statistical analysis of this project, is used for the data collected on a quantitative dependent variable at multiple levels of two categorical independent variables, as well as the interaction between them. A categorical variable represents types or categories of things and a level is an individual category within the categorical variable [94].

The ANOVA tests for significance using the F-test for statistical significance, which is a groupwise comparison test, meaning it compares the variance in each group mean to the overall variance in the dependent variable.

A two-way ANOVA with interaction tests three different situations at the same time, both with a null and an alternate hypothesis, expressed in Table 27:

Table 27 – Hypothesis test in a two-way ANOVA

Null hypothesis (H_0)	Alternate hypothesis (H_0)
There is no difference in group means at any level of the first independent variable.	There is a difference in group means by the first independent variable.
There is no difference in group means at any level of the second independent variable.	There is a difference in group means by the second independent variable.
The effect of one independent variable does not depend on the effect of the other independent variable (no interaction effect).	There is an interaction effect between the first and the second independent variables on group means.

The p-value is the probability of obtaining a test statistic equal to or more extreme than that observed in a sample, under the null hypothesis. For example, in hypothesis testing, one can reject the null hypothesis at 5% if the p-value is less than 5%. This is the most common p-value and will be used for this analysis.

The variables considered for this test and its respective categories are:

- Laser Power (P) – P≤20 ; P=25; P≥30
- Incidence Time (T) – T5; T10; T20; T30
- Beam speed (V) – V3; V5; V10; V20

The three described variables correspond to the laser system's parameters which had an influence of the final outcome, the repaired defects, being the ΔE^* the characteristic in study. The Lens Use parameter wasn't chosen, since from the samples analyzed with the colourimeter, only 6 out of 54 had the lens. For this reason, the data which is subject of the ANOVA test had 48 samples, all of them without lens, as even during the practical experiments it was realized that without lens the results were far better.

All the described categories include the totality of the data within the three variables. The laser power had a higher variance, so its categories were established in intervals, instead of fixed values. Figure 90 represents a boxplot diagram with a 0.8 delta blue line for reference, showing that the laser powers which produced the best results (lower delta) in both types of defects were for values above P30. The P25 laser powers also had a great outcome for pinholes; however, for cracks, its variance was excessively high due to the experiments with the concentrated PL960 ink, which burned with the laser interaction, causing the delta values to rise, as the recovery attempt had a colour far from the intended white.

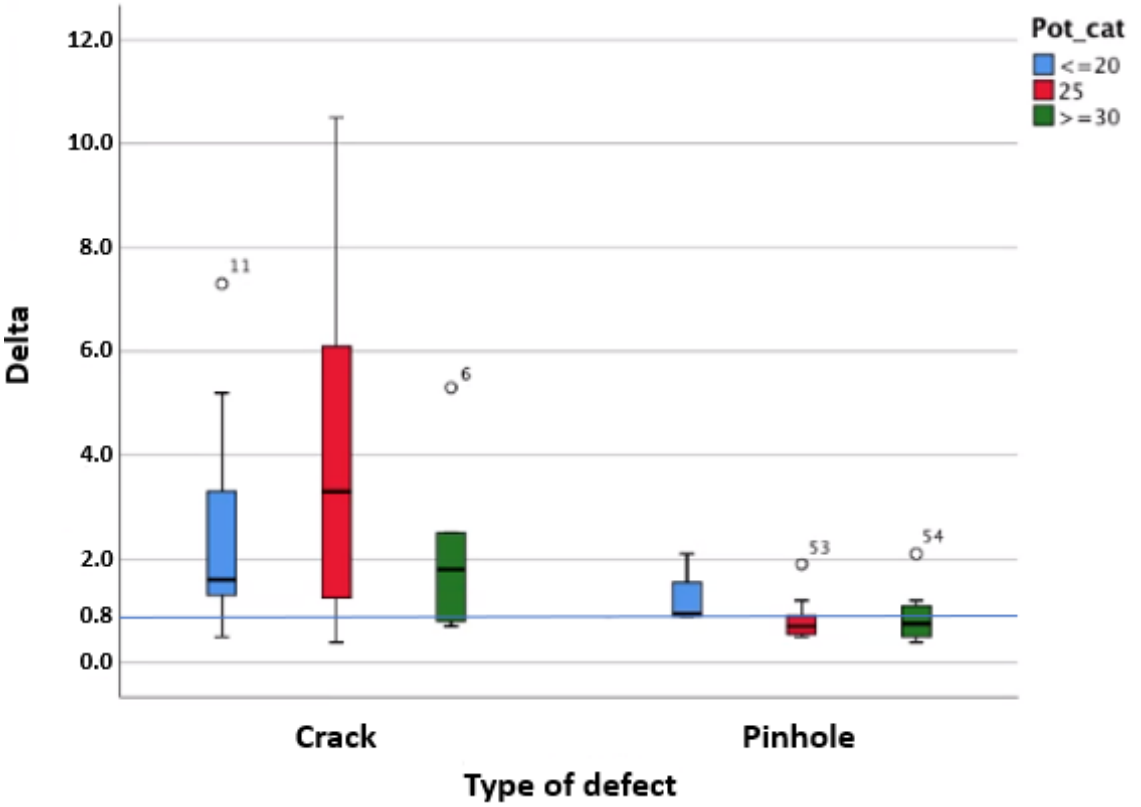

Figure 90 – Influence of the laser power in the delta by type of defect

Considering all the data available and the combined influence of the factors involved in the experiments (Laser power, Beam speed and Incidence time), the results in the delta value for the two types of defects experimented are present in Table 28.

Table 28 – Mean and Variance for the delta value by defect

Crack	Mean		2.8517
	95% Confidence Interval for Mean	Lower bound	1.9322
		Upper bound	3.7712
	Variance		5.8430
Pinhole	Mean		0.9120
	95% Confidence Interval for Mean	Lower bound	0.7129
		Upper bound	1.1111
	Variance		0.2330

These results sustain the graphic representation from Figure 90, in which both the mean and the variance of the pinholes' delta values are much lower than the cracks' ones, meaning that the pinholes had a better recovery ratio with the laser incidence than the cracks. This can also be explained with the set of crack experiments which had a bad ink formulation, resulting in various poor results with the crack defects. A suggestion to improve the recovery processes regarding the cracks is to use, from hereby forward, just

an ink formed by white powder mixed with ethyl alcohol and use the parameters which had a good effect on the pinholes, for then the results with the cracks will certainly be better.

Then, the two-way ANOVA test was performed for two different groups. The first one compared the Laser Power with the Incidence Time, with a total of 35 samples in study, and the second did a comparison between the Laser Power and the Beam Speed, contemplating just 13 samples.

- Laser Power / Incidence Time (Table 29)

Table 29 – Two-way ANOVA test for Laser Power vs Incidence Time

Parameter	F	p-value
Laser Power	0.030	0.971
Incidence Time	3.145	0.043
Interaction	0.904	0.476

The two-way ANOVA test was intended to evaluate if the tested parameters had a significant effect on the ΔE^* values, i.e., if the p-value is lower than 5%. By regarding Table 29, it is possible to see that only the Incidence Time has an impact on the ΔE^* values, whereas the Laser Power and the interaction between these two factors have a high p-value, therefore their variance contributes little to the variance of the ΔE^*.

- Laser Power / Beam Speed (Table 30)

Table 30 – Two-way ANOVA test for Laser Power vs Beam Speed

Parameter	F	p-value
Laser Power	0.652	0.560
Beam Speed	1.087	0.435
Interaction	0.769	0.511

As for the case of Table 30, neither of the two parameters has an impact on the ΔE^* values and not even the interaction between them stands with a significant influence on the colour of the repaired ink-filled defects through the laser recovery process.

This last result is not completely reliable, since it only has 13 samples for analysis. The first ANOVA test had the Incidence Time, which was used for both pinholes and cracks, being the latter test used only for cracks. For this reason, it is understandable why the conclusions considering significance couldn't be completely well drawn. In order to perform an ANOVA test closer to reality, this had to contemplate many more values, for the more data there is, the better is the conclusion.

3.3.3 Optical microscope analysis

An optical microscope was used, after the colourimeter data was statistically analysed, for a specific set of samples' surface and sectional detailed view.

In order to begin this analysis, there was a specimen, the (3,1), which broke during a laser interaction, factor that was actually positive, since the fracture crossed exactly one of the defects, the (3,1,1), revealing its sectional view, seen in Figure 91. The vitrified phase along the pinhole's depth is clearly visible, proving that the laser incidence did not only fuse the superficial zone of the defect, but also its interior. In Figure 92 is a top view of the same sample, resembling the half circle of the defect's geometry and the fused glaze in the middle. These images have 2x and 4x amplification factors, respectively.

In Appendix 3 the retrieved images for the entire set of optical microscope analysis done in the remaining samples may be consulted.

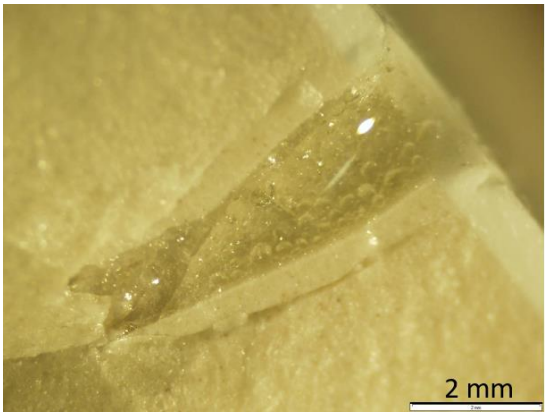

Figure 91 – Sample (3,1,1) microscopic sectional view

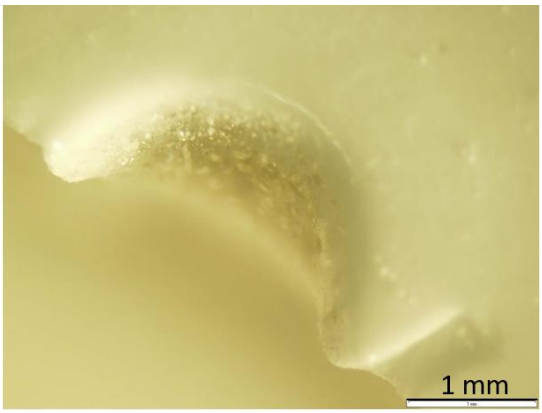

Figure 92 – Sample (3,1,1) microscopic top view

The next defects to be analysed were the (3,2,1) and (3,2,2), with a 4x amplification, present in Figure 93 and Figure 94. The first one shows three distinct zones where the ink did not spread as it should have, marked with faded shadows. The remaining areas, however, present a great fusion of the ink and almost no transition zone to the specimen's glaze. The second pinhole, however, shows more cavities on the left and top sides, but at the bottom the result is also positive, with a good transition zone.

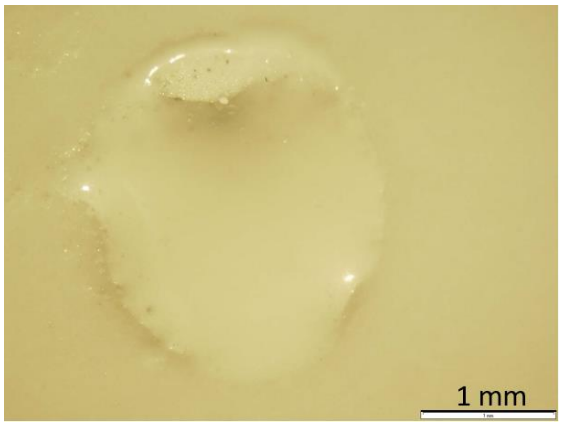

Figure 93 – Sample (3,2,1) microscopic view

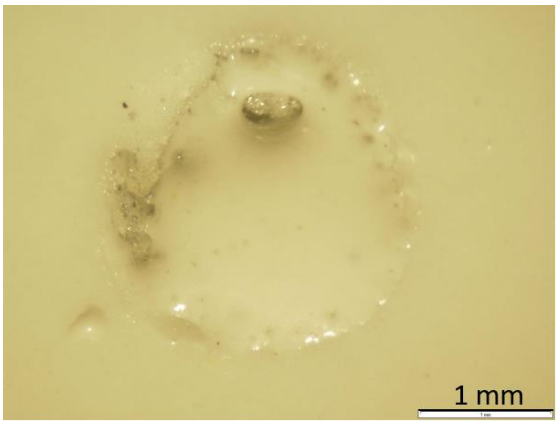

Figure 94 – Sample (3,2,2) microscopic view

In order to finish the set of pinholes, the (3,2,3) and (3,2,5) had results, through the naked eye, as good as or better than the previous shown samples from the same specimen. The following microscopic pictures, Figure 95 and Figure 96, prove this statement, with an almost complete fusion of both of the defects, being the transition from the ink filled defect to the glaze surface of the specimen so smooth that it is barely not visible at a 4x amplification factor. The dark bubbles on the left side of both pictures are a sign of an incomplete ink spread and trapped air presence, which demonstrates that although the result is satisfactory, it is not perfect.

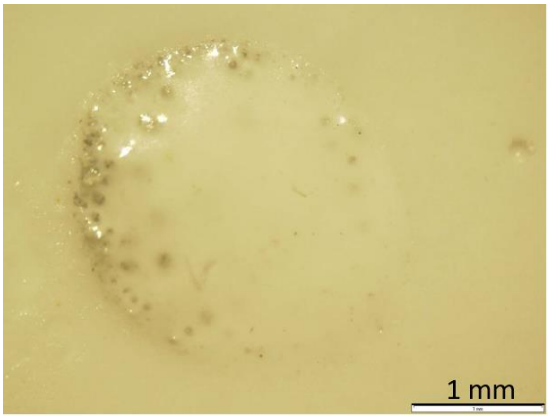

Figure 95 – Sample (3,2,3) microscopic view

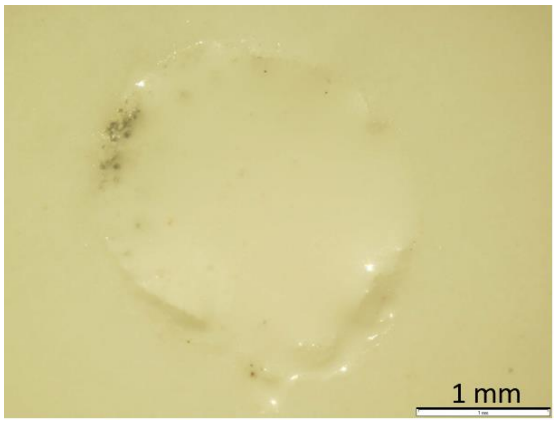

Figure 96 – Sample (3,2,5) microscopic view

Last but not least, it were the cracks which had a greater difficulty in spreading the ink due to the larger geometry of this type of defect. In Figure 97 is represented the (6,2,6) crack and in Figure 98 the (6,2,9) one. As it can be observed, the first crack shows a much smoother ink surface geometry than the second one, which has a rough presentation. This is explained by the fact that the (6,2,6) sample possesses more ink, so when the laser beam performed its irradiation, despite having formed bubbles, the ink maintained the expected configuration. As for the (6,2,9) defect, on the other hand, there is a lack of ink which was deposited above the provoked defect, which led to an ink jump. Either way, the cracks still need more experiments to have a satisfying result, such as performing more tests with the optimal parameters and using the proper ink, which allowed good results in the pinholes.

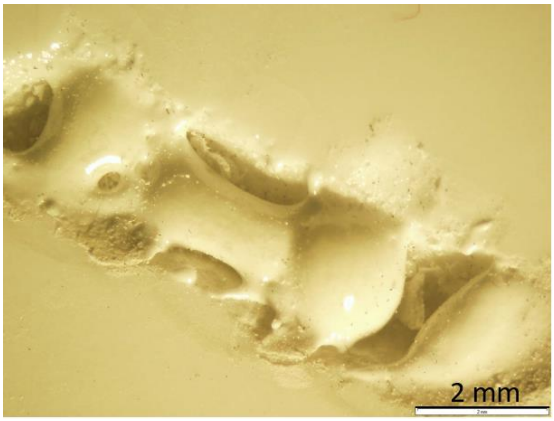

Figure 97 – Sample (6,2,6) microscopic view

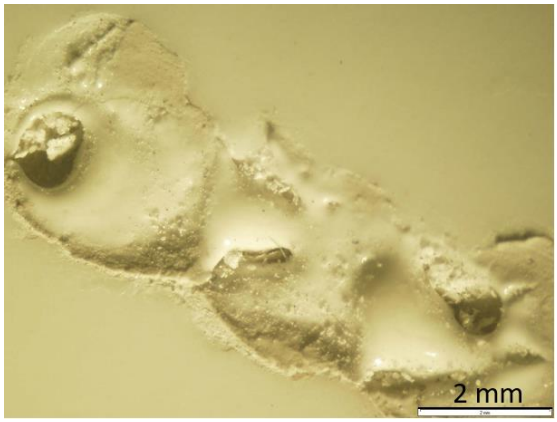

Figure 98 – Sample (6,2,9) microscopic view

3.3.4 Electronic microscope (SEM) analysis

Ceramic tile cutter

As explained earlier, before the SEM analysis begun, the samples' preparation had to be carried out, namely, cutting the 150x150 mm tiles into small cubicles of 3x3 mm maximum, which was done in a ceramic tile cutter tool. Firstly, the tile had to be positioned and scratched with the diamond tip for a notch. Then, a lever was pulled downwards to exert pressure on both of the uncut ceramic tiles' edges, in order to perform an even break throughout the notch and resulting in two separate pieces.

After several repetitive operations with this tool, ten different samples were obtained, being nine of them defects experimented with the laser beam (six pinholes and three cracks) and the last one a standard, with no defect, for comparison. The small samples are represented in Figure 99, alongside the respective codifications for each one.

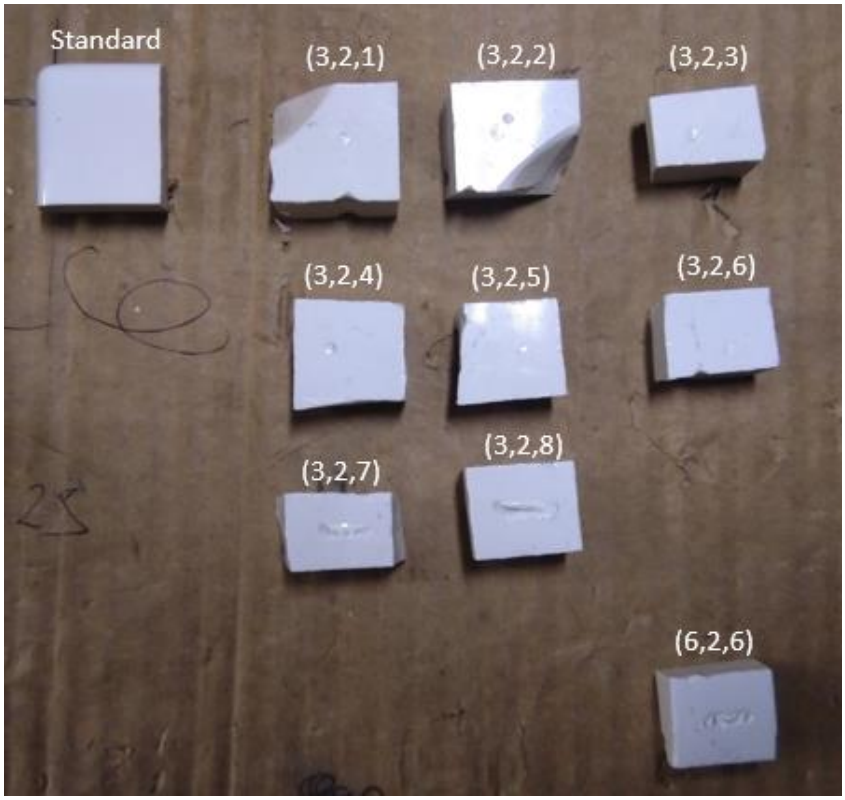

Figure 99 – Ceramic tile cutter finished samples

In spite of this, in the end only five of the ten intended samples were actually analysed over the SEM, due to the reduced time permitted to use this microscope. In this manner, the samples analysed in the SEM were: (3,2,1), (3,2,3), (6,2,6), (3,2,7) and Standard, listed by order of importance considering their defect recovery nature. The Standard sample had to be analysed so as to establish a comparison to the laser-recovered defects. As for the remaining ones, the (3,2,1) defect was almost unnoticeable, just like the (3,2,3), due to their good recover, having just the drawback of having downed a little. In addition to this, and because it would be interesting to analyse cracks and not

only pinholes, the (6,2,6) and the (3,2,7) samples were chosen, given that although the results weren't as good as the pinholes beforementioned, of every crack tested, these two had the best recoveries, with their ink fusing correctly, but forming small bubbles.

Electronic microscope

The scanning electron microscopy – electron dispersive spectroscopy (SEM-EDS) consists of an x-ray photon spectrum which shows the number of detected photons by energy in kiloelectrons-volt. A film of graphite is deposited in the samples' surface in order for them to be conductive and react with the electrons' beam, a primary radiation incidence used to excite the samples, after which the material's reaction is studied (following the pattern: excitement, decay, analysis). A detailed examination is possible, given that the elements feature different behaviours according to the detected energy, for each element has a unique electronic configuration.

The electronic microscope analyses just a surface composition, i.e., down to a 2 μm depth, and is essentially divided in two different kinds of images:

- Topography image

In this group, the brightness is associated to the surface edges and inclination. It is also capable of identifying the surface's micro constitution.

- Backscattered electron image

On the other hand, here the brightness is related to the atomic number of the elements, reason why it offers a more heterogeneous picture. The shinier areas translate into a denser compound.

Figure 100 and Figure 101 represent the two kinds of images mentioned before, at a 75x amplification, to reflect the differences between both of them. In the topography image, there can be seen some dark zones, which represent small contaminations in the sample. There can also be seen some grey zones in the defect area, mainly at the top of the pinhole, where the ink didn't spread completely, although the result in this matter is very satisfying. As for the backscattered electron image, the difference between the fused ink and the surrounding tile's glaze is reduced. However, a bright line is visible around the defect, as well as some contamination and trapped air in the middle.

A complete footage for the SEM-EDS analysis performed in the referred samples can be consulted in Appendix 4.

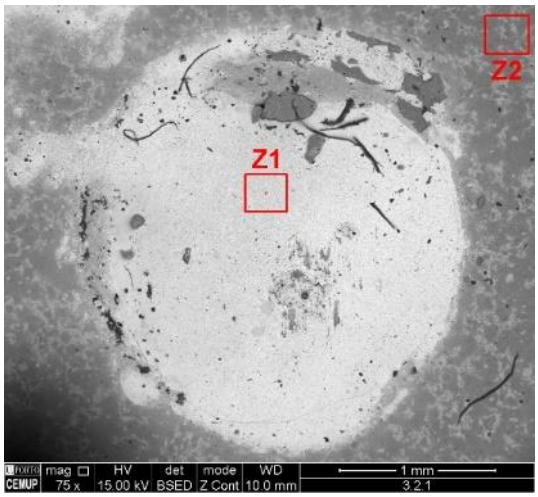

Figure 100 – Sample (3,2,1) backscattered electron image

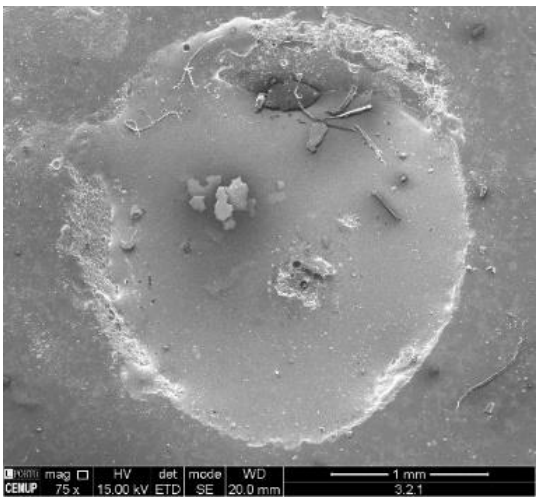

Figure 101 – Sample (3,2,1) topography image

The squared labels in the backscattered electron image were used to analyse the chemical composition in those specific zones through the EDS function of the electronic microscope, being the results of the first one, Z1, present in Figure 102. Here the silicate and zirconium are obviously the most abundant elements, although there are also smaller traces of oxygen, aluminium, lead, and a few of carbon, sodium, potassium and zinc. As for Z2, which may be consulted in Appendix 4, the results are close, with the largest distinction being the reduction of zirconium, and the appearance of magnesium and cadmium.

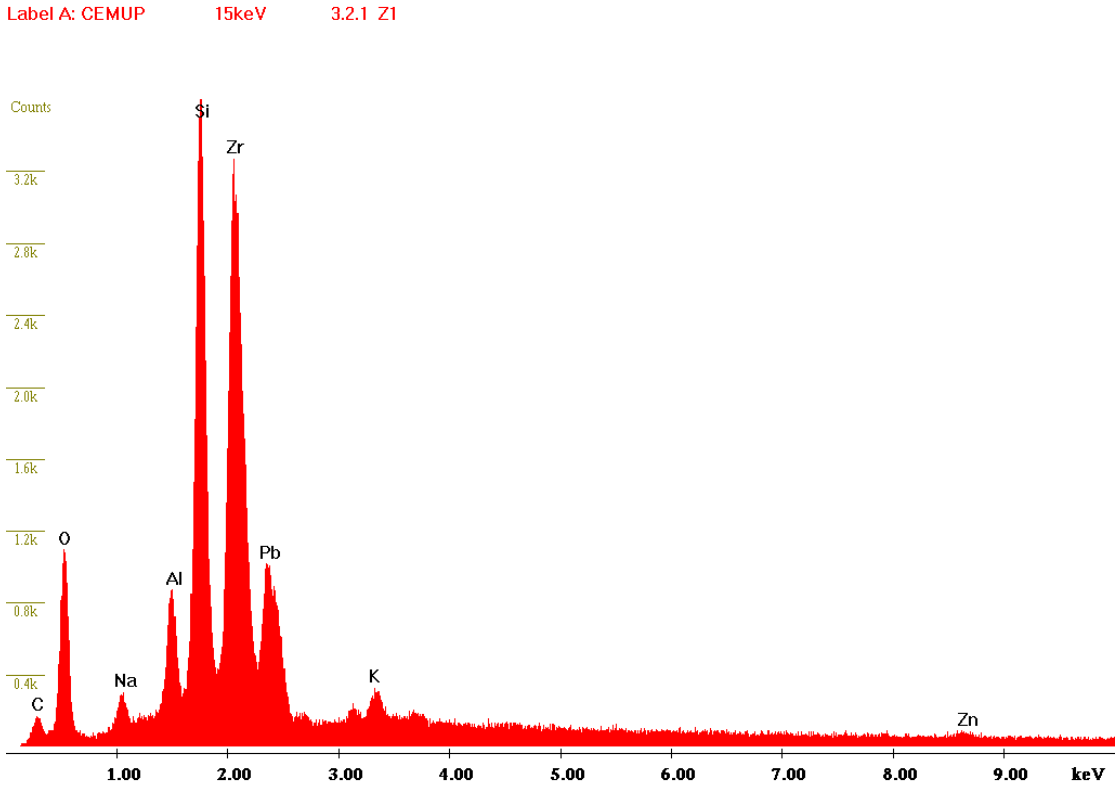

Figure 102 – Sample (3,2,1) EDS image from Z1

The pinhole in the (3,2,3) sample has also registered a great result, confirmed by Figure 103's top, where the fusion with the specimen was well performed. Despite this, Figure 104 shows a fracture of 766.6 nm wideness with a 5000x amplification factor, meaning that microscopically the ink bonds were broken in that specific zone.

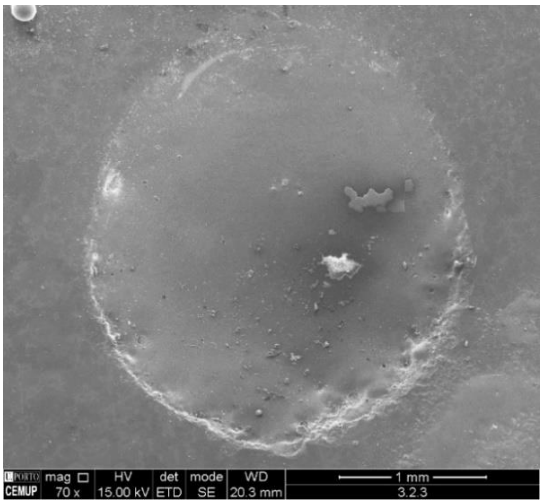

Figure 103 – Sample (3,2,3) SEM-EDS with a 70x amplification

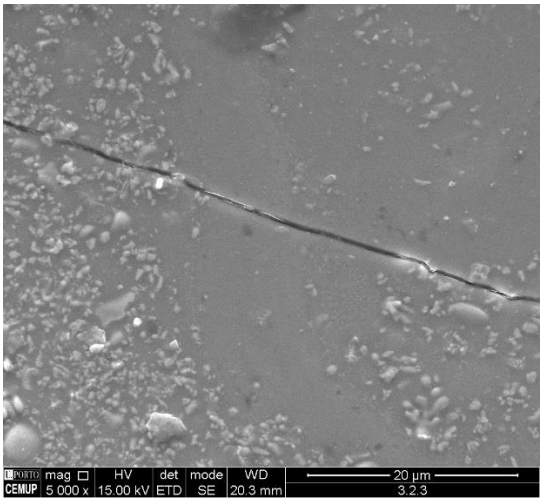

Figure 104 – Sample (3,2,3) SEM-EDS with a 5000x amplification

As for the cracks' analysis, in the (6,2,6) sample, with a 70x amplification, there is a clear distinction between the bubble formed ink and the remaining defect where it did not spread correctly in Figure 105. In the case of Figure 106, it is possible to notice a 250x amplified zone on the lower left corner of the first picture, that belongs to the defect's centre left side. This shows several spreading fractures, revealing that the ink broke due to a contraction in the cooling phase.

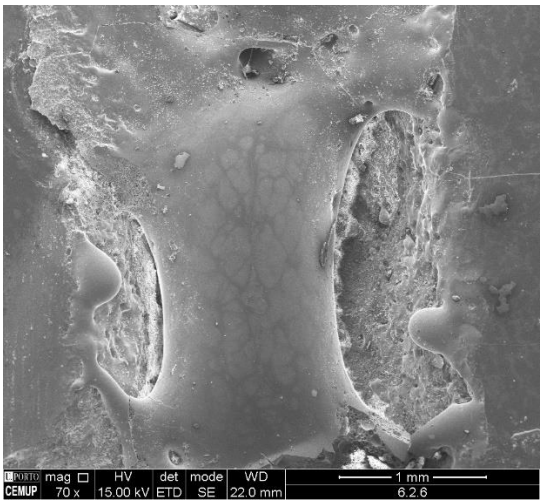

Figure 105 – Sample (6,2,6) SEM-EDS with a 70x amplification

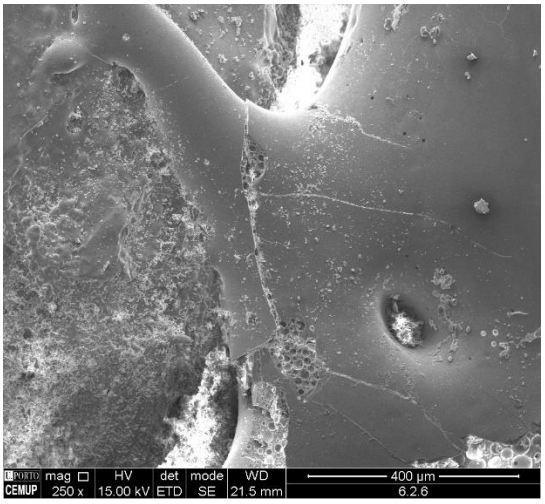

Figure 106 – Sample (6,2,6) SEM-EDS with a 250x amplification

In Figure 107 is represented the lower left corner of the Figure 106's fractures, amplified a thousand times, so that the presence of trapped air in the ink may be perceived, meaning that it only fused at the surface. Figure 108 shows exactly the same

phenomena; however, this time it is in the lower right side of the same sample. The presence of such an occurrence clearly signifies that although the laser power fused most of the ink, some zones, even inside those better looking through the naked eye, were not completely well repaired.

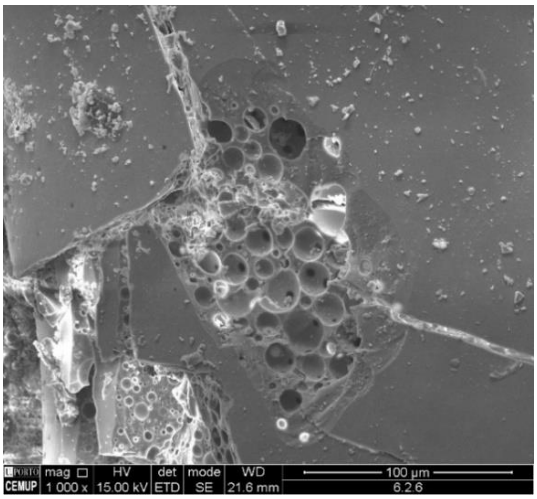

Figure 107 – Sample (6,2,6) SEM-EDS with 1000x amplification

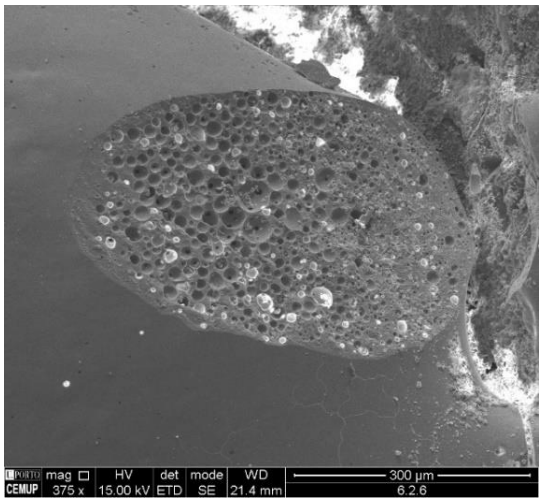

Figure 108 – Sample (6,2,6) SEM-EDS with a 375x amplification

The (3,2,7) sample, yet another crack, represented in Figure 109, depicts some rough zones, the pits formed by the ink that did not spread. On the other hand, the laser fused ink possesses a great similarity with the ceramic tile's glaze around the defect, in addition to most of the left side but essentially on the upper left corner of the picture, almost no transition zone is visible between the ink and the glaze, proof of a good result. In Figure 110 is visible the standard sample, a homogeneous structure, with a pattern characteristic of the surface material composition, a dispersion of glaze particles.

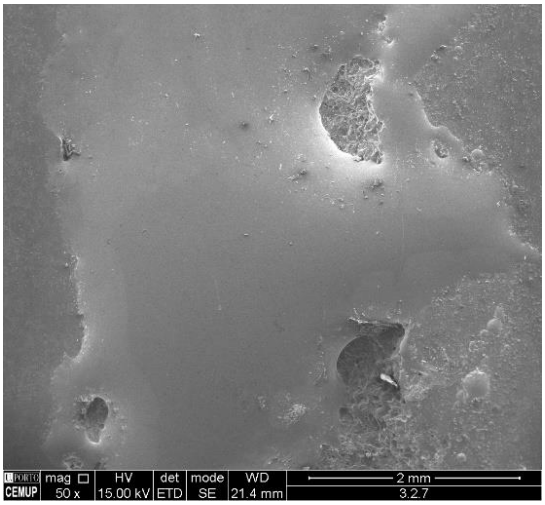

Figure 109 – Sample (3,2,7) SEM-EDS with a 50x amplification

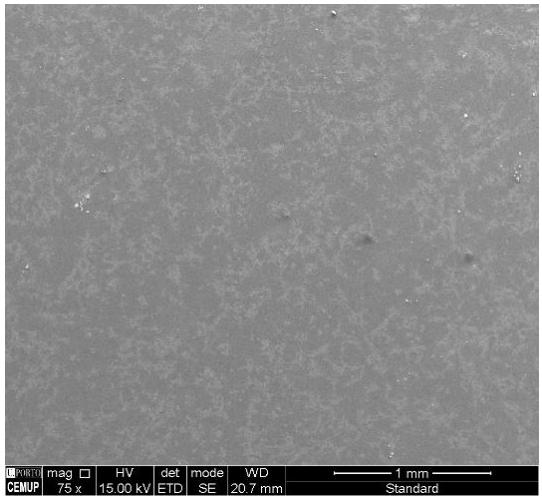

Figure 110 – Standard sample SEM-EDS with a 75x amplification

Finally, Figure 111 and Figure 112**Erro! A origem da referência não foi encontrada.** both depict analyses performed at a 10,000x amplification taken from the (3,2,7) sample's

fused ink and the standard sample's surface glaze, respectively. This leads to the conclusion that, despite the possibility of the two formulations being different from one another (white ink with ethyl alcohol for the first case and regular glaze for the second), the ink's formulation was well developed, as through a thorough analysis achieved with a 10,000x expansion factor, it is very similar to the comparison factor, the glaze used in the hot recovery method. The two images share the presence of tiny little white crystals, representative of their identical chemical composition.

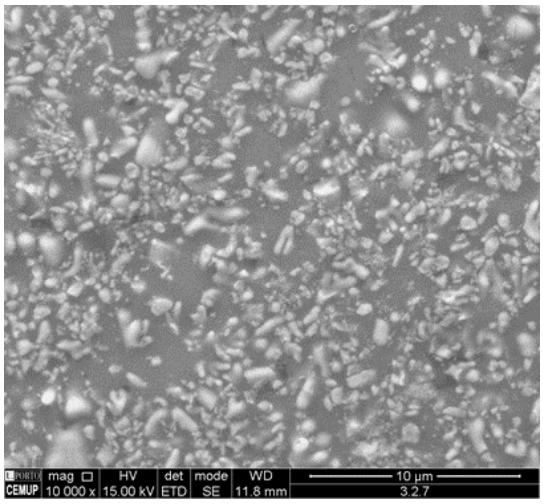

Figure 111 – Sample (3,2,7) with a 10,000x amplification

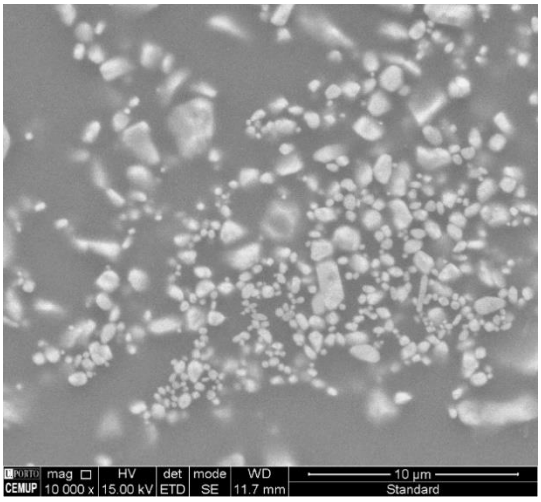

Figure 112 – Standard sample with a 10,000x amplification

3.3.5 Quality tests

The final step after every experiment concluded to the sanitary ware tiles, the specimens for this project, was to perform the quality tests necessary to evaluate the resistance these workpieces possess when carrying out their everyday function.

Although there were various tests presented which are done to the usual sanitary ware products, not all apply to the study focus ceramic tiles. For example, the hanging base load test only applies to products hanging from a wall, like wash basins or toilets, so it doesn't make sense when referring to ceramic tiles. As for the water absorption test, its main objective stands in assessing the percentage of water a workpiece may engross. However, the area which absorbs water is the main ceramic body, which is not glazed. Since the experiments done throughout this project only affected the glazed area of the products, this test is not appliable.

Bearing all these factors in mind, the two quality tests undertaken to finalize the experimental part of the project were the autoclave test and the resistance to acids, bases and staining agents (ABS).

3.3.5.1 Autoclave test

The purpose of the autoclave test stands in evaluating the existence or formation of crazing in the working piece's glazed surface. This test was performed to three different specimens, being the first two with defects corrected by laser, (4,1) and (5,2), and the last one through the hot recovery process in the kiln, employed for comparison with the others.

The choice of the two ceramic tiles (eighteen samples in total) for the crazing trial was done based on the fact of having the best results from the laser interaction to evaluate if, other than visually, they were still able to be considered good after being submitted to the pressure and time factors, simulating the wear they suffer during their lifetime.

In this context, the described specimens were put inside the autoclave (Figure 113), as seen in Figure 114, at a pressure corresponding to 3.2 kgf/cm^2 for fifteen hours.

Note: The second picture contains more than just the three specimens in study, because of the need to use the autoclave for the daily work in ARCH's laboratories.

Figure 113 – Autoclave

Figure 114 – Specimens in the autoclave

Subsequently, the specimens were removed from the autoclave, being then dived in an aniline solution, an organic compound, for twenty-four hours. The objective was to reveal possible fractures present in the corrected white ink, should they exist.

As expected, the standard tile (Figure 115), with its defects so well corrected in the kiln that appear to have never existed at all, shows no signs of the aniline presence, remaining exactly the same as before the contact with this solution, excepting to a barely visible vertical line in the left zone of the specimen, due to poor cleaning after the test. This will be the comparison factor for both of the tested specimens following up.

Figure 115 – Standard tile after autoclave test

In Figure 116 stands the result of the (4,1) specimen after the autoclave experiment. In the picture only the last three defects are present because the remaining ones of this ceramic tile were not experimented.

Although there is a dark halo around the defects, due to the incomplete spreading of the white ink in the pinholes, the glazed surface was not affected whatsoever by the aniline, which is a good result. Moreover, the (4,1,7) sample has the best white ink spread across the defect hole, reason why the aniline dark colour is faded around it.

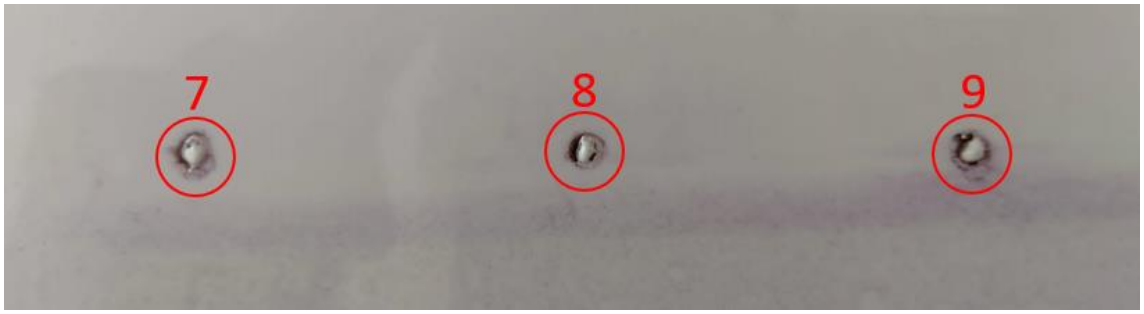

Figure 116 – Specimen (4,1) autoclave test results

On the other hand, the (5,2) specimen depicted in Figure 117 just contains the cracks, since the pinholes' ink present in this tile jumped the defect. The ink in the cracks numbers 1 and 4 also fell apart, leaving the ceramic body exposed, which was clearly revealed by the aniline. As for the (5,2,2) and (5,2,5) samples, some dark zones are visible in the defects' surrounding area, having the aniline revealed more precisely the thermally affected zones provoked by the laser interaction with the concentrated PL960 ink. Besides that, the bubbles formed by the fused white ink and spread across the defect were unaltered after this experiment's impact, meaning that specific part had a good result.

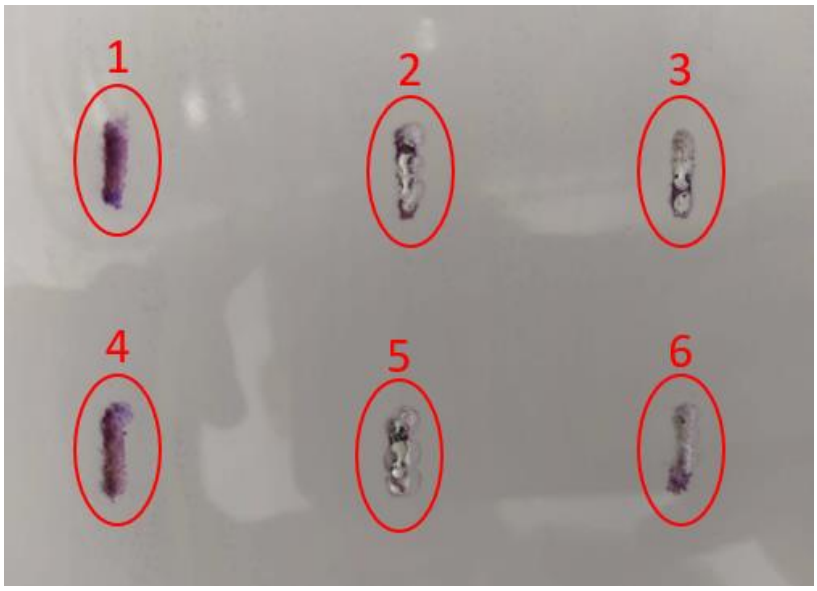

Figure 117 – Specimen (5,2) autoclave test results

3.3.5.2 Resistance to acids, bases and staining agents (ABS)

The ABS test was performed to a single specimen, the (4,2) tile, in its three pinholes, which were some of the best results achieved in terms of defect correction with the laser incidence.

For that, three different solutions were tested, as seen in Figure 118, from the left to the right, respectively:

- 10% acetic acid for the (4,2,7) defect;
- 5% sodium hydroxide as a base for the (4,2,8) sample;
- 1% methylene blue (or methylthioninium chloride) for the (4,2,9) pinhole.

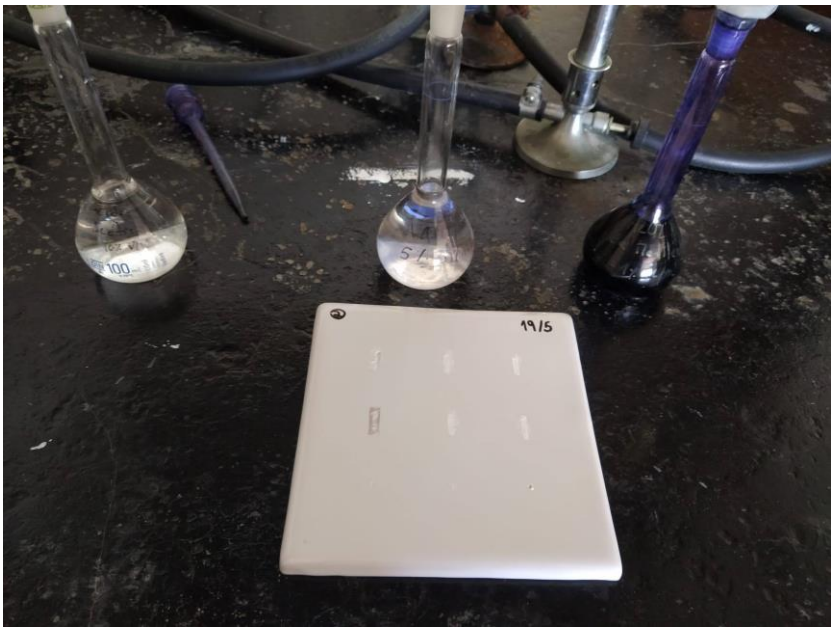

Figure 118 – Acids, bases and staining agents (ABS)

In Figure 119 are depicted the three solutions which were poured on the respective samples, with the assistance of a pipette, reacting with the laser corrected pinholes.

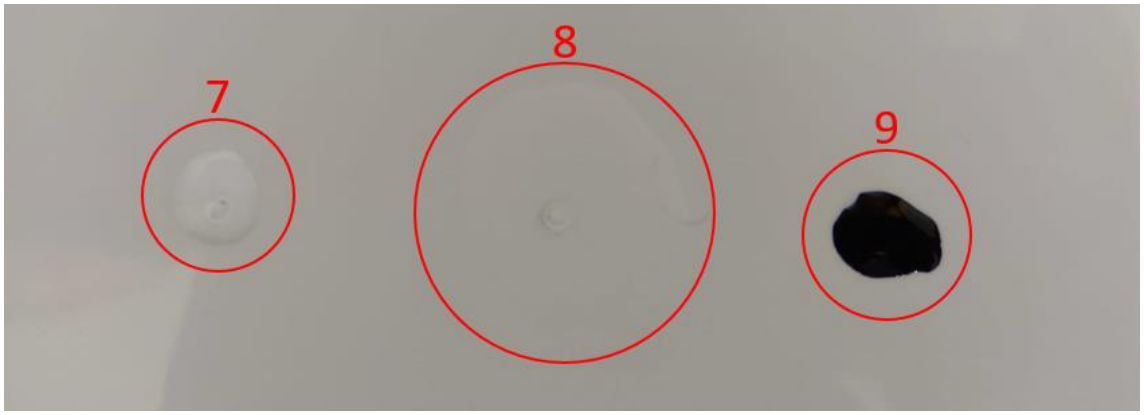

Figure 119 – ABS test reaction on the defects

The following step was to leave the liquids in reactive contact for one hour, in an attempt to develop a chemical reaction with the laser-fused ink. After that, the reagents were removed by water cleaning to verify the results, observable in Figure 120.

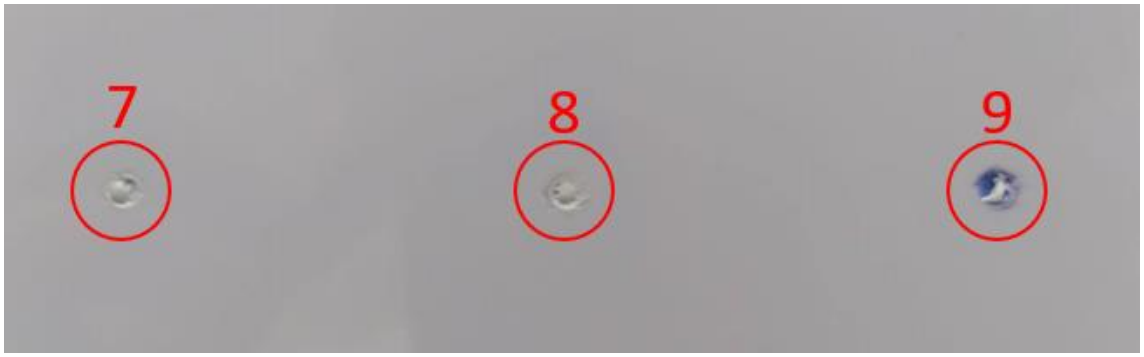

Figure 120 – ABS test results

The meaning of this test was to figure the existence of a chemical reaction between the reagents and the white ink, resembling the glaze surface of the ceramic part. The first two defects, if reacted with the solutions, should have faced a colour transformation, usually to yellow. As for the last one, as explained before, the defect was not completely filled with the white ink, due to the bubble formation in the middle. For this reason, the blue dye only penetrated the non-glazed area, leaving the white ink in an equal state.

In conclusion, the three defects had their white ink fused with laser showing absolutely no signs of being affected by the reagents, which means they successfully passed the test.

CONCLUSIONS

4.1 Conclusions

4.2 Proposals of future works

4 CONCLUSIONS AND PROPOSALS OF FUTURE WORKS

4.1 Conclusions

In order to conclude this dissertation, an overview is made, alongside a balance of the advantages and drawbacks that this project has had.

As a summary of the whole work done considering the initial goals, six different ink formulations were experimented, with arrows pointing out the good and the bad ones:

- Production glaze - ↓
- Frit - ↓
- Grey ink with ethyl alcohol - ↓
- White ink with ethyl alcohol - ↑↑
- White ink with diluted PL960 - ↑
- White ink with concentrated PL960 - ↓↓

Out of these, the concentrated PL960 medium offered the worst results, as it burned and created a heat affected area surrounding the defects. The production glaze and the frit, although presenting perfect results in the hot recovery process, through the kiln they did not react so well when submitted to the laser interaction. The grey ink was experimented mostly to perform markings for the parameters testing; it could be used in grey sanitary ware products' defects, to evaluate the results. Finally, the white ink with ethyl alcohol and with diluted PL960 had the best results.

Considering the parameters, Table 31 shows the best results obtained for each parameter that was experimented throughout this project. Although the outcomes were better when performed with the manual firing method (laser power and incidence time) for both the pinholes and cracks, some samples were correctly repaired using the beam speeds shown below, but the incidence time was still the most important parameter.

Table 31 – Best results obtained with each parameter

Parameter	Best result
Laser power	P25, P30, P35
Incidence time	T10, T20, T30
Beam speed	V3, V5, V10
Lens use	No lens
Focal length	2.5''

Finally, regarding the defects repaired with the laser technology, the pinholes had much better results than the cracks. Besides this, the experimental tests for both of the defects have to continue, in order to manage to perform a perfect recovery process for the sanitary ware defects comparable to the hot recovery method. Nevertheless, the samples with a better result, either in the qualitative or the quantitative analysis, are:

- Pinholes – (3,2,1); (3,2,2); (3,2,3); (3,2,4); (3,2,5); (3,2,6); (4,2,7); (4,2,8).
- Cracks – (6,2,6); (6,2,9); (3,2,7).

A comparison of the objectives proposed at the beginning and the respective results is presented in Table 32.

Table 32 – Dissertation's balance considering its objectives and results

Objective	Accomplishment	Result
To create a set of glazes (both white and coloured) which fuse with the laser beam interaction.		Both the grey and the white ink showed a good result fusing with the laser beam.
To create a set of white glazes whose colour difference does not exceed 0.8 in the colourimeter reading, so as not to be distinguishable from the standard in the user's perspective.	 	In spite of just a third of the total experiments being able to be analysed in the colourimeter (54/153), out of this value, 37% of the colourimeter readings had a colour difference which did not exceed 0.8, a total of 20 samples. On the other hand, no defect was completely well repaired compared to the hot recovery process, although in 6 of them the difference to the standard tile was tenuous.
To create a technique using a laser system that can reach the necessary temperature to achieve a tone identical to the one of the glass.		Through the manoeuvre of the laser system's parameters, such as the Laser Power, Incidence Time, Beam Speed and Lens Use, it was possible to vary each factor bearing in mind the result from the immediate previous test and enabling the achievement of the required tone, alongside with the ink formulation adjustment through chemical methods.

To create a technique using a laser system that allows the fusion of the glaze only in the place where it is required to cover the defect.		The laser system employed was a fixed set. However, some problems arose considering the beam positioning on the tile's surface. With a careful observation of the experimental tests, it was possible to identify whether the beam was impacting the correct zone or not, readjusting the position manually or through the computer software in order for the laser to fuse the ink just in the place where the defect was placed.

4.2 Proposals of future works

Although good results were achieved using a completely innovative technique in the ceramic sanitary ware field, there is still a long journey ahead and new objectives to achieve. Every great invention that is nowadays embedded in the modern society and that brings countless benefits in each sector, for example considering the industry, had to start with a simple idea and a few set of experimental tests before reaching success. The same happens to the development of a recovery process for sanitary ware using a new technology, in this case a laser system. Now that the first steps have been taken considering the development of this technology, the proposals of future works are:

- Continuation of the research method, considering as a base the accomplished results in this project, so as to optimize the parameters' values, increase the tested data in order to achieve a more accurate statistical relevance and manage to obtain a perfect defects' recovery, both in pinholes and cracks, extending this technique to other defects found in the sanitary ware production process, with different lengths and depths;

- Performance of experimental tests with the best results acquired, but to specimens of different colours, other than white. In the case of grey products, for example, the grey ink tested only for the laser markings can be used, filling in the defects and using the laser interaction to fuse them, evaluating later the colourimeter reading difference between the ink in the defects and the specimen;

- Implementation of this concept in a flexible laser system, using a robotic arm for the laser head instead of a fixed machine. This way, it will be possible to reach difficult zones of any sanitary ware product, which is impossible with a rigid laser machine due to the workpieces' complex geometry;

- Application of the laser recovery process in sanitary ware products, such as washbasins, toilets or shower trays, now that it was already experimented on ceramic tiles;
- Automatization of the laser technology, implementing it in the daily production of the sanitary ware production factories.

With a well succeeded repairing method using the laser technology, 9 € per product will be spared, which converted in an annual production in ARCH company of 200,000 products, considering the laser use in 5% of them, results in an annual 90,000 € save.

REFERENCES AND OTHER SOURCES OF INFORMATION

5 REFERENCES AND OTHER SOURCES OF INFORMATION

[1] J. M. P. Q. Delgado and A. G. Barbosa de Lima, *Transport processes and separation technologies*. Springer, 2020.

[2] J. William D. Callister and David G. Rethwisch, *Fundamentals of materials science and engineering: an integrated approach*, no. 5th Edition. 2015.

[3] A. F. Dericioglu, "Fabrication of ceramics by die pressing and firing," 1984.

[4] DreamsTime, "Composição de blocos cerâmicos dos tijolos vermelhos." [Online]. Available: https://pt.dreamstime.com/composição-de-blocos-cerâmicos-dos-tijolos-vermelhos-em-um-fundo-branco-image125232941. [Accessed: 28-Nov-2020].

[5] Gardenista, "Pure white ceramic vases." [Online]. Available: https://www.gardenista.com/products/pure-white-ceramic-vases/. [Accessed: 28-Nov-2020].

[6] Z. Keshavarz and D. Mostofinejad, "Porcelain and red ceramic wastes used as replacements for coarse aggregate in concrete," *Constr. Build. Mater.*, vol. 195, pp. 218–230, 2019.

[7] Ansys, "Granta EduPack, formerly CES EduPack: materials education support." [Online]. Available: https://www.ansys.com/products/materials/granta-edupack. [Accessed: 16-Nov-2020].

[8] R. K. Nishihora, P. L. Rachadel, M. G. N. Quadri, and D. Hotza, "Manufacturing porous ceramic materials by tape casting - a review," Elsevier Ltd, 2018.

[9] T. Mori *et al.*, "Sanitary ware and method of manufacturing sanitary ware," 2019.

[10] Arch Valadares, "Sanitários Valadares." [Online]. Available: https://www.archvaladares.com. [Accessed: 14-Nov-2020].

[11] Jika, "Ceramics production in the new millennium." [Online]. Available: https://www.jika.eu/technology/ceramics-production-in-the-new-millennium. [Accessed: 21-Nov-2020].

[12] Data Bridge Market Research, "Sanitary ware market - global industry trends and forecast to 2026." [Online]. Available: https://www.databridgemarketresearch.com/reports/global-sanitary-ware-market#. [Accessed: 11-Dec-2020].

[13] Associação Portuguesa das Indústrias de Cerâmica e Cristalaria (APICER), "Capacitação da indústria cerâmica portuguesa - Um cluster, uma estratégia, mercados prioritários." p. 178, 2016.

[14] European Comission, “Internal market, industry, entrepreneurship and SMEs.” [Online]. Available: https://ec.europa.eu/growth/sectors/raw-materials/industries/non-metals/ceramics_en. [Accessed: 11-Dec-2020].

[15] Union of International Associations, “European federation of ceramic sanitary ware manufacturers.” [Online]. Available: https://uia.org/s/or/en/1100055992. [Accessed: 11-Dec-2020].

[16] Instituto Nacional de Estatística (Portugal), “Classificação portuguesa das actividades económicas.” Lisboa, p. 322, 2007.

[17] Instituto Nacional de Estatística (Portugal), “Portal do INE.” [Online]. Available: https://www.ine.pt/xportal/xmain?xpid=INE&xpgid=ine_indicadores&userLoadSave=Load&userTableOrder=9964&tipoSeleccao=0&contexto=pq&selTab=tab1&submitLoad=true&xlang=pt. [Accessed: 14-Nov-2020].

[18] Banco de Portugal Eurosistema, “Quadros do setor.” [Online]. Available: https://www.bportugal.pt/QS/qsweb/Dashboards. [Accessed: 14-Nov-2020].

[19] K. Kim, K. Kim, and J. Hwang, “LCD waste glass as a substitute for feldspar in the porcelain sanitary ware production,” *Ceram. Int.*, vol. 41, no. 5, pp. 7097–7102, 2015.

[20] S. De Miranda, L. Patruno, M. Ricci, R. Saponelli, and F. Ubertini, “Ceramic sanitary wares: prediction of the deformed shape after the production process,” *J. Mater. Process. Technol.*, vol. 215, no. 1, pp. 309–319, 2015.

[21] M. Ricci, L. Patruno, S. de Miranda, R. Saponelli, and F. Ubertini, “A numerical strategy for predicting the mould of ceramic sanitary wares,” *Int. J. Adv. Manuf. Technol.*, vol. 90, no. 5–8, pp. 2233–2241, 2017.

[22] A. Ruggieri, A. M. Braccini, S. Poponi, and E. M. Mosconi, “A meta-model of inter-organisational cooperation for the transition to a circular economy,” *Sustain.*, vol. 8, no. 11, pp. 1–17, 2016.

[23] Whitech, “Ceramic division - robotised and automated solutions.” [Online]. Available: https://www.whitech-it.com/ceramic-division/. [Accessed: 01-Dec-2020].

[24] M. Beheary and F. El-matary, “Management of heat stress in sanitary ware industry,” in *9th International Conference on The Role Of Engineering Towards A Better Environment*, 2012.

[25] Z. Qian, M. QingLong, X. YongQian, and G. Lin, “The robot intelligent spraying glazing system for sanitary ceramics industry,” *J. Phys. Conf. Ser.*, vol. 1653, no. 1, 2020.

[26] E. Martini, “An industrial approach to ceramics: sanitaryware,” no. November 2017, pp. 138–145, 2018.

[27] Associação Empresarial de Portugal (AEP), “BenchMark A + E.” p. 156, 2011.

[28] JSC Keramin, “Sanitary ware production technologies.” [Online]. Available: https://eng.keramin.com/products/sanitary-ware/technologies. [Accessed: 02-Dec-2020].

[29] R. Li *et al.*, “Development of sapphirine opaque glazes for ceramic tiles,” *J. Eur. Ceram. Soc.*, vol. 38, no. 16, pp. 5632–5636, 2018.

[30] T. Pradell and J. Molera, “Ceramic technology. How to characterise ceramic glazes,” *Archaeol. Anthropol. Sci.*, vol. 12, no. 8, 2020.

[31] G. Topateş, B. Tarhan, and M. Tarhan, “Chemical durability of zircon containing glass-ceramic glazes,” *Ceram. Int.*, vol. 43, no. 15, pp. 12333–12337, 2017.

[32] J. Cai *et al.*, “Development of spinel opaque glazes for ceramic tiles,” *J. Eur. Ceram. Soc.*, vol. 38, no. 1, pp. 297–302, 2018.

[33] K. Pekkan, E. Taşçı, and Y. Gün, “Development of temmoku glazes and their applications onto different tiles under industrial fast firing conditions at 1180 °C,” *J. Aust. Ceram. Soc.*, vol. 56, no. 2, pp. 489–497, 2020.

[34] V. B. Tezza, M. Scarpato, L. F. O. Silva, and A. M. Bernardin, “Effect of firing temperature on the photocatalytic activity of anatase ceramic glazes,” *Powder Technol.*, vol. 276, pp. 60–65, 2015.

[35] GSI Ceramica, “Ceramic elements - italian made.” [Online]. Available: https://www.gsiceramica.it/it/. [Accessed: 15-Jan-2021].

[36] A. S. Rieck, “Methods for vitrescent marking,” 2007.

[37] M. Matin, M. Tite, and O. Watson, “On the origins of tin-opacified ceramic glazes: New evidence from early Islamic Egypt, the Levant, Mesopotamia, Iran, and Central Asia,” *J. Archaeol. Sci.*, vol. 97, no. January, pp. 42–66, 2018.

[38] International Finance Corporation (World Bank Group), “Environmental, health and safety guidelines for ceramic tile and sanitary ware manufacturing,” *Corrosion*, 2007.

[39] M. Kavanová, A. Kloužková, and J. Kloužek, “Characterization of the interaction between glazes and ceramic bodies,” *Ceram. - Silikaty*, vol. 61, no. 3, pp. 267–275, 2017.

[40] M. Kumru, “Assessing the visual quality of sanitary ware by fuzzy logic,” *Appl. Soft Comput. J.*, vol. 13, no. 8, pp. 3646–3656, 2013.

[41] S. H. Hanzaei and A. Afshar, “Automatic detection and classification of the ceramic tiles’ surface defects,” *Pattern Recognit.*, vol. 66, pp. 174–189, 2016.

[42] R. P. Monteiro and C. J. A. Bastos-Filho, “Detecting defects in sanitary wares using deep learning,” *IEEE*, vol. 19, 2019.

[43] M. Kesharaju, R. Nagarajah, T. Zhang, and I. Crouch, “Ultrasonic sensor based defect detection and characterisation of ceramics,” *Ultrasonics*, vol. 54, no. 1, pp. 312–317, 2014.

[44] N. Bao, X. Ran, Z. Wu, Y. Xue, and K. Wang, “Design of inspection system of glaze defect on the surface of ceramic pot based on machine vision,” *Proc. 2017 IEEE 2nd Inf. Technol. Networking, Electron. Autom. Control Conf. ITNEC 2017*, vol. 17, pp. 1486–1492, 2018.

[45] B. Teng, H. Zhao, P. Jia, J. Yuan, and C. Tian, “Research on ceramic sanitary ware defect detection method based on improved vgg network,” *J. Phys. Conf. Ser.*, vol. 1650, no. 2, 2020.

[46] M. Romagnoli, M. Burani, G. Tari, and J. M. F. Ferreira, “A non-destructive method to assess delamination of ceramic tiles,” *J. Eur. Ceram. Soc.*, vol. 27, no. 2–3, pp. 1631–1636, 2007.

[47] Imerys Ceramics, “Glaze defects.” [Online]. Available: https://www.imerys-performance-minerals.com/your-market/ceramics/sanitaryware-troubleshooting/glaze-defects. [Accessed: 07-Dec-2020].

[48] H. Bazargan and A. Dehghanzadeh, “Modeling pinhole phenomenon in sanitary porcelains case study: isatis sanitary porcelain plant, Yazd, Iran,” *J. Stat. Theory Appl.*, vol. 17, no. 3, pp. 572–586, 2018.

[49] Lakeside Pottery, “Understanding and solving glaze shivering.” [Online]. Available: http://www.lakesidepottery.com/HTML Text/Tips/Shivering.html. [Accessed: 05-May-2021].

[50] J. Lv, F. Gu, W. Zhang, and J. Guo, “Life cycle assessment and life cycle costing of sanitary ware manufacturing: A case study in China,” *J. Clean. Prod.*, vol. 238, 2019.

[51] J. M. Miranda Fernandes, “Estudo da tecnologia laser na reparação de defeitos em louças cerâmicas,” 2017.

[52] InfoEscola, “Espectro eletromagnético.” [Online]. Available: https://www.infoescola.com/fisica/espectro-eletromagnetico/. [Accessed: 26-Dec-2020].

[53] InfoEscola, “Laser - aplicações e tipos de lasers.” [Online]. Available: https://www.infoescola.com/optica/laser/. [Accessed: 21-Jan-2021].

[54] Cerinnov, “Máquina de marcação a laser.” [Online]. Available: www.cerinnov.com. [Accessed: 14-Apr-2021].

[55] GearBest, “Laser engraving machine.” [Online]. Available: https://pt.gearbest.com/community/mjfL80. [Accessed: 14-Apr-2021].

[56] MM Cortes e Dobras, “Corte a laser em aço.” [Online]. Available: https://www.mmcortesedobra.com.br/corte-a-laser-em-aco. [Accessed: 14-Apr-2021].

[57] Ideias Únicas, “Marcação em garrafa térmica.” [Online]. Available: https://ideiasunicas.pt/. [Accessed: 15-Apr-2021].

[58] U. Enzyklopaedie, U. Enzyklopaedie, U. Enzyklopaedie, F. Application, P. Data, and P. E. L. Schilling, “Laser marking of ceramic materials, glazes, glass ceramics and glasses,” 1988.

[59] D. S. A. Mahmod, A. A. Khan, M. A. Munot, N. Glandut, and J. C. Labbe, “Laser surface treatment of porous ceramic substrate for application in solid oxide fuel cells,” *IOP Conf. Ser. Mater. Sci. Eng.*, vol. 146, no. 1, 2016.

[60] S. S. Yilmaz, “Ytterbium doped all-fiber integrated high power laser,” 2013.

[61] N. Basile, M. Gonon, F. Petit, and F. Cambier, “Processing of a glass ceramic surface by selective focused beam laser treatment,” *Ceram. Int.*, vol. 42, no. 1, pp. 1720–1727, 2016.

[62] Oerlikon Metco, “Laser cladding process.” [Online]. Available: https://www.oerlikon.com/metco/en/solutions-technologies/technology/process-solutions/laser-cladding-process/. [Accessed: 31-Dec-2020].

[63] C. Leyens and E. Beyer, “Innovations in laser cladding and direct laser metal deposition,” *Laser Surf. Eng. Process. Appl.*, pp. 181–192, 2015.

[64] S. Rodríguez-López *et al.*, “Laser cladding of glass-ceramic sealants for SOFC,” *J. Eur. Ceram. Soc.*, vol. 35, no. 16, pp. 4475–4484, 2015.

[65] A. Goulas and R. J. Friel, “Laser sintering of ceramic materials for aeronautical and astronautical applications,” in *Laser Additive Manufacturing*, Elsevier Ltd, 2017, pp. 373–398.

[66] B. Chang, J. Blackburn, C. Allen, and P. Hilton, “Studies on the spatter behaviour when welding AA5083 with a Yb-fibre laser,” *Int. J. Adv. Manuf. Technol.*, vol. 84, no. 9–12, pp. 1769–1776, 2016.

[67] J. Ahn, L. Chen, E. He, J. P. Dear, and C. M. Davies, “Optimisation of process parameters and weld shape of high power Yb-fibre laser welded 2024-T3 aluminium alloy,” *J. Manuf. Process.*, vol. 34, no. April, pp. 70–85, 2018.

[68] B. Fotovvati, S. F. Wayne, G. Lewis, and E. Asadi, “A Review on Melt-Pool Characteristics in Laser Welding of Metals,” *Adv. Mater. Sci. Eng.*, vol. 2018, 2018.

[69] TWI, “The fibre laser: A newcomer for material welding and cutting.” [Online]. Available: https://www.twi-global.com/technical-knowledge/published-papers/the-fibre-laser-a-newcomer-for-material-welding-and-cutting-august-2005. [Accessed: 07-Aug-2021].

[70] F. Silva, *Tecnologia da Soldadura - Uma Abordagem Técnico-Didática*, 2ª edição. 2016.

[71] D. Wang, C. Yu, J. Ma, W. Liu, and Z. Shen, “Densification and crack suppression in selective laser melting of pure molybdenum,” *Mater. Des.*, vol. 17, 2017.

[72] R. He, Z. Qu, and D. Liang, “Rapid heating thermal shock study of ultra high

temperature ceramics using an in situ testing method," *J. Adv. Ceram.*, vol. 6, no. 4, pp. 279–287, 2017.

[73] C. E. Protasov, R. S. Khmyrov, S. N. Grigoriev, and A. V Gusarov, "Selective laser melting of fused silica: interdependent heat transfer and powder consolidation," *Int. J. Heat Mass Transf.*, vol. 104, pp. 665–674, 2017.

[74] D. E. Murnick, "Localized surface glazing of ceramic articles," 1995.

[75] R. L. Lehman, Y. Umezu, J. Li, and E. Al., "Method of thermally glazing an article," 2000.

[76] K. Osvay, I. Képíró, and O. Berkesi, "Laser treatment of white china surface," vol. 252, pp. 4516–4522, 2006.

[77] Minitab, "Experimentos fatoriais e fatoriais fracionados ." [Online]. Available: https://support.minitab.com/pt-br/minitab/18/help-and-how-to/modeling-statistics/doe/supporting-topics/factorial-and-screening-designs/factorial-and-fractional-factorial-designs/. [Accessed: 17-Apr-2021].

[78] A. J. A. Gama, J. M. R. Figueirêdo, A. L. F. Brito, M. A. Gama, G. A. Neves, and H. C. Ferreira, "Factorial design and statistical analysis of smectite clay treatment by hydrocyclone," *Cerâmica*, vol. 64, no. 369, pp. 57–63, 2018.

[79] C. Decker Jr., E. Henning, J. C. E. Ferreira, and B. Zappelino, "Comparison of complete and fractured factor projects in a simulation model to discrete events of a manufacture system for virtual cellylar and cellular layouts," *GEPROS*, pp. 23–57, 2020.

[80] Toda Matéria, "Variância e desvio padrão." [Online]. Available: https://www.todamateria.com.br/variancia-e-desvio-padrao/. [Accessed: 17-Apr-2021].

[81] U. Kucuk, M. Eyuboglu, H. O. Kucuk, and G. Degirmencioglu, "Importance of using proper post hoc test with ANOVA," *Int. J. Cardiol.*, vol. 209, p. 346, 2016.

[82] Norma Portuguesa, "NP EN 997:2012 + A1 2017 - Sanitas e conjunto sanita e autoclismo com sifão incorporado," 2017.

[83] ISO, "BS EN ISO 10545-11:1996 - crazing resistance of ceramic tiles - test method," 1996.

[84] The Art of Asia, "Kuan ware - guide to chinese ceramics." [Online]. Available: http://www.artsmia.org/art-of-asia/ceramics/early-chinese-ceramics-kuan.cfm. [Accessed: 05-May-2021].

[85] M. A.-Y. Oliveira and R. Gonçalves, "Estratégia, inovação e mudança: casos de estudo sobre competitividade," Universidade de Aveiro, 2017.

[86] ARCH - Advanced Research Ceramic Heritage, "Arch Valadares." [Online]. Available: http://arch.pt/. [Accessed: 14-Nov-2020].

[87] Valadares, "Arch ." [Online]. Available: http://site2020.archvaladares.com/.

[Accessed: 23-Jun-2021].

[88] Trotec, “Laser engravers and laser cutters.” [Online]. Available: https://www.troteclaser.com/en/. [Accessed: 15-Apr-2021].

[89] Tabor, “Sheet metal works.” [Online]. Available: http://www.tabor.pt/. [Accessed: 04-Aug-2021].

[90] B. C. K. Ly, E. B. Dyer, J. L. Feig, A. L. Chien, and S. Del Bino, “Research techniques made simple: cutaneous colorimetry: a reliable technique for objective skin color measurement,” *J. Invest. Dermatol.*, vol. 140, no. 1, pp. 3-12.e1, 2020.

[91] ISEP, “Instituto Superior de Engenharia do Porto.” [Online]. Available: https://www.isep.ipp.pt/. [Accessed: 04-Aug-2021].

[92] CEMUP, “Centro de materiais de Universidade do Porto.” [Online]. Available: https://www.cemup.up.pt/. [Accessed: 04-Aug-2021].

[93] SelectScience, “Zeiss Sigma VP from Zeiss Research Microscopy Solutions.” [Online]. Available: https://www.selectscience.net/products/zeiss-sigma-vp/?prodID=113791. [Accessed: 05-Jul-2021].

[94] Scribbr, “The two-way ANOVA test.” [Online]. Available: https://www.scribbr.com/statistics/two-way-anova/. [Accessed: 31-Aug-2021].

[95] IBM, “SPSS Software.” [Online]. Available: https://www.ibm.com/analytics/spss-statistics-software. [Accessed: 05-Sep-2021].

APPENDIX

6.1 ARCH 2020 Organogram

6.2 Trotec SP1500 Laser Technical Sheet

6.3 Optical Microscope Analysis complete footage

6.4 SEM-EDS Analysis complete footage

6.5 Colourimeter Analysis complete set of values

6.6 Experimental work resume table

6 APPENDIX

6.1 Appendix 1 – ARCH 2020 Organogram

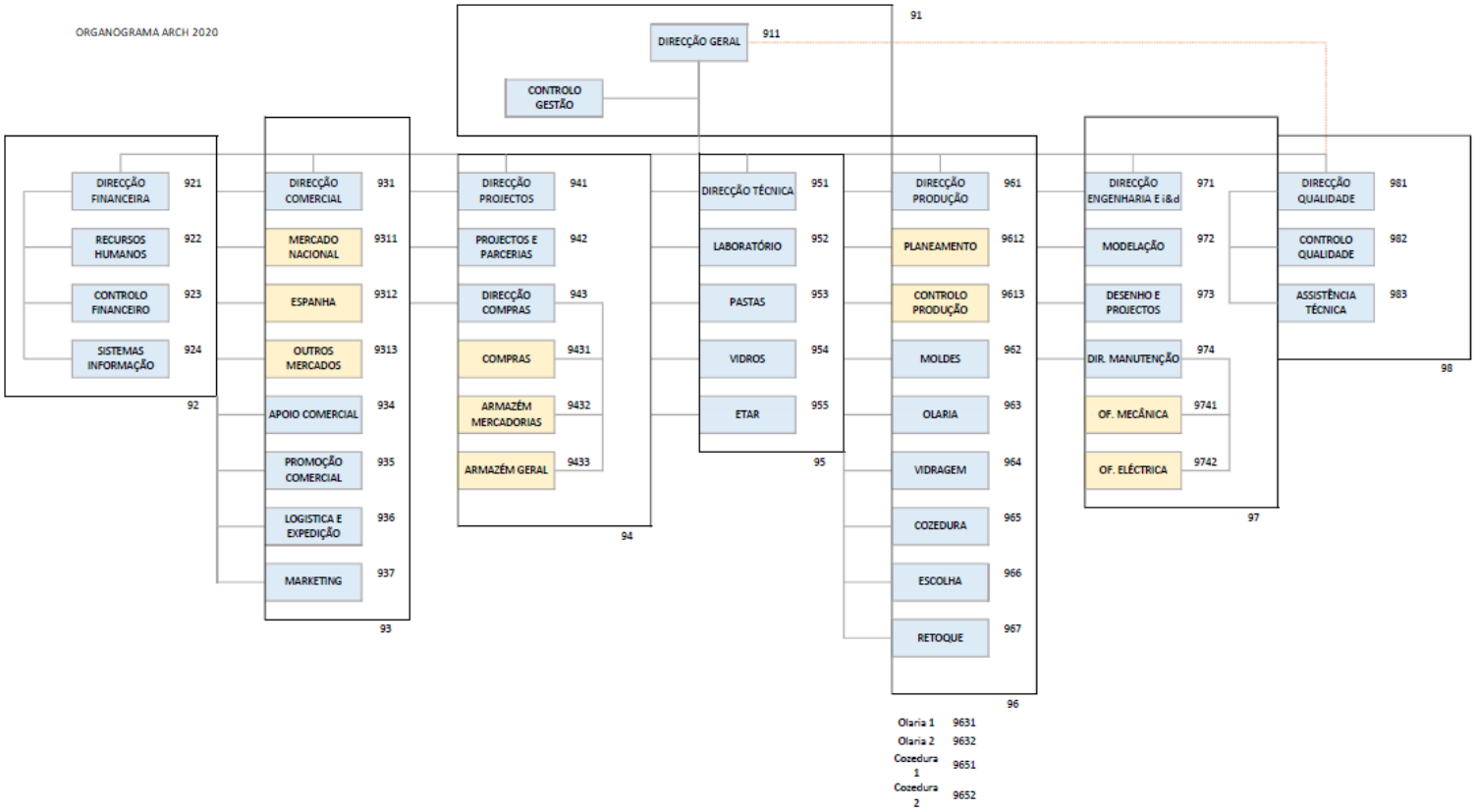

6.2 Appendix 2 – Trotec SP1500 Laser Technical Datasheet

A simple calculation

→ Profitability

Raise your profits with SP1500 from Trotec!

The SP1500 to the most profitable laser cutting and engraving system in its class. It combines highest productivity, a working area of a standard acrylic sheet size, highest system life span and lowest maintenance costs.

First-class components

The individual components like motion system, optics, electronics, working head and laser source feature highest quality and performance. The proven InPack-Technology™ protects all valuable components from dust and gases and ensures a long-term reliability and trouble-free operation. SP1500 stands for top quality with minimum maintenance. The base frame weighs 900 kgs and offers a robust, stable working area for laser cutting and engraving.

Standard

→ Trotec IPC – Intelligent Path Control™

This new laser control module allows the dynamic adjustment of speed and acceleration depending on the cutting path. This reduces processing time and increases the cutting results.

Air-flushed optics

All optics are air-flushed, providing for maintenance-free operation and long life.

Enclosed working cabin

The SP 1500 has a unique housing design and meets the requirements of laser safety class 2. You will not need a special design to protect your employees, or a laser safety officer. As an added benefit, the self-contained system allows dust to be efficiently evacuated.

Cutting table

With the cutting table system the SP1500 is configured to process thicker materials. Material support on low reflection anodized aluminum plates (may be replaced by acrylic plates)

Options

Extraction on working head

Flame-polished cut of acrylics up to 40 mm

Extraction on working head

An extraction hose is mounted directly on the working head and removes dust and smoke from the material surface during processing.

Gas kit

Select between two gases for processing (e.g. compressed air, N2). Reduces flame-up, improves dust dispersal and also protects the lens. Activation and deactivation are controlled by the JobControl® software.

JobControl® Vision

Archive perfect results when cutting printed materials (acrylic, MDF, polyester, cardboard, and many more). A camera is mounted on the processing head of the laser and registers the dimensions and position of the printed design by "reading" the registration marks prior to the cutting process.

Vacuum table

Thin and light materials that tend to lie unevenly on the base can be engraved, cut or marked in combination with the vacuum table.

Professional CAD/CAM software

The CAD/CAM software TroCAM is best for obtaining excellent cutting results. Only the SP1500 is equipped with professional CAD/CAM software. Benefit from functions like correction of cutting width, different lead-in/lead out paths, material database and many more.

Standard

JobControl® Lasersoftware

Die Trotec Lasersoftware unterstützt Sie perfekt bei allen Schneid- und Gravuraufgaben. Sie verfügt über eine Vielzahl an nützlichen und intelligenten Funktionen, die Ihre Arbeit erleichtern: z.B. die bi-direktionale Kommunikation zwischen PC und Laser, der Job Time Calculator oder die Positionsmarker.

Lenses 2.5 and 5.0 inch

For flexible material processing with maximum quality.

InPack-Technology™

A high-quality cut depends on several factors. The perfect function of the axis system is most important. The InPack-Technology™, with its closed design, protects the axis. Consequently guide components are perfectly protected against dust. This guarantees years of trouble-free processing even under intensive use. Additional costs for wear parts that have to be exchanged regularly with machines from other manufactureres are thus eliminated.

Options

Cutting table

Heavy-load table

Exhaust systems

The exhaust system evacuates dust and vapors created when operating the laser. The exhaust system guarantees an uninterrupted, safe and reliable laser operation for many years to come. Trotec offers a wide variety of suction systems—from simple ventilators to high-tech filter systems.

Lens 7.5 inch

For perfect results when cutting thick materials.

Heavy-Load Table

The heavy-load table for SP1500 has been developed to carry heavy objects like monuments, tombstones, natural stone, marble and granite plates, tiles, etc. up to 50 kg and 120 mm in height. With this new laser engraver option Trotec is the only supplier of a heavy-load table combined with laser safety class 2.

The technology of SP1500

Working area:	1500 x 1250 mm
Overall dimensions (W x D x H):	2850 x 2200 x 1300 mm
Material size:	1700 x 1600 mm
Material height:	185 mm
Laser power:	60 W - 400 W „sealed-Off" CO2 Laser
Max. processing speed:	165 cm/sec.
Weight:	1300 kg (depending on laser power)
Precision:	+/- 0,1 mm
Addressable accuracy:	Encoder +/- 0,001 mm
Static repeat accuracy:	<+/- 15 µm
Software:	JobControl™ Expert, TroCAM CAD/CAM software or i-cut® Control via Trotec printer driver or HPGL

Trotec laser – developed and built in Austria

A COMPANY OF THE **trodat** GROUP

34747

Send us your materials and samples: Our application engineers support you in looking for the optimal laser system for you.



Printed on FSC certified paper

www.troteclaser.com

Trotec Produktions u. Vertriebs GmbH
Linzer Str. 156, A-4600 Wels, trotec@troteclaser.com
Tel. +43 / 72 42 / 239-7002, Fax +43 / 72 42 / 239-7380

www.facebook.com/trotec
twitter.com/TrotecLaser

6.3 Appendix 3 – Optical Microscope Analysis complete footage

Sample description	Optical Microscope analysis
(1,1,8) sample 2x amplification	
(1,1,8) sample 4x amplification Left side	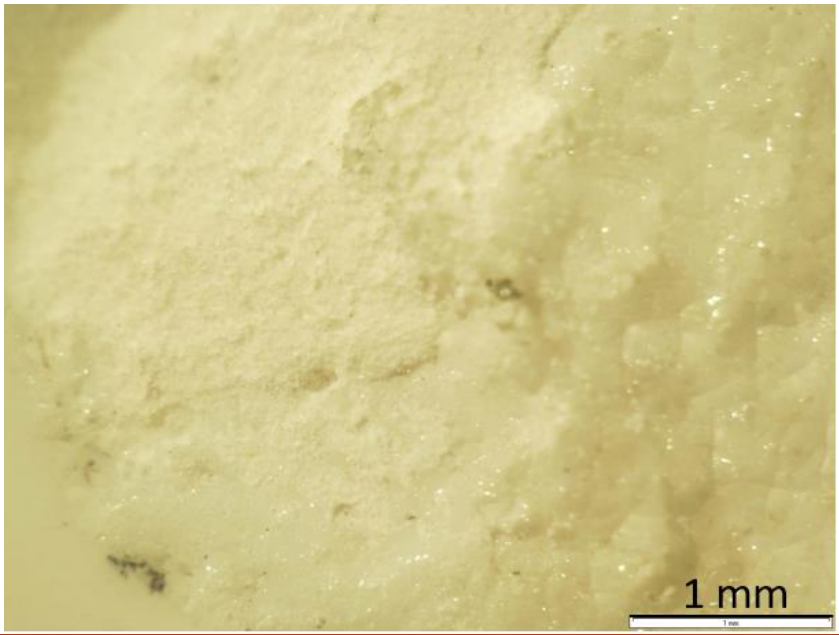

(1,1,8) sample
4x amplification
Right side

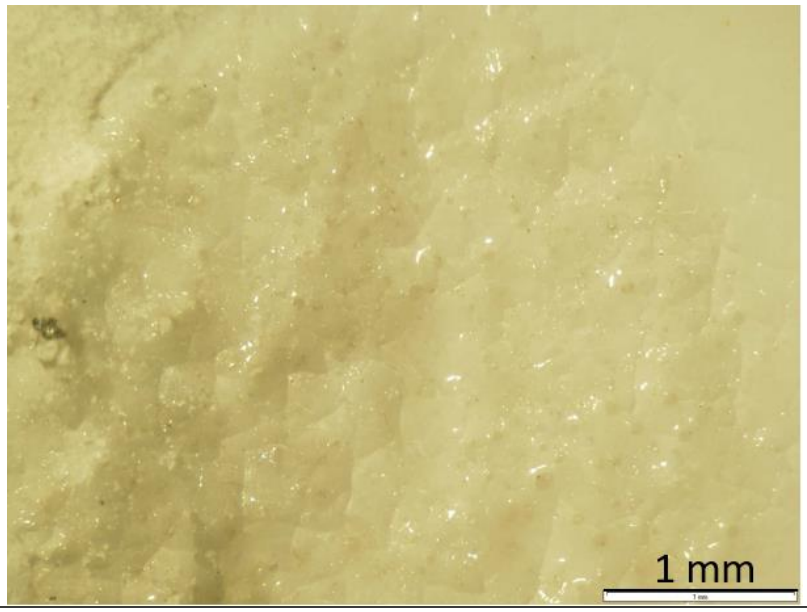

(1,2,1) sample
2x amplification

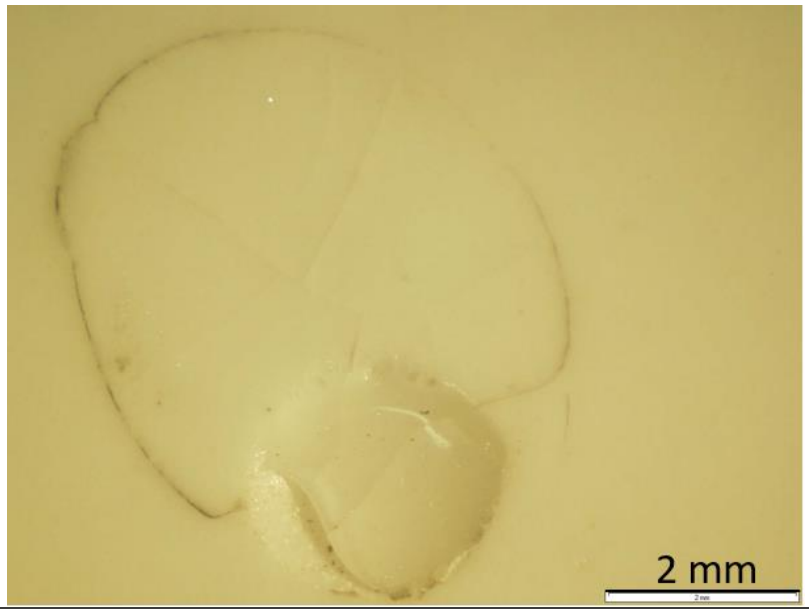

(1,2,1) sample
4x amplification

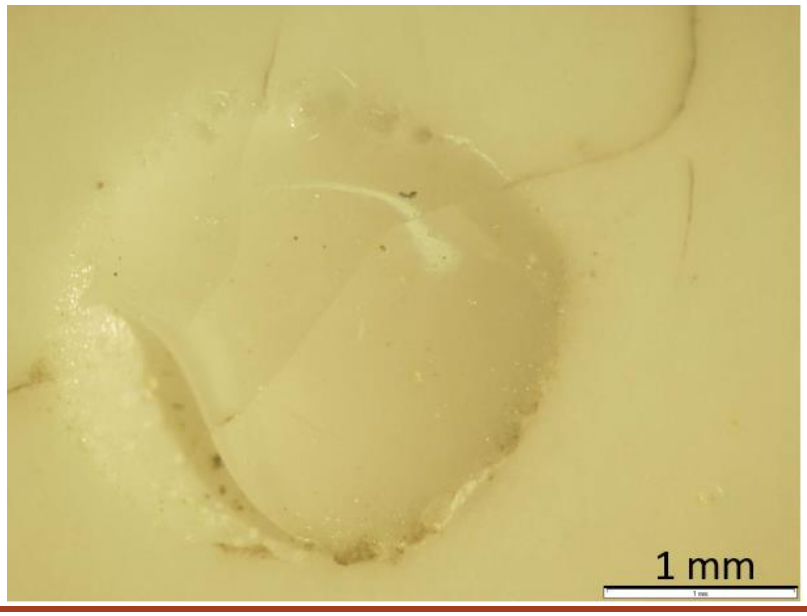

(2,1,13) sample 2x amplification Left side	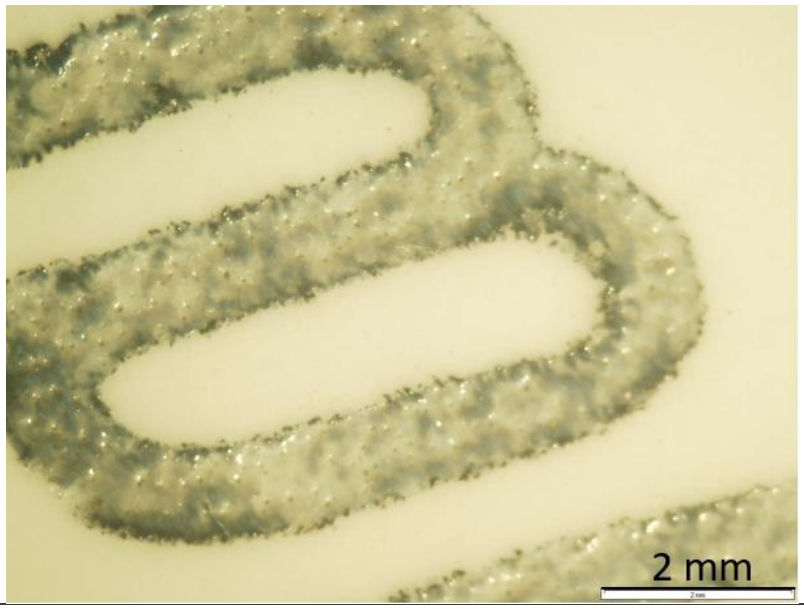
(2,1,13) sample 2x amplification Right side	
(2,1,13) sample 4x amplification	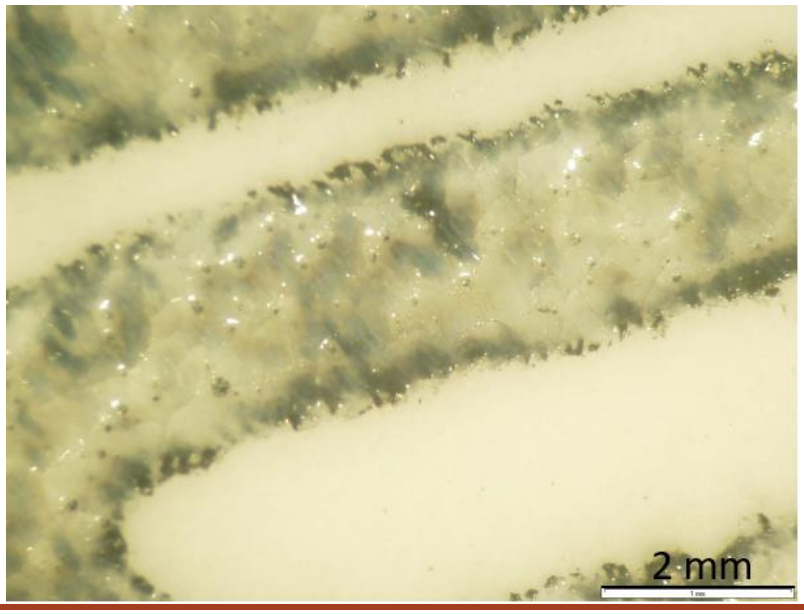

(2,1,13) sample 6x amplification	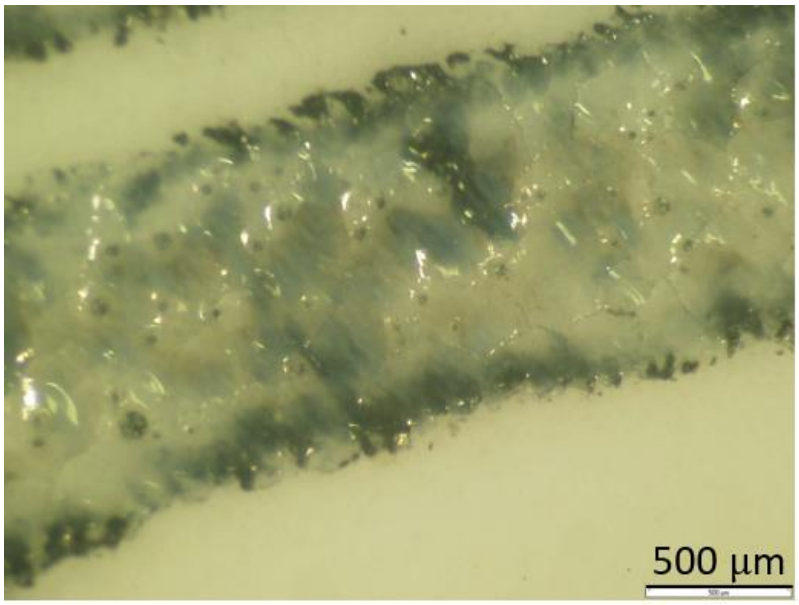
(2,1,13) sample 11x amplification	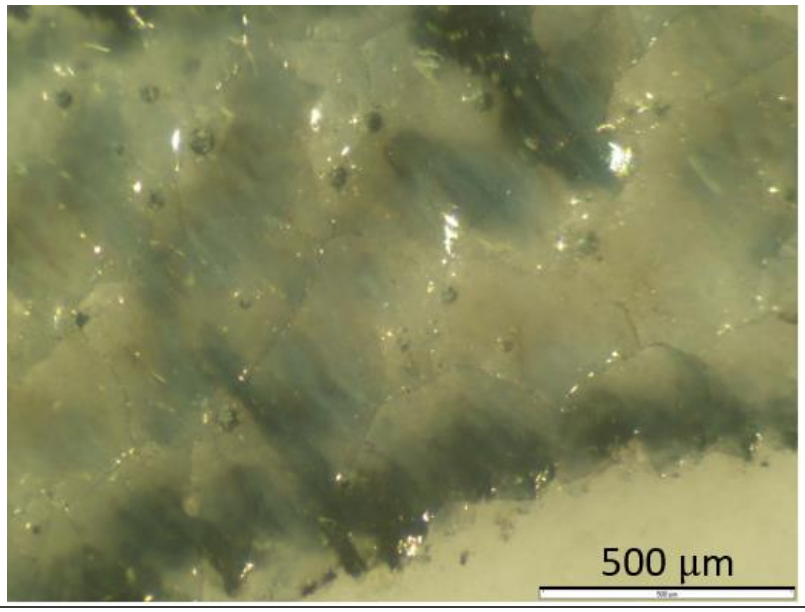
(2,1,14) sample 2x amplification	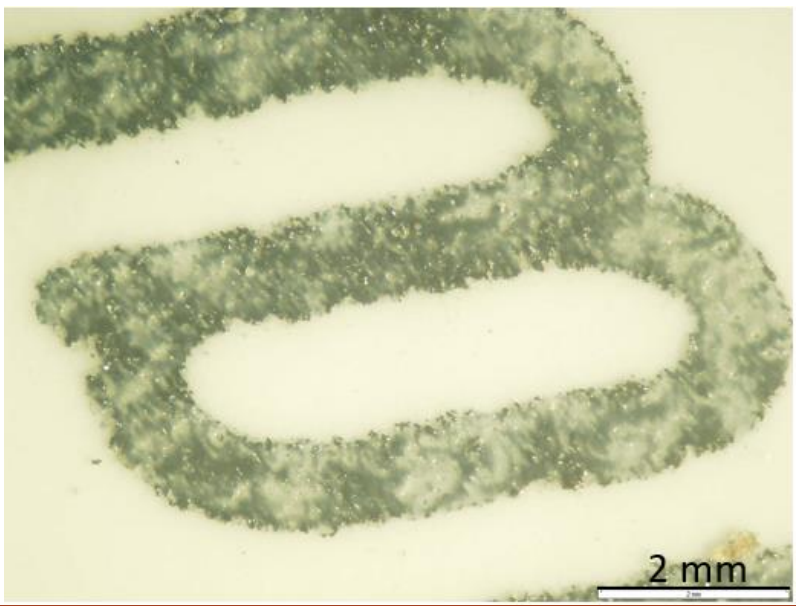

(2,1,14) sample
4x amplification

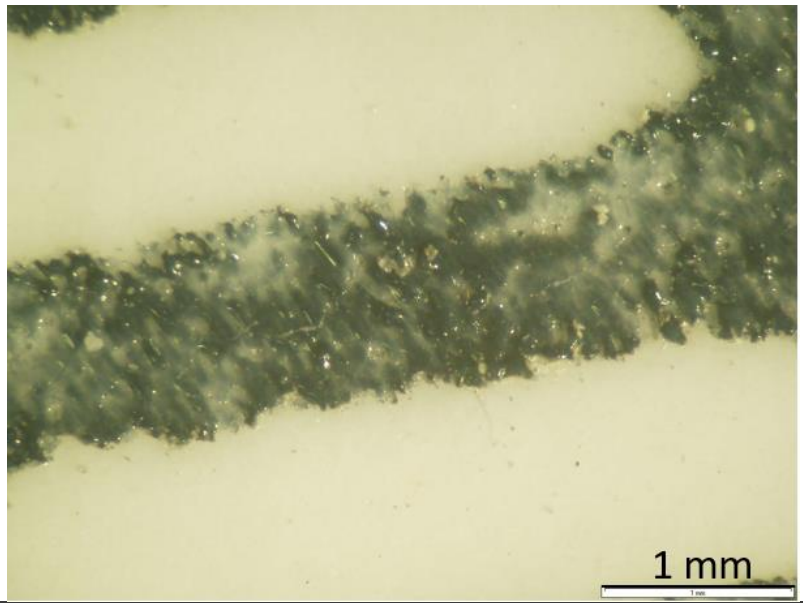

(2,1,14) sample
6x amplification

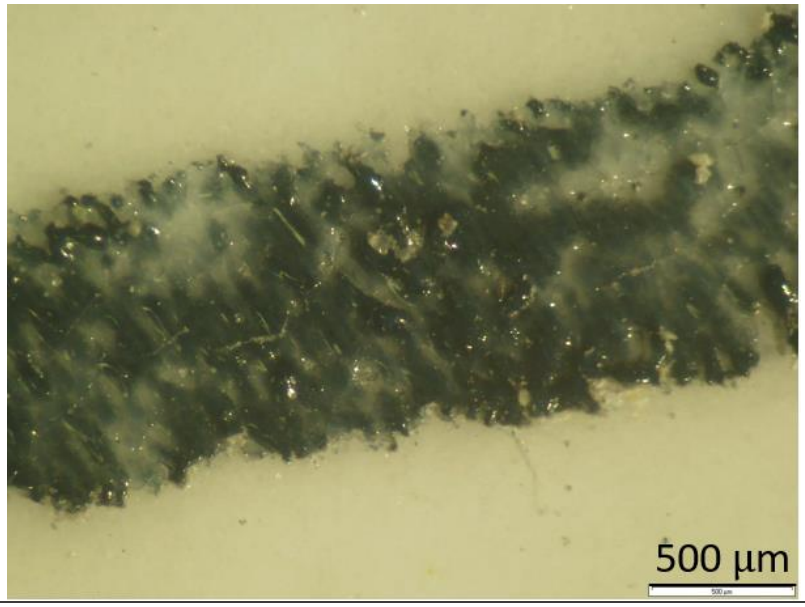

(2,1,14) sample
11x amplification

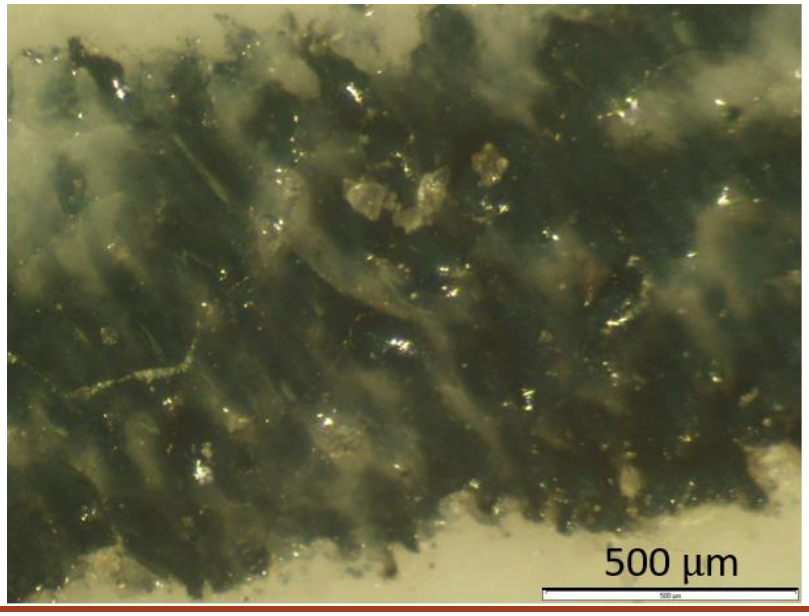

(2,2,1) sample
2x amplification

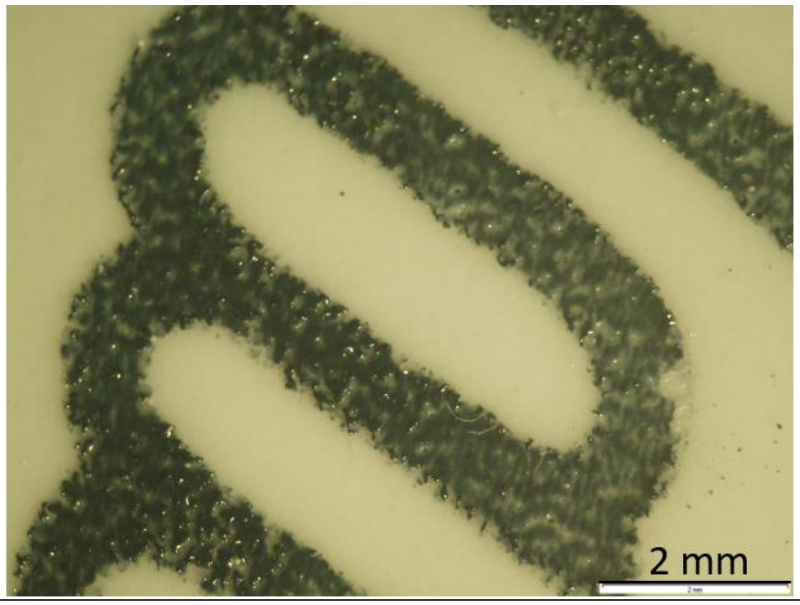

(2,2,2) sample
2x amplification

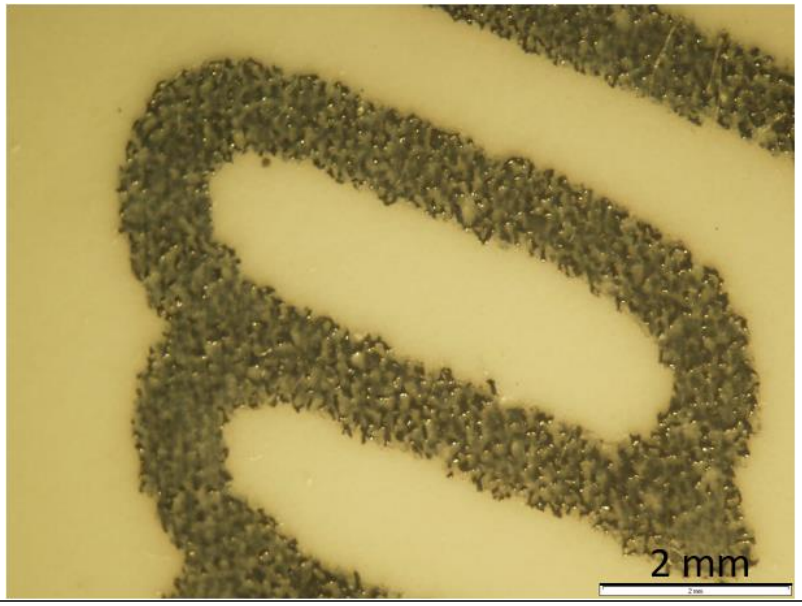

(2,2,2) sample
4x amplification

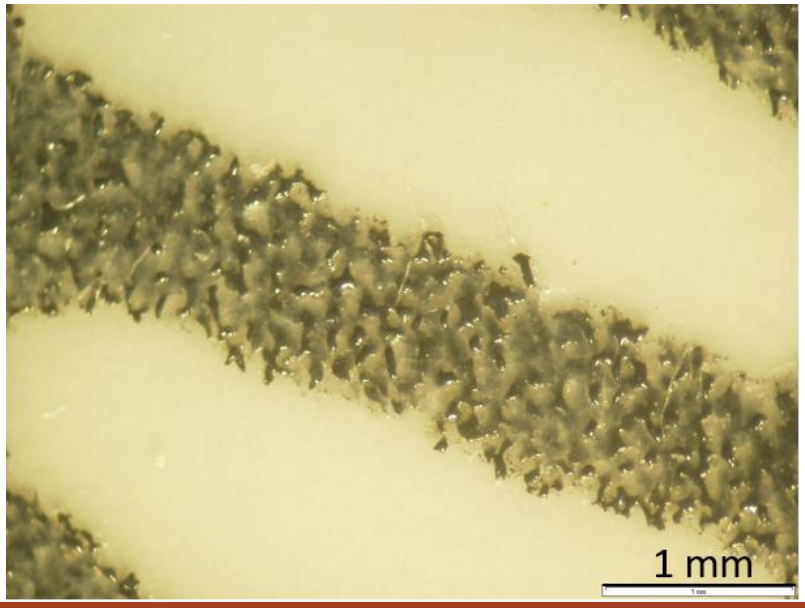

(3,1,1) sample
2x amplification
Top view

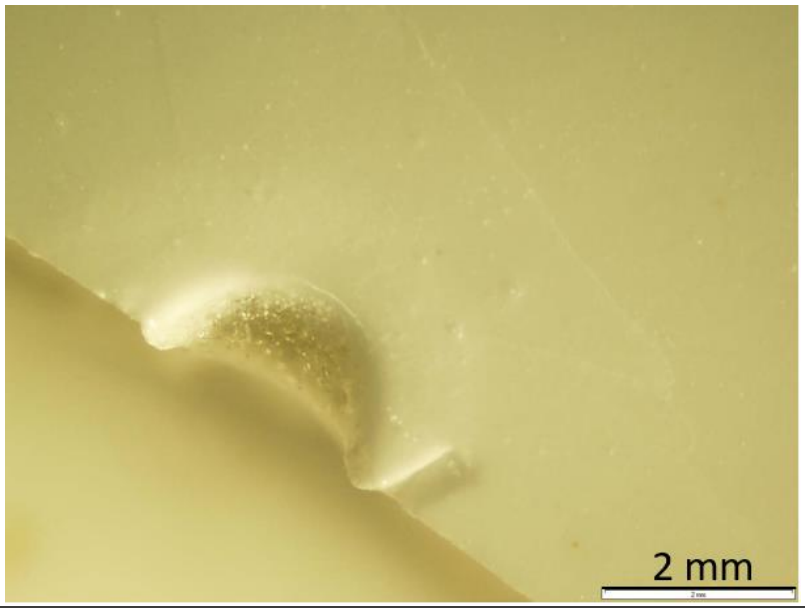

(3,1,1) sample
4x amplification
Sectional view

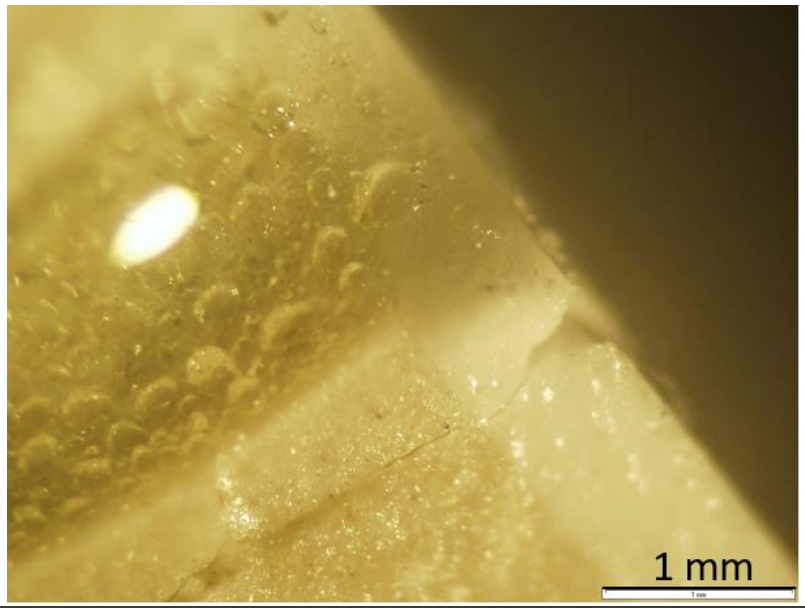

(3,1,5) sample
2x amplification

(3,1,5) sample
4x amplification

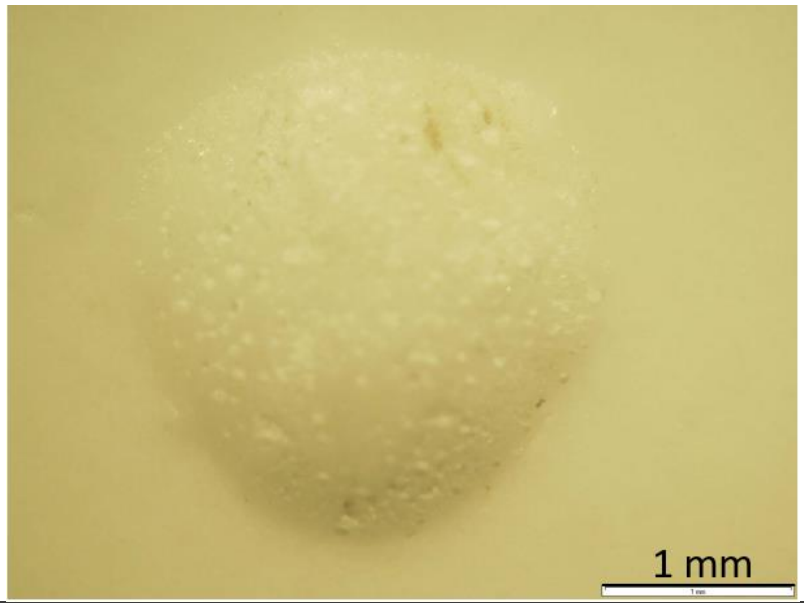

(3,1,6) sample
2x amplification

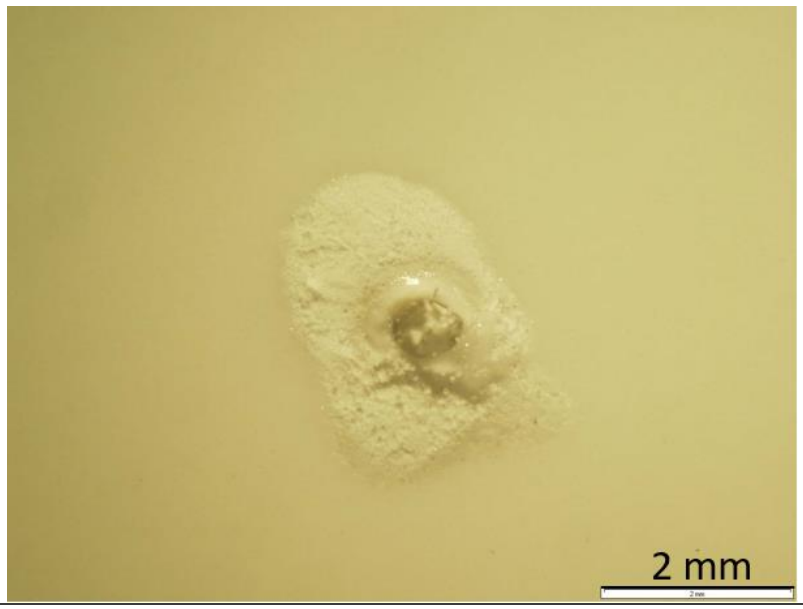

(3,1,6) sample
4x amplification

(3,1,6) sample
6x amplification

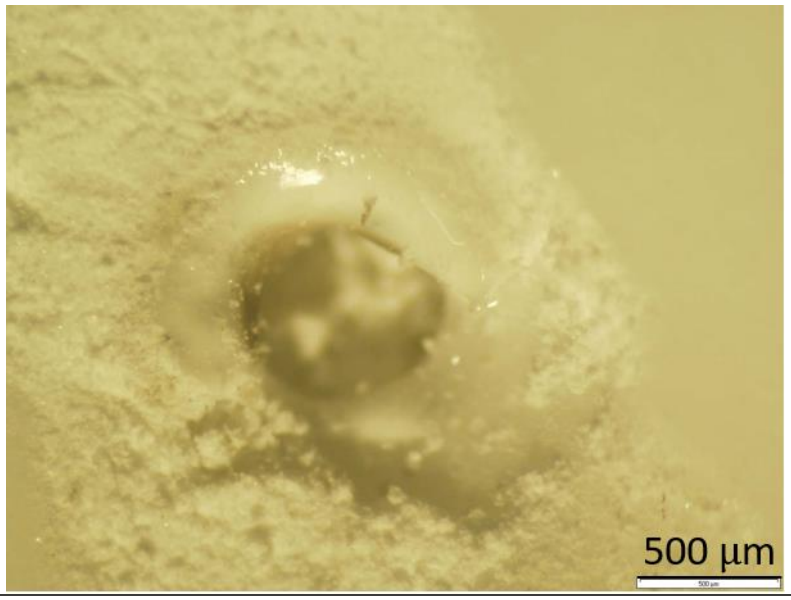

(3,2,1) sample
2x amplification

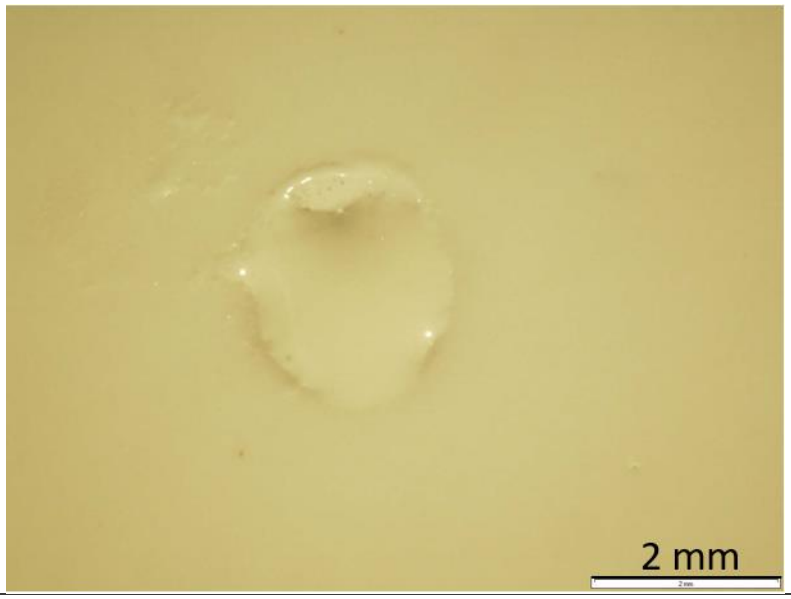

(3,2,2) sample
2x amplification

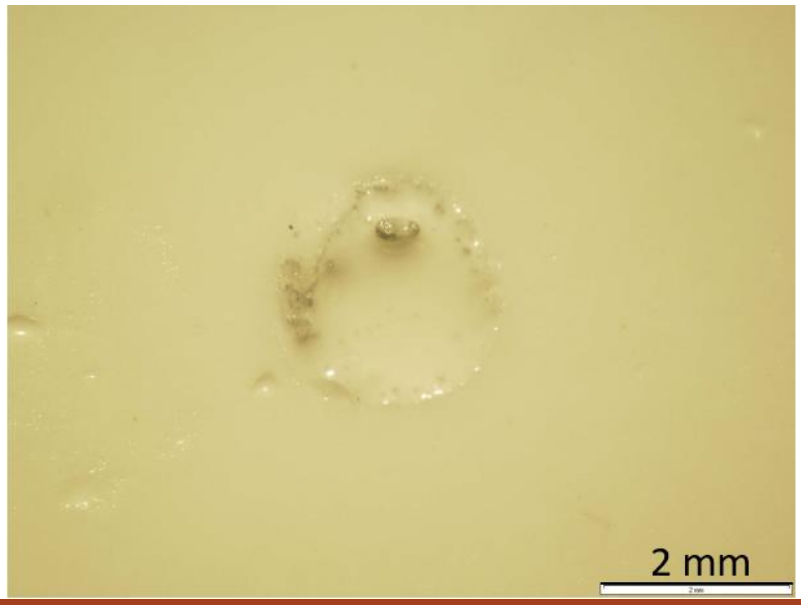

(3,2,3) sample
2x amplification

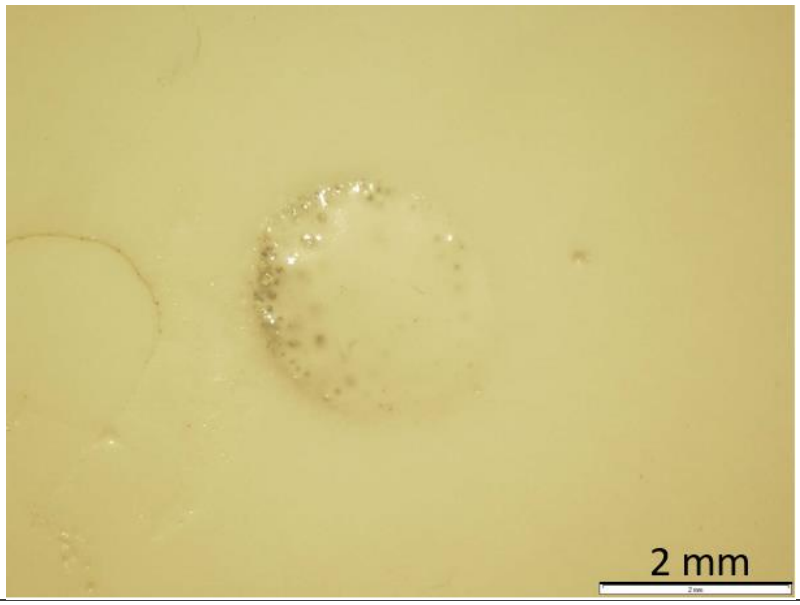

(3,2,4) sample
2x amplification

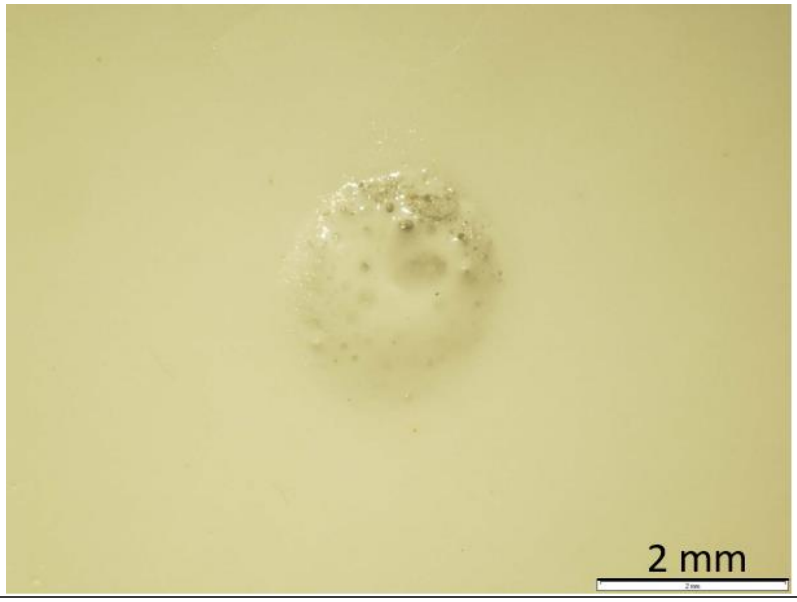

(3,2,4) sample
4x amplification

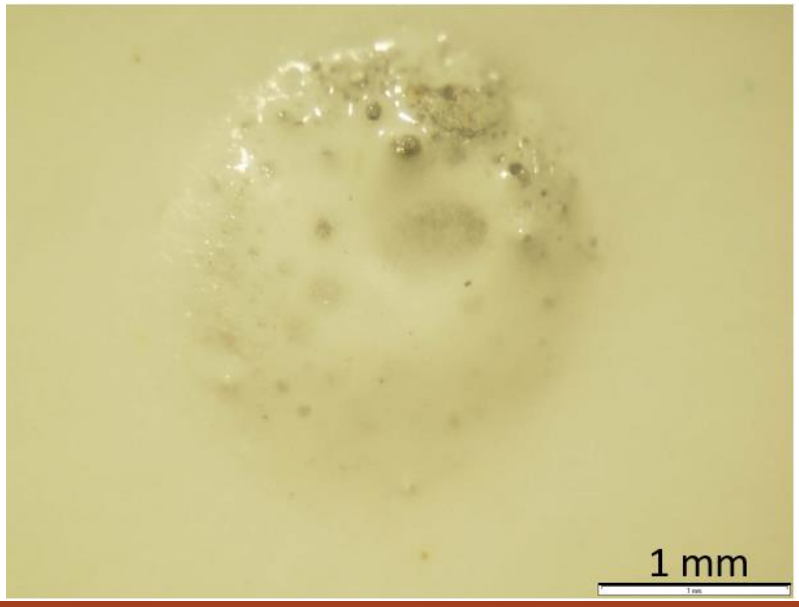

(3,2,5) sample
2x amplification

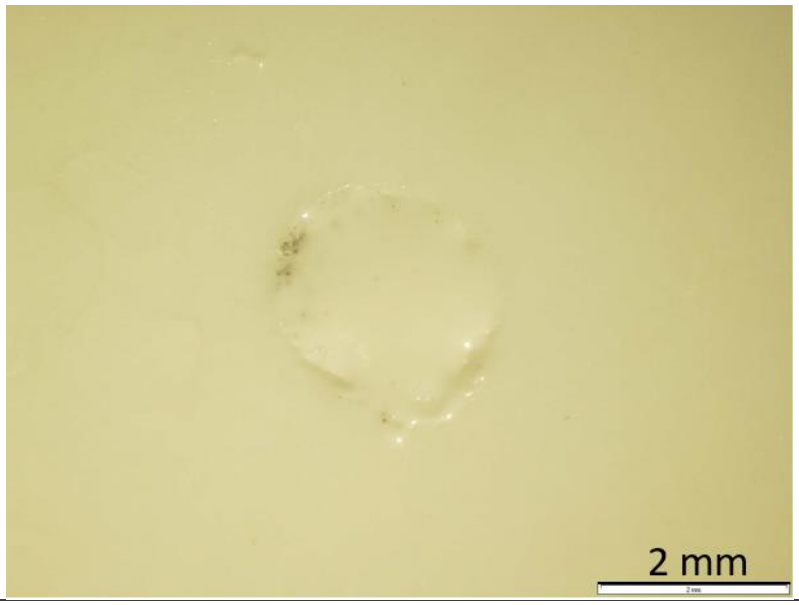

(3,2,6) sample
2x amplification

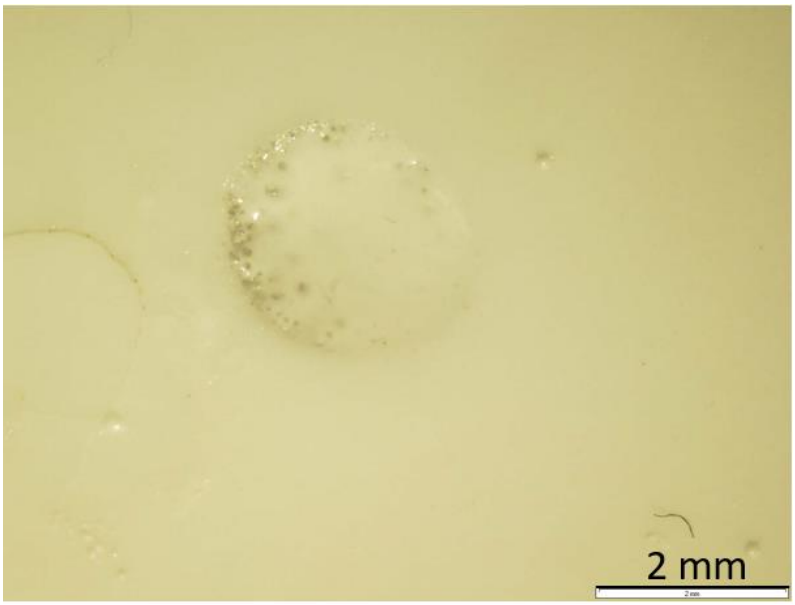

(3,2,6) sample
4x amplification

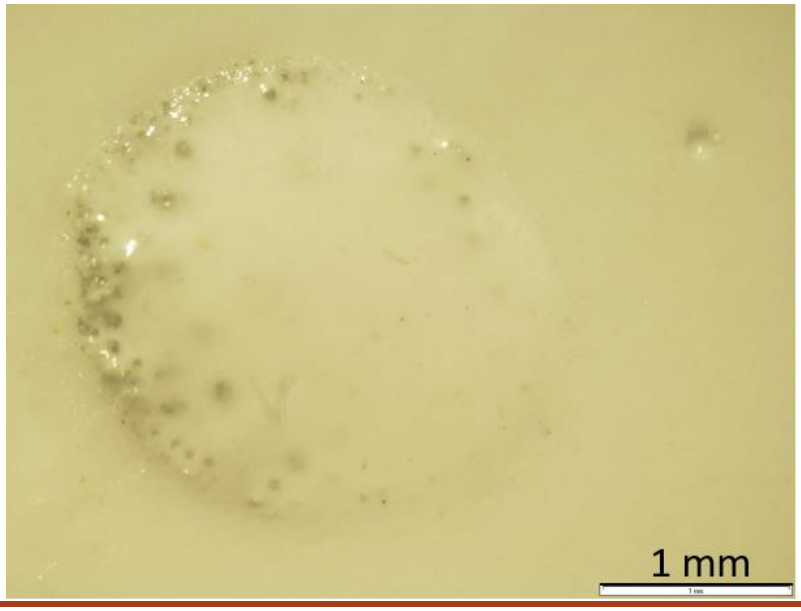

(3,2,4) sample 2x amplification Top view	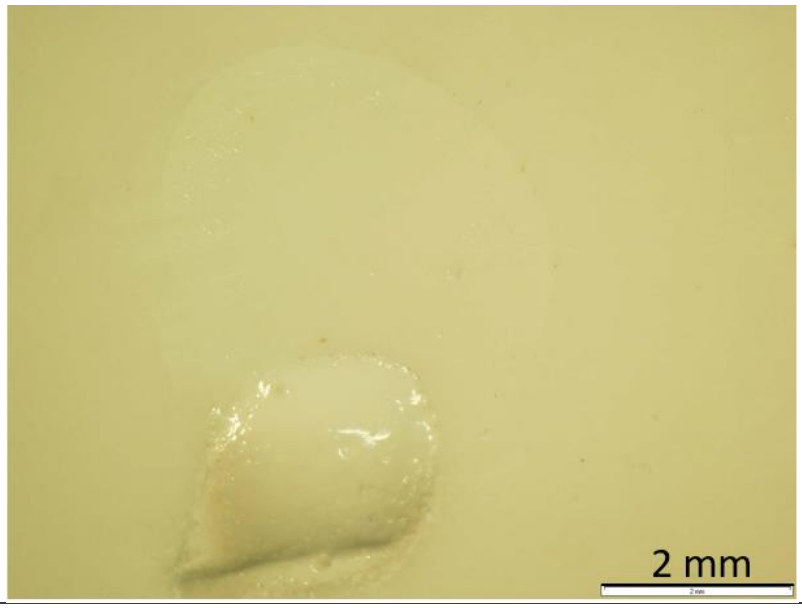
(3,2,4) sample 2x amplification Centre view	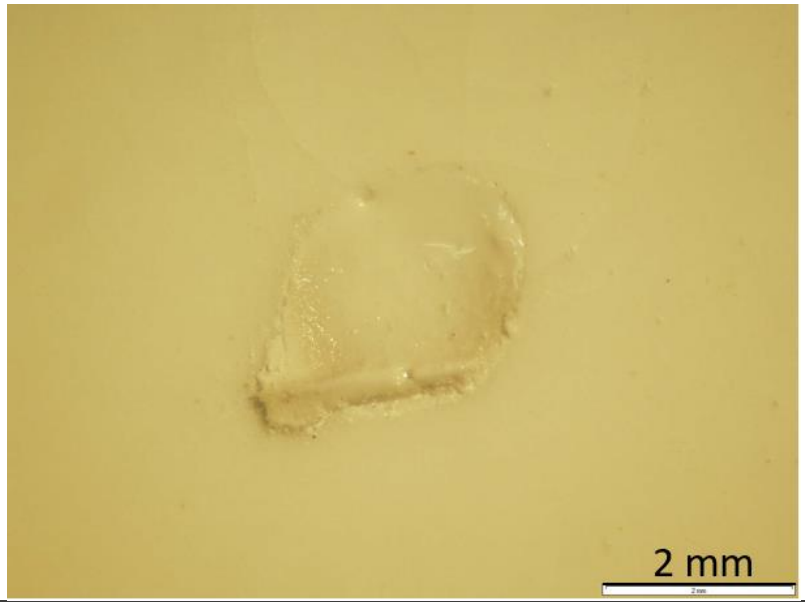
(3,3,4) sample 4x amplification	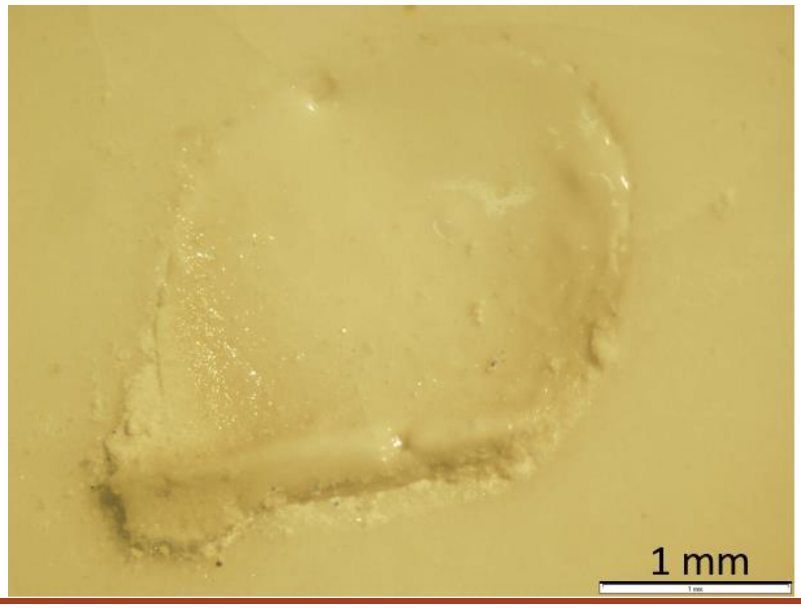

(4,1,5) sample
2x amplification

(4,1,7) sample
2x amplification

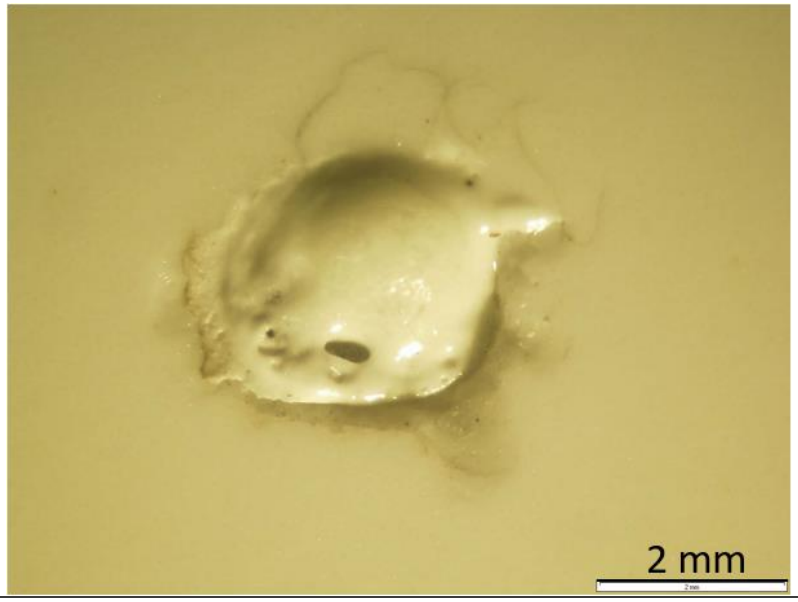

(4,1,7) sample
4x amplification

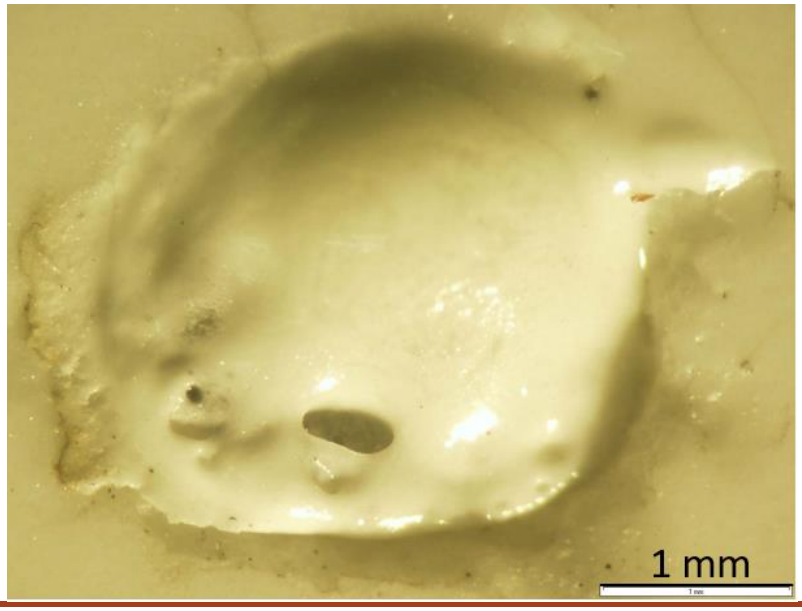

(4,1,8) sample
2x amplification

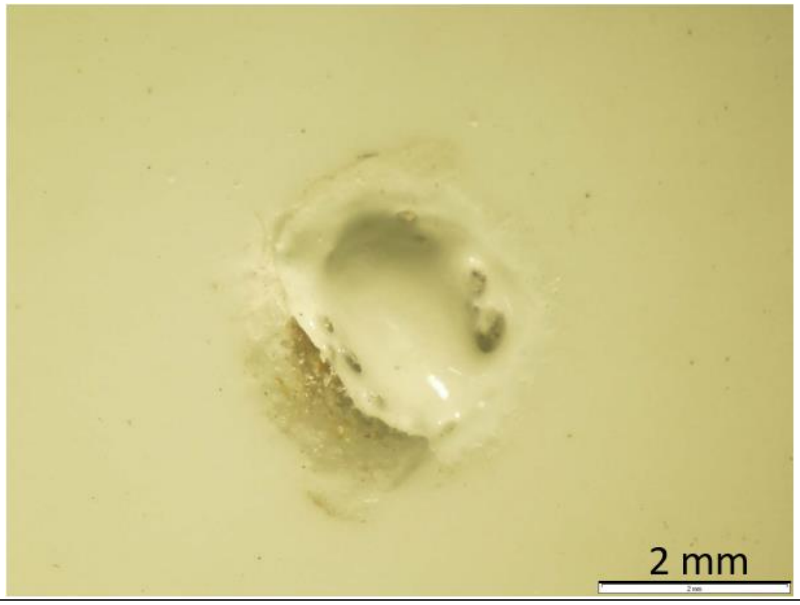

(4,1,8) sample
4x amplification

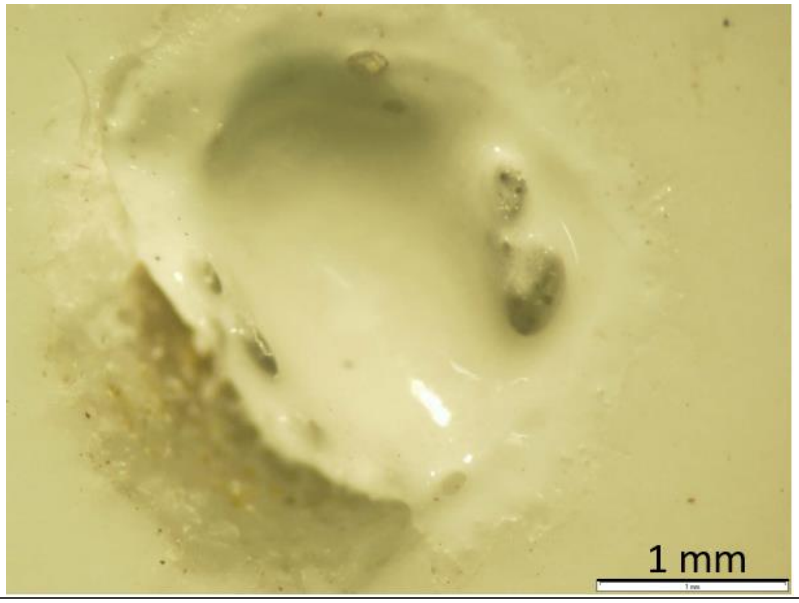

(4,1,9) sample
2x amplification

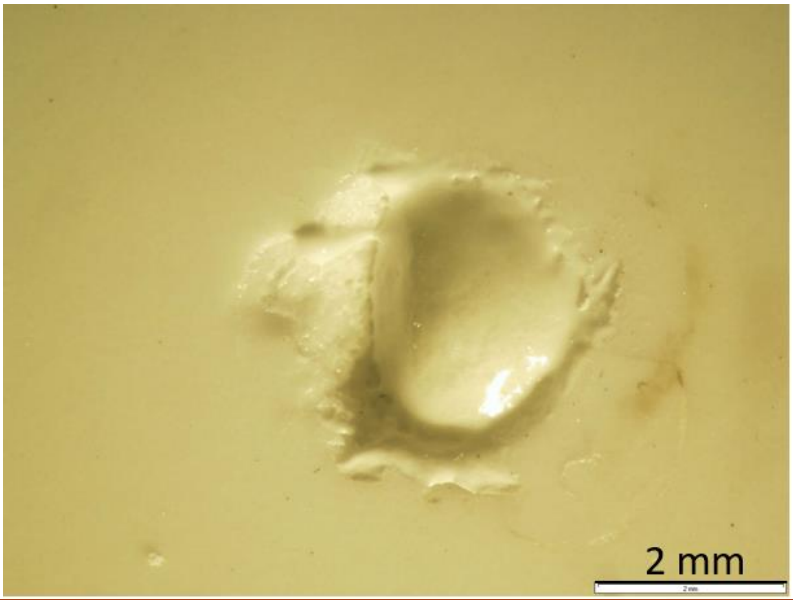

(4,1,9) sample 4x amplification	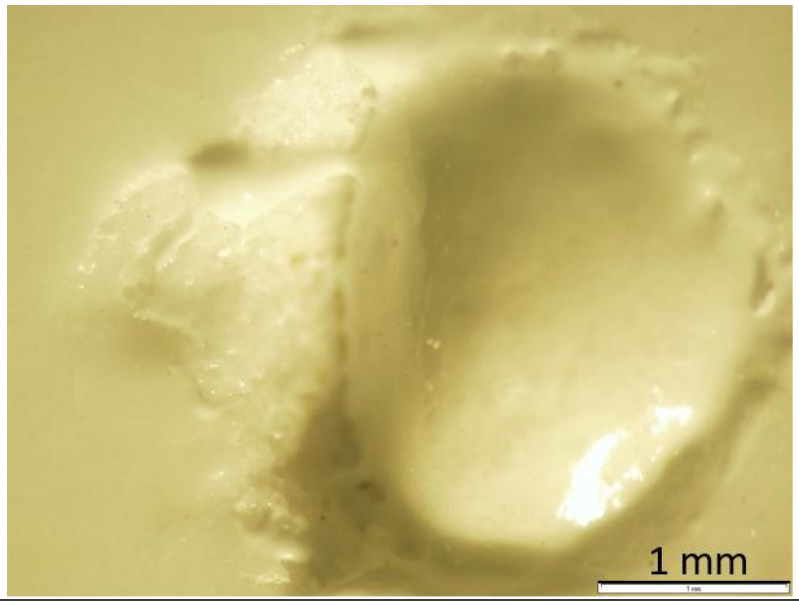
(5,1,5) sample 2x amplification Left side	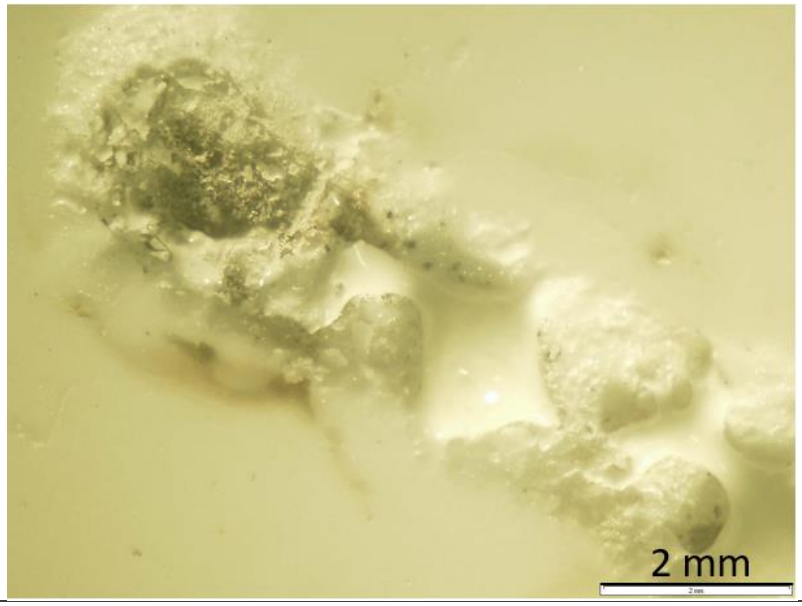
(5,1,5) sample 2x amplification Right side	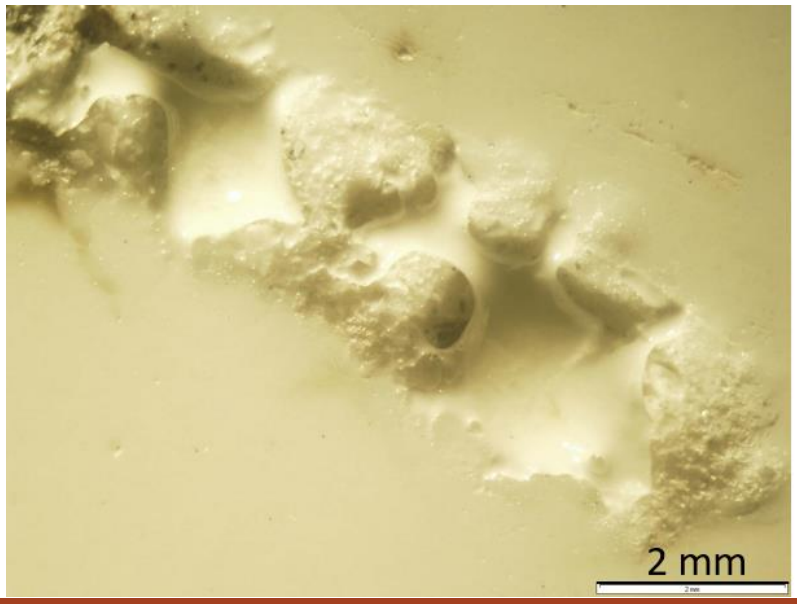

(5,1,6) sample
2x amplification

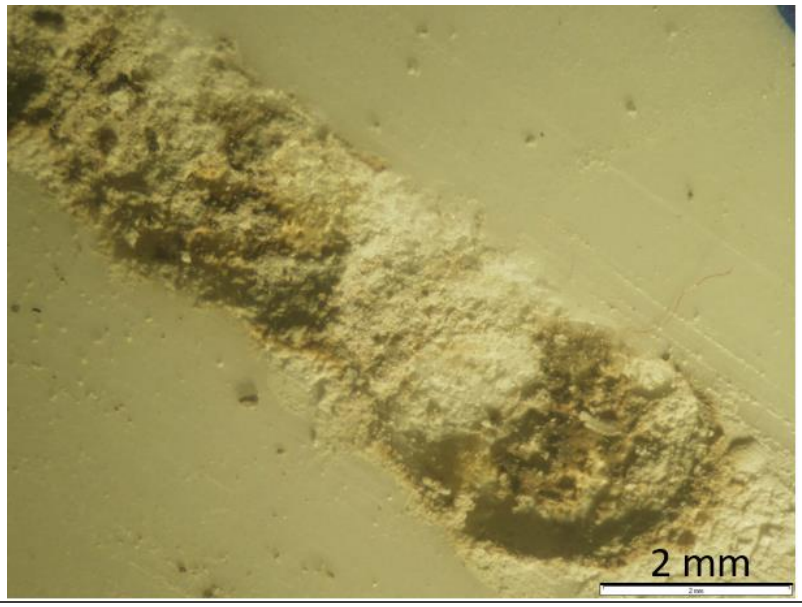

(5,2,2) sample
2x amplification

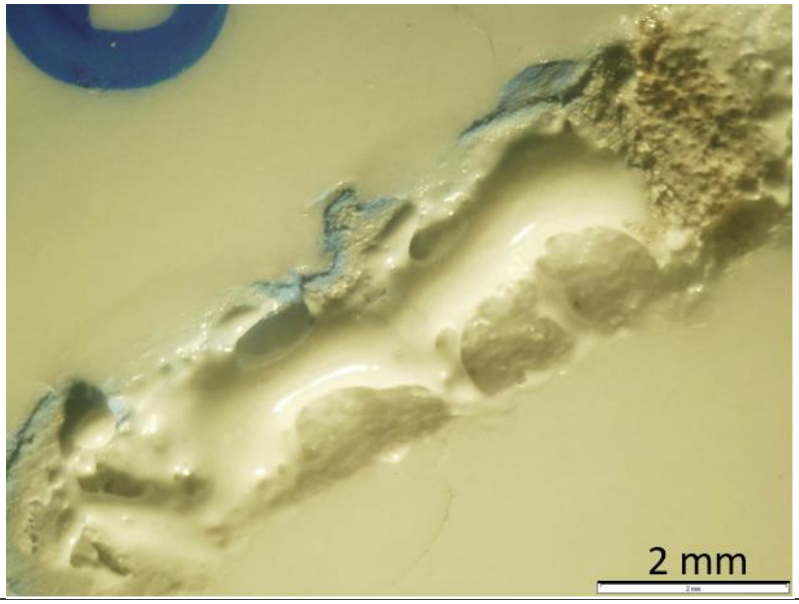

(5,2,4) sample
2x amplification

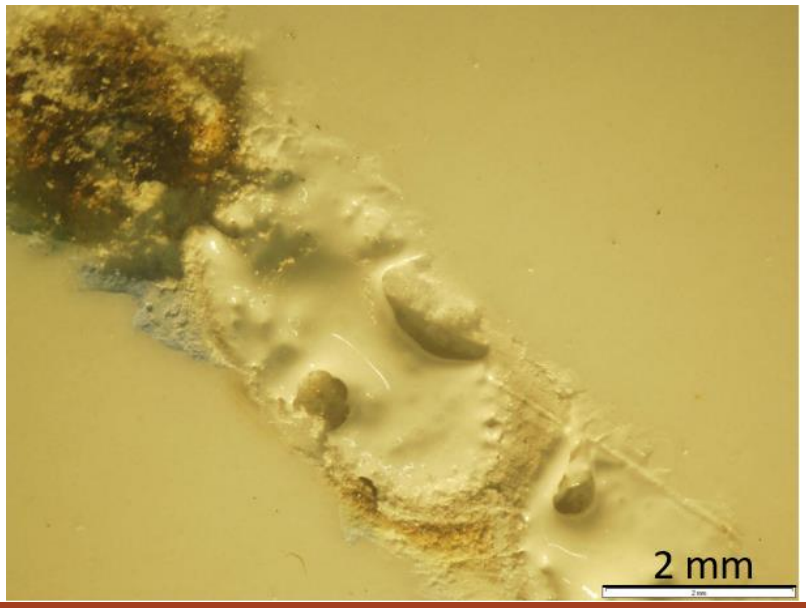

(5,2,6) sample 2x amplification	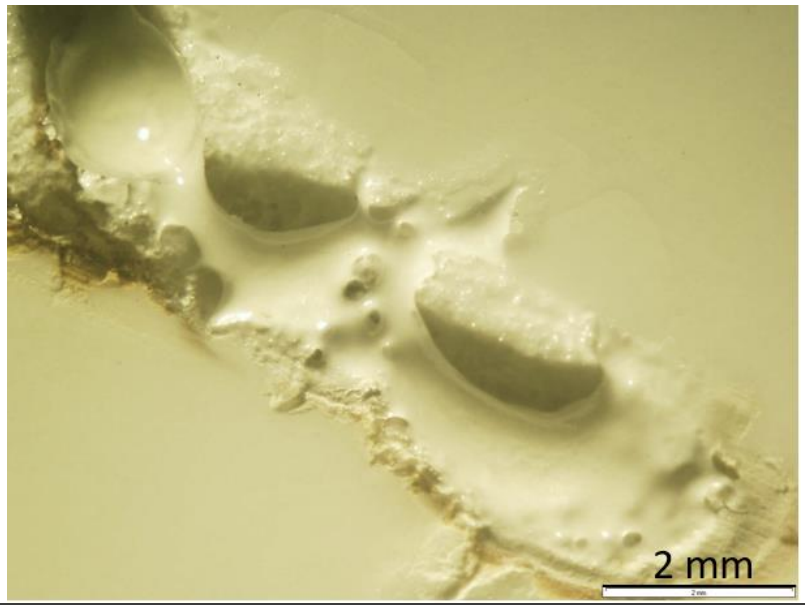
(5,2,6) sample 3x amplification	
(5,2,6) sample 4x amplification Left side	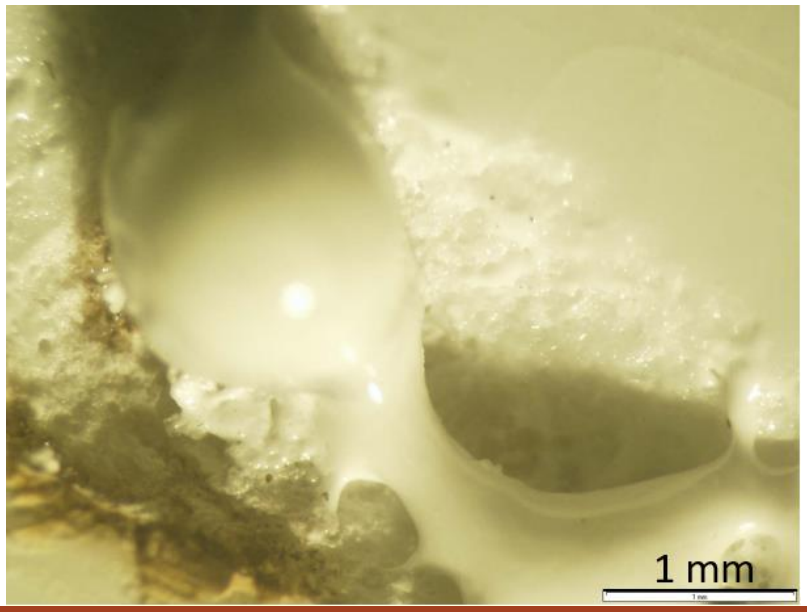

(5,2,6) sample
4x amplification
Right side

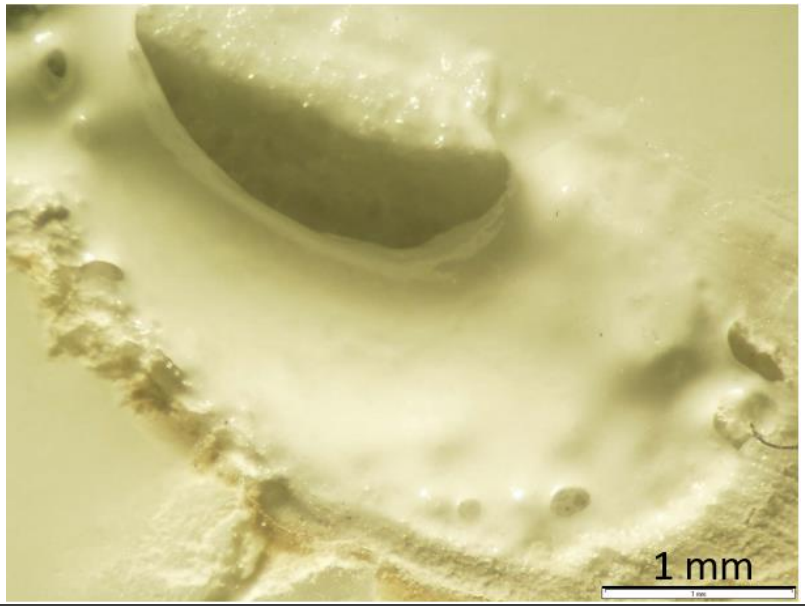

(6,2,9) sample
4x amplification
Left side

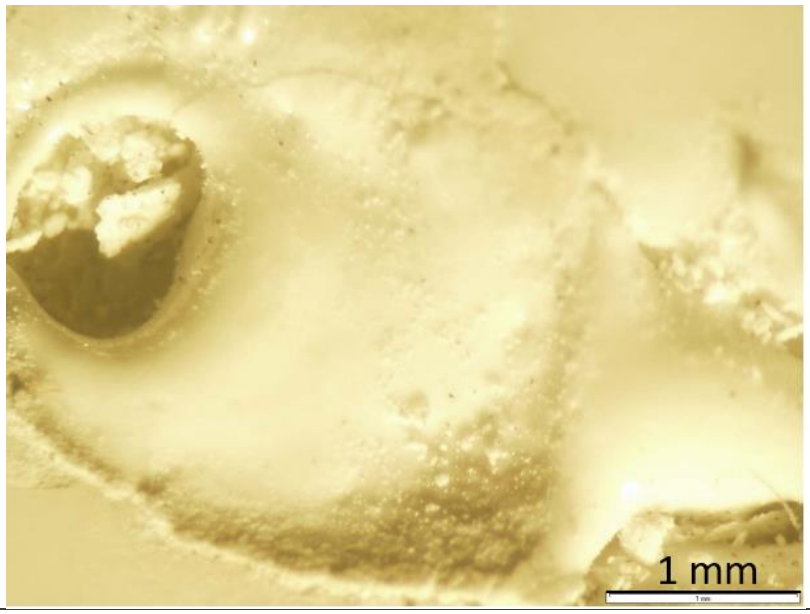

(6,2,9) sample
4x amplification
Right side

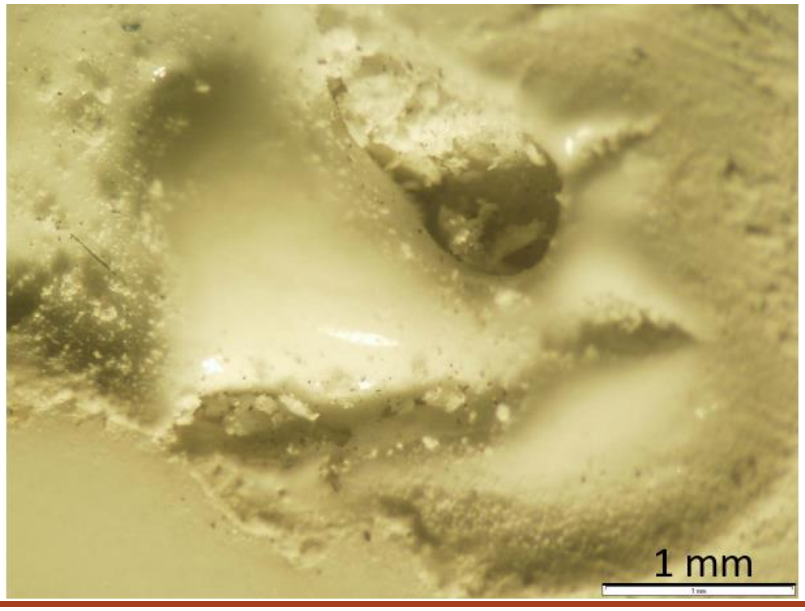

6.4 Appendix 4 – SEM-EDS Analysis complete footage

Sample description	SEM-EDS analysis
(3,2,1) sample 75x amplification Backscattered electron image	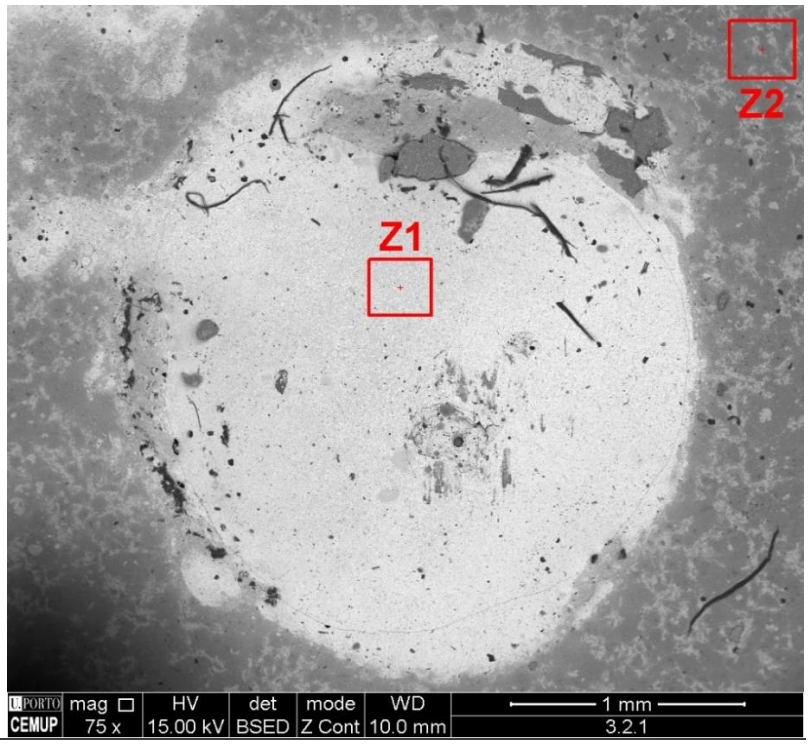
(3,2,1) sample Z2 region Micro constitution	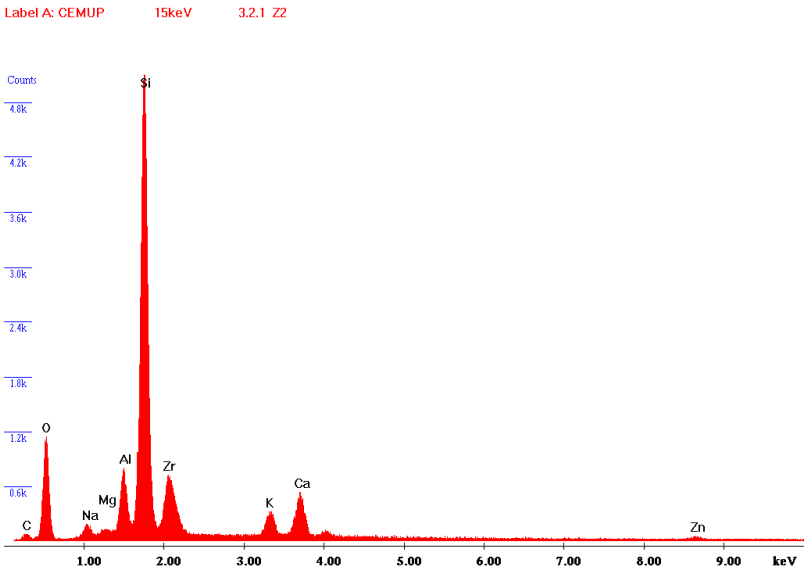

(3,2,1) sample
250x amplification
Centre left side
Topography image

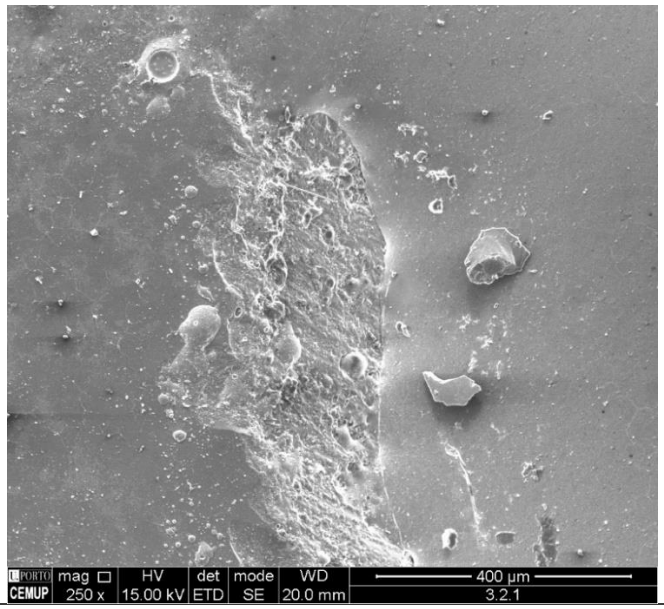

(3,2,1) sample
500x amplification
Centre left side
Topography image

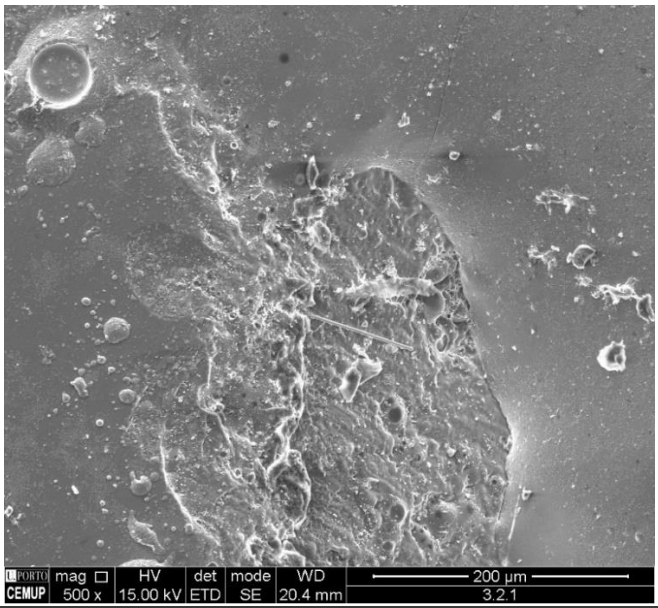

(3,2,1) sample
2000x amplification
Centre left side
Topography image

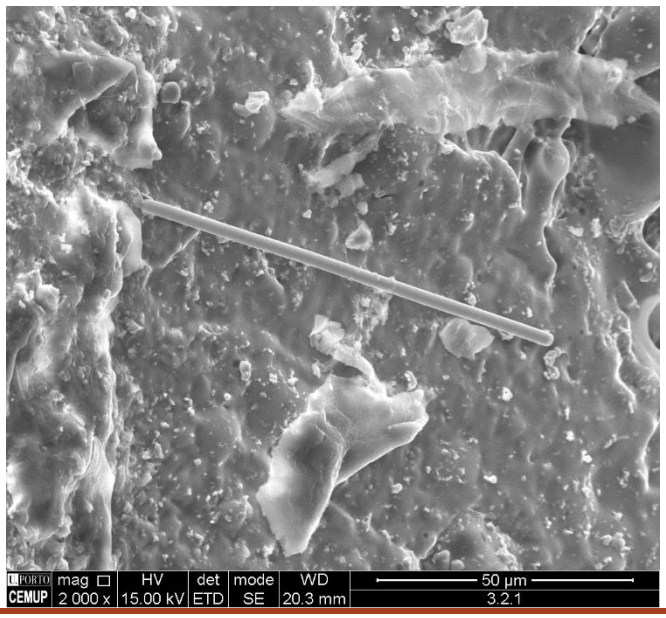

(3,2,1) sample
500x amplification
Centre
Topography image

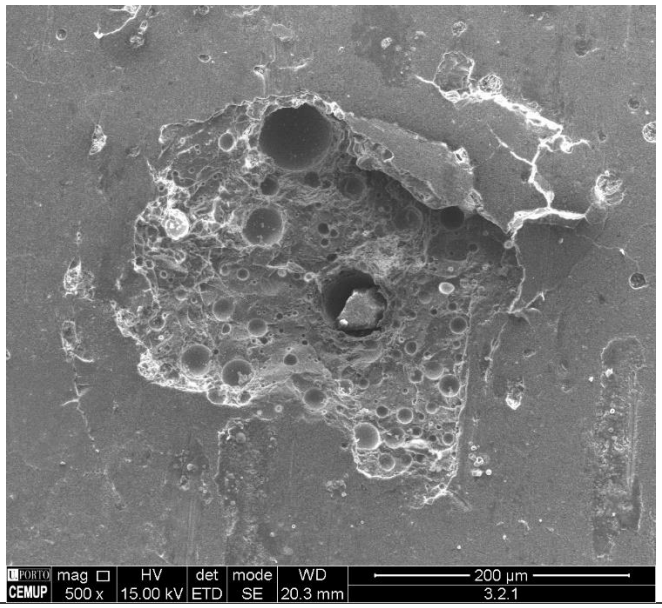

(3,2,3) sample
500x amplification
Centre left side
Topography image

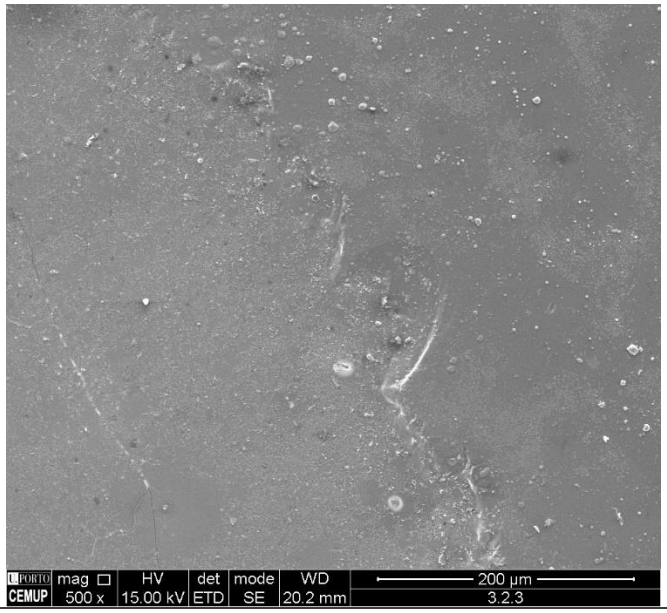

(3,2,3) sample
2000x amplification
Centre left side
Topography image

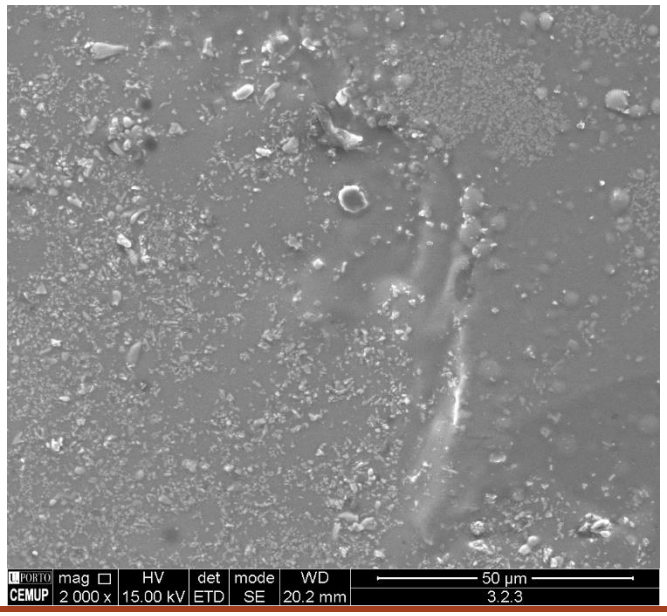

(3,2,3) sample
250x amplification
Lower right side
Topography image

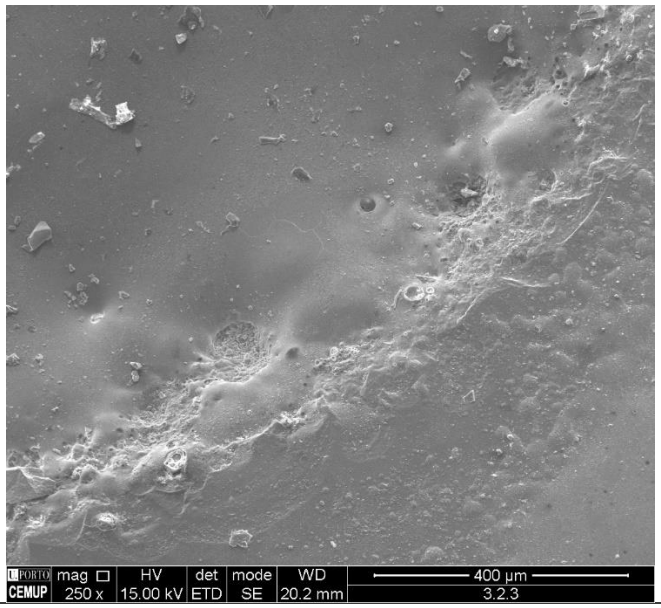

(3,2,3) sample
500x amplification
Lower right side
Topography image

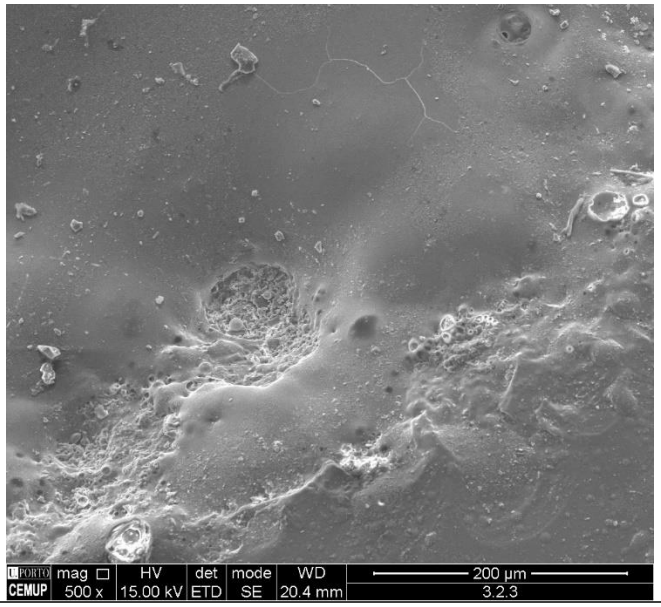

(3,2,3) sample
5000x amplification
Lower right side
Topography image

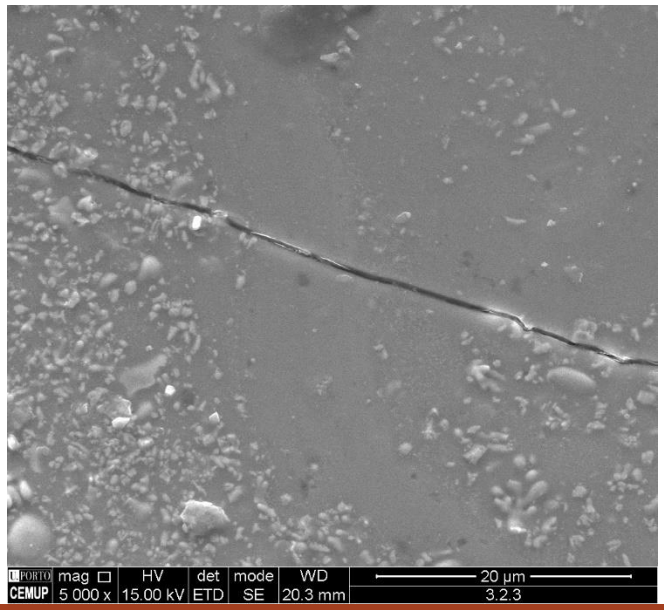

(3,2,3) sample
20,000x amplification
Lower right side
Topography image

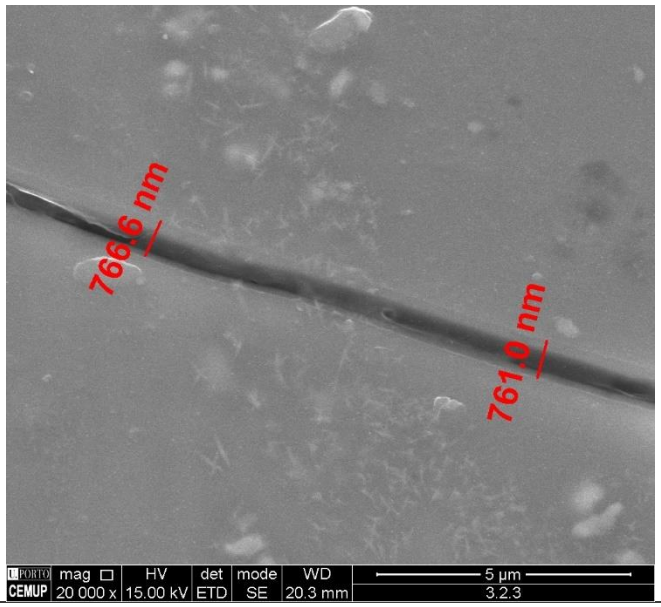

(3,2,3) sample
500x amplification
Lower left side
Topography image

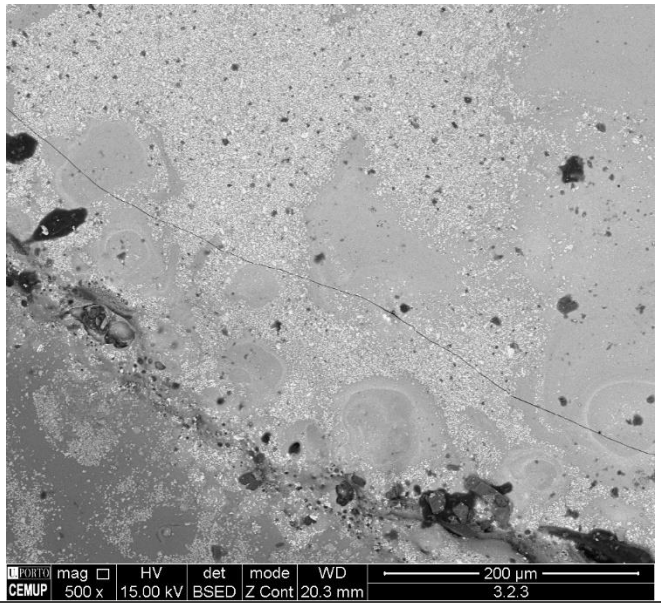

(3,2,7) sample
70x amplification
Upper centre side
Topography image

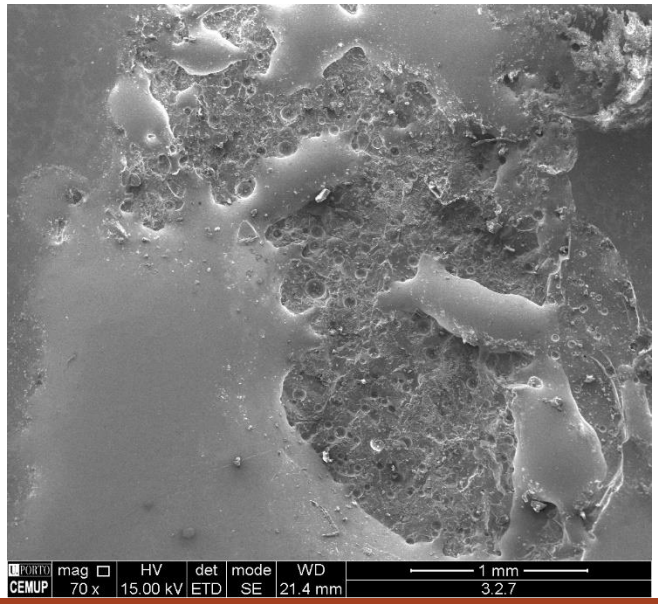

(3,2,7) sample
250x amplification
Upper centre side
Topography image

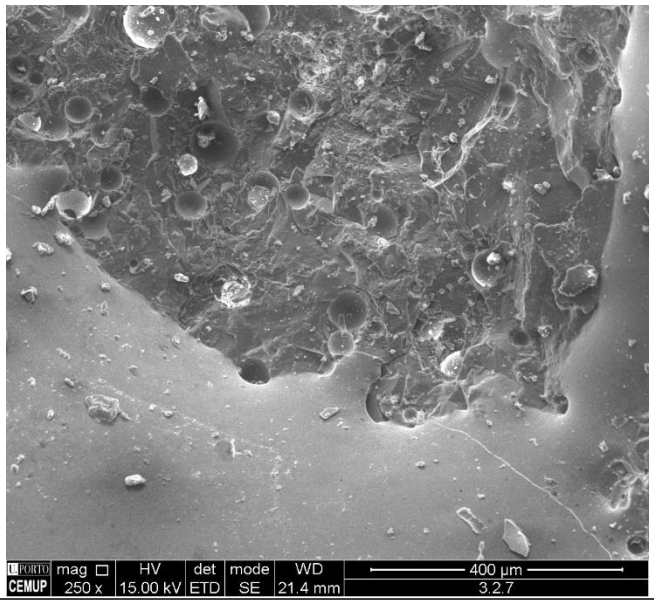

(3,2,7) sample
50x amplification
Centre
Backscattered electron image

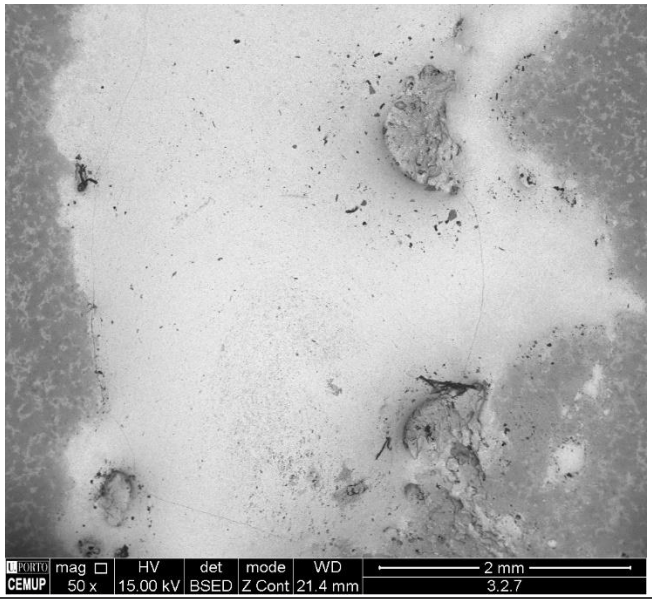

(3,2,7) sample
250x amplification
Upper right side
Topography image

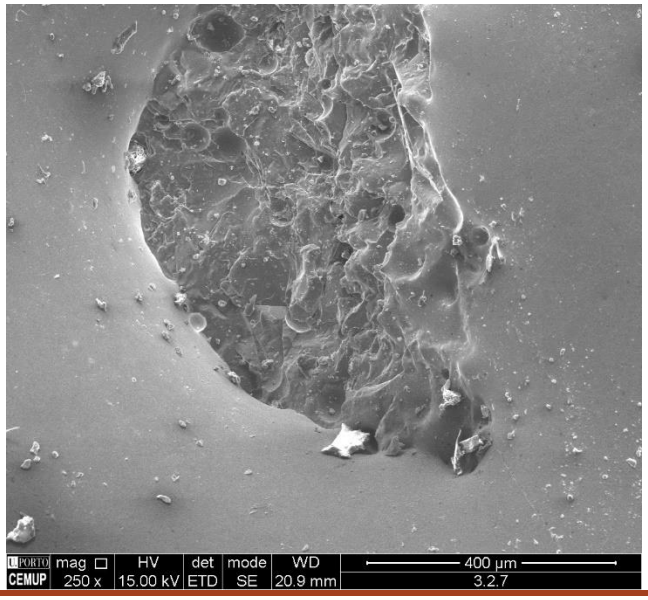

(3,2,7) sample
50x amplification
Lower centre side
Topography image

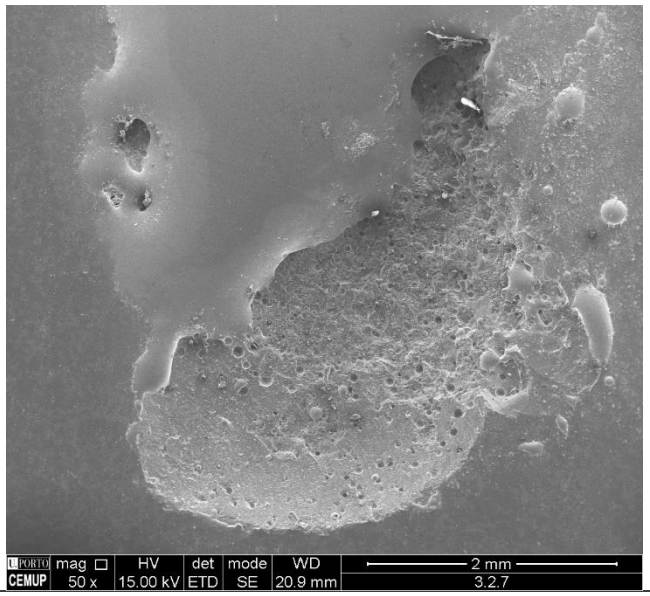

(3,2,7) sample
150x amplification
Lower centre side
Topography image

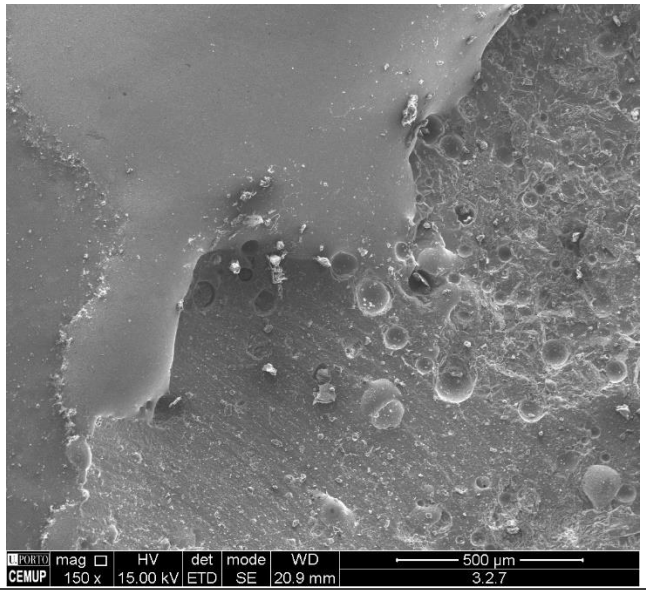

(3,2,7) sample
2500x amplification
Lower centre side
Topography image

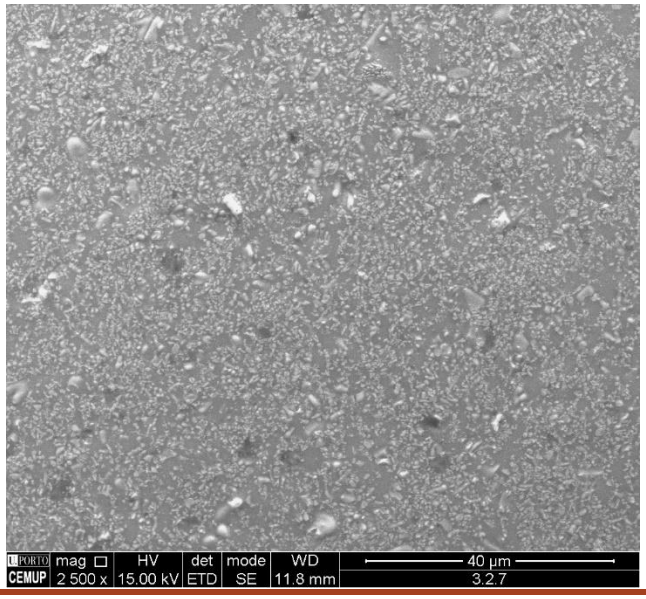

(6,2,6) sample
70x amplification
Upper centre side
Topography image

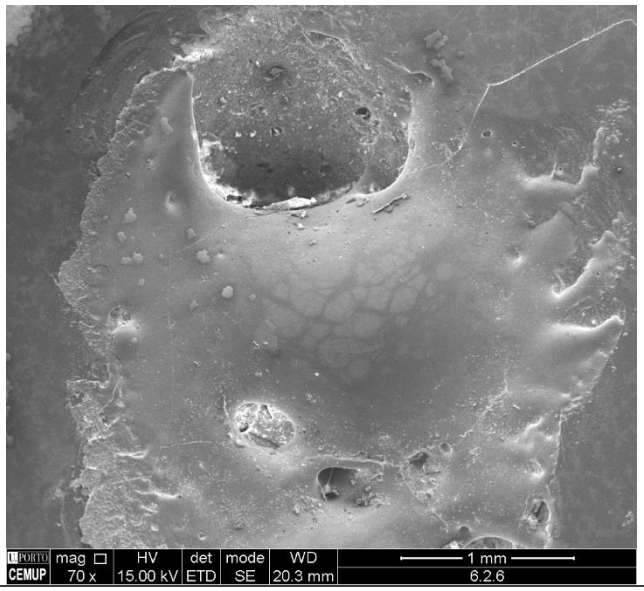

(6,2,6) sample
250x amplification
Upper centre side
Topography image

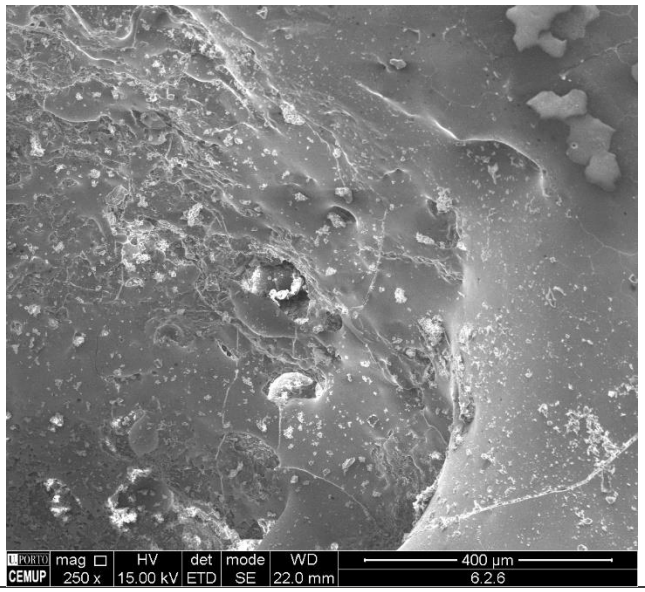

(6,2,6) sample
70x amplification
Lower side
Backscattered electron image

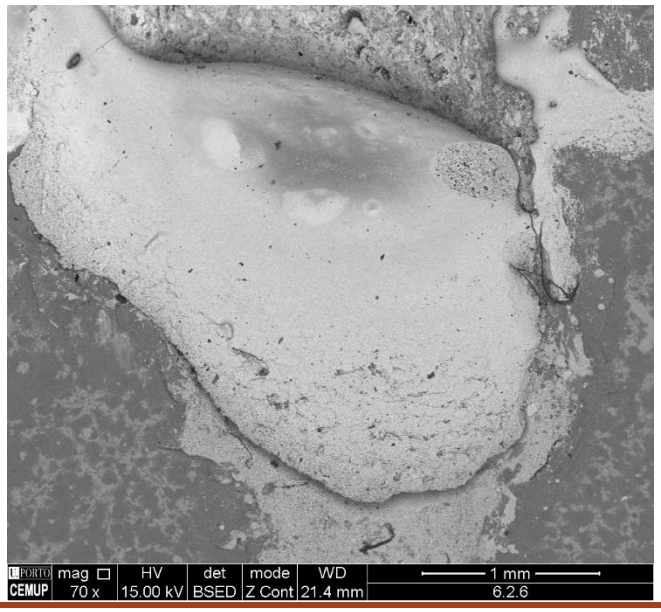

Standard sample

250x amplification

Topography image

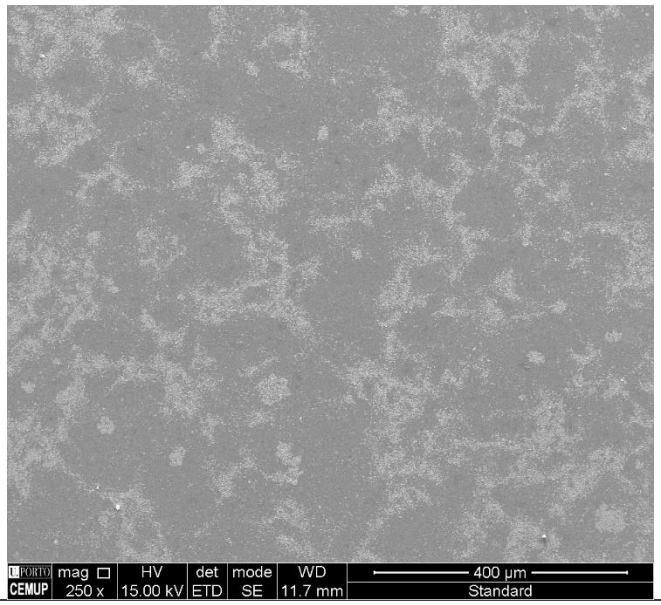

Standard sample

500x amplification

Topography image

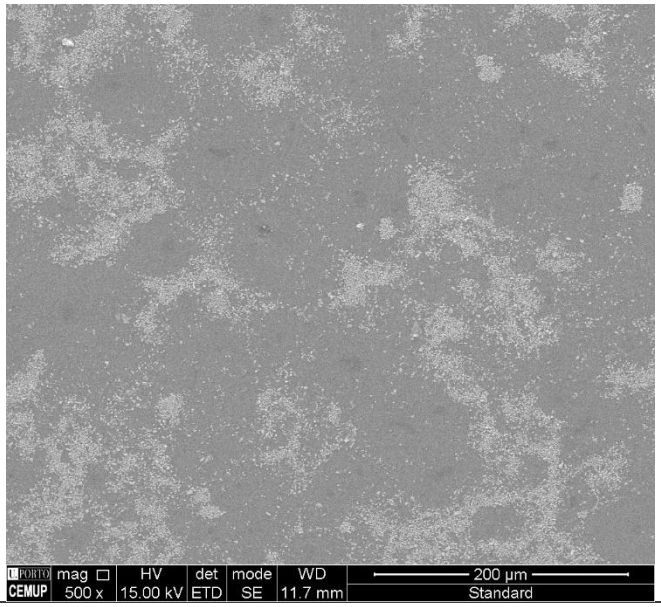

Standard sample

2500x amplification

Topography image

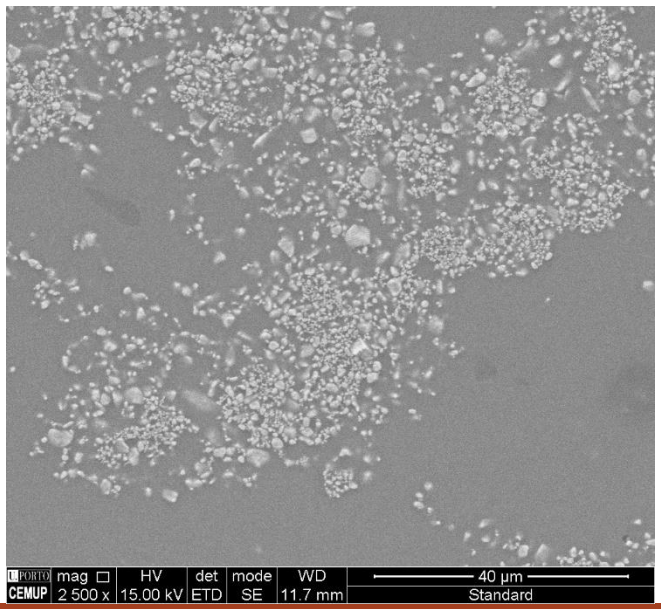

6.5 Appendix 5 – Colourimeter Analysis complete set of values

The ink from the samples (3,3,2) and (6,1,5), a pinhole and a crack, respectively, jumped, being both of the colourimeter reading values associated with the ceramic tile's provoked defect directly in the specimen's non glazed zone. Also, the sample (5,2,6), a crack, has not had any laser incidence; therefore, its colourimeter reading values are relative to the non-experimented ink formed by a white powder mixed with concentrated PL960.

In addition, the values for the L^*, a^* and b^* axles were registered regarding the glazed area of every specimen whose defects have been analysed by the colourimeter, in order to have a comparative term. This way, the ΔE^* value for each sample is taken directly from the colourimeter and is relative to the parameters' values for the standard specimen (highlighted in bold) each defect belongs to.

Location	Defect	Power	Time/ Speed	With Lens/ No Lens	L^*	a^*	b^*	ΔE^*
(1,1)	Standard	-	-	-	90.9	0.0	1.1	-
(1,1,3)	Pinhole	P25	V45	WL2.5''	89.3	0.3	1.6	1.9
(1,1,8)	Pinhole	P35	V45	WL2.5''	88.9	0.4	1.7	2.1
(1,2)	Standard	-	-	-	91.3	0.1	1.1	-
(1,2,1)	Pinhole	P60	T10	NL	91.9	0.0	0.9	1.0
(3,1)	Standard	-	-	-	92.1	0.2	1.3	-
(3,1,1)	Pinhole	P60	T5	WL2.5''	91.6	0.2	1.3	1.1
(3,1,2)	Pinhole	P30	T3	WL2.5''	91.9	0.3	0.9	0.8
(3,1,3)	Pinhole	P30	T5	WL2.5''	91.1	0.2	0.8	1.2
(3,1,4)	Pinhole	P25	T5	NL	91.8	0.3	1.0	0.7
(3,1,5)	Pinhole	P25	T20	NL	91.8	0.2	1.3	0.5
(3,1,6)	Pinhole	P25	T5	WL2.5''	92.3	0.3	0.9	0.7
(3,2)	Standard	-	-	-	91.8	0.4	1.3	-
(3,2,1)	Pinhole	P25	T30	NL	91.2	0.3	1.1	0.5
(3,2,2)	Pinhole	P35	T30	NL	91.4	0.2	1.5	0.5
(3,2,3)	Pinhole	P35	T30	NL	91.3	0.3	1.5	0.6
(3,2,4)	Pinhole	P30	T20	NL	91.0	0.3	1.1	0.5
(3,2,5)	Pinhole	P30	T30	NL	91.4	0.2	1.7	0.7

Location	Defect	Power	Time/ Speed	With Lens/ No Lens	L^*	a^*	b^*	ΔE^*
(3,2,6)	Pinhole	P35	T30	NL	91.7	0.3	1.2	0.4
(3,2,7)	Crack	P25	T30	NL	91.3	0.2	1.6	0.7
(3,2,8)	Crack	P25	T30	NL	91.4	0.3	1.5	0.8
(3,2,9)	Crack	P25	T30	NL	91.3	0.3	1.6	0.8
(3,3)	Standard	-	-	-	92.4	0.0	1.1	-
(3,3,2)	Pinhole	P20	T70	NL	92.8	0.1	1.3	0.4
(3,3,4)	Pinhole	P40	T10	NL	91.0	0.0	1.4	0.9
(3,3,6)	Pinhole	P40	T10	NL	92.1	0.2	1.0	0.8
(4,1)	Standard	-	-	-	91.5	0.2	1.2	-
(4,1,7)	Pinhole	P25	T20	NL	89.0	0.3	2.1	0.6
(4,1,8)	Pinhole	P20	T20	NL	90.7	0.3	1.5	1.0
(4,1,9)	Pinhole	P25	T20	NL	90.9	0.1	2.1	1.2
(4,2)	Standard	-	-	-	91.6	0.1	1.2	-
(4,2,1)	Crack	P20	V3	NL	90.2	0.0	1.8	1.8
(4,2,7)	Pinhole	P25	T20	NL	92.0	0.0	1.6	0.6
(4,2,8)	Pinhole	P25	T20	NL	91.8	0.2	0.6	0.5
(4,2,9)	Pinhole	P25	T20	NL	91.1	0.2	0.7	1.0
(5,1)	Standard	-	-	-	91.2	0.1	1.1	-
(5,1,1)	Crack	P20	V3	NL	89.3	1.0	3.2	4.5
(5,1,2)	Crack	P20	V3	NL	89.3	1.4	4.3	2.6
(5,1,3)	Crack	P20	V5	NL	89.4	1.2	3.3	3.6
(5,1,4)	Crack	P20	V10	NL	92.0	0.2	1.0	3.0
(5,1,5)	Crack	P25	3xT10	NL	91.3	0.1	0.9	1.5
(5,1,6)	Crack	P25	3xT5	NL	87.8	1.3	3.6	5.1
(5,1,8)	Pinhole	P15	T10	NL	90.3	0.6	2.2	2.1
(5,1,9)	Pinhole	P10	T10	NL	91.6	0.3	0.9	0.9
(5,2)	Standard	-	-	-	91.6	-0.1	0.8	-
(5,2,1)	Crack	P20	V3	NL	91.6	0.1	0.6	1.6

Location	Defect	Power	Time/ Speed	With Lens/ No Lens	L^*	a^*	b^*	ΔE^*
(5,2,2)	Crack	P25	3xT10	NL	87.3	-0.4	1.0	5.3
(5,2,3)	Crack	P20	3xT10	NL	83.8	0.3	2.7	7.1
(5,2,4)	Crack	P20	3xT5	NL	88.2	1.1	4.2	5.2
(5,2,5)	Crack	P30	3xT10	NL	91.1	-0.3	0.6	1.9
(5,2,6)	Crack	P25	3xT10	NL	87.7	0.4	0.6	3.6
(5,3)	Standard	-	-	-	91.6	0.1	1.1	-
(5,3,2)	Crack	P25	V5	NL	89.5	0.7	2.4	3.0
(5,3,3)	Crack	P10	3xT10	NL	87.0	1.3	3.9	7.3
(5,3,5)	Crack	P40	3xT10	NL	91.4	0.2	1.1	1.2
(5,3,6)	Crack	-	-	-	91.8	0.7	1.0	1.1
(5,4)	Standard	-	-	-	91.3	0.2	1.1	-
(5,4,3)	Crack	P20	V10	NL	91.8	1.3	1.6	1.3
(5,4,4)	Crack	P30	V50	NL	90.8	0.2	1.1	1.7
(5,4,6)	Crack	P50	V20	NL	89.9	0.4	2.4	2.5
(5,4,7)	Crack	P25	V5	NL	84.0	1.6	4.2	10.5
(5,4,8)	Crack	P25	3xT10	NL	91.0	0.2	1.0	1.5
(5,4,9)	Crack	P20	3xT10	NL	91.1	0.3	1.0	1.3
(6,1)	Standard	-	-	NL	92.6	0.0	1.5	-
(6,1,1)	Crack	P25	V10	NL	93.3	-0.1	1.7	1.7
(6,1,5)	Crack	P30	V1	NL	89.9	0.5	2.8	2.6
(6,2)	Standard	-	-	NL	92.1	0.2	1.5	-
(6,2,4)	Crack	P28	V3	NL	92.2	0.3	2.0	0.4
(6,2,6)	Crack	P20	3xT10	NL	91.7	0.0	2.1	0.7
(6,2,9)	Crack	P15	3xT10	NL	92.4	0.1	1.3	0.5

6.6 Appendix 6 – Experimental work resume table

The following tables consist of a summary of the entire experimental work performed throughout the entire project englobed in this dissertation. Every specimen (a, b) is taken into consideration, including the standard obtained by the hot recovery method, and sample (a, b, c), being pinholes, cracks or markings, to which the laser interaction was employed in, added to the provoked defects that, in the end, were never experimented. Furthermore, to each and every one of these samples, is displayed the types of analysis performed: visual inspection, colourimeter reading, optical microscope, quality tests and electronic microscope (SEM). A first table containing the total values for the experimental tests is presented, in order to provide a reference for the quantitative part of the practical work.

Samples	Pinholes	Cracks	Markings	Tiles	Laser	Visual	Colourimeter	Optical	Quality	SEM
198	81	72	24	21	154	154	70	27	22	5
	153									
	177									

Sample	Pinholes	Cracks	Markings	Tiles	Laser	Visual	Colourimeter	Optical	Quality	SEM
Standard				X					X	X
(1,1)				X			X			
(1,1,1)	X				X	X				
(1,1,2)	X				X	X				
(1,1,3)	X				X	X	X			
(1,1,4)	X				X	X				
(1,1,5)	X				X	X				
(1,1,6)	X				X	X				
(1,1,7)	X				X	X				
(1,1,8)	X				X	X	X	X		
(1,1,9)	X				X	X				
(1,1,10)	X				X	X				
(1,1,11)	X				X	X				

Sample	Pinholes	Cracks	Markings	Tiles	Laser	Visual	Colourimeter	Optical	Quality	SEM
(1,1,12)	X				X	X				
(1,2)				X			X			
(1,2,1)	X				X	X	X	X		
(1,2,2)	X				X	X				
(1,2,3)	X				X	X				
(1,2,4)	X				X	X				
(1,2,5)	X				X	X				
(1,2,6)	X				X	X				
(1,2,7)	X				X	X				
(1,2,8)	X				X	X				
(1,2,9)	X				X	X				
(1,3)				X						
(1,3,1)	X				X	X				
(1,3,2)	X				X	X				
(1,3,3)	X				X	X				
(1,3,4)	X				X	X				
(1,3,5)	X				X	X				
(1,3,6)	X				X	X				
(1,3,7)	X				X	X				
(1,3,8)	X				X	X				
(1,3,9)	X				X	X				
(1,3,10)	X				X	X				
(1,3,11)	X				X	X				
(1,3,12)	X				X	X				
(1,4)				X						
(1,4,1)	X				X	X				
(1,4,2)	X				X	X				
(1,4,3)	X				X	X				
(1,4,4)	X				X	X				

Sample	Pinholes	Cracks	Markings	Tiles	Laser	Visual	Colourimeter	Optical	Quality	SEM
(1,4,5)	X				X	X				
(1,4,6)	X				X	X				
(1,4,7)			X		X	X				
(2,1)				X						
(2,1,1)			X		X	X				
(2,1,2)			X		X	X				
(2,1,3)			X		X	X				
(2,1,4)			X		X	X				
(2,1,5)			X		X	X				
(2,1,6)			X		X	X				
(2,1,7)			X		X	X				
(2,1,8)			X		X	X				
(2,1,9)			X		X	X				
(2,1,10)			X		X	X				
(2,1,11)			X		X	X				
(2,1,12)			X		X	X				
(2,1,13)			X		X	X		X		
(2,1,14)			X		X	X		X		
(2,1,15)			X		X	X				
(2,2)				X						
(2,2,1)			X		X	X		X		
(2,2,2)			X		X	X		X		
(2,2,3)			X		X	X				
(2,2,4)			X		X	X				
(2,2,5)			X		X	X				
(2,2,6)			X		X	X				
(2,3)				X						
(2,3,1)			X		X	X				
(2,3,2)			X		X	X				

Sample	Pinholes	Cracks	Markings	Tiles	Laser	Visual	Colourimeter	Optical	Quality	SEM
(2,4)				X						
(2,4,1)	X				X	X				
(2,4,2)	X				X	X				
(2,4,3)	X				X	X				
(2,4,4)	X				X	X				
(2,4,5)	X				X	X				
(2,4,6)	X				X	X				
(3,1)				X			X			
(3,1,1)	X				X	X	X	X		
(3,1,2)	X				X	X	X			
(3,1,3)	X				X	X	X			
(3,1,4)	X				X	X	X			
(3,1,5)	X				X	X	X	X		
(3,1,6)	X				X	X	X	X		
(3,1,7)		X								
(3,1,8)		X								
(3,1,9)		X								
(3,2)				X			X			
(3,2,1)	X				X	X	X	X		X
(3,2,2)	X				X	X	X	X		
(3,2,3)	X				X	X	X	X		X
(3,2,4)	X				X	X	X	X		
(3,2,5)	X				X	X	X	X		
(3,2,6)	X				X	X	X	X		
(3,2,7)		X			X	X	X			X
(3,2,8)		X			X	X	X			
(3,2,9)		X			X	X	X			
(3,3)				X			X			
(3,3,1)	X				X	X				

Sample	Pinholes	Cracks	Markings	Tiles	Laser	Visual	Colourimeter	Optical	Quality	SEM
(3,3,2)	X				X	X	X			
(3,3,3)	X				X	X				
(3,3,4)	X				X	X	X	X		
(3,3,5)	X				X	X				
(3,3,6)	X				X	X	X			
(3,3,7)		X								
(3,3,8)		X								
(3,3,9)		X								
(3,4)				X						
(3,4,1)	X				X	X				
(3,4,2)	X				X	X				
(3,4,3)	X				X	X				
(3,4,4)	X				X	X				
(3,4,5)	X				X	X				
(3,4,6)	X				X	X				
(3,4,7)		X								
(3,4,8)		X								
(3,4,9)		X								
(4,1)				X			X			
(4,1,1)		X							X	
(4,1,2)		X							X	
(4,1,3)		X							X	
(4,1,4)		X							X	
(4,1,5)		X						X	X	
(4,1,6)		X							X	
(4,1,7)	X				X	X	X	X	X	
(4,1,8)	X				X	X	X	X	X	
(4,1,9)	X				X	X	X	X	X	
(4,2)				X			X			

Sample	Pinholes	Cracks	Markings	Tiles	Laser	Visual	Colourimeter	Optical	Quality	SEM
(4,2,1)		X			X	X	X			
(4,2,2)		X								
(4,2,3)		X								
(4,2,4)		X			X	X				
(4,2,5)		X								
(4,2,6)		X								
(4,2,7)	X				X	X	X		X	
(4,2,8)	X				X	X	X		X	
(4,2,9)	X				X	X	X		X	
(5,1)				X			X			
(5,1,1)		X			X	X	X			
(5,1,2)		X			X	X	X			
(5,1,3)		X			X	X	X			
(5,1,4)		X			X	X	X			
(5,1,5)		X			X	X	X	X		
(5,1,6)		X			X	X	X	X		
(5,1,7)	X				X	X				
(5,1,8)	X				X	X	X			
(5,1,9)	X				X	X	X			
(5,2)				X			X			
(5,2,1)		X			X	X	X		X	
(5,2,2)		X			X	X	X	X	X	
(5,2,3)		X			X	X	X	X	X	
(5,2,4)		X			X	X	X		X	
(5,2,5)		X			X	X	X		X	
(5,2,6)		X			X	X	X	X	X	
(5,2,7)	X				X	X			X	
(5,2,8)	X				X	X			X	
(5,2,9)	X				X	X			X	

Sample	Pinholes	Cracks	Markings	Tiles	Laser	Visual	Colourimeter	Optical	Quality	SEM
(5,3)				X			X			
(5,3,1)		X			X	X				
(5,3,2)		X			X	X	X			
(5,3,3)		X			X	X	X			
(5,3,4)		X			X	X				
(5,3,5)		X			X	X	X			
(5,3,6)		X					X			
(5,3,7)		X								
(5,3,8)		X								
(5,3,9)		X								
(5,4)				X			X			
(5,4,1)		X			X	X				
(5,4,2)		X			X	X				
(5,4,3)		X			X	X	X			
(5,4,4)		X			X	X	X			
(5,4,5)		X			X	X				
(5,4,6)		X			X	X	X			
(5,4,7)		X			X	X	X			
(5,4,8)		X			X	X	X			
(5,4,9)		X			X	X	X			
(6,1)				X			X			
(6,1,1)		X			X	X	X			
(6,1,2)		X			X	X				
(6,1,3)		X			X	X				
(6,1,4)		X			X	X				
(6,1,5)		X			X	X	X			
(6,1,6)		X			X	X				
(6,1,7)		X			X	X				
(6,1,8)		X			X	X				

Sample	Pinholes	Cracks	Markings	Tiles	Laser	Visual	Colourimeter	Optical	Quality	SEM
(6,1,9)		X			X	X				
(6,2)				X			X			
(6,2,1)		X			X	X				
(6,2,2)		X			X	X				
(6,2,3)		X			X	X				
(6,2,4)		X			X	X	X			
(6,2,5)		X			X	X				
(6,2,6)		X			X	X	X	X		X
(6,2,7)		X			X	X				
(6,2,8)		X			X	X				
(6,2,9)		X			X	X	X	X		